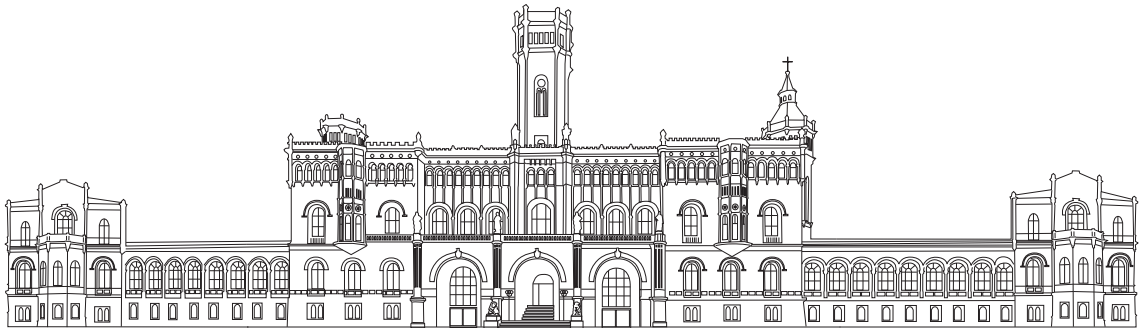# THE INFLUENCE OF BOUNDARY CONDITIONS ON THE EMERGENCE OF NON-COMPACT DEGREES OF FREEDOM IN THE SCALING LIMIT OF INTEGRABLE LATTICE MODELS

Von der Fakultät für Mathematik und Physik
der Gottfried Wilhelm Leibniz Universität Hannover zur Erlangung des Grades

Doktor der Naturwissenschaften
Dr. rer. nat.

genehmigte Dissertation von

M.A.St. Sascha Gehrmann

2024

ABSTRACT

One-dimensional critical integrable lattice models with a finite-dimensional degree of freedom attached to each lattice site can exhibit the remarkable phenomenon of the emergence of continuous degrees of freedom in the scaling limit. The most studied system in which this occurrence has been observed is the staggered six-vertex model with twisted boundary conditions. Here, we study the influence of different boundary conditions and higher-rank generalisations on/of this model. Our analysis is based on the Bethe ansatz and the formulation of a conserved quantity — the so-called quasi-momentum — which parametrises the non-compact degree of freedom directly on the lattice. Moreover, we carry over the powerful approach of the correspondence between ordinary differential equations and integrable quantum field theories to the case of open boundary conditions. Using this methodology, we can fully classify the scaling limit of the alternating six-vertex model with $U_q(\mathfrak{sl}(2))$ boundary conditions. Furthermore, we demonstrate the incompatibility of antidiagonal boundary conditions with a non-compact degree of freedom in the scaling limit. Finally, we provide numerical evidence that the higher rank generalisation, the $D_3^{(2)}$ model, possesses two independent continuous components.

Keywords: integrability, Bethe ansatz, six-vertex model, boundary conditions, scaling limit, lattice models, conformal field theory, critical exponents.

LIST OF ABBREVIATIONS

1D one-dimensional

2D two-dimensional

AdS Anti de Sitter space

BAE Bethe ansatz equations

BC boundary condition

BCFT boundary conformal field theory

CFT conformal field theory

IQFT integrable quantum field theory

irreps irreducible representations

LHS left hand side

NLIE non-linear integral equation

NLSM non-linear sigma model

ODE ordinary differential equation

ONB orthonormalized basis

OPE operator product expansion

QFT quantum field theory

RHS right hand side

RG renormalisation group

WKB Wentzel-Kramers-Brillouin

WZW Wess-Zumino-Witten

YBE Yang-Baxter equation

CONTENTS

1 | INTRODUCTION

The beginning of the era of investigating phase transitions via solvable systems can undoubtedly be dated back 100 years ago[1] to the formulation of the Ising model [1]. In that work, Ising showed the absence of a ferromagnetic phase for any finite temperature in *one* dimension. He concluded — based on the results for the one-dimensional (1D) case — the general failure of the model to describe ferromagnetism in solids for *any* dimension. Shortly after, Ising's conclusions concerning the higher dimensional case were called into question, in particular, by Peierls [2]. Later, Kramers and Wannier [3] deduced the critical temperature, if it exists, of a phase transition for the two-dimensional (2D) Ising model. Their arguments make use of a map between the partition functions at temperatures T and T^{-1}, which is a prototype of strong/weak coupling dualities that nowadays attract a lot of attention in quantum field theory (QFT), in particular in String Theory. Further attempts at clarification using approximate methods led to contradictory results. It was only after Onsager solved the 2D square lattice Ising model exactly [4] that the matter was finally settled. His analytical results proved the existence of a phase transition at the critical temperature predicted in [3]. It also laid the foundation for the development of key concepts such as the scaling hypothesis, universality, and the transfer matrix approach to statistical systems.

The success of the square lattice Ising model stimulated interest in other simplified statistical systems. One of these is the so-called Potts model. In the antiferromagnetic case, Berker and Kadanoff observed a remarkable phenomenon. In their work [5], they showed that $T = 0$ is not a fixed point of the renormalisation group (RG) flow. This is connected to the presence of a macroscopically large residual entropy. The universal behaviour was further studied in [6] via the mapping of the critical Potts model to the (inhomogeneous) six-vertex model, which can be solved exactly [7]. Phases exhibiting properties such as macroscopic residual entropy attract a lot of attention in condensed matter physics. Recent examples are fracton systems, which have been studied with a view towards possible realizations in nature [8] and applications to quantum information theory [9].

At the critical temperature, which is a fixed point under the renormalisation group flow, a system develops universal behaviour. The latter is insensitive to the details of the microscopic Hamiltonian. Thus, even studies of highly simplified, exactly solvable systems

---

[1]If one considers the date at which Ising has submitted his article.

exhibiting a phase transition yield results that apply to a class of models, some of which may be realised in nature.

The critical six-vertex model develops universal behaviour, which is described by a free massless bosonic field, taking values on the circle. Such 'compact' conformal field theories (CFTs) were commonly believed to arise also in the scaling limit of other critical lattice systems, where the local number of degrees of freedom is finite. On the other hand, theories with non-compact target space describe many interesting problems in modern physics. For example, they appear in theoretical high-energy physics in the context of the correspondence between quantum gravity in Anti de Sitter space (AdS) and CFT [10, 11, 12, 13, 14]. Moreover, non-compact QFTs have applications in the context of condensed matter theory. For instance, they have been argued to describe the multifractal scaling of the critical wave functions at the integer quantum Hall plateau transition and other disorder-driven quantum phase transitions [15, 16]. Such non-compact field theories and their lattice counterparts — where the degrees of freedom at each lattice site are infinite — are significantly more challenging to study. Even in the case of integrable models, the standard techniques meet difficulties. However, there has been significant progress for specific models, e.g. for the Sinh-Gordon QFT [17].

The common belief that non-compact CFTs only admit lattice regularisations with an infinite number of local degrees of freedom made the results of [18] all the more remarkable. In that work, a critical integrable $sl(2|1)$ superspin chain with alternating three-dimensional quark and antiquark representations at each site is studied. A finite-size analysis provided evidence for the presence of a continuous component in the spectrum of critical exponents — a hallmark of a CFT with non-compact target space. This opens the way to approach non-compact field theories via the analysis of the scaling limit of integrable lattice systems where the Hilbert space is finite-dimensional. The latter can be treated within the standard Bethe ansatz approach.

The emergence of a continuous component in the spectrum of scaling dimensions was later found to occur in other critical lattice models as well [19, 20, 21, 22, 23]. The simplest of these is the so-called staggered six-vertex model, which possesses three different phases. For one of them, it was conjectured in [24] that the scaling limit is governed by a non-linear sigma model (NLSM) in $(1+1)$-dimensional space-time, whose target space is the so-called 2D Euclidean Black Hole. The solution of the spectral problem for this CFT, which includes determining the density of states for the continuous spectrum, was achieved in the later work [25]. The results are based on a detailed study of the staggered six-vertex model with twisted boundary conditions (BCs).

The analysis of critical integrable systems exhibiting a continuous spectrum of critical exponents presents various technical challenges. These require the application of novel techniques based on the study of the family of commuting operators on the lattice and in the CFT. Previous works have mostly focused on the case when periodic (or, more generally, twisted) BCs are imposed. This thesis aims to extend the analysis to integrable lattice models with open BCs. This would be of prime interest from the point of view of 2D boundary conformal field theory (BCFT). As a testing ground, two extreme cases for

the staggered six-vertex model are considered. Namely, a particular choice of diagonal BCs for which the $U(1)$ symmetry is enlarged to a continuous $U_q(\mathfrak{sl}(2))$ symmetry and those where the $U(1)$ is broken down to a discrete $\mathbb{Z}_2$ one (antidiagonal BCs). The former case has already been investigated from the perspective of the Potts model [26, 27]. In these works, it was shown that different choices of BCs in the Potts model have a profound effect. Namely, depending on their choice, the continuous component of the conformal spectrum may disappear completely. We explain this phenomenon within a unified framework. In addition, we study a higher-rank generalisation of the staggered six-vertex model based on the twisted affine Lie-algebra $D_3^{(2)}$.

The second chapter of the thesis introduces basic concepts which underpin the later analysis. In particular, we will state some fundamental facts about CFT using the examples of the free massless boson and the Black Hole CFTs which are relevant to this thesis. Also, the framework of Yang-Baxter integrable models for various BCs is introduced. We briefly comment on the relationship between CFT and critical lattice models.

In the third chapter, we discuss integrable vertex models with two-site periodically repeating inhomogeneities, the so-called staggered vertex models. We describe their algebraic structure for periodic and open BCs. In the latter case, it turns out that only two types of staggering, named alternating and quasi-periodic, lead to a local Hamiltonian. The scaling limits of these Hamiltonians for the particular case of the six-vertex model with so-called $U_q(\mathfrak{sl}(2))$ invariant BCs will be examined in chapter four.

For the model with alternating staggering, we demonstrate the power of the correspondence between ordinary differential equations (ODEs) and integrable quantum field theories (IQFTs) for the analysis of the scaling limit. The ODE/IQFT correspondence was first observed and developed in [28, 29, 30]. Using the uniform framework introduced in chapter three, the case of the quasi-periodic staggering is then studied by a spectral flow to the alternating case.

We briefly discuss the results of our numerical investigation for the case of antidiagonal BCs in the fifth chapter.

Finally, the framework from chapter three allows a straightforward generalisation from the staggered six-vertex model to the *homogeneous* $D_3^{(2)}$ model, whose underlying symmetry algebra is of a higher rank. A detailed numerical finite-size analysis of a class of states is performed.

A visualisation of the relationship of the key sections of this thesis is given below. This thesis is based on the author's works [31, 32, 33, 34]. We omit the referencing of these works repeatedly.
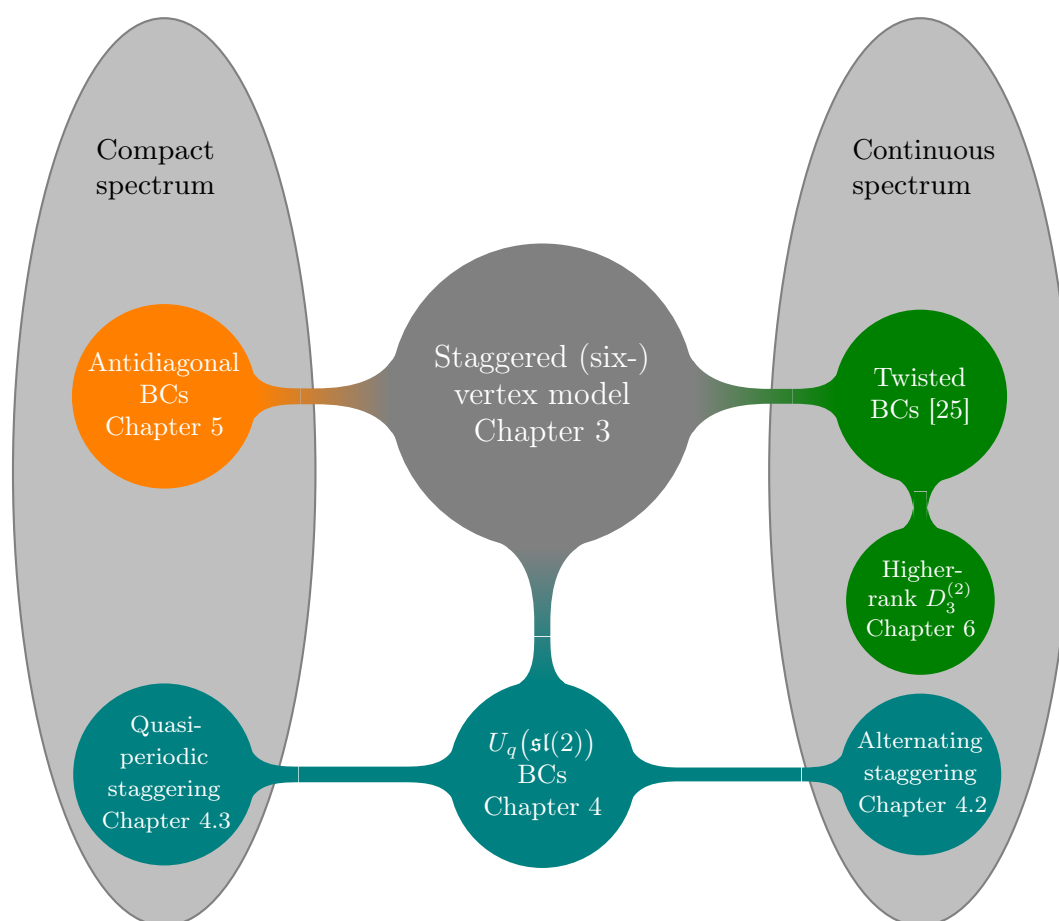
Figure 1.1: A visualisation of the key chapters of this thesis

2 | PRELIMINARIES

This thesis concerns the study of the scaling limit of critical integrable lattice models. By scaling limit, we mean a certain limit where the system size tends to infinity, and one just considers the low energy excitations around the ground state. This procedure leads to an effective description of the low-energy regime of the lattice model in terms of a field theory [35]. While it seems natural to introduce the lattice side first, then present the procedure of taking the scaling limit, and finally discuss the field theory content in detail, the reverse way is more convenient for coherently presenting the methodology used.

The first section is devoted to the field theory side. It is mainly centred around a detailed discussion of the free massless boson in 2D. Along the way, we will use this simple example to recall and demonstrate elementary facts about CFT. This lays the foundation to introduce the so-called 2D Black Hole CFTs, which play a significant role in this thesis. The content is based on the introductory chapters of [36, 37]. We have adapted the presentation for our purposes and omitted referencing these works repeatedly.

The bridge to the lattice part of this introductory chapter is a short discussion about the concept of finite-size scaling.

In the second half of this chapter, we introduce Yang-Baxter integrable lattice models; the presentation is partly adapted from [32]. In the course of the discussion, we present a toolbox of analytic and numerical methods, which we will often refer to in later chapters. We put emphasis on the analysis of the scaling limit of an integrable lattice system. Again, we illustrate the technique with a simple example: the spin-$\frac{1}{2}$ XXZ chain. Along the way, we will also discuss the powerful ODE/IQFT approach.

2.1 The free massless boson in 2D

Consider the real scalar field defined on the infinite cylinder $(-\infty, \infty) \times [0, L)$ with circumference L

$$\varphi(t, x) : (-\infty, \infty) \times [0, L) \longrightarrow \mathbb{R} \,. \tag{2.1}$$

In the literature, the domain of the field is often called the worldsheet, while its image is called the target space. We use this convention in the following. The dynamics of the field is described by the following action functional

$$S[\varphi] = \frac{1}{2} \int_{-\infty}^{\infty} \mathrm{d}t \int_0^L \mathrm{d}x \, \left(\partial_t \varphi\right)^2(t, x) - \left(\partial_x \varphi\right)^2(t, x) \,. \tag{2.2}$$

Requiring that the action is stationary under a variation of the field $\varphi \mapsto \varphi + \delta\varphi$ leads to the following equations of motion as well as the extra condition[1]

$$\partial_\mu \partial^\mu \varphi(t, x) = 0 \,, \qquad \int_{-\infty}^{\infty} \mathrm{d}t \, \partial_x \varphi(t, x) \delta\varphi(t, x) \Big|_{x=0}^{x=L} = 0 \,. \tag{2.3}$$

To satisfy the latter, we impose that the quantity $\partial_x \varphi(t, x)$ is periodic[2] in x with period L, i.e., $\partial_x \varphi(t, x + L) = \partial_x \varphi(t, x)$. In the Hamiltonian formalism, the conjugate momentum to φ is given by $\pi(t, x) = \partial_t \varphi(t, x)$ and is assumed also to be L-periodic in the spatial direction. Hence, for a given time slice — we choose $t = 0$ for simplicity — we can introduce the following Fourier expansions for the two chiral fields $\partial_\pm \varphi$

$$(\partial_- \varphi)(0, x) := \frac{1}{2} \left(\pi(0, x) - \partial_x \varphi(0, x)\right) = \sqrt{\frac{\pi}{2}} \frac{p}{L} + \frac{\sqrt{2\pi}}{L} \sum_{n \in \mathbb{I}} a_n \mathrm{e}^{\frac{2\mathrm{i}\pi n x}{L}} \,, \tag{2.4}$$

$$(\partial_+ \varphi)(0, x) := \frac{1}{2} \left(\pi(0, x) + \partial_x \varphi(0, x)\right) = \sqrt{\frac{\pi}{2}} \frac{\bar{p}}{L} + \frac{\sqrt{2\pi}}{L} \sum_{n \in \mathbb{I}} \bar{a}_n \mathrm{e}^{-\frac{2\mathrm{i}\pi n x}{L}} \,. \tag{2.5}$$

Here, we used the light cone derivatives $\partial_\pm = \partial_t \pm \partial_x$ and the index set $\mathbb{I}$ is $\mathbb{Z} \backslash \{0\}$. To quantise the theory, we promote the fields to be operator-valued with the fundamental commutation relations

$$\begin{aligned} [\varphi(t, x), \pi(t, y)] &= \mathrm{i}\delta(x - y) \,, \\ [\pi(t, x), \pi(t, y)] &= 0 \,, \\ [\varphi(t, x), \varphi(t, y)] &= 0 \,. \end{aligned} \tag{2.6}$$

These in turn induce relations on the Fourier modes p, $\bar{p}$, a_n and $\bar{a}_n$. In fact, they are mutually commuting except for $[a_m, a_n] = \frac{m}{2} \delta_{n+m,0}$ and $[\bar{a}_m, \bar{a}_n] = \frac{m}{2} \delta_{n+m,0}$. We will call the modes with positive indices the annihilation and those with negative subscripts the creation operators.

Let us proceed to define the theory's Hamiltonian and momentum operator. They do not depend on time and are given by

$$H = \int_0^L \mathrm{d}x \, \frac{1}{2} \left(\pi^2(t, x) + (\partial_x \varphi)^2(t, x)\right) = \int_0^L \mathrm{d}x \, (\partial_+ \varphi)^2(0, x) + (\partial_- \varphi)^2(0, x) \,, \tag{2.7}$$

$$P = -\int_0^L \mathrm{d}x \, \pi(t, x) \partial_x \varphi(t, x) = -\int_0^L \mathrm{d}x \, (\partial_+ \varphi)^2(0, x) - (\partial_- \varphi)^2(0, x) \,. \tag{2.8}$$

---

[1] We assume here for simplicity that the variation of the field decays to zero as $t \to \pm\infty$.
[2] —and so the variation $\delta\varphi$ is also periodic—

The expressions above contain composite operators such as $(\partial_\pm\varphi)^2(0,x)$. A proper definition of such operators can be subtle since the product of two local operators generically diverges when evaluated at the same space-time point. For example

$$
\begin{aligned}
(\partial_-\varphi)(0,x)(\partial_-\varphi)(0,y) =& \frac{p^2\pi}{2L^2} + \frac{\pi p}{L}\sum_{n\neq 0} a_n\left(\mathrm{e}^{\frac{2\mathrm{i}\pi nx}{L}} + \mathrm{e}^{\frac{2\mathrm{i}\pi ny}{L}}\right) \\
&+ \frac{2\pi}{L^2}\sum_{n,m\neq 0} :a_n a_m: \mathrm{e}^{\frac{2\mathrm{i}\pi(n+m)x}{L}} - \frac{\pi}{4L^2\sin^2\left(\frac{\pi(x-y)}{L}\right)}\,,
\end{aligned}
\tag{2.9}
$$

where $:\!...\!:$ denotes the normal ordering where we place all annihilation operators to the right. We see that $(\partial_-\varphi)^2(0,x)$ is diverging due to the last term in (2.9). One suitable regularisation scheme is to subtract the most divergent term. The latter can be obtained via the expansion

$$
\frac{\pi}{4L^2\sin^2\left(\frac{\pi(x-y)}{L}\right)} = \frac{1}{4\pi(x-y)^2} + \frac{\pi}{12L^2} + O\left((x-y)^1\right)\,.
\tag{2.10}
$$

From now on, we define any composite operators to be implicitly regularised by subtracting the divergent part, e.g.,

$$
(\partial_\pm\varphi)^2(0,x) = \lim_{y\to x}(\partial_\pm\varphi)(0,x)(\partial_\pm\varphi)(0,y) + \frac{1}{4\pi(x-y)^2}\,.
\tag{2.11}
$$

By this definition, the Hamiltonian and the momentum operator can be expressed in terms of the oscillator modes

$$
H = \frac{\pi\left(p^2+\bar{p}^2\right)}{2L} + \frac{4\pi}{L}\left(\sum_{n>0} a_{-n}a_n + \bar{a}_{-n}\bar{a}_n\right) - \frac{1}{12}\frac{2\pi}{L}\,,
\tag{2.12}
$$

$$
P = \frac{\pi\left(p^2-\bar{p}^2\right)}{2L} + \frac{4\pi}{L}\left(\sum_{n>0} a_{-n}a_n - \bar{a}_{-n}\bar{a}_n\right)\,.
\tag{2.13}
$$

This explicit form of the Hamiltonian can be used to determine the time evolution of the fields. The Heisenberg equations lead to

$$
a_n(t) = \mathrm{e}^{-\frac{2\mathrm{i}\pi nt}{L}} a_n\,,
\tag{2.14}
$$

$$
\bar{a}_n(t) = \mathrm{e}^{-\frac{2\mathrm{i}\pi nt}{L}} \bar{a}_n\,,
\tag{2.15}
$$

while p and $\bar{p}$ are constant in time. One can utilise this to restore the time dependence in the fields. Furthermore, we can integrate suitable linear combinations of $\partial_\pm\varphi$ to obtain the following expressions for the fundamental quantities

$$
\varphi(t,x) = \varphi_0 + \sqrt{\frac{\pi}{2}}\frac{p+\bar{p}}{L}t - \sqrt{\frac{\pi}{2}}\frac{p-\bar{p}}{L}x + \frac{\mathrm{i}}{\sqrt{2\pi}}\sum_{n\in\mathbb{I}}\frac{1}{n}\left(a_n\mathrm{e}^{\frac{2\mathrm{i}\pi n(x-t)}{L}} + \bar{a}_n\mathrm{e}^{-\frac{2\mathrm{i}\pi n(x+t)}{L}}\right)\,,
\tag{2.16}
$$

$$
\pi(t,x) = \sqrt{\frac{\pi}{2}}\frac{p+\bar{p}}{L} + \frac{\sqrt{2\pi}}{L}\sum_{n\in\mathbb{I}} a_n\mathrm{e}^{\frac{2\mathrm{i}\pi n(x-t)}{L}} + \bar{a}_n\mathrm{e}^{-\frac{2\mathrm{i}\pi n(x+t)}{L}}\,,
\tag{2.17}
$$

where φ_0 is the constant zero mode. Its commutation relations with the other operators are deduced to be

$$[\varphi_0, a_n] = 0, \qquad [\varphi_0, \bar{a}_n] = 0, \tag{2.18}$$

$$\left[\varphi_0, \sqrt{\frac{\pi}{2}}(p - \bar{p})\right] = 0, \qquad \left[\varphi_0, \sqrt{\frac{\pi}{2}}(p + \bar{p})\right] = \mathrm{i}. \tag{2.19}$$

Note that the last equation is the defining relation of the Heisenberg algebra. Hence, as the target space of the fields is $\mathbb{R}$, the operator $p + \bar{p}$ has a continuous spectrum [38].

The Virasoro algebra

To discuss the symmetry properties of the present theory, it is useful to map the infinite cylinder to the complex plane $\mathbb{C}$ (in fact, the Riemann sphere) via the following transformation (and going to imaginary time $t \mapsto -\mathrm{i}t$)

$$z = \exp\left[\frac{2\pi}{L}(t - \mathrm{i}x)\right], \qquad \bar{z} = \exp\left[\frac{2\pi}{L}(t + \mathrm{i}x)\right]. \tag{2.20}$$

Then, time flows in the radial direction while space plays the role of the phase. Note that the compactification $x \sim x + L$ of the cylinder is consistent with the periodicity of $2\pi\mathrm{i}$ of the exponential function. Further, the infinite past is mapped to the origin of $\mathbb{C}$, while the infinite future is mapped to complex infinity.

In general, for a given space-time equipped with the coordinates x^μ and the contravariant metric tensor $g^{\mu\nu}(x)$, a mapping $x^\mu \mapsto w^\mu(x)$ is defined to be conformal if the transformed tensor is the original one up to some scalar function $\lambda(x)$, i.e.

$$g^{\mu\nu}(x) \mapsto \tilde{g}^{\mu\nu}(w) = \lambda(x)\, g^{\mu\nu}(x). \tag{2.21}$$

For the case at hand, the above condition, locally, takes the same form as the Cauchy-Riemann equations for either a holomorphic or anti-holomorphic function. Hence, each local (anti-)holomorphic function defines a local conformal transformation on the complex plane[3] which are, in general, given by

$$z \mapsto z + \sum_{n \in \mathbb{Z}} c_n z^{n+1}, \tag{2.22}$$

and analogously for the anti-holomorphic part. In the following, we will use the barred and unbarred notation for quantities which are[4] anti-holomorphic and holomorphic, respectively. The generators of the local conformal transformations on the space of functions — this means on the classical level — can be easily deduced:

$$l_n = -z^{n+1}\partial_z, \quad \bar{l}_n = -\bar{z}^{n+1}\partial_{\bar{z}} \qquad \text{with} \qquad n \in \mathbb{Z}. \tag{2.23}$$

These form a realisation of the De Witt algebra whose defining commutation relations are given by the following

$$[l_n, l_m] = (n - m)\, l_{n+m}, \quad [\bar{l}_n, \bar{l}_m] = (n - m)\, \bar{l}_{n+m}, \quad [l_n, \bar{l}_m] = 0. \tag{2.24}$$

---

[3]Note that we do not make any restrictions on the function to be well-defined on the whole complex plane. We just require this locally. Further, in the context of our discussion of the free bosonic field, we mean here (anti-)holomorphicity on the Riemann sphere with both poles $\{0, \infty\}$ removed.

[4]— or which are associated to (anti-)holomorphic quantities —

From the commutation relations, it is clear that $l_{\pm 1}, l_0$ and their anti-holomorphic counter-parts form a subalgebra. This is the algebra of *global* conformal transformations defined on the whole complex plane. From (2.23), it is apparent that $l_{-1} = -\partial_z$ generates translations on the complex plane. Further, $l_1 = z^2 \partial_z$ induces the so-called special conformal transformations. Linear combinations of $l_0 = -z \partial_z$ and its anti-holomorphic counterpart correspond to rotations and scale transformations. Namely, dilatations are generated by $l_0 + \bar{l}_0$ while the application of $\mathrm{i}(l_0 - \bar{l}_0)$ results in a rotation. Hence, $l_0 + \bar{l}_0$ and $\mathrm{i}(l_0 - \bar{l}_0)$ play the role of translation in time and space, respectively.

A field $\phi(z, \bar{z})$ is called quasi-primary if it transforms under global conformal transformations $z \mapsto w(z)$ as

$$\phi(z, \bar{z}) \mapsto \left(\frac{\mathrm{d}w}{\mathrm{d}z}\right)^{-\Delta} \left(\frac{\mathrm{d}\bar{w}}{\mathrm{d}\bar{z}}\right)^{-\bar{\Delta}} \phi(z, \bar{z}), \tag{2.25}$$

where Δ and $\bar{\Delta}$ are the eigenvalues of l_0 and $\bar{l}_0$ respectively. If the field transforms as (2.25) under any local transformation, we call the field a primary field.

The field φ itself is not primary, but the chiral fields $\partial_{\pm}\varphi$ are. Due to the latter, one can show that the action of bosonic theory (2.2) is invariant under conformal transformations. We call this property classical conformal symmetry.

An important general fact about conformal invariance is that it restricts the energy-momentum tensor to be symmetric[5] and traceless. Combined with the conservation law $\partial_\mu T^{\mu\nu}$ its non-trivial entries are, in complex coordinates,

$$T(z) = T_{11} - T_{22} - 2\mathrm{i}\, T_{12}, \qquad \bar{T}(\bar{z}) = T_{11} - T_{22} + 2\mathrm{i}\, T_{12}, \tag{2.26}$$

which are (anti-)holomorphic functions i.e. $\partial_{\bar{z}} T(z) = 0$ and $\partial_z \bar{T}(\bar{z}) = 0$. As usual, the elements of the stress energy-momentum tensor $T(z), \bar{T}(\bar{z})$ are the local densities of the Noether charges associated with translations. It turns out that the conserved charges built from $z^{n+1} T(z)$, $\bar{z}^{n+1} \bar{T}(\bar{z})$ generate through Poisson brackets all the other infinitesimal conformal transformations just like (2.23). The expression of the generators of the conformal transformations in terms of the energy-momentum tensor allows for the standard quantization procedure.

In order to quantise the theory, we promote the Noether charges to operators and replace the Poisson bracket with the commutator. As discussed above, the underlying algebraic structure of conformal invariance of the quantum theory can then be conveniently expressed in terms of the modes of the quantised energy-momentum tensor

$$L_n = \frac{1}{2\pi\mathrm{i}} \oint \mathrm{d}z\, z^{n+1} T(z), \tag{2.27}$$

$$\bar{L}_n = \frac{1}{2\pi\mathrm{i}} \oint \mathrm{d}z\, \bar{z}^{n+1} \bar{T}(\bar{z}), \tag{2.28}$$

---

[5]In fact, we can always symmetrize the energy-momentum tensor [37] for theories with rotational/Lorentz invariance.

where the contour is taken to be at constant time, i.e., a circle. For the case at hand, the free massless boson, we can easily express these operators in terms of the oscillator operators

$$L_m = \sum_{n\in\mathbb{Z}} a_{m-n}a_n \,, \qquad \bar{L}_m = \sum_{n\in\mathbb{Z}} \bar{a}_{m-n}\bar{a}_n \,, \qquad m \neq 0 \,, \tag{2.29}$$

$$L_0 = \frac{p^2}{4} + 2\sum_{n>0} a_{-n}a_n \,, \qquad \bar{L}_0 = \frac{\bar{p}^2}{4} + 2\sum_{n>0} \bar{a}_{-n}\bar{a}_n \,. \tag{2.30}$$

It is easy to work out their commutations relations

$$[L_n, L_m] = (n-m)L_{n+m} + \frac{c}{12}n(n^2-1)\delta_{n+m,0} \,, \tag{2.31}$$

$$\left[\bar{L}_n, \bar{L}_m\right] = (n-m)\bar{L}_{n+m} + \frac{c}{12}n(n^2-1)\delta_{n+m,0} \,, \tag{2.32}$$

$$\left[L_n, \bar{L}_m\right] = 0 \,, \tag{2.33}$$

where $c = 1$. These above equations are the defining relations of the so-called Virasoro algebra, which underlies, in general, conformal quantum field theory in two dimensions. The central charge c is an important characteristic quantity of the model.

The Hamiltonian and momentum operator can be expressed in terms of the Virasoro generators L_0 and $\bar{L}_0$ as

$$H = \frac{2\pi}{L}\left(L_0 + \bar{L}_0 - \frac{1}{12}\right) \,, \qquad P = \frac{2\pi}{L}\left(L_0 - \bar{L}_0\right) \,. \tag{2.34}$$

Note that this is the quantum version of our discussion about the De Witt algebra on the classical level where $l_0 + \bar{l}_0$ and $\mathrm{i}(l_0 - \bar{l}_0)$ play the role of translation in time and space respectively.

The Hilbert space

So far, we have not discussed the space of states. In the following, we present two analogous constructions of the latter, which use the annihilation and creation operators of either the Heisenberg or Virasoro algebra.

The Hamiltonian and $p, \bar{p}$ commute amongst each other. Hence, the eigenvalues of $p, \bar{p}$ can be used to label the eigenstates of the Hamiltonian. Define now the Fock vacuum, denoted by $|p, \bar{p}\rangle$ and the Virasoro vacuum, called $|\Omega\rangle_{p,\bar{p}}$ as the simultaneous eigenstate of H and $p, \bar{p}$ which is annihilated by all $a_n, \bar{a}_n$ or $L_n, \bar{L}_n$ for $n > 0$:

$$L_n |\Omega\rangle_{p,\bar{p}} = 0 \quad \& \quad \bar{L}_n |\Omega\rangle_{p,\bar{p}} = 0 \,, \tag{2.35}$$

$$a_n |p, \bar{p}\rangle = 0 \quad \& \quad \bar{a}_n |p, \bar{p}\rangle = 0 \,. \tag{2.36}$$

The eigenvalues $\Delta = p^2/4$ and $\bar{\Delta} = \bar{p}^2/4$ of the zero modes $L_0, \bar{L}_0$ will be referred to as the conformal weights or dimensions.

Based on the reference state, we define the so-called level-spaces as

$$\mathcal{V}_{\mathtt{L}}^{p,\bar{p}} = \text{span}\left\{ \prod_{\sum_i n_i \ell_i = \mathtt{L}} L_{-n_i}^{\ell_i} |\Omega\rangle_{p,\bar{p}} \right\}, \quad \bar{\mathcal{V}}_{\bar{\mathtt{L}}}^{p,\bar{p}} = \text{span}\left\{ \prod_{\sum_i \bar{n}_i \bar{\ell}_i = \bar{\mathtt{L}}} \bar{L}_{-\bar{n}_i}^{\bar{\ell}_i} |\Omega\rangle_{p,\bar{p}} \right\}, \quad (2.37)$$

$$\mathcal{F}_{\mathtt{F}}^{p,\bar{p}} = \text{span}\left\{ \prod_{\sum_i n_i \ell_i = \mathtt{F}} a_{-n_i}^{\ell_i} |p,\bar{p}\rangle \right\}, \quad \bar{\mathcal{F}}_{\bar{\mathtt{F}}}^{p,\bar{p}} = \text{span}\left\{ \prod_{\sum_i \bar{n}_i \bar{\ell}_i = \bar{\mathtt{F}}} \bar{a}_{-\bar{n}_i}^{\bar{l}_i} |p,\bar{p}\rangle \right\}, \quad (2.38)$$

Note that the number of basis vectors in each level space is given by the number of integer partitions of $\mathtt{L}$ or $\mathtt{F}$ and is independent of $p, \bar{p}$. For a given integer x, we will call the number of its integer partition $\text{par}(x)$. Its generating function reads

$$\sum_{\mathtt{d}=0}^{\infty} \text{par}(\mathtt{d})\, \mathtt{q}^{\mathtt{d}} = \prod_{j=1}^{\infty} \frac{1}{(1 - \mathtt{q}^j)} \ . \quad (2.39)$$

Finally, the Fock space $\mathcal{F}_{p,\bar{p}}$ or Verma module $\mathcal{V}^{p,\bar{p}}$ over the vacuum $|p,\bar{p}\rangle$, $|\Omega\rangle_{p,\bar{p}}$ is defined to be[6]

$$\mathcal{F}_{p,\bar{p}} = \bigoplus_{\mathtt{F},\bar{\mathtt{F}}=0}^{\infty} \mathcal{F}_{\mathtt{F}}^{p,\bar{p}} \otimes \bar{\mathcal{F}}_{\bar{\mathtt{F}}}^{p,\bar{p}}, \quad \mathcal{V}_{p,\bar{p}} = \bigoplus_{\mathtt{L},\bar{\mathtt{L}}=0}^{\infty} \mathcal{V}_{\mathtt{L}}^{p,\bar{p}} \otimes \bar{\mathcal{V}}_{\bar{\mathtt{L}}}^{p,\bar{p}} \quad (2.40)$$

while the total Hilbert space can be written as a direct sum

$$\mathcal{H} = \bigoplus_{p,\bar{p}} \mathcal{F}_{p,\bar{p}} = \bigoplus_{p,\bar{p}} \mathcal{V}_{p,\bar{p}} \ . \quad (2.41)$$

The Verma module construction appears to be the same as the Fock space one for the case at hand. However, in general, there are significant differences. For instance, while the Fock space will always be an irreducible representation of the Heisenberg algebra, the Verma module might become a reducible one for the Virasoro algebra. In particular, this is the case when the Verma module contains so-called nullstates. These are states in the $\mathtt{L}$-level-subspace with $\mathtt{L} > 0$ which are annihilated by all the positive Virasoro modes.

2.1.1 TOROIDIAL PARTITION FUNCTION OF THE PERIODIC BOSON

In the following, we consider the periodic boson. This means that instead of imposing that the first derivative of the field φ is spatially periodic, we require the stronger condition $\varphi(t, x + L) = \varphi(t, x)$. With regard to (2.16), this additional assumption enforces the equality $p = \bar{p}$ of the two chiral zero modes. Besides spatial periodicity, we also require the same property in the time direction, leading to the geometry of a torus [37]. Again, the mapping to the complex plane is useful to illustrate the effects of conformal invariance. Let us recall in general how a torus can be constructed from the complex plane: one way of defining a torus is to pick two complex numbers t_1, t_2 of different phases and identify

---

[6]Here, by the tensor product we mean the span of all possible combinations of the applications of barred and unbarred operators on the vacuum.

points which differ by an integer combination of these numbers. As our theory is invariant under conformal transformations — in particular, it does not depend on a length scale or an absolute orientation — our results should just depend on the ratio $\tau = t_2/t_1$. This fact is known as modular invariance, and τ is called the modular parameter.

Not only does the theory depend just on the modular parameter, but it must also be invariant under the so-called modular transformations. To explain this point, let t_1' and t_2' be two other complex numbers generating the same — up to some global scale transformation — torus as t_1 and t_2. It follows that we must have the relation

$$\begin{pmatrix} t_1' \\ t_2' \end{pmatrix} = \begin{pmatrix} a & b \\ c & d \end{pmatrix} \begin{pmatrix} t_1 \\ t_2 \end{pmatrix} \quad \text{with} \quad ad - bc = 1, \quad a, b, c, d \in \mathbb{Z}. \tag{2.42}$$

Under the above transformation, the modular parameter is changed according to

$$\tau \longrightarrow \frac{a\,\tau + b}{c\,\tau + d}. \tag{2.43}$$

All results must be invariant under (2.43).

Let us now define the partition function on the torus. Without loss of generality, we choose for the generating numbers of the latter $t_1 = L$ and $t_2 = \alpha + \mathrm{i}\beta$ with $\alpha, \beta \in \mathbb{R}$. Then, the partition function is defined as

$$\mathcal{Z} = \mathrm{Tr}_{\mathcal{H}} \left(e^{-\beta H + \mathrm{i}\alpha P} \right) = \mathrm{Tr}_{\mathcal{H}} \left(q^{L_0 - \frac{1}{24}} \bar{q}^{\bar{L}_0 - \frac{1}{24}} \right), \tag{2.44}$$

where, in the second step, we have used the expression of the Hamiltonian and the momentum operator in terms of the Virasoro modes (2.34), and we have introduced the quantities

$$\begin{aligned} q &= \exp\left(2\mathrm{i}\pi\tau\right), & \bar{q} &= \exp\left(-2\mathrm{i}\pi\bar{\tau}\right), \\ \tau &= (\alpha + \mathrm{i}\beta)/L, & \bar{\tau} &= (\alpha - \mathrm{i}\beta)/L. \end{aligned} \tag{2.45}$$

Note that τ is the modular parameter and that $\bar{q}$ is the complex conjugate of q.

The trace in (2.44) can be evaluated in any basis. We choose to describe the Hilbert space as a Verma module. This way, a direct computation shows that

$$\mathcal{Z} = \int_{-\infty}^{\infty} \mathrm{d}p\, 1 \sum_{\mathrm{L}, \bar{\mathrm{L}} = 1}^{\infty} \mathrm{par}(\mathrm{L})\mathrm{par}(\bar{\mathrm{L}})\, e^{\frac{\ln(q) + \ln(\bar{q})}{4} p^2} q^{\mathrm{L} - \frac{1}{24}} \bar{q}^{\bar{\mathrm{L}} - \frac{1}{24}}, \tag{2.46}$$

where the 1 was placed for further reference, and we integrate over all possible values of the zero mode momentum $p = \bar{p}$. Evaluation of the Gaussian integral gives

$$\begin{aligned} \mathcal{Z} &= \frac{\sqrt{4\pi}}{\sqrt{-\ln(q) - \ln(\bar{q})}} \sum_{\mathrm{L}, \bar{\mathrm{L}} = 1}^{\infty} \mathrm{par}(\mathrm{L})\mathrm{par}(\bar{\mathrm{L}}) q^{\mathrm{L} - \frac{1}{24}} \bar{q}^{\bar{\mathrm{L}} - \frac{1}{24}}, \\ &= \frac{\sqrt{4\pi}}{\sqrt{-\ln(q) - \ln(\bar{q})}} \frac{1}{\eta(q)\eta(\bar{q})}, \\ &= \frac{1}{\sqrt{\Im m(\tau)}} \frac{1}{|\eta(q)|^2}, \end{aligned} \tag{2.47}$$

where we have restricted to q being of modulus less than 1 to make use of the series expansion of the Dedekind η-function

$$(\eta(x))^{-1} = x^{-\frac{1}{24}} \sum_{n=0}^{\infty} \mathrm{par}(n)\, x^n \quad \text{for} \quad |x| < 1\,. \tag{2.48}$$

Using the transformation properties of the Dedekind η-function, one can show that the partition function (2.47) is modular invariant [37, 39].

The above calculation has been carried out in the operator formalism of QFT. An equivalent treatment is the path integral approach [40]. For the reader's convenience, we have presented the above calculation also in this equivalent methodology in appendix A.

2.1.2 COMPACTIFIED BOSON

In contrast to the previous section, where the target space of the field was $\mathbb{R}$, we can also consider the case of a circle of radius R instead. This means we identify field configurations if they differ by an integer multiple — the so-called winding number — of the circumference of the circle

$$\varphi(t,x) \sim \varphi(t,x) + 2\pi\vartheta R \quad \vartheta \in \mathbb{Z}\,. \tag{2.49}$$

Under this identification, the periodicity condition of the field does not imply the equality of the zero modes, as was pointed out for the non-compactified case. Rather, they obey

$$\sqrt{\frac{\pi}{2}}(p - \bar{p}) = 2\pi R\vartheta\,. \tag{2.50}$$

For notational clarity, we put in the following hats on operators while their eigenvalues are denoted without hats. In view of (2.19), the standard representation of the Heisenberg algebra with $\hat{\varphi}_0$ being the multiplication operator and $\hat{p} + \hat{\bar{p}}$ being the differential is suitable to compute the eigenvalues $p + \bar{p}$:

$$\hat{\varphi}_0 = \varphi_0\,, \qquad \sqrt{\frac{\pi}{2}}(\hat{p} + \hat{\bar{p}}) = -\mathrm{i}\frac{\partial}{\partial\varphi_0}\,. \tag{2.51}$$

As φ_0 is defined on a circle, we have that the plane waves $\exp\left[\frac{\mathrm{i}j\varphi_0}{R}\right]$ with $j \in \mathbb{Z}$ are a complete set of eigenfunctions of $\hat{p} + \hat{\bar{p}}$ and so we have

$$\sqrt{\frac{\pi}{2}}(p + \bar{p}) = \frac{n}{R}\,. \tag{2.52}$$

Combining this with (2.50) yields

$$\sqrt{2\pi}p = \frac{n}{R} + 2\pi R\vartheta\,, \qquad \sqrt{2\pi}\bar{p} = \frac{n}{R} - 2\pi R\vartheta\,. \tag{2.53}$$

In turn, the conformal weights of the vacuum are given by

$$\Delta_{n,\vartheta} = \frac{1}{8\pi}\left(\frac{n}{R} + 2\pi R\vartheta\right)^2\,, \qquad \bar{\Delta}_{n,\vartheta} = \frac{1}{8\pi}\left(\frac{n}{R} - 2\pi R\vartheta\right)^2\,, \tag{2.54}$$

while the partition function becomes

$$\mathcal{Z} = \mathrm{Tr}_0 \left(q^{L_0 - \frac{1}{24}} \bar{q}^{\bar{L}_0 - \frac{1}{24}} \right) = \sum_{n, \vartheta \in \mathbb{Z}} \frac{q^{\Delta_{n,\vartheta}} \bar{q}^{\bar{\Delta}_{n,\vartheta}}}{|\eta(\tau)|^2} . \tag{2.55}$$

The partition function is invariant under the modular transformations (2.43). In addition, the expression (2.55) exhibits the remarkable T-duality $R \mapsto (2\pi R)^{-1}$. In view of (2.54) this mapping interchanges n and ϑ. The latter leaves the partition function, which involves a sum over all integer values of n and ϑ, unchanged.

Like in the last section, we present the calculation of the above partition function in the path integral formalism in the second part of appendix A.

2.1.3 FREE BOSON ON THE STRIP

So far, we have considered CFT on the cylinder or the infinite plane. These two manifolds do not have any boundaries. In this section, we give some facts concerning the free massless boson with the worldsheet, instead of the cylinder, now being the infinite sheet $(t, x) \in (-\infty, \infty) \times [0, L]$. We stress that the points on the boundaries $x = 0$ and $x = L$ are not identified. The equations of motion and the additional constraint read as in (2.3). To satisfy the latter, Dirichlet or Neumann conditions can be imposed. Using the canonical momentum, we can write out all possible BCs and their constraints on the mode expansions in (2.16),(2.17) in the convenient form

(NN) $\partial_x \varphi(t, 0) = 0$ & $\partial_x \varphi(t, L) = 0$ $\implies$ $a_n - \bar{a}_n = 0 , \quad p - \bar{p} = 0 , \quad \mathbb{I} = \mathbb{Z}/\{0\}$
(ND) $\partial_x \varphi(t, 0) = 0$ & $\pi(t, L) = 0$ $\implies$ $a_n - \bar{a}_n = 0 , \quad p - \bar{p} = 0 , \quad \mathbb{I} = \mathbb{Z} + \frac{1}{2}$
(DN) $\pi(t, 0) = 0$ & $\partial_x \varphi(t, L) = 0$ $\implies$ $a_n + \bar{a}_n = 0 , \quad p + \bar{p} = 0 , \quad \mathbb{I} = \mathbb{Z} + \frac{1}{2}$
(DD) $\pi(t, 0) = 0$ & $\pi(t, L) = 0$ $\implies$ $a_n + \bar{a}_n = 0 , \quad p + \bar{p} = 0 , \quad \mathbb{I} = \mathbb{Z}/\{0\}$

The above imply the following restriction on the Virasoro modes[7]

$$L_n - \bar{L}_n = 0 \quad \implies \quad T(z) = \bar{T}(\bar{z}) . \tag{2.56}$$

Hence, the holomorphic and anti-holomorphic parts are no longer independent. The fact that the symmetry algebra is just one copy of the Virasoro algebra is general for any BCFT [36, 37]. The partition function then takes the form

$$\mathcal{Z} = \mathrm{Tr}(q^{L_0 - \frac{c}{24}}) . \tag{2.57}$$

Evaluating it[8] for the different BCs of the bosonic theory yields [36]

$$\mathcal{Z}^{(D,D)} = \mathrm{e}^{\frac{i\tau}{4\pi}(\varphi_0^L - \varphi_0^0)^2} \frac{1}{\eta(\tau)} , \tag{2.58}$$

$$\mathcal{Z}^{(\mathrm{MIX})} = \sqrt{\frac{\eta(\tau)}{\vartheta_4(\tau)}} , \tag{2.59}$$

$$\mathcal{Z}^{(N,N)} = \frac{1}{2\sqrt{-i\tau}} \frac{1}{\eta(\tau)} , \tag{2.60}$$

---

[7]Note that, we have $a_n = \pm\bar{a}_n$ and that the expressions (2.29) and (2.30) are quadratic in a_n and $\bar{a}_n$.
[8]These are cylinder partition functions. For more details on their derivation and physical meaning see e.g. [36].

where $\vartheta_4(\tau)$ is the Jacobi theta function. Also, for the case of Dirichlet-Dirichlet BCs, φ_0^j is the value of the fields at the boundary $j = 0, L$. The prefactor originates from the constraint

$$\sqrt{2\pi}p = \varphi_0^0 - \varphi_0^L . \tag{2.61}$$

2.2 THE 2D BLACK HOLE CFTS

The subjects of interest in this section are the so-called 2D Black Hole CFTs, which were introduced in string theory by Witten [10], see also [41]. The Euclidean Black Hole CFT appeared slightly earlier in the work of Elitzur *et al.* [42]. It attracted attention in the context of the AdS/CFT correspondence and was used as a setup for the development of methods of non-rational CFT [12]. We will not go into these interesting applications. Instead, we just briefly sketch its origin, elaborate on the name and then import the results necessary for our purposes from the literature.

A starting point to define the Black Hole CFTs is the Wess-Zumino-Witten (WZW) model [43, 44, 45] whose action functional takes the form

$$S_{\text{WZW}}[\mathbf{g}] = -\frac{k}{16\pi} \int \mathrm{d}t\,\mathrm{d}x\,\sqrt{-\eta}\,\eta^{\mu\nu}\mathrm{Tr}\left(\mathbf{g}^{-1}(\partial_\mu\mathbf{g})\,\mathbf{g}^{-1}\partial_\nu\mathbf{g}\right) - k\,W[\mathbf{g}] . \tag{2.62}$$

We focus on the case where the target space of the model is $\mathrm{SL}(2,\mathbb{R})$ and the worldsheet is taken to be the torus. Further, $\eta^{\mu\nu}$ denotes the Minkowski metric on the worldsheet, k is a coupling constant, and $W(\mathbf{g})$ is the so-called Wess-Zumino term. The latter is crucial to ensure conformal invariance [37]. It takes the form

$$W[\mathbf{g}] = \frac{1}{24\pi} \int_B \mathrm{d}^3 y\,\epsilon^{\mu\nu\lambda}\mathrm{Tr}\left(\mathbf{g}^{-1}(\partial_\mu\mathbf{g})\mathbf{g}^{-1}(\partial_\nu\mathbf{g})\mathbf{g}^{-1}\partial_\lambda\mathbf{g}\right) , \tag{2.63}$$

where $\epsilon^{\mu\nu\lambda}$ is the Levi-Civita tensor, and B is a three-dimensional manifold with the worldsheet as its boundary. In writing the above integral, we have implicitly extended the field $\mathbf{g}$ from the worldsheet to B. It turns out that the theory is not dependent on the particular extension of $\mathbf{g}$ nor the choice of B.

An important property of the above action is that it is invariant under the transformation

$$\mathbf{g}(t,x) \mapsto \mathbf{g}_L\,\mathbf{g}(t,x)\,\mathbf{g}_R . \tag{2.64}$$

where $\mathbf{g}_{L,R} \in \mathrm{SL}(2,\mathbb{R})$ are constant matrices. In other words, the model possesses a global $\mathrm{SL}(2,\mathbb{R}) \times \mathrm{SL}(2,\mathbb{R})$ symmetry. In the following, we want to gauge the theory with respect to a subgroup $\mathfrak{H} \in \mathrm{SL}(2,\mathbb{R}) \times \mathrm{SL}(2,\mathbb{R})$. This means [40], to introduce gauge fields $\mathbf{a}_L, \mathbf{a}_R$ such that the theory — now described by a modified action $S_{\text{WZW}}[\mathbf{g}, \mathbf{a}_L, \mathbf{a}_R]$ containing the gauge fields — is invariant under the infinitesimal transformations

$$\begin{aligned}
\mathbf{g} &\mapsto \mathbf{g} + \mathrm{i}(\mathbf{h}_L(t,x)\,\mathbf{g} + \mathbf{g}\,\mathbf{h}_R(t,x)) , \\
\mathbf{a}_{L,\mu} &\mapsto \mathbf{a}_{L,\mu} - \partial_\mu\mathbf{h}_L + [\mathbf{a}_{L,\mu}, \mathbf{h}_L] , \\
\mathbf{a}_{R,\mu} &\mapsto \mathbf{a}_{R,\mu} - \partial_\mu\mathbf{h}_R + [\mathbf{a}_{R,\mu}, \mathbf{h}_R] .
\end{aligned} \tag{2.65}$$

Here, $\mathbf{h}_L(t,x) \oplus \mathbf{h}_R(t,x)$ is an element of the Lie algebra of $\mathfrak{H}$ and is related to the group element via the exponential mapping $e^{i\mathbf{h}_L} \otimes e^{i\mathbf{h}_R} \in \mathfrak{H}$. We emphasise that $\mathbf{h}_{L,R}$ are allowed to vary with the worldsheet variables. Further, note that, as a consequence of this symmetry, two field configurations of $\mathbf{g}$ must be identified if they differ by a gauge transformation. Hence, the space of the physical degrees of freedom is reduced to fields taking values in $\mathrm{SL}(2,\mathbb{R})/\mathfrak{H}$.

The gauged action for a general WZW model for any group $\mathfrak{G}$ is known. By using the notation for the light cone indices $\pm$ introduced in section 2.1, it takes the form

$$S_{\mathrm{WZW}}[\mathbf{g}, \mathbf{a}_L, \mathbf{a}_R] = S_{\mathrm{WZW}}[\mathbf{g}] + \frac{k}{2i\pi} \int dt\, dx\, \mathrm{Tr}\left(\mathbf{a}_{R,-}\mathbf{g}^{-1}\partial_+\mathbf{g} + \mathbf{a}_{L,+}(\partial_-\mathbf{g})\mathbf{g}^{-1}\right)$$
$$+ \frac{k}{2\pi} \int dt\, dx\, \mathrm{Tr}\left(\mathbf{a}_{R,-}\mathbf{a}_{R,+} + \mathbf{g}\,\mathbf{a}_{R,-}\mathbf{g}^{-1}\right). \tag{2.66}$$

This action is invariant under (2.65) provided the gauge anomaly condition[9]

$$\mathrm{Tr}\left(\mathbf{h}_R, \partial_-\mathbf{a}_{R,+} - \partial_+\mathbf{a}_{R,-}\right) - \mathrm{Tr}\left(\mathbf{h}_L, \partial_-\mathbf{a}_{L,+} - \partial_+\mathbf{a}_{L,-}\right) = 0 \tag{2.67}$$

is satisfied [10].

Let us consider gauging the $U(1)$-subgroup of $\mathrm{SL}(2,\mathbb{R})$ corresponding to the transformation

$$\mathbf{g} \mapsto e^{\frac{i}{2}h(t,x)\sigma^y}\, \mathbf{g}\, e^{\frac{i}{2}h(t,x)\sigma^y} \approx \mathbf{g} + \frac{ih(t,x)}{2}\left(\sigma^y\mathbf{g} + \mathbf{g}\,\sigma^y\right), \tag{2.68}$$

$$\mathbf{a}_{R,\mu} = \mathbf{a}_{L,\mu} = \frac{1}{2}a_\mu\sigma^y \implies a_\mu \mapsto a_\mu - \partial_\mu h(t,x). \tag{2.69}$$

Clearly, the anomaly condition (2.67) is satisfied. For the explicit calculations, it is convenient to parametrise $\mathbf{g}$ in terms of the Euler angles

$$\mathbf{g}(\omega(t,x), \phi(t,x), \rho(t,x)) = e^{\frac{i}{2}(\omega+\phi)\sigma^y}e^{\rho\sigma^z}e^{\frac{i}{2}(\omega-\phi)\sigma^y}. \tag{2.70}$$

Note that the gauge transformation is then expressed as a shift in the field $\omega \mapsto \omega + h$. Using this parameterisation, the gauged action (2.66) can be brought to the form

$$\tilde{S}_{\mathrm{EBH}}[\phi, \rho, \omega, a_\pm] = \frac{k}{2\pi} \int dt dx\, \sinh^2(\rho)\Big(\partial_+\phi\partial_-\phi + \partial_-\phi(\partial_+\omega + a_+) - \partial_+\phi(\partial_-\omega + a_-)\Big)$$
$$+ \partial_+\rho\partial_-\rho - \cosh^2(\rho)(\partial_+\omega + a_+)(\partial_-\omega + a_-). \tag{2.71}$$

The gauge fields can be eliminated by inserting their equations of motion/integrating them out; see for details [10]. In this way, the action is reduced to

$$S_{\mathrm{EBH}}[\phi, \rho] = \frac{k}{2\pi} \int dx\, dt\, \partial_-\rho\partial_+\rho + \tanh^2(\rho)\partial_+\phi\partial_-\phi. \tag{2.72}$$

---

[9]The anomaly-free condition can be formulated purely in terms of the Lie algebra of the to-be gauged subgroup. Namely, $\mathrm{Tr}(h_L^1, h_L^2) - \mathrm{Tr}(h_R^1, h_R^2) = 0$ for any two elements $h^{1,2} = h_L^{1,2} \oplus h_R^{1,2}$ of the Lie algebra of the subgroup $\mathfrak{H}$. Recall that the gauge field is generally valued in the Lie algebra so that (2.67) follows from the above condition. Furthermore, it turns out [46] that it is impossible to gauge a WZW model by a subgroup $\mathfrak{H}$ if the anomaly condition is not satisfied by its Lie algebra.
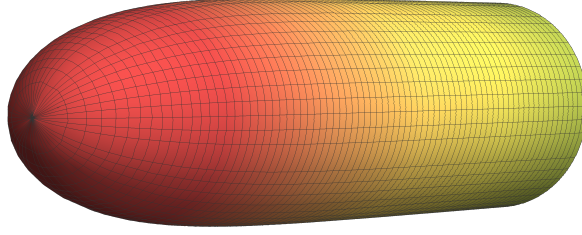
Figure 2.1: Displayed is an embedding of the manifold with the metric (2.75) in $\mathbb{R}^3$. The realisation is given as $z = \log\left(\frac{\sqrt{2-x^2-y^2}+1}{\sqrt{1-x^2-y^2}}\right) - \sqrt{2-x^2-y^2}$. Due to the shape of the embedded manifold, the theory was coined the cigar CFT or simply the cigar.

It can be further simplified via the following coordinates

$$U = \sinh(\rho)\mathrm{e}^{\mathrm{i}\phi}, \qquad \bar{U} = \sinh(\rho)\mathrm{e}^{-\mathrm{i}\phi} \tag{2.73}$$

in which it finally takes the convenient form

$$S_{\mathrm{EBH}}[U,\bar{U}] = \frac{k}{8\pi}\int \mathrm{d}x\,\mathrm{d}t\,\frac{\partial_\mu U \partial^\mu \bar{U}}{1+|U|^2}\,. \tag{2.74}$$

The obtained action can be interpreted as governing a field moving on a manifold with the metric

$$\mathrm{d}s^2_{\mathrm{EBH}} = \frac{\mathrm{d}U\mathrm{d}\bar{U}}{1+|U|^2}\,. \tag{2.75}$$

Let us examine this result with regards to the geometry of the target space $\mathrm{SL}(2,\mathbb{R})/U(1)$. The above metric is invariant under rotations $U \mapsto U\mathrm{e}^{\mathrm{i}\alpha}$. Moreover, one can see that the curvature takes its maximum value at the point where $|U| = 0$. In contrast, in the regime where $|U| \gg 1$, the metric becomes nearly flat as then the denominator can be approximated in the following way

$$\mathrm{d}s^2_{\mathrm{EBH}} \approx \frac{\mathrm{d}U\mathrm{d}\bar{U}}{|U|^2} = \mathrm{d}\rho^2 + \mathrm{d}\phi^2\,. \tag{2.76}$$

In the second step, we have made the coordinate transformation $U = \mathrm{e}^{\rho+\mathrm{i}\phi}$. Hence, in this chart, we obtain the flat metric of a cylinder. From these three facts, it is clear that one may visualize the target space as a half-infinite cigar. For the reader's convenience, an embedding of the target space as a surface in the higher dimensional space $\mathbb{R}^3$ has been displayed in Figure 2.1.

In the above, we have gauged a compact $U(1)$ subgroup. However, there exists also a non-compact abelian subgroup of $\mathrm{SL}(2,\mathbb{R})$ corresponding to the transformation

$$\mathbf{g} \mapsto \mathrm{e}^{h(t,x)\sigma^z}\,\mathbf{g}\,\mathrm{e}^{h(t,x)\sigma^z} \approx \mathbf{g} + h(t,x)\left(\sigma^z\,\mathbf{g} + \mathbf{g}\,\sigma^z\right)\,, \tag{2.77}$$

$$\mathbf{a}_{R,\mu} = \mathbf{a}_{L,\mu} = \frac{\mathrm{i}}{2}a_\mu\sigma^z \implies a_\mu \mapsto a_\mu + \partial_\mu h(t,x)\,. \tag{2.78}$$

Performing similar steps, one arrives at the action

$$S_{\text{LBH}} = \frac{k}{8\pi} \int \mathrm{d}x\,\mathrm{d}t\,\frac{\partial_\mu U \partial^\mu V}{1 - UV}\,,\tag{2.79}$$

where U and V are real fields. The metric is given by

$$\mathrm{d}s^2_{\text{LBH}} = \frac{\mathrm{d}U\mathrm{d}V}{1 - UV}\,.\tag{2.80}$$

The name Black Hole CFT was given to the theory (2.79) as the target space geometry — see Figure 2.2 — resembles the usual Schwarzschild one in Kruskal coordinates, one can see the curvature singularity at $UV = 1$. Further, the coordinate axes where $U = 0$ or $V = 0$ mark the event horizon. Instead of a globally defined time coordinate, the Killing vector $U\partial_U - V\partial_V$ is timelike in regions I and II while it is spacelike in regions III and IV.

Note that — neglecting an overall minus sign — the metric (2.80) becomes the previous one (2.75) under a Wick rotation in the *target-space*[10]. Due to this fact, the latter is also called the 2D *Euclidean* Black Hole CFT while (2.80) is known as the 2D *Lorentzian* Black Hole. This explains the choice of the subscripts EBH and LBH in (2.74) and (2.79).

The quantum versions of the above theories are, of course, of great interest. However, the quantization of the Lorentzian Black Hole faces the usual problem of unboundedness due to the Lorentzian signature of the target space. In contrast, the quantum Euclidean Black Hole was widely studied. It reveals itself as a unitary CFT with central charge

$$c = 2 + \frac{6}{k - 2}\,.\tag{2.81}$$

The spectrum of conformal dimensions splits into two parts [47]. The first is a continuous family of weights given by

$$\begin{aligned}\Delta &= \frac{p^2}{k} - \frac{J(J-1)}{k-2}\,,\\ \bar{\Delta} &= \frac{\bar{p}^2}{k} - \frac{J(J-1)}{k-2}\end{aligned} \quad \text{with} \quad \begin{aligned}p &= \frac{(m+kw)}{2}\\ \bar{p} &= \frac{(m-kw)}{2}\end{aligned} \quad \text{and} \quad \begin{aligned}J &= \frac{1}{2} + \mathrm{i}s\,,\\ s &\in \mathbb{R}_0^+\end{aligned}\tag{2.82}$$

where the integers $m \in \mathbb{Z}$ and $w \in \mathbb{Z}$ label the momentum and winding in the compact direction of the semi-infinite cigar-shaped target space of the CFT for large $|U|$. The quantity $\mathrm{i}s = J - 1/2$ is the conserved ingoing momentum along the uncompactified direction. Besides the continuous spectrum, there is another family, the discrete states, where the conformal dimensions are given by (2.82) but J takes a set of discretized values [48, 49]

$$J \in \left[\frac{1-k}{2}, -\frac{1}{2}\right) \cap \left(\mathbb{N} - \frac{1}{2}|kw| + \frac{1}{2}|m|\right)\,.\tag{2.83}$$

These correspond to bound states localized near the tip of the cigar-shaped target space of the model [50, 49, 48]. The restriction (2.83) can be seen as a condition that the states are normalizable.

---

[10]We extend U, V to be complex-valued and set $\bar{U} = -V$. This makes the time coordinate in region I to be purely imaginary.
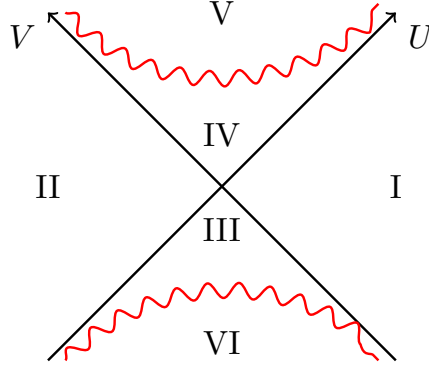
Figure 2.2: Displayed is the space-time diagram of the metric (2.80). The event horizon, where $U = 0$ or $V = 0$, coincides with the coordinate axes. The wiggled curve displays the curvature singularity, where $UV = 1$.

The calculation of the partition function of the Euclidean Black Hole via the path integral formalism starting from (2.71) has been carried out in [49, 51]. The evaluation boils down to a computation of the Ray-Singer Torsion [52]. The latter involves a regularisation procedure similar to the case of the free boson on the line that we present in appendix A. As this matter is somewhat technical and long, we do not reproduce it here.

The partition function obtained from the path integral approach enables one to make conjectures about the density of states, i.e. the measure over which the continuous spectrum must be integrated, e.g. see (2.46) for the non-compact free boson, where the integration measure was trivial, i.e. $\equiv 1$. For the continuous component of the Black Hole CFT, it was conjectured in the works [49, 51] to be given by

$$\rho_{\mathrm{EBH}}^{(\bar{\mathrm{L}},\mathrm{L})}(s \,|\, \bar{p}, p) = \mathrm{par}_2(\mathrm{L}) \, \mathrm{par}_2(\bar{\mathrm{L}}) \, \rho^{(0)}(s \,|\, p, \bar{p}) \,,$$

$$\rho^{(0)}(s) = \frac{1}{\pi} \log(\Lambda) + \frac{1}{4\mathrm{i}\pi} \frac{\mathrm{d}}{\mathrm{d}s} \log \left(\frac{\Gamma\left(\frac{1}{2} + p - \mathrm{i}s\right) \Gamma\left(\frac{1}{2} + \bar{p} - \mathrm{i}s\right)}{\Gamma\left(\frac{1}{2} + p + \mathrm{i}s\right) \Gamma\left(\frac{1}{2} + \bar{p} + \mathrm{i}s\right)} \right) \,. \tag{2.84}$$

Here Λ plays the role of a regularising cut-off, and $\mathrm{par}_2(\mathrm{L})$ is the number of bipartitions of the integer L (see (4.96)).

In a series of recent works [20, 24, 53, 54, 55], in particular [25], new results for the 2D Euclidean Black Hole sigma model were obtained via a detailed study of an integrable lattice system. It led, among other things, to a corrected formula for the density of states for the continuous part of the spectrum. Explicitly one has

$$\rho_{\mathrm{EBH}}^{(\bar{\mathrm{L}},\mathrm{L})}(s \,|\, \bar{p}, p) = \frac{2}{\pi} \, \mathrm{par}_2(\mathrm{L}) \, \mathrm{par}_2(\bar{\mathrm{L}}) \log(\Lambda) + \frac{1}{2\pi\mathrm{i}} \frac{\mathrm{d}}{\mathrm{d}s} \log \left[\left(\mathfrak{D}_{\bar{p}}^{(\bar{\mathrm{L}})}(s)\right)^{\mathrm{par}_2(\mathrm{L})} \left(\mathfrak{D}_p^{(\mathrm{L})}(s)\right)^{\mathrm{par}_2(\bar{\mathrm{L}})} \right] \tag{2.85}$$

where

$$\mathfrak{D}_p^{(\mathrm{L})}(s) = \left(\frac{\Gamma(\frac{1}{2} + p - \mathrm{i}s)}{\Gamma(\frac{1}{2} + p + \mathrm{i}s)} \right)^{\mathrm{par}_2(\mathrm{L})} \prod_{a=0}^{\mathrm{L}-1} \left[\frac{\left(\frac{1}{2} + a + p - \mathrm{i}s\right) \left(\frac{1}{2} + a - p - \mathrm{i}s\right)}{\left(\frac{1}{2} + a + p + \mathrm{i}s\right) \left(\frac{1}{2} + a - p + \mathrm{i}s\right)} \right]^{\mathrm{par}_2(\mathrm{L}) - d_a(\mathrm{L})} \tag{2.86}$$

and the integers $\mathtt{d}_a(\mathtt{L})$ are defined by the series expansion of the following generating function

$$\left(\prod_{m=1}^{\infty} \frac{1}{(1 - \mathtt{q}^m)^2} \right) \sum_{m=0}^{\infty} (-1)^m \, \mathtt{q}^{\frac{1}{2}m \, (m+2a+1)} = \sum_{\mathtt{L}=0}^{\infty} d_a(\mathtt{L}) \, \mathtt{q}^{\mathtt{L}} \, . \tag{2.87}$$

Notice that for the case $\mathtt{L} = \bar{\mathtt{L}} = 0$, this density of states coincides with eq. (2.84).

2.3 FINITE-SIZE SCALING

Since the pioneering work of Polyakov [56], it has been widely accepted that the scaling behaviour of a critical isotropic and homogeneous statistical system can be effectively described in the framework of CFT. While a general proof is lacking, there is extensive supporting evidence [57, 58, 59], much of which arises from examining two-dimensional classical statistical models. In numerous instances, these models can be rephrased as one-dimensional quantum spin chains. Consequently, identifying the underlying CFT can be pursued by investigating the scaling limit of the spin chain Hamiltonian. In the following, we will elaborate on this point borrowing from the discussion in [60, 61].

Consider the two-point function of a primary field ϕ subject to periodic BCs in space. In the path integral formalism, it would be given by

$$\langle \phi(z_1, \bar{z}_1)\phi(z_2, \bar{z}_2) \rangle = \frac{1}{\mathcal{Z}} \int \mathcal{D}\phi \; \phi(z_1, \bar{z}_1)\phi(z_2, \bar{z}_2) \exp\left[-S[\phi]\right] . \tag{2.88}$$

Conformal invariance dictates the form of the two-point function and its transformation behaviour under conformal mappings [37]. On the complex plane $z \in \mathbb{C}$ we have that

$$\langle \phi(z_1, \bar{z}_1)\phi(z_2, \bar{z}_2) \rangle = (z_1 - z_2)^{-2\Delta} \left(\bar{z}_1 - \bar{z}_2\right)^{-2\bar{\Delta}} . \tag{2.89}$$

Further, under a conformal mapping $z, \bar{z} \mapsto w(z), \bar{w}(\bar{z})$ the following identity holds true

$$\langle \phi(w_1, \bar{w}_1)\phi(w_2, \bar{w}_2) \rangle = \left[\left.\frac{\partial w}{\partial z}\right|_{z_1} \left.\frac{\partial w}{\partial z}\right|_{z_2}\right]^{-\Delta} \left[\left.\frac{\partial \bar{w}}{\partial \bar{z}}\right|_{\bar{z}_1} \left.\frac{\partial \bar{w}}{\partial \bar{z}}\right|_{\bar{z}_2}\right]^{-\bar{\Delta}} \langle \phi\left(z_1, \bar{z}_1\right) \phi\left(z_2, \bar{z}_2\right) \rangle . \tag{2.90}$$

Let us now evaluate the right hand side (RHS) with z substituted for w according to $w = \frac{2\pi}{L} \log(z)$ (analogously for $\bar{w}$ and $\bar{z}$). One obtains

$$\begin{aligned}
\langle \phi\left(w_1, \bar{w}_1\right) \phi\left(w_2, \bar{w}_2\right) \rangle &= \left(\frac{2\pi}{L}\right)^{2(\Delta + \bar{\Delta})} \left(\frac{z_1^{1/2} z_2^{1/2}}{z_1 - z_2}\right)^{2\Delta} \left(\frac{\bar{z}_1^{1/2} \bar{z}_2^{1/2}}{\bar{z}_1 - \bar{z}_2}\right)^{2\bar{\Delta}} \\
&= \left(\frac{\pi}{L \sinh\left(\frac{\pi}{L}(w_1 - w_2)\right)}\right)^{2\Delta} \left(\frac{\pi}{L \sinh\left(\frac{\pi}{L}(\bar{w}_1 - \bar{w}_2)\right)}\right)^{2\Delta} \\
&\approx \left(\frac{2\pi v_{\mathrm{F}}}{L}\right)^{2(\Delta + \bar{\Delta})} \sum_{\mathrm{L}, \bar{\mathrm{L}}=1}^{\infty} \left(c_{\mathrm{L}, \bar{\mathrm{L}}} \, e^{-\frac{2\pi v_{\mathrm{F}}}{L}(\Delta + \bar{\Delta} + \mathrm{L} + \bar{\mathrm{L}})(t_1 - t_2)} \right. \\
&\qquad \left. \times \, e^{-\frac{2\pi \mathrm{i}}{L}(\Delta - \bar{\Delta} + \mathrm{L} - \bar{\mathrm{L}})(x_1 - x_2)}\right) ,
\end{aligned} \tag{2.91}$$

where in the last step we have splitted w into its real and imaginary parts, $w = v_{\mathrm{F}}\, t + \mathrm{i}x$, and expanded the resulting expression for large $|v_{\mathrm{F}}\left(t_1 - t_2\right)| \gg L$. Here $c_{\mathrm{L}, \bar{\mathrm{L}}}$ are some coefficients which are easily calculable and we restored the constant v_{F}, the velocity of light, relating time and space.

Let us assume that the CFT governs the universal behaviour of a critical lattice model. In the transfer matrix approach — where the field ϕ appears in the scaling limit of a

regularised lattice version ϕ^{reg} — one can express the two-point function as the ground state expectation value

$$\langle 0|\phi^{\text{reg}}(t_1, x_1)\,\phi^{\text{reg}}(t_2, x_2)\,|0\rangle = \sum_n \langle 0|\phi^{\text{reg}}(t_1, x_1)|n\rangle\langle n|\phi^{\text{reg}}(t_2, x_2)|0\rangle$$

$$= \sum_n |\langle n|\phi^{\text{reg}}(0,0)|0\rangle|^2 \mathrm{e}^{-(E_n - E_0)(t_1 - t_2)}\mathrm{e}^{-\mathrm{i}P_n(x_1 - x_2)}\,. \quad (2.92)$$

In the first step, we have inserted a complete set of eigenstates of H and P with eigenvalues E_n and P_n, respectively, while the second line follows since the Hamiltonian and momentum operators generate translations in time and space. A comparison with (2.91) suggests the relations between the conformal weights and the finite-size corrections of the low-lying energy states of the lattice regularisation:

$$E_n(L) - E_0(L) \asymp \frac{2\pi v_{\text{F}}}{L}(\Delta + \bar{\Delta} + \mathtt{L} + \bar{\mathtt{L}})\,, \quad (2.93)$$

$$P_n(L) - P_0(L) \asymp \frac{2\pi}{L}\left(\Delta - \bar{\Delta} + \mathtt{L} - \bar{\mathtt{L}}\right) + 2Dk_F\,. \quad (2.94)$$

In the above, we have accounted for the possibility [62] of a macroscopic momentum $2Dk_F$ of the state $\phi|0\rangle$ measured in units of the Fermi momentum k_F.

The ground state energy of a 1+1 dimensional critical spin chain should behave as [61, 63]

$$E_0(L) \asymp Le_\infty - \frac{\pi v_{\text{F}}}{6L}c\,, \quad (2.95)$$

where e_∞ is the energy density in the thermodynamic limit. Combining this with (2.93), we obtain the formula

$$E(L) \asymp Le_\infty + \frac{2\pi v_{\text{F}}}{L}X_{\text{eff}}\,, \qquad X_{\text{eff}} = -\frac{c}{12} + \Delta + \bar{\Delta} + \mathtt{L} + \bar{\mathtt{L}}\,. \quad (2.96)$$

The above results can be generalized to open BCs [59]. They read

$$E(L) \asymp Le_\infty + f_\infty + \frac{\pi v_{\text{F}}}{L}X_{\text{eff}}\,, \qquad X_{\text{eff}} = -\frac{c}{24} + \Delta + \mathtt{d}\,, \quad (2.97)$$

where $\mathtt{d} = 0, 1, 2, \ldots$ denotes the level of the descendent[11] and f_∞ is the surface energy density.

Formulae like (2.96) or (2.97) are of great practical importance. They allow one to study the spectrum of scaling dimensions of the CFT underlying the critical behaviour of a lattice system by considering the energy of the low-lying energy states at large L. However, it should be stressed that the central charge and the conformal weights enter as a sum. As such, one cannot read them off separately from the lattice data but only their combination. Let us discuss this matter in the context of the continuous family of conformal primaries in the Euclidean Black Hole CFT with periodic BCs. By inserting (2.81) and (2.82) in (2.96), we obtain for the effective scaling dimensions

$$X_{\text{eff}}^{\text{EBH}} = -\frac{2}{12} + \frac{p^2}{k} + \frac{\bar{p}^2}{k} + \frac{2s^2}{k - 2}\,, \quad (2.98)$$

---

[11]Recall, that we have for the open case $L_n = \bar{L}_n$. We denote the level instead of as $\mathtt{L}$ as $\mathtt{d}$.

where we have expressed J in terms of s. This looks like $\Delta + \bar{\Delta} - \frac{c}{12}$ for two non interacting massless bosons. Indeed, the second and third terms $p^2/k, \bar{p}^2/k$ resemble the chiral zero mode momenta of a compact boson with compactification radius $R = \sqrt{\frac{k}{2\pi}}$ (see (2.54)). The fourth term can be identified — up to a multiplicative factor — with the zero mode momentum of a periodic non-compact boson (see (2.30), the discussion after section 2.1.1 and after (2.18)). The first term would correspond to $c = 1 + 1$, one for each boson. Hence, we conclude the following: the additive constant from $J = 1/2 + \mathrm{i}s$ combines with the central charge term in a way that the effective scaling dimensions of the conformal primaries will mimic the ones of a CFT consisting of two bosonic (compact and non-compact) fields. Thus, to identify the Black Hole CFT as the effective field theory describing the low energy regime of a given lattice model, it is necessary to show the existence of the discrete states (2.83) and to determine the non-trivial density of states (2.84), which distinguish the Black Hole CFT from the free field theory.

Ignoring the fact that we have not yet defined any conformal invariant BCs for the Euclidean Black Hole CFT, the application of formula (2.97) for the open case yields

$$X_{\text{eff}}^{\text{EBH}} = -\frac{1}{12} + \frac{p^2}{k} + \frac{s^2}{k-2} \, . \tag{2.99}$$

2.4 Yang-Baxter integrable models

The first part of this chapter is based on the author's publication [32].

The basic element for the systematic construction of an integrable lattice model is the R-matrix. Written as $R_{a,b}(u)$ the R-matrix depends on the so-called spectral parameter $u \in \mathbb{C}$ and acts as an endomorphism on the tensor product $\mathscr{V}_a \otimes \mathscr{V}_b$ of some vector spaces $\mathscr{V}_a$ and $\mathscr{V}_b$. The explicit form of the vector spaces defines the physical properties of the lattice model, but their specification is not strictly necessary in order to formulate the abstract notion of integrability. In the rest of the manuscript, we use the following convention unless stated otherwise. Given $R_{a,b}(u)$, we extend it to the larger spaces such as $\mathscr{V}_a \otimes \mathscr{V}_b \otimes \mathscr{V}_c$ by demanding its action on $\mathscr{V}_c$ to be the identity. We do the same for any other lattice operator as well. Using this convention, the defining relation of the R-matrix can be stated as

$$R_{a,b}(u-v)\,R_{a,c}(u)\,R_{b,c}(v) \,=\, R_{b,c}(v)\,R_{a,c}(u)\,R_{a,b}(u-v)\,. \tag{2.100}$$

The equation (2.100) is called the Yang-Baxter equation (YBE) after their two inventors C. N. Yang [64, 65] and R. J. Baxter [66] (see also [67]). By depicting the matrix element[12] $R_{\alpha\beta}^{\gamma\delta}(u)$ of the R-matrix as in the left panel of Figure 2.3, the YBE can be illustrated as on the right side of Figure 2.3, where a summation over the indices associated with the internal lines is being assumed.

Often [68], the R-matrix has additional properties such as the so-called regularity, i.e. it becomes proportional to the permutation operator P when evaluated at zero

$$R_{a,b}(0) \propto P_{a,b}\,. \tag{2.101}$$

From this and the YBE, it follows that the R-matrix obeys[13]

$$R_{a,b}(u)R_{b,a}(-u) = \xi(u)\xi(-u)\mathbf{1}\,, \tag{2.102}$$

where $\xi(u)$ is a scalar function, which we assume to be regular at $u = 0$. The above relation is called unitarity. An inspection of (2.101), keeping in mind (2.102), suggests that the proportionality constant therein can be arranged to be $\xi(0)$. We will assume this to be true in the following.

Several other properties are common, such as the so-called PT-symmetry

$$R_{i,j}^{t_i t_j}(u) = R_{j,i}(u)\,, \tag{2.103}$$

where we denote by the superscripts t_j the transpose in the space j. Further, we will assume that we have an invertible matrix V and the so-called crossing parameter $\eta \in \mathbb{C}$ such that

$$R_{i,j}(u) = V_i R_{i,j}^{t_j}(-u-\eta)V_i^{-1}. \tag{2.104}$$

---

[12]Here, we use the index pair $|_\alpha^\gamma$ for the first space, and $|_\beta^\delta$ for the second space.

[13]To be precise, it just follows that $R_{a,b}(u)R_{b,a}(-u) \propto \mathbf{1}$. For simplicity, we assume that the proportionality function factorises in this convenient manner, as this is the case for all explicit R-matrices in this thesis.
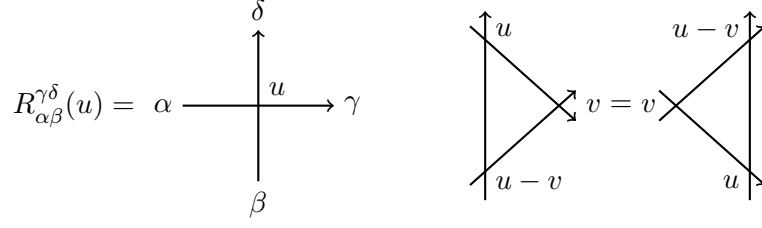
Figure 2.3: The left hand side (LHS) shows the R-matrix in graphical notation. The right panel illustrates the Yang-Baxter equation, where we have suppressed the free indices and summation over indices of connected lines is implicit.

It will be convenient to combine unitarity and the crossing symmetry into the so-called crossing unitarity:

$$R_{i,j}^{t_i}(u)M_i R_{i,j}^{t_j}(-u-2\eta)M_i^{-1} = \xi(u+\eta)\xi(-u-\eta)\,\mathbf{1}\,, \tag{2.105}$$

where $M = V^t V$. Besides the above properties, some [68, 69] R-matrices are also quasi-periodic in their spectral parameter. That means, there exist a non-zero constant $\mathsf{p} \in \mathbb{C}$ and an invertible matrix U such that

$$R_{a,b}(u+\mathsf{p}) = \pm U_a R_{a,b}(u)U_a^{-1}\,, \tag{2.106}$$

where the sign depends on the specific model. In fact, one can show that U is either a symmetric or antisymmetric matrix. Furthermore, one has $U^{-1} \propto V^{-1}UV$. We depict U as in Figure 2.4.

Given a solution of the YBE, we define the Yang-Baxter algebra for the so-called monodromy matrix T_a

$$R_{a,b}(u-v)T_a(u)T_b(v) = T_b(v)T_a(u)R_{a,b}(u-v)\,, \tag{2.107a}$$

$$T_a(u)R_{a,b}(u+v)T_b^{-1}(-v) = T_b^{-1}(-v)R_{a,b}(u+v)T_a(u)\,, \tag{2.107b}$$

$$R_{a,b}(u-v)T_a^{-1}(u)T_b^{-1}(v) = T_b^{-1}(v)T_a^{-1}(u)R_{a,b}(u-v)\,. \tag{2.107c}$$

where T_a acts on $\mathscr{V}_a \otimes \mathscr{H}$. Here, $\mathscr{H}$ denotes the Hilbert space of the quantum system while $\mathscr{V}_a$ is called the auxiliary space. By tracing out the auxiliary space, we obtain a family of commuting operators [70]. The generating function is called the transfer matrix $\mathfrak{t}(u)$ of the integrable system

$$\mathfrak{t}(u) = \mathrm{Tr}_a\left(T_a(u)\right)\,, \qquad [\mathfrak{t}(u), \mathfrak{t}(v)] = 0\,. \tag{2.108}$$

Assuming that the matrix elements of $\mathfrak{t}(u)$ are analytical in some domain of the complex u-plane, including the origin, one can expand the commutator above in a power series in u and v. This makes the family of commuting operators explicit

$$\mathfrak{t}(u) = \mathbb{I}_0 + u\,\mathbb{I}_1 + u^2\,\mathbb{I}_2 + \ldots\,, \qquad [\,\mathbb{I}_k\,,\,\mathbb{I}_j\,] = 0\,. \tag{2.109}$$

It is important to mention that a solution of (2.100) automatically generates one of (2.107a) with $\mathscr{H} = \mathscr{V}_c$ by taking $T_a(u) = R_{a,c}(u+\delta_c)$ where $\delta_c \in \mathbb{C}$ is an arbitrary parameter

$$U_\alpha^\beta = \alpha \longrightarrow\!\!\bullet\!\!\longrightarrow \beta \quad (U^{-1})_\alpha^\beta = \alpha \longrightarrow\!\!\ominus\!\!\longrightarrow \beta$$

$$\varpi_\alpha^\beta = \alpha \longrightarrow\!\!\blacktriangle\!\!\longrightarrow \beta \quad (\varpi^{-1})_\alpha^\beta = \alpha \longrightarrow\!\!\triangle\!\!\longrightarrow \beta$$

Figure 2.4: The figure illustrates the matrices U and ϖ in graphical notation.

which is called the inhomogeneity. Further, equation (2.107a) possesses the comultiplication property, i.e. solutions of the RTT-relation can be combined together to form another solution with an enlarged Hilbert space. Hence, a R-matrix naturally leads to the transfer matrix

$$\mathbb{t}(u) = \text{Tr}_a \left(R_{a,L}(u + \delta_L) R_{a,L-1}(u + \delta_{L-1}) \dots R_{a,1}(u + \delta_1) \right) \tag{2.110}$$

of an integrable system with Hilbert space $\mathscr{H} = \mathscr{V}_L \otimes \dots \otimes \mathscr{V}_1$.

To define a quantum mechanical system, the space of states is not enough. The dynamics are encoded in a Hamiltonian. In principle, any choice of the operators $\mathbb{I}_j$ for the Hamiltonian is possible if we disregard the question of its meaning or utility in describing physical phenomena. In this thesis, $\mathbb{I}_0$ corresponds to either the translation or the identity operator, while $\mathbb{I}_1$ will be taken as the Hamiltonian. For example we have, provided the inhomogeneities $\{\delta_m\}_{m=1}^L$ are all set to zero,

$$\mathbb{H} \propto \sum_{i=1}^L P_{i,i+1} R'_{i,i+1}(0) \,, \tag{2.111}$$

where the prime denotes the derivative with respect to the spectral parameter, and we identify the $(L+1)^{\text{th}}$ space with the first one.

The transfer matrix in (2.108) can only generate systems with periodic BCs as is evidenced in formula (2.111). The case of twisted or open BCs is incorporated in the following way. Starting with the former, we need additional symmetry properties of the R-matrix. Namely, if we find a scalar-valued solution ϖ_a of (2.107a) i.e.

$$\left[\varpi_a \varpi_b, R_{a,b}(u) \right] = 0 \,, \tag{2.112}$$

then we can construct an integrable model with twisted BCs controlled by ϖ by inserting it in the transfer matrix as

$$\mathbb{t}(u) = \text{Tr}_a \left(\varpi_a R_{a,L}(u + \delta_L) R_{a,L-1}(u + \delta_{L-1}) \dots R_{a,1}(u + \delta_1) \right) \,. \tag{2.113}$$

Any operator $\mathcal{O}$ acting on the lattice site $(L + j)$ would be identified as acting on the jth space up to an additional conjugated action of ϖ

$$\mathcal{O}_{L+j} = \varpi_j \mathcal{O}_j \varpi_j^{-1} \,. \tag{2.114}$$

When it comes to open or free BCs, the property (2.112) is not enough. It turns out that one has to introduce reflection algebras [71, 72, 73]. The right reflection algebra $\mathscr{F}_R$ is built from solutions K^R of the following equation

$$R_{a,b}(u - v) \, K_a^R(u) \, R_{b,a}(u + v) \, K_b^R(v) = K_b^R(v) \, R_{a,b}(u + v) \, K_a^R(u) \, R_{b,a}(u - v) \,, \tag{2.115}$$
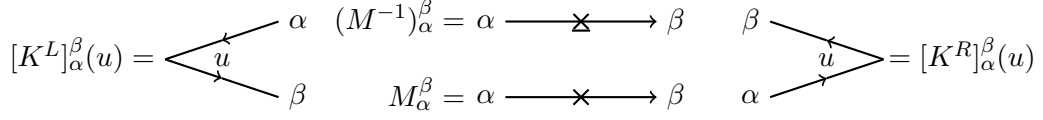
Figure 2.5: The figure illustrates the K- and M-matrices in graphical notation.

while the defining relation of the left analogue, $\mathscr{F}_L$, can be stated as

$$
\begin{aligned}
R_{a,b}(-u+v) & K_a^{L,t_a}(u) M_a^{-1} R_{a,b}(-u-v-2\eta) M_a K_b^{L,t_b}(v) \\
&= K_b^{L,t_b}(v) M_a R_{a,b}(-u-v-2\eta) M_a^{-1} K_a^{L,t_a}(u) R_{b,a}(-u+v) \, .
\end{aligned}
\tag{2.116}
$$

Similar to the periodic case, the K-matrices and the reflection algebras can be depicted graphically, as done in Figures 2.5 and 2.6.

Note that the two algebras are isomorphic. Given an element K^R of the right reflection algebra, one obtains a solution of equation (2.116) by the mapping

$$
K^R(u) \mapsto K^{R,t}(-u-\eta) \in \mathscr{F}_L \, .
\tag{2.117}
$$

We will require the K-matrices to have some additional properties. We will discuss just the imposed assumptions for the right K-matrix as the ones for the left directly follow by the above isomorphism. The first relation we want to impose is the K-analogue of unitarity:

$$
K^R(u) K^R(-u) \propto \mathbf{1} \, ,
\tag{2.118}
$$

which can be shown to hold for a large number of K-matrices, see [72, 73, 74, 75] and references therein. If the R-matrix is quasi-periodic (2.106), we further assume the compatibility condition

$$
K^R(u+\mathsf{p}) \propto U K^R(u) U \, .
\tag{2.119}
$$

Finally, it is natural, especially with regard to *local* Hamiltonian to assume that $K^R(u)$ is meromorphic in u, and obeys

$$
K^R(0) \propto \mathbf{1} \, , \quad K^R\left(\frac{\mathsf{p}}{2}\right) \propto U \, .
\tag{2.120}
$$

Having at hand solutions K^R, K^L, and a solution of the RTT-relation, we can again construct commuting transfer matrices

$$
\mathtt{t}(u) = \mathrm{Tr}_a \left(K_a^L(u) \, T_a(u) \, K_0^R(u) \, T_a^{-1}(-u) \right) \, .
\tag{2.121}
$$

Taking $T(u)$ as the L-fold coproduct of R-matrices, we can resolve the inverse in (2.121) by using the unitarity (2.102) of the R-matrix. We obtain

$$
\begin{aligned}
\mathtt{t}(u) = \mathrm{Tr}_a \big(& K_a^L(u) \, R_{0,L}(u+\delta_L) \, ... \, R_{0,1}(u+\delta_1) \\
& \times K_0^R(u) \, R_{1,0}(u-\delta_1) \, ... \, R_{L,0}(u-\delta_L) \big) \, ,
\end{aligned}
\tag{2.122}
$$

whereby we have ignored upcoming scalar factors[14].

---

[14]We can always absorb overall factors in a redefinition of the R-matrix without spoiling integrability.
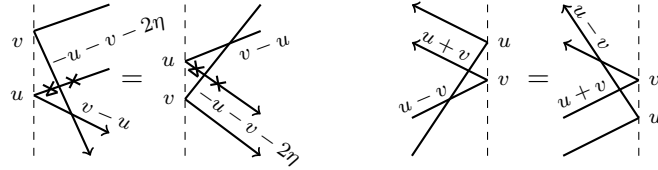
Figure 2.6: Graphical representation of the left and right reflection algebra, respectively. The dashed line has no meaning in the graphical notation but has been added to emphasise the meaning of the name *reflection* algebras.

Additional symmetries

It often appears that a model has additional symmetries. By a symmetry, we mean a quantity $\mathbb{G}$ such that

$$[\mathfrak{t}(u), \mathbb{G}] = 0 \,. \tag{2.123}$$

Note that for periodic or twisted BCs, equation (2.112) already implies the symmetry $\prod_{i=1}^{L} \varpi_i$. Besides the twist matrix ϖ, there are two other natural symmetries[15] based on the properties of the R-matrix. Namely, one can show that the crossing matrix M (see (2.105)) and the matrix U in (2.106) also always generate symmetries[16].

Turning to open BCs, the general picture remains the same provided the elementary building block of the symmetry also commutes with the reflection matrices K^L and K^R.

2.4.1 Famous example: the six-vertex model

Let us illustrate the above abstract notion of integrability on a concrete example by following [7]. Among the most prominent examples are the so-called ice-type models [76, 77]. When water freezes, a crystal structure arises in which the oxygen atoms arrange in a lattice with coordination number four [78], i.e. each oxygen atom has four neighbouring oxygen atoms. The hydrogen atoms position themselves in between the oxygen according to hydrogen bonding. This means each oxygen atom is surrounded by two close-by hydrogen atoms and two more distant ones. The lattice is three-dimensional. However, a toy model that is easier to study is the two-dimensional version of it. The structure of the oxygen in the latter is then the one of a square lattice. One possible configuration is depicted in the left panel of Figure 2.7. The hydrogen bonds between the oxygen atoms induce electric dipoles whose direction either points towards the oxygen atom (near hydrogen) or away from it (far away hydrogen). Such a dipole structure is illustrated on the right of Figure 2.7. One can notice that the only six vertices arising from the dipole structure are given by

---
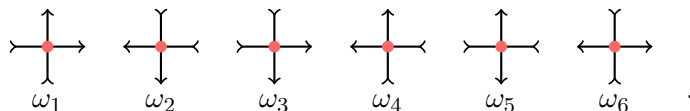
[15]Under the assumption that these matrices also commute with the twist matrix if twisted BCs are considered.

[16]For the proof for U one needs to use the PT-symmetry in the transposed version of (2.106) with the spaces interchanged.
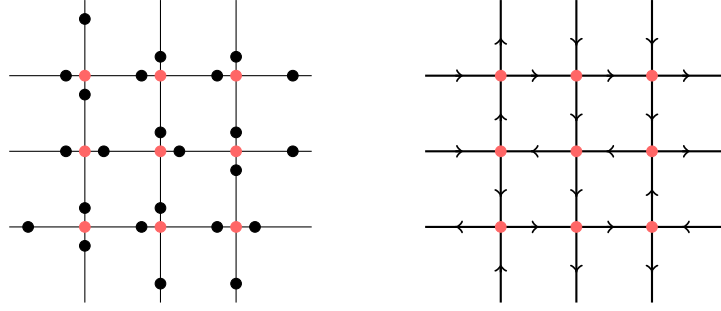
Figure 2.7: On the left panel the square lattice of the oxygen atoms (red) is visualised. A possible configuration of the hydrogen atoms (black) is displayed. On the right, the corresponding dipole structure is illustrated.

For the ice model, we would assign to each of these vertices the same energy [7]. However, in general, each vertex can be assigned a different Boltzmann weight ω_i. In this most general case, the partition function of the statistical system would be given by

$$\mathcal{Z} = \sum_{\text{confi}} \exp\left[-\frac{E^{\text{confi}}}{k_B T}\right] = \sum_{\text{confi}} \prod_{j=1}^{6} \omega_j^{n_j}, \tag{2.124}$$

where the sum is over all possible configurations and n_j is the number of appearing vertices of type j in a given configuration. If we consider a periodic $L \times M$ lattice with periodic BCs, it is easy to show that the partition function can be written as

$$\mathcal{Z} = \text{Tr}\left(\mathfrak{t}^M(u)\right), \tag{2.125}$$

where $\mathfrak{t}$ is given by (2.110) with all the inhomogeneities set to zero, $\mathcal{V}_a = \mathbb{C}^2$ and

$$R(u) = \begin{pmatrix} \omega_1 & 0 & 0 & 0 \\ 0 & \omega_3 & \omega_6 & 0 \\ 0 & \omega_5 & \omega_4 & 0 \\ 0 & 0 & 0 & \omega_2 \end{pmatrix}. \tag{2.126}$$

For general ω_j, the above matrix is not a solution of the YBE, so the model is not exactly solvable. However, if we set

$$\omega_1 = \omega_2 = \sinh(u + \mathrm{i}\gamma), \quad \omega_3 = \omega_4 = \sinh(u), \quad \omega_5 = \omega_6 = \sinh(\mathrm{i}\gamma) \tag{2.127}$$

the model becomes integrable[17]. The extra parameter $\gamma \in \mathbb{C}$ is called the anisotropy. It is related to the crossing parameter by $\eta = \mathrm{i}\gamma$. The other quantities involved in the relations, such as unitarity, crossing symmetry and quasi-periodicity (negative sign), take the explicit form

$$\xi(u) = \sinh(u + \mathrm{i}\gamma), \qquad V = \begin{pmatrix} 0 & 1 \\ -1 & 0 \end{pmatrix}, \qquad U = \begin{pmatrix} 1 & 0 \\ 0 & -1 \end{pmatrix}, \qquad \mathrm{p} = \mathrm{i}\pi. \tag{2.128}$$

The above R-matrix commutes with the tensor products $\sigma^j \otimes \sigma^j$ of all Pauli matrices $j = x, y, z$ and also with the matrix exponential $\mathrm{e}^{\mathrm{i}k\sigma^z} \otimes \mathrm{e}^{\mathrm{i}k\sigma^z}$ for $k \in \mathbb{C}$. Hence, suitable

---

[17]Note, that one always has the gauge freedom to set $\omega_5 \neq \omega_6$.

BCs can be generated by[18]

$$\varpi = \begin{pmatrix} e^{ik\pi} & 0 \\ 0 & e^{-ik\pi} \end{pmatrix}, \qquad \varpi = \begin{pmatrix} 0 & 1 \\ 1 & 0 \end{pmatrix}. \qquad (2.129)$$

We will refer to $\mathbf{k}$ as the twist parameter in the following. While the first choice in (2.129) is compatible with the $U(1)$ symmetry. i.e. $\mathbb{S}^z = \sum_j \sigma_j^z$ is a conserved quantity, for the antidiagonal BCs only one a discrete $\mathbb{Z}_2$ symmetry exists. The Hamiltonian of the homogeneous six-vertex model as in (2.111) is the one of the XXZ chain of interacting $\frac{1}{2}$-spins:

$$\mathbb{H}_{\text{XXZ}} = -\frac{1}{2\sin(\gamma)} \sum_{j=1}^{L} \sigma_j^x \sigma_{j+1}^x + \sigma_j^y \sigma_{j+1}^y + \cos(\gamma)(\sigma_j^z \sigma_{j+1}^z - \mathbf{1}), \qquad (2.130)$$

where we recall that the BCs (2.129) are reflected in (2.114).

The most general K-matrix for open BCs in the six-vertex model depends on three additional parameters s_1, s_2 and ξ^R and takes the form [79]

$$K^R(u) = \begin{pmatrix} \sinh(u + \xi^R) & s_1 \sinh(2u) \\ s_2 \sinh(2u) & -\sinh(u - \xi^R) \end{pmatrix}. \qquad (2.131)$$

2.4.2 THE BETHE ANSATZ

In this section, we briefly sketch a method for how the spectrum and eigenvectors of the transfer matrix $\mathbb{t}(u)$ can be found exactly. Note that this yields the simultaneous diagonalization of the whole family of commuting operators $\mathbb{I}_k$.

We start by illustrating the *algebraic* Bethe ansatz for the simple case of a periodic model with $\mathfrak{sl}(2)$ symmetry, e.g. the six-vertex model. It turns out that for this symmetry, the auxiliary space of the monodromy matrix T_a is isomorphic to $\mathbb{C}^2$. Hence, we can write T_a as a two by two matrix

$$T_a(u) = \begin{pmatrix} \mathcal{A}(u) & \mathcal{B}(u) \\ \mathcal{C}(u) & \mathcal{D}(u) \end{pmatrix}, \qquad (2.132)$$

where the entries $\mathcal{A}(u)$, $\mathcal{B}(u)$, $\mathcal{C}(u)$ and $\mathcal{D}(u)$ are operators acting on $\mathscr{H}$. These operators obey the commutation relation dictated by the RTT-relation (2.107a). The transfer matrix $\mathbb{t}(u)$, given as the trace over the auxiliary space, can easily be expressed as

$$\mathbb{t}(u) = \mathcal{A}(u) + \mathcal{D}(u). \qquad (2.133)$$

The starting point of the algebraic Bethe ansatz is to identify an obvious simultaneous eigenvector of $\mathcal{A}(u)$ and $\mathcal{D}(u)$. Further, one needs that this eigenvector is either annihilated by $\mathcal{B}(u)$ or $\mathcal{C}(u)$ and must not be by the other. A vector with these properties is called a pseudo vacuum or simply the reference state. For the six-vertex model, a suitable reference state is the product state of all spins up. Once a reference state $|\phi\rangle$ is found, one constructs the so-called Bethe states by applying the non-annihilating operator on it. In the following,

---

[18]Note that the BC produced by σ^y can be generated by a combination of the ones given in (2.129).

we pick the convention that $\mathcal{C}(u)$ will annihilate $|\phi\rangle$, and $\mathcal{B}(u)$ does not. In this case, the Bethe state is defined as

$$|u_1 \dots u_M\rangle := \prod_{j=1}^{M} \mathcal{B}(u_j) |\phi\rangle \, , \tag{2.134}$$

where $u_j \in \mathbb{C}$ are extra — yet unknown — parameters. Using the explicit form of the commutation relation of $\mathcal{A}(u)$ and $\mathcal{D}(u)$ with $\mathcal{B}(u)$, the action of the transfer matrix on the Bethe state can be worked out explicitly, e.g. for the six-vertex model the necessary commutation relations would look like

$$
\begin{aligned}
\mathcal{A}(u)\mathcal{B}(v) &= \mathcal{B}(v)\mathcal{A}(u)\frac{\omega_1(v-u)}{\omega_4(v-u)} - \mathcal{B}(u)\mathcal{A}(v)\frac{\omega_6(v-u)}{\omega_4(v-u)} \, , \\
\mathcal{D}(u)\mathcal{B}(v) &= \mathcal{B}(v)\mathcal{D}(u)\frac{\omega_2(u-v)}{\omega_4(u-v)} - \mathcal{B}(u)\mathcal{D}(v)\frac{\omega_5(u-v)}{\omega_4(u-v)} \, .
\end{aligned}
\tag{2.135}
$$

Imposing that the Bethe state is an eigenstate, i.e. cancelling all contributions arising from the second terms in (2.135), will lead to a set of algebraic constraints for the parameters u_j. These constraints are called the Bethe ansatz equations (BAE), and the solution set $\{u_j\}_{j=1}^{M}$ are named Bethe roots. For the inhomogeneous six-vertex model with twisted[19] BCs the BAE take the form (after a redefinition of $u_j \mapsto u_j - \frac{\mathrm{i}\gamma}{2} + \frac{\mathrm{i}\pi}{2}$)

$$\prod_{l=1}^{L} \frac{\cosh\left(u_m + \delta_l + \frac{\mathrm{i}\gamma}{2}\right)}{\cosh\left(u_m + \delta_l - \frac{\mathrm{i}\gamma}{2}\right)} = \mathrm{e}^{2\mathrm{i}\pi\mathtt{k}} \prod_{j \neq m}^{M} \frac{\sinh\left(u_m - u_j + \mathrm{i}\gamma\right)}{\sinh\left(u_m - u_j - \mathrm{i}\gamma\right)} \, , \tag{2.136}$$

while the eigenvalue of the transfer matrix would read

$$
\begin{aligned}
t(u) = & \mathrm{e}^{\mathrm{i}\pi\mathtt{k}} \prod_{j=1}^{L} \sinh(u + \delta_j + \mathrm{i}\gamma) \prod_{j=1}^{M} \frac{\sinh(u - u_j - \frac{\mathrm{i}\pi}{2} - \frac{\mathrm{i}\gamma}{2})}{\sinh(u - u_j - \frac{\mathrm{i}\pi}{2} + \frac{\mathrm{i}\gamma}{2})} \\
& + \mathrm{e}^{-\mathrm{i}\pi\mathtt{k}} \prod_{j=1}^{L} \sinh(u + \delta_j) \prod_{j=1}^{M} \frac{\sinh(u - u_j - \frac{\mathrm{i}\pi}{2} + \frac{3\mathrm{i}\gamma}{2})}{\sinh(u - u_j - \frac{\mathrm{i}\pi}{2} + \frac{\mathrm{i}\gamma}{2})} \, .
\end{aligned}
\tag{2.137}
$$

The eigenvalue of $\mathbb{I}_k$ on the corresponding Bethe state can then be simply expressed in terms of the Bethe roots. Hence, the problem of determining the spectrum of the commuting family of operators has been reduced to obtain all solutions of an algebraic system of equations. For example, the energies given by the eigenvalues of (2.130) can be expressed in terms of the corresponding Bethe roots solving (2.136) as

$$E_{\mathrm{XXZ}} = \sum_{j=1}^{M} \epsilon_0(u_j) = -\sum_{j=1}^{M} \frac{2\sin(\gamma)}{\cosh(2u_j) + \cos(\gamma)} \, . \tag{2.138}$$

Here, we call ϵ_0 the bare energies of the model for further reference. Remarkably, the above procedure can also be generalised to higher-rank models where the minimal dimension of

---

[19] Note that the above derivation is strictly speaking only valid for the periodic case $\mathtt{k} = 0$. However, the above procedure can be simply generalized to the twisted case by adding the phase factors $\mathrm{e}^{\pm\mathrm{i}\pi\mathtt{k}}$ in (2.133).

the auxiliary space is larger than two. For the case of a rank 3 model, the monodromy matrix would be of the form

$$
\begin{pmatrix} \tilde{\mathcal{A}} & \tilde{\mathcal{B}} \\ \tilde{\mathcal{C}} & \tilde{\mathcal{D}} \end{pmatrix} , \tag{2.139}
$$

where $\tilde{\mathcal{A}}$ is just an operator but $\tilde{\mathcal{B}}$ and $\tilde{\mathcal{C}}$ are operator-valued two-row and two-column vectors respectively while $\tilde{\mathcal{D}}$ is an 2×2 operator valued matrix. Nevertheless, applying the framework of algebraic Bethe ansatz will lead to a diagonalization problem of reduced rank. The latter can be again solved by a second algebraic Bethe ansatz. Hence, one ends up applying the above scheme two times. This is a general pattern. A n rank problem needs a hierarchy of $n-1$ Bethe ansätze [80, 81, 82].

The generalisation to models with other BCs is also straightforward provided the associated matrices ϖ, K^L and K^R are diagonal (see [72, 73] for the open case). The case of non-zero off-diagonal elements is more delicate due to the lack of an obvious reference state. Hence, the treatment of this model requires more advanced methods, e.g. separation of variables [83, 84] or off-diagonal Bethe ansatz [85].

The algebraic Bethe ansatz gives important insights through the explicit construction of the eigenstates. However, in this thesis, we are primarily interested in the spectrum of the transfer matrix. The latter can be obtained through the analytic Bethe ansatz, which we will review in the next section.

2.4.3 Commuting transfer matrices: the Q-operator

Another powerful concept in integrable lattice systems is known as the method of commuting transfer matrices. The method has been developed by Baxter to solve the eight vertex model [86]. It can also be applied to the six-vertex model [87] and is based on the so-called Q-operator, which commutes with the transfer matrix and itself

$$
[\mathbb{Q}(u), \mathbb{Q}(v)] = [\mathbb{t}(u), \mathbb{Q}(v)] = 0 . \tag{2.140}
$$

Note that (2.140) implies the existence of a common system of eigenvectors of $\mathbb{Q}(u)$ and $\mathbb{t}(u)$. Further, the transfer matrix and the Q-operator are intertwined by the so-called TQ-equation. This is a functional relation of the kind

$$
\mathbb{t}(u)\mathbb{Q}(u) = f_1(u)\mathbb{Q}(u+a) + f_2(u)\mathbb{Q}(u+b) , \tag{2.141}
$$

where $f_{1,2}(u)$ are scalar functions and $a, b \in \mathbb{C}$.

The method of commuting transfer matrices is, in particular, useful for systems where the algebraic Bethe ansatz fails, such as models with off-diagonal boundary matrices, e.g. the second one in (2.129). Based on [88, 89], we briefly sketch how the Q-operator can be constructed for the general inhomogeneous six-vertex model with antidiagonal BCs. In the later section 4.1 we will discuss the case of open BCs.

The starting point of the derivation is to apply the transfer matrix given by (2.113), (2.126) and (2.129) on a general product state, denoted as

$$
\mathbf{y} = g_1 \otimes g_2 \otimes \cdots \otimes g_L , \qquad g_i = \begin{pmatrix} g_j^1 \\ g_j^2 \end{pmatrix} , \qquad g_j^i \in \mathbb{C} . \tag{2.142}
$$

The result can be written in multi index notation $\beta = (\beta_1, \ldots, \beta_L)$

$$(\mathfrak{t}(u)\mathbf{y})^\beta = \mathrm{Tr}\left(\mathcal{G}_L(\beta_L) \ldots \mathcal{G}_1(\beta_1)\varpi\right),\tag{2.143}$$

where the matrix $\mathcal{G}$ is given by

$$\mathcal{G}_i(1) = \begin{pmatrix} \omega_1(u+\delta_i)g_i^1 & \omega_3(u+\delta_i)g_i^2 \\ \omega_5(u+\delta_i)g_i^2 & 0 \end{pmatrix}, \quad \mathcal{G}_i(2) = \begin{pmatrix} 0 & \omega_5(u+\delta_i)g_i^1 \\ \omega_3(u+\delta_i)g_i^1 & \omega_1(u+\delta_i)g_i^2 \end{pmatrix}\tag{2.144}$$

The key is now to find a matrix $P_i = \begin{pmatrix} p_i(1) & * \\ p_i(2) & * \end{pmatrix}$ to write $\mathcal{G}_i(\beta_i) = P_{i+1}H_i(\beta_i)P_i^{-1}$ where $H_i(\beta_i)$ is an upper triangular matrix. A necessary and sufficient condition for the existence of such matrices leads to the recurrence relation

$$2\cos(\gamma) = \frac{r_i}{r_{i+1}} + \frac{r_{i+1}}{r_i}\tag{2.145}$$

for $r_i = \frac{p_i(1)}{p_i(2)}$. This equation can be solved leading to $r_i = r_{i-1}e^{i\gamma\sigma^{(i-1)}}$ where $\sigma^{(i-1)}$ can either be $+1$ or -1. Note that for each $i = 1, \ldots L$, the choice of the sign of $\sigma^{(i-1)}$ can be made independently. This yields 2^L different combinations in total, equal to the dimension of the Hilbert space $\mathscr{H}$. The initial condition, $r_1 = r$ is fixed by the antiperiodicity of the model such that $r^2 = e^{i\gamma\sum_{j=1}^L \sigma^j}$.

Using the above solution for r_i, the diagonal elements of the matrix $H_i(\beta_i)$ are easily found, and so equation (2.143) can be evaluated using its upper triangular form for all 2^L different sign choices. Grouping all 2^L different vectors into one matrix $\mathbb{Q}$ leads using an appropriate normalisation to the following TQ-relation

$$\mathfrak{t}(u)\mathbb{Q}(u) = \prod_{j=1}^L \sinh(u+\delta_j+i\gamma)\mathbb{Q}(u-i\gamma) - \prod_{j=1}^L \sinh(u+\delta_j)\mathbb{Q}(u+i\gamma),\tag{2.146}$$

whereby we have found the matrix elements of $\mathbb{Q}$ to be given by ($z = e^u$)

$$\mathbb{Q}_{i,j}(z) = \frac{Q_{i,j}^E(z)}{Q_{j,j}^E(z)}\tag{2.147}$$

with

$$\begin{aligned}
Q_{i,j}^E(z) &= z^{\frac{1}{2}\sum_{k=1}^L \sigma_k(j)} \prod_{k=1}^L h_{k,w_k(i)}(\sigma(j)),\\
h_{i,j}(\sigma(k)) &= 1 + \delta_{j,2}(-1 + r_i(\sigma(k))z^{-\sigma_i(k)}e^{-\delta_i\sigma_i(k)}),\\
r_i(\sigma(k)) &= e^{-\frac{i\gamma}{2}\sum_{j=1}^L \sigma_j(k)}e^{i\gamma\sum_{j=i+1}^L \sigma_j(k)},\\
\sigma_j(k) &= -1 + 2\,\mathtt{IntDig}(k-1,2,L,j),\\
w_j(k) &= 1 + \mathtt{IntDig}(k-1,2,L,j)
\end{aligned}\tag{2.148}$$

and $\mathtt{IntDig}(a,b,c,j)$ is the jth entry of the list of the base-b-digits in the integer a of length c. In fact, it just transforms the indices of the canonical basis into the ones of the tensor basis notation in a convenient way. We should stress that this formula is truly explicit

and does not contain any implicit operations such as matrix inversion or multiplications in contrast to [89]. Hence, this form of the operator is particularly useful for numerical implementations.

The above operator equation induces, in turn, a similar equation for the eigenvalues $t(u)$, $Q(u)$ of the transfer matrix and the Q-operator:

$$t(u)Q(u) = \prod_{j=1}^{L} \sinh(u + \delta_j + i\gamma)Q(u - i\gamma) - \prod_{j=1}^{L} \sinh(u + \delta_j)Q(u + i\gamma). \qquad (2.149)$$

Note the similarity with the eigenvalues $t(u)$ for the twisted BCs (2.137). The above equation (2.149) for $Q(u)$ can be solved [89, 90] by the knowledge of the asymptotics of $t(u)$: Using the fact that the transfer matrix is a Laurent polynomial in e^u one obtains the following asymptotic behaviour of its eigenvalues regarding the spectral parameter u:

$$\lim_{u \to \infty} t(u)e^{-Lu} = O(e^{-u}). \qquad (2.150)$$

Taking this scaling into account one can deduce from (2.149) that $Q(u)$ has the form

$$Q(u) = \prod_{k=1}^{L} \sinh\left(\frac{1}{2}\left(u - u_k + \frac{i\gamma}{2}\right)\right), \qquad (2.151)$$

where the u_k's are unknown parameters. The eigenvalue of the transfer matrix is given in terms of the u_k:

$$\begin{aligned}
t(u) = \prod_{j=1}^{L} \sinh(u + \delta_j + i\gamma) \prod_{k=1}^{L} \frac{\sinh\left(\frac{1}{2}(u - u_k - \frac{i\gamma}{2})\right)}{\sinh\left(\frac{1}{2}(u - u_k + \frac{i\gamma}{2})\right)} \\
- \prod_{j=1}^{L} \sinh(u + \delta_j) \prod_{k=1}^{L} \frac{\sinh\left(\frac{1}{2}(u - u_k + \frac{3i\gamma}{2})\right)}{\sinh\left(\frac{1}{2}(u - u_k + \frac{i\gamma}{2})\right)}.
\end{aligned} \qquad (2.152)$$

From the form of the transfer matrix and its analytic dependence on its spectral parameter, the eigenvalue must also be an analytic function. Prima facie, the expression in (2.152) has simple poles at $u = u_k - \frac{i\gamma}{2}$. However, provided $\{u_k\}$ satisfies the equations

$$\prod_{j=1}^{L} \frac{\sinh\left(u_k + \delta_j + \frac{i\gamma}{2}\right)}{\sinh\left(u_k + \delta_j - \frac{i\gamma}{2}\right)} = \prod_{m=1}^{L} \frac{\sinh\left(\frac{1}{2}(u_k - u_m + i\gamma)\right)}{\sinh\left(\frac{1}{2}(u_k - u_m - i\gamma)\right)}, \qquad (2.153)$$

all residues vanish, and so the singularities are removable. This scheme of deriving the eigenvalue of the transfer matrix by requiring it to be an analytical function is called the *analytical* Bethe ansatz.

Systematic extraction of Bethe roots

Above we have seen that different Bethe ansätze have in common that the solution of the spectral problem reduces to finding all solutions of the Bethe ansatz equations. However, finding all of the possible solution sets of the latter, even for $L \lesssim 20$, is impossible to carry
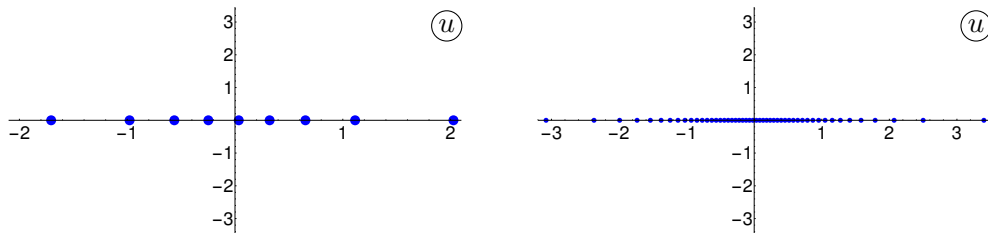
Figure 2.8: The left panel displays the Bethe root configuration of the ground state for $L = 18$ of the Hamiltonian (2.130) with twisted BC in the complex u-plane obtained within the Q-operator approach while the right panel depicts the root pattern extended to $L = 100$. The parameters are given by $\gamma = \frac{\pi}{5}$ and $\mathtt{k} = 0.05$.

out on a modern consumer-PC because the system is too complicated. Moreover, many searching algorithms, e.g. the Newton method, are based on the quality of the guess of an initial approximation. The try-and-error approach is time-consuming and not guaranteed to work. A more sophisticated method is required. Note that the zeros of the eigenvalue of $\mathbb{Q}$ are given essentially by the Bethe roots see e.g. (2.151). This allows for an efficient and systematic way to extract the Bethe roots for system sizes $L \sim 20$, as we will describe in the following [91].

First, one should choose from the family of commuting operators $\mathbb{I}_k$ an operator which is of sparse form, e.g. the Hamiltonian as given in (2.111). Due to its sparse form, it can be easily implemented on a standard computer for relatively large system sizes $L \sim 20$ without running out of memory. Using the Arnoldi-Krylov method [92, 93], one can obtain its first few hundred eigenvalues and corresponding eigenvectors, whereby we order the spectrum by its real parts. Using the shifted operator $\mathbb{H} - \lambda \mathbf{1}$ instead of $\mathbb{H}$ where $\lambda \in \mathbb{C}$ is called the Arnoldi shift, one can iteratively diagonalize the whole Hamiltonian by suitable choices of λ.

Once the spectrum and eigenstates of the Hamiltonian are found, one finds, e.g. by the Gram–Schmidt process, an orthonormalized basis (ONB) $\psi^{(j)}$ $j = 1, \ldots d$ in each d-times degenerated energy level. Due to (2.140), each eigenspace is left invariant under the action of $\mathbb{Q}$. Hence, we can project $\mathbb{Q}(u)$ onto one of these subspaces. Let us denote this projected version by $\mathbb{Q}^{\mathrm{proj}}(u)$. As $\mathbb{Q}^{\mathrm{proj}}(u)$ still commutes with itself for different arguments, its eigenvectors do not depend on the spectral parameter. Hence, it is enough to finds its eigenvectors $\mathfrak{a}_j$ for some numerical value $u = u_0$. Then we obtain the d eigenvalues of $\mathbb{Q}(u)$ in the given energy level via

$$Q_j(u) = \frac{\mathfrak{a}_j^\dagger \mathbb{Q}^{\mathrm{proj}}(u) \mathfrak{a}_j}{||\mathfrak{a}_j||^2}, \qquad j = 1, \ldots, d. \tag{2.154}$$

Using simple root-finding algorithms such as the Newton method, one determines the associated Bethe roots. The Bethe roots of the ground state and one excited state of the twisted XXZ chain are displayed in Figures 2.8 and 2.9. Furthermore, looping this algorithm over all accessible energy levels, we systematically generate all corresponding Bethe roots.

It should be stressed that in the above procedure, the rational notation $\zeta = \mathrm{e}^{-2u}$ should be used when implementing the algorithm on a computer. The advantage is that instead of

working with a growing number of unevaluated functions such as $\sinh(u + \ldots)$, one works with Laurent polynomials in ζ. Numerical manipulations of the latter are simply reduced to computations of their purely numerical coefficients.

2.4.4 The critical twisted homogeneous XXZ model

To extract properties such as the critical behaviour of a lattice system, often small system sizes such as $L \sim 20$ are not enough to capture the essential physics. However, studying larger system sizes is limited by the growth of necessary memory or computational time.

The advantage of *integrable* lattice systems, such as the XXZ chain, is that they allow for either direct analytical treatment or that the complexity of certain numerical problems grows polynomially. One particular task facilitated by integrability is the construction of individual RG trajectories. We mean by that the extension of a given state $|\psi_{L_{\text{in}}}\rangle$ for the system of L_{in} sites to larger system sizes[20] e.g. $L = L_{\text{in}} + 2$. In an integrable system, we can assign a set of Bethe roots to each state. Suppose one has at hand the Bethe roots for a Bethe state for a lattice of L_{in} sites. The state $|\Psi_{L_{\text{in}}+2}\rangle$ is specified such that the pattern of Bethe roots qualitatively remains the same. They can be obtained by numerically solving the Bethe ansatz equations, where the initial approximation for the solution is constructed from the Bethe roots corresponding to $|\Psi_{L_{\text{in}}}\rangle$. By iterating this procedure, a RG trajectory $\{|\Psi_L\rangle\}$ for increasing L is obtained. Examples of the Bethe root configuration for the ground state and an excited state for the twisted XXZ model are displayed in Figures 2.8 and 2.9, respectively.

Note that having at hand the Bethe roots of a RG trajectory $\{|\Psi_L\rangle\}$, we can study how the properties, e.g. energy or momentum of that individual state, behave as $L \to \infty$. This is, in particular, useful concerning the discussion in section 2.3, especially for formulae like (2.96) and (2.94). There, it has been shown that the asymptotic behaviour of the energies and momenta of a lattice regularisation of a conformal field theory is dictated by its field theory content. On the other hand, given an integrable lattice model and the hypothesis that its infra-red limit tends to a conformal fix point, information about this fix point can be accessed via the study of the scaling behaviour of the pattern of Bethe roots. Essentially, the latter is the subject of the rest of the thesis.

A sketch of the root density approach

The above numerical method relies on the assumption — the so-called Bethe hypothesis — that the Bethe roots are arranged in a regular pattern as $L \to \infty$. Based on the numerical data of the roots for an increasing number of system sizes, one can guess what the limiting pattern is. Starting from a hypothesis for a particular class of states, one can treat them in an analytic fashion [94] valid in the limit $L \to \infty$. For the so-called root density approach, two main properties of the limiting root pattern are essential.

First, one needs to know the limiting imaginary part as a function of the real part. Often, the imaginary part has branches, i.e. given a real number x, there can be multiple choices for the possible imaginary part. One needs to incorporate each branch.

---

[20]Since the two Hilbert spaces are not isomorphic, this question only makes sense if one restricts to a certain energy regime, e.g. the low-energy excitations.

Secondly, the distance between neighbouring roots on the same branch needs to decrease as $\sim L^{-1}$. Suppose we have ordered the roots u_j by their real part x_j such that $x_{j+1} > x_j$. Then the quantity

$$\rho(x_{j+\frac{1}{2}}) = \frac{1}{L(x_{j+1} - x_j)} \qquad \text{with } x_{j+\frac{1}{2}} = \frac{(x_j + x_{j+1})}{2} \tag{2.155}$$

tends to a continuous function in the thermodynamic limit $L \to \infty$, describing the density of the root distribution on the associated branch. As the Bethe ansatz equations involve all roots, the densities on different branches are not independent of each other but rather are coupled to each other via a system of integral equations. The latter follows by inserting the Bethe hypothesis into the logarithmic form of the Bethe ansatz equations and performing a series expansion in L^{-1} whereby sums over the roots of a given branch can be replaced by a convolution with the associated density.

For instance, the lowest energy state in a given sector of S^z of the twisted XXZ model has $L/2 - S^z$ real roots if the twist parameter $\mathtt{k}$ is not too large. For an illustration of the roots of the ground state, which appears in the sector $S^z = 0$, see Figure 2.8. By comparing the two panels, it is apparent that the above conditions are satisfied. Then we can bring (2.136) by taking its logarithm to the form

$$2\pi\, I_m = Z_L(u_m)\,, \tag{2.156}$$

where I_m are a certain set of (half-)integers, labelling the branch of the logarithm. Further, we have introduced the so-called counting function

$$Z_L(u) = 2\pi\mathtt{k} + Lf_1(u) + \sum_{m=1}^{\frac{L}{2}-S^z} f_2(u - u_m)\,, \tag{2.157}$$

where

$$f_1(u) = 2\arctan\left(\tanh(u)\tan\left(\frac{\gamma}{2}\right)\right)\,, \qquad f_2(u) = 2\arctan\left(\tanh(u)\cot(\gamma)\right)\,. \tag{2.158}$$

In the derivation of (2.157) we have chosen the branches of the logarithm such that $f_1(u)$ and $f_2(u)$ are continuous functions in the strips $|\Im m(u)| < \frac{\pi-\gamma}{2}$ and $|\Im m(u)| < \gamma$, respectively, such that (the star denotes the complex conjugation)

$$f_j(u^*) = \left(f_j(u)\right)^*\,, \qquad\qquad f_j(0) = 0 \qquad\qquad (j = 1,2)\,. \tag{2.159}$$

Different choices of the I_m correspond to different solution sets of the Bethe ansatz equations. For simplicity, let's focus on the case when $\frac{L}{2} - S^z$ is even. Then, for the considered lowest energy states in a sector S^z, the I_m are the half integers and symmetrically distributed around zero. Further, the counting function (2.157) for the solution set $\{u_j\}$ is a real, monotonically increasing function. The above facts read

$$Z_L(u_m) = \pi\left(2m - 1 + S^z - \tfrac{L}{2}\right)\,, \tag{2.160}$$

$$u_m < u_{m'} \quad \Longleftrightarrow \quad m < m'\,. \tag{2.161}$$

Also, we have the asymptotics

$$Z_L(u) \to \pm\pi\left(\tfrac{L}{2} - S^z\right) \pm 2\gamma S^z + 2\pi\mathtt{k} \qquad \text{as} \qquad u \to \pm\infty\,. \tag{2.162}$$
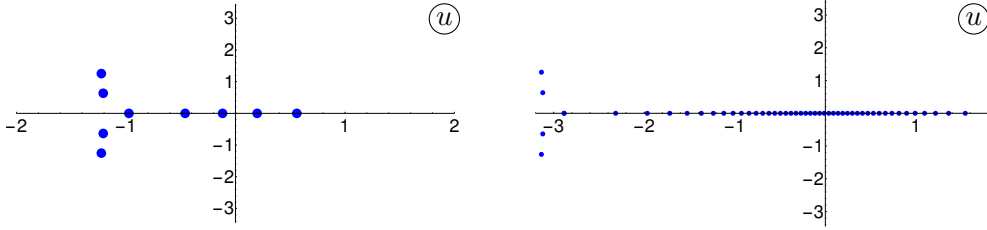
Figure 2.9: The left panel displays the Bethe root configuration of an excited state for $L = 18$ of the anti-ferromagnetic XXZ spin chain in the complex u-plane obtained within the Q-operator approach while the right panel depicts the root pattern extended to $L = 100$. The parameters are given by $\gamma = \frac{\pi}{5}$ and $\mathbf{k} = 0.05$.

Note that, for $L \to \infty$, the bounds of the counting function approach $\pm\infty$. Now, in regard to the continuous version of (2.155), we define the root density to be

$$\rho(u) = \frac{\mathrm{d}}{\mathrm{d}u} \frac{Z_L(u)}{2\pi L}. \tag{2.163}$$

By differentiating the equation (2.157) and approximating the sum via the Euler MacLaurin formula as $L \to \infty$, we obtain in the first order of L^{-1}, the integral equation for the ground state density

$$2\pi\rho(u) = f_1'(u) + \int_{-\infty}^{\infty} \mathrm{d}u' f_2'(u - u')\rho(u'). \tag{2.164}$$

This integral equation can be solved via the Fourier transform. This yields

$$\rho(u) = \frac{1}{2(\pi - \gamma)} \frac{1}{\cosh(\frac{u}{\pi - \gamma})}. \tag{2.165}$$

Having this density at hand, we can calculate the energy density in the thermodynamic limit by approximating the sum over the roots in (2.138) again by the convolution with the root density. This way, we obtain

$$e_\infty = -\frac{1}{\pi - \gamma} \int_{-\infty}^{\infty} \mathrm{d}\omega \, \frac{\sinh\left(\frac{\gamma\omega}{\pi - \gamma}\right)}{\cosh(\omega)\sinh\left(\frac{\pi\omega}{\pi - \gamma}\right)}. \tag{2.166}$$

Further, one can determine the dressed energies $\epsilon(u)$, defined by the same integral equation as (2.164) but where the driving term f_1' is replaced by the bare energies ϵ_0 given in (2.138). The form of dressed energy shows that one has gapless excitations with linear dispersion. The corresponding Fermi velocity is given by

$$v_{\mathrm{F}} = \lim_{\Lambda \to \infty} \frac{1}{2\pi\rho(\Lambda)} \frac{\mathrm{d}}{\mathrm{d}\Lambda} \epsilon(\Lambda) = \frac{\pi}{\pi - \gamma}. \tag{2.167}$$

Now, we have everything at hand to extract the conformal weights of the underlying CFT. By numerically solving the Bethe ansatz equations, we can extract a finite-size approximation $X_{\mathrm{eff}}(L)$ of effective scaling dimensions given in (2.96), i.e.

$$X_{\mathrm{eff}}(L) = \frac{L}{2\pi v_{\mathrm{F}}}(E(L) - Le_\infty). \tag{2.168}$$

In the rest of this thesis, we will often suppress the argument L of the finite-size estimate $X_{\text{eff}}(L)$ of X_{eff} when it is clear from the context what is meant.

By considering various states in different sectors of S^z, we obtain the formula

$$X_{\text{eff}}(L) = -\frac{1}{12} + \frac{\gamma S_z^2}{2\pi} + \frac{(\mathbf{k}+w)^2}{2\gamma} + \mathbf{L} + \bar{\mathbf{L}} + o(1)\,, \qquad (2.169)$$

where $w \in \mathbb{Z}$ and $\mathbf{L} + \bar{\mathbf{L}}$ are positive integers. Comparing (2.169) with (2.54), we conclude that the CFT underlying the XXZ model is a compactified boson of radius $R = \sqrt{2\gamma}^{-1}$. Also, one can check that the degeneracy (2.39) of the level space $\text{par}(\mathbf{L})\text{par}(\bar{\mathbf{L}})$ works out.

Comment on ODE/IQFT correspondence

In the last section, we have seen that the CFT Hamiltonian of a compact boson appears in the scaling limit of the Hamiltonian of the XXZ model. A natural question to ask is what operators built from the free bose field appear in the scaling limit of the Q-operator or the transfer matrix $\mathfrak{t}$. It turns out that the CFT analogues are well known. They form a communting family which is referred to as the qKdV integrable structure in the CFT [95, 96, 97]. In the later work [29], it was shown that the spectral problem for the integrals of motion of the IQFT can be equivalently described in terms of spectral properties of a class of ODEs. The latter offers a much simpler and convenient treatment. A detailed explanation of the lattice, IQFT and ODE's threefold interplay is outside this thesis' scope. We will limit ourselves to stating the relation between the lattice operators and the ODEs and pointing out some numerical checks.

A good starting point for the discussion is the expression of the eigenvalues of the lattice $\mathbb{Q}_{\pm}$ operators — below and above the equator — in the rational notation $\zeta = \mathrm{e}^{-2u}$

$$A_{\pm}(\zeta) = \prod_{m=1}^{\frac{L}{2} \mp S_z} \left(1 - \frac{\zeta}{\zeta_m^{\pm}} \right)\,, \qquad (2.170)$$

where we neglect an inessential overall factor. A manifestation of the ODE/IQFT correspondence, which is important for our purposes, is that the scaling limit (slim) of $A_{\pm}$ for the vacuum coincides with the spectral determinants of a certain ODE:

$$\operatorname*{slim}_{L\to\infty} A_{\pm}((L/L_0)^{\left(\frac{2\gamma}{\pi}-2\right)}E) = D_{\pm}(E)\,. \qquad (2.171)$$

Let us explain the quantities appearing in the above formula. In the LHS L_0 is a non-universal constant:

$$L_0 = \frac{\sqrt{\pi}\,\Gamma\left(\frac{1}{2} + \frac{\pi}{2\pi - 2\gamma}\right)}{2\Gamma\left(1 + \frac{\pi}{2\pi - 2\gamma}\right)}\,. \qquad (2.172)$$

The functions $D_{\pm}(E)$ are the spectral determinants of the ODE

$$\left(\partial_x^2 + E - x^{2\alpha} - \frac{l(l+1)}{x^2}\right)\Psi(x) = 0\,. \qquad (2.173)$$

39

Here the relation between the parameters is given by

$$S_z + \frac{\pi \mathsf{k}}{\gamma} = l + \frac{1}{2}, \qquad \gamma = \frac{\pi}{1+\alpha}. \tag{2.174}$$

Also in (2.171) we make the technical assumption that $0 < \gamma < \frac{\pi}{2}$.

As a definition of the spectral determinant $D_+(E)$ (for $D_-(E)$ see below) we will use the following. Denote by ψ^+ the solution of the ODE, which is characterised by its asymptotic behaviour at $x \to 0^+$

$$\psi^+(x) \asymp \sqrt{\frac{2\pi}{1+\alpha}} \frac{(2+2\alpha)^{-\frac{2l+1}{2+2\alpha}}}{\Gamma(1+\frac{2l+1}{2+2\alpha})} x^{l+1} \qquad \text{as} \quad x \to 0^+. \tag{2.175}$$

Note that this specifies $\psi^+(x)$ uniquely only for $\Re e(l+1) \geq 0$. Let $\chi^+(x)$ be another solution of the ODE which decays as $x \to +\infty$. We fix its normalisation by means of the Wentzel-Kramers-Brillouin (WKB) approximation

$$\chi^+(x) \asymp x^{-\frac{\alpha}{2}} \exp\left[-\frac{x^{\alpha+1}}{\alpha+1}\right] \qquad \text{as} \quad x \to +\infty. \tag{2.176}$$

The spectral determinant of the ODE is defined as the Wronskian of the solution which decays at $x = 0$ with the one which decays at $x = \infty$:

$$D_+(E) = \frac{1}{2} W[\chi^+, \psi^+] = \frac{1}{2}\left(\chi^+ \partial_x \psi^+ - \psi^+ \partial_x \chi^+\right). \tag{2.177}$$

For the values $E = E_m$ at which there exists a normalisable solution of the ODE (2.173), ψ^+ is proportional to χ^+ and so their Wronskian vanishes:

$$D_+(E_m) = 0. \tag{2.178}$$

Also the normalisation factors in (2.175) and (2.176) are chosen such that

$$D_+(0) = 1. \tag{2.179}$$

An essential ingredient that allows one to argue for the scaling relation (2.171) is the so-called *quantum Wronskian relation*. On the lattice/IQFT side, it can be derived from the representation theory of $U_q(\widehat{\mathfrak{sl}}(2))$ (for an irrep see (4.8) and (4.9)) with $q = e^{i\gamma}$, which underlies the integrability of the XXZ spin chain [97]. It reads

$$(e^{i\pi \mathsf{k}} q^{S_z} - e^{-i\pi \mathsf{k}} q^{-S_z})(1+\zeta)^L = e^{i\pi \mathsf{k}} q^{S_z} A_+(q\,\zeta) A_-(q^{-1}\zeta) - e^{-i\pi \mathsf{k}} q^{-S_z} A_-(q\,\zeta) A_+(q^{-1}\zeta). \tag{2.180}$$

In the scaling limit where $L \to \infty$ and $\zeta \sim L^{\left(\frac{2\gamma}{\pi}-2\right)}$ the factor $(1+\zeta)^L$ tends to one and can be ignored (recall the technical assumption $0 < \gamma < \pi/2$). In the following, we derive along the lines of the work [29] the same functional relation (2.180), without the factor $(1+\zeta)^L$, for the spectral determinants $D_\pm(E)$. Among other things, it yields the identification between the parameters of the lattice model and the ones of the ODE (2.174). The derivation is

based on the Bazhanov-Lukyanov-Zamolodchikov symmetry transformations [29] of the ODE (2.173)

$$\hat{\Lambda}: \quad x \mapsto x\,, \qquad E \mapsto E\,, \qquad l \mapsto -l-1\,, \qquad (2.181)$$

$$\hat{\Omega}: \quad x \mapsto q_0 x\,, \quad E \mapsto q_0^{-2}E\,, \qquad l \mapsto l\,, \qquad (2.182)$$

which act non-trivially on the solutions but leave the ODE the same. In the above, we have defined[21] q_0 to be

$$q_0 = e^{\frac{i\pi}{1+\alpha}} \implies q_0^{\alpha+1} = -1\,. \qquad (2.183)$$

Let us denote the transformed solutions by ψ^- and χ^-

$$\psi^-(x,E,l) = \psi^+(x,E,-l-1)\,, \qquad (2.184)$$

$$\chi^-(x,E,l) = iq_0^{-\frac{1}{2}} \chi^+(q_0 x, q_0^{-2}E, l)\,. \qquad (2.185)$$

The Wronskian of these with the original solutions are

$$W[\psi^+,\psi^-] = 2i\left(q_0^{l+\frac{1}{2}} - q_0^{-l-\frac{1}{2}} \right)\,, \qquad (2.186)$$

$$W[\chi^+,\chi^-] = 2\,. \qquad (2.187)$$

A non-vanishing Wronskian means that the two solutions are linearly independent. As the ODE is of second order, both sets $\{\psi^+,\psi^-\}$ and $\{\chi^+,\chi^-\}$ individually form bases of all solutions of the ODE for generic l. Therefore, we can express ψ^+ in terms of $\chi^\pm$:

$$\psi^+(x,E,l) = C(E,l)\chi^+ + D(E,l)\chi^-\,. \qquad (2.188)$$

For future reference, we mention that D and C are referred to as connection coefficients. Due to (2.187) and $W[f,f] = 0$ for any function f, we have

$$D(E,l) = \frac{1}{2}W[\chi^+,\psi^+]\,. \qquad (2.189)$$

Other relations between the coefficients C and D can be deduced by considering the action of the transformations given in (2.181) and (2.182) on the solutions $\psi^\pm, \chi^\pm$. One finds

$$\hat{\Lambda}\psi^\pm(x,E,l) = \psi^\mp(x,E,l)\,, \qquad \hat{\Lambda}\chi^\pm(x,E,l) = \chi^\pm(x,E,l)\,, \qquad (2.190)$$

$$\hat{\Omega}\psi^\pm(x,E,l) = q_0^{l+1}\psi^\pm(x,E,l)\,, \qquad \hat{\Omega}\chi^+(x,E,l) = -iq_0^{\frac{1}{2}}\chi^-(x,E,l)\,, \qquad (2.191)$$

and also the following identity where $u(E,l)$ is an unknown function that is not important for our purposes

$$\hat{\Omega}\chi^-(x,E,l) = -iq_0^{\frac{1}{2}}\chi^+(x,E,l) + u(E,l)\chi^-(x,E,l)\,. \qquad (2.192)$$

If we apply $\hat{\Omega}$ to the equation (2.188) we get

$$\begin{aligned} q_0^{l+1}\psi^+(x,E,l) = &-iq^{\frac{1}{2}} C(q_0^{-2}E,l)\,\chi^-(x,E,l) - iq_0^{\frac{1}{2}} D(q_0^{-2}E,l)\,\chi^+(x,E,l) \\ &+ u(E,l)\,D(q_0^{-2}E,l)\,\chi^-(x,E,l)\,. \end{aligned} \qquad (2.193)$$

---

[21]We have chosen almost the same letter q_0 for $e^{\frac{i\pi}{\alpha+1}}$ as for the anisotropy q of the XXZ model, since they turn out to coincide.

Equating the LHS of the last equation with (2.188), we obtain by comparing the prefactors in front of χ^+ (possible due to the linear independence of the solutions $\{\chi^+, \chi^-\}$) that

$$C(E, l) = -\mathrm{i} q_0^{-l-\frac{1}{2}} D(q_0^{-2} E, l) \,. \tag{2.194}$$

Substituting this into the $\hat{\Lambda}$ transformed version of (2.188), yields

$$\psi^- = -\mathrm{i} q_0^{l+\frac{1}{2}} D(q_0^{-2} E, -l-1) \chi^+ + D(E, -l-1) \chi^- \,. \tag{2.195}$$

Having all these identities at hand, we can now derive the quantum Wronskian relation for the connection coefficients. We start by inserting (2.195) into (2.186):

$$2\mathrm{i} \left(q_0^{l+\frac{1}{2}} - q_0^{-l-\frac{1}{2}} \right) = -\mathrm{i} q_0^{l+\frac{1}{2}} D(q_0^{-2} E, -l-1) W[\psi^+, \chi^+] + D(E, -l-1) W[\psi^+, \chi^-] \,. \tag{2.196}$$

The first factor can be rewritten by using (2.189). For the second factor we insert (2.188) and further apply (2.187):

$$2\mathrm{i} \left(q_0^{l+\frac{1}{2}} - q_0^{-l-\frac{1}{2}} \right) = 2\mathrm{i} q_0^{l+\frac{1}{2}} D(q_0^{-2} E, -l-1) D(E, l) + 2 D(E, -l-1) C(E, l) \,. \tag{2.197}$$

Keeping in mind (2.194) one obtains

$$2\mathrm{i} \left(q_0^{l+\frac{1}{2}} - q_0^{-l-\frac{1}{2}} \right) = 2\mathrm{i} q_0^{l+\frac{1}{2}} D(q_0^{-2} E, -l-1) D(E, l) - 2\mathrm{i} q_0^{-l-\frac{1}{2}} D(E, -l-1) D(q_0^{-2} E, l) \,. \tag{2.198}$$

Finally, we just have to do some cosmetic manipulations: namely, dividing by $2\mathrm{i}$ and shift $E \mapsto q_0 E$, to arrive at

$$q_0^{l+\frac{1}{2}} - q_0^{-l-\frac{1}{2}} = q_0^{l+\frac{1}{2}} D(q_0 E, l) D(q_0^{-1} E, -l-1) - q_0^{-l-\frac{1}{2}} D(q_0^{-1} E, l) D(q_0 E, -l-1) \,. \tag{2.199}$$

Hence, we obtain the same functional relation as (2.180) — without the factor $(1+\zeta)^L$ — upon the following identifications

$$\operatorname*{slim}_{L \to \infty} A_+(\zeta) = D(E, l) = D_+(E, l) \,, \qquad \operatorname*{slim}_{L \to \infty} A_-(\zeta) = D(E, -l-1) = D_-(E, l) \,, \tag{2.200}$$

and

$$\zeta = (L/L_0)^{\left(\frac{2\gamma}{\pi} - 2\right)} E \,, \qquad S_z + \frac{\pi \mathbf{k}}{\gamma} = l + \frac{1}{2} \,, \qquad q = q_0 \,, \qquad \left(\gamma = \frac{\pi}{1+\alpha} \right) \,. \tag{2.201}$$

We have proven that $D_\pm$ satisfies the same functional relation that appears in the scaling limit of (2.180). One can further show that the analytic properties and asymptotic behaviour of the functions $D_\pm$ and $\operatorname{slim}_{L \to \infty} A_\pm$ are also the same [96, 29]. It turns out that the quantum Wronskian relation combined with the analytic and asymptotic properties determines the functions uniquely and so their equality follows.

Let us sketch how the uniqueness can be easily deduced from the ODE side. By its definition, the spectral determinant $D_+(E,l)$ is an entire function in E while it is meromorphic in l and analytic for $\Re e(l) > -\frac{1}{2}$. A detailed WKB analysis determines the asymptotic behaviour in E and l. Due to its analyticity in E, the logarithm of the spectral determinant can be expanded in a power series in E:

$$\log(D_+(E,l)) = \sum_{s=1}^{\infty} J_s(l)\, E^s \tag{2.202}$$

with a finite radius of convergence. It can be plugged into the quantum Wronkian relation (2.199). This yields a recursive sequence of equations for the $J_s(l)$. For example, the first one reads

$$J_1(l)\sin\left(\frac{\pi\,(2l+3)}{2\alpha+2}\right) + J_1(-l-1)\sin\left(\frac{\pi(2l-1)}{2\alpha+2}\right) = 0\,. \tag{2.203}$$

The punch line is that the above equation and also all others of higher order are simply Riemann Hilbert problems as $J_s(l)$ is analytic for $\Re e(l) > -\frac{1}{2}$. The solution of a Riemann Hilbert problem is unique if one takes into account the known asymptotic. Hence, all coefficients are fixed, and so is the function.

On the side of the IQFT/lattice, the formulation of the Bethe ansatz equations as non-linear integral equation (NLIE) is needed to determine the analytical properties of $A_{\pm}(\zeta)$ defined in (2.170), e.g. see [98] for the lattice. The asymptotics in l can then be derived from the Wiener Hopf analysis of a linearized version of the NLIE in the large l limit; see [96] for details.

For practical purposes, having at hand a way of numerically validating the ODE/IQFT correspondence is often extremely useful. A suitable approach is based on the study of what we refer to as the sum rules. This was originally introduced in the works [91, 55] and we give a brief description for the XXZ model. One expands the logarithm of the LHS of (2.171) and compares it with (2.202) which yields

$$\operatorname*{slim}_{L\to\infty}\left(\frac{L}{L_0}\right)^{-2s\left(\frac{\gamma}{\pi}-1\right)} h_s^{(L)} = J_s\,, \tag{2.204}$$

and we defined

$$h_j^{(L)} = \frac{1}{j}\sum_{m=1}^{M}\zeta_m^{-j}. \tag{2.205}$$

Both sides of the above formula can be computed numerically and verified that they are equal to one another. The relation (2.204) and its variants are known as the sum rules. They turn out to be very important tools for deducing the ODE governing the scaling of a given integrable lattice model.

The sum rules sometimes meet technical problems related to the numerical evaluation of the limit in the LHS of (2.204). An alternative approach is to focus on the scaling behaviour of individual roots. Note that the Bethe roots are the zeros of the function (2.170). Hence, their scaled version should become the zeros of the spectral determinant, i.e. the eigenvalues

E_k of the Sturm-Liuville operator (2.173). The latter can be easily computed numerically by integrating the ODE. Therefore, one can check if the following relation holds true

$$\lim_{L \to \infty} \left(\frac{L}{L_0} \right)^{2 - \frac{2\gamma}{\pi}} \zeta_k = E_k \qquad (2.206)$$

where ζ_k is the kth smallest Bethe root, equivalently, in the $u = -\frac{1}{2} \log(\zeta)$ plane the root with the kth largest real part.

3 | STAGGERED VERTEX MODELS

This chapter is based on the author's publication [32].

Yang-Baxter integrable lattice models with periodically repeating inhomogeneities (or so-called staggered models) have proven to be applicable to a wide range of problems. Apart from the construction of spin chains with larger unit cells [99, 100], they are used, for example, in the quantum transfer matrix approach to thermodynamics [101] or to formulate the Potts model as a $\mathbb{Z}_2$-staggered six-vertex model [102]. They also serve as lattice regularisation of field theories such as the principal chiral model [103, 104] or can be utilised to study integrable perturbations of CFTs [105].

In this chapter, we take a different perspective on staggered models by reformulating these as homogeneous models. This is interesting as staggered models naturally possess two different classes of integrals of motions: one stemming from the product of elementary transfer matrices and the other from the quotient. The definition of the latter is not directly possible from the perspective of a homogeneous model. Further, we will see in subsequent chapters that the definition/identification of the scaling limit of certain integrable lattice models requires operators of both families. Namely, the Hamiltonian from the 'product family' and the so-called quasi-momentum operator from the 'quotient family'. We hope that the presented alternative approach facilitates the study of the critical behaviour of homogeneous models.

We start this chapter by constructing *composite* $\mathcal{R}$-matrices using the co-multiplication property of the Yang-Baxter algebra. These $\mathcal{R}$-matrices satisfy a generalised Yang-Baxter equation (3.2) and depend on the original inhomogeneities through additional arguments. For periodic BCs, this allows us to define a homogeneous transfer matrix generating the two classes of integrals of motions.

Then, we generalise our findings to the case of open BCs, where we express composite boundary matrices in terms of the elementary ones. Depending on the properties of the elementary R-matrices (and unlike in the periodic case), we identify two different choices of the staggering leading to a transfer matrix constructed from the composite $\mathcal{R}$-matrix and boundary matrices, which generates a Hamiltonian with local interactions (similar as in the works [106, 107]). For one of these choices, a second homogeneous transfer matrix with boundary matrices satisfying a different reflection equation generates the quasi-momentum. The commutativity of these objects is guaranteed by a set of intertwining relations between the two sets of boundary matrices.
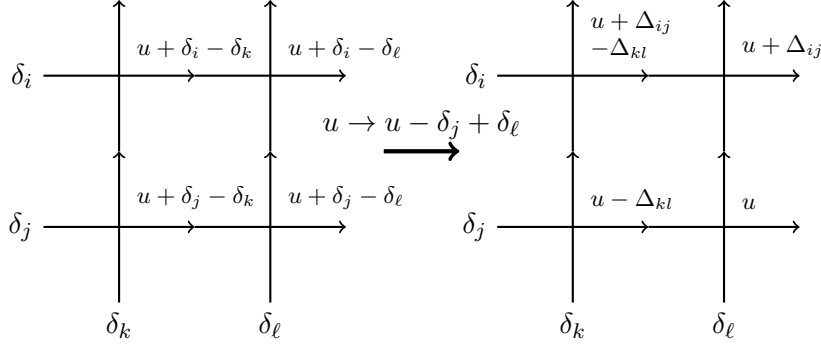
Figure 3.1: The composite $\mathcal{R}$-matrix (3.1), where $\Delta_{ij} = \delta_i - \delta_j$.

3.1 The composite $\mathcal{R}$-matrix

The coproduct structure of the Yang-Baxter algebra allows one to extend a solution R of the YBE (2.100) acting on $\mathcal{V} \otimes \mathcal{V}$ to one acting on $(\mathcal{V} \otimes \mathcal{V}) \otimes (\mathcal{V} \otimes \mathcal{V})$ (or, more generally, the n-fold tensor products of the vector space $\mathcal{V}$). We define the composite $\mathcal{R}$-matrix to be

$$\mathcal{R}_{i,j|k,\ell}(u, \Delta_{ij}, \Delta_{k\ell}) = R_{i,\ell}(u + \Delta_{ij})R_{i,k}(u + \Delta_{ij} - \Delta_{k\ell})R_{j,\ell}(u)R_{j,k}(u - \Delta_{k\ell}), \qquad (3.1)$$

where $\Delta_{ij}, \Delta_{k\ell}$ are arbitrary parameters. The explicit form in equation (3.1) is motivated by a general choice of inhomogeneities in both the horizontal and vertical direction as displayed in Figure 3.1. The introduced index notation, including the vertical line, should emphasise that $\mathcal{R}_{i,j|k,\ell}$ acts on the tensor product of the two copies $(\mathcal{V}_i \otimes \mathcal{V}_j)$ and $(\mathcal{V}_k \otimes \mathcal{V}_\ell)$. By construction, $\mathcal{R}$ satisfies the generalized Yang-Baxter equation

$$\begin{aligned}
\mathcal{R}_{i,j|k,\ell}(u - v, \Delta_{ij}, \Delta_{k\ell})\mathcal{R}_{i,j|m,n}(u, \Delta_{ij}, \Delta_{mn})\mathcal{R}_{k,\ell|m,n}(v, \Delta_{k\ell}, \Delta_{mn}) = \\
\mathcal{R}_{k,\ell|m,n}(v, \Delta_{k\ell}, \Delta_{mn})\mathcal{R}_{i,j|m,n}(u, \Delta_{ij}, \Delta_{mn})\mathcal{R}_{i,j|k,\ell}(u - v, \Delta_{ij}, \Delta_{k\ell}),
\end{aligned} \qquad (3.2)$$

and therefore allows for the definition of commuting transfer matrices similar to the procedure explained in section 2.4. Since this construction relies on the properties (2.102)-(2.106) of the elementary matrix $R(u)$ it is natural to ask which of these are inherited to the $\mathcal{R}$-matrix. One can work out that the $\mathcal{R}$-matrix obeys the following properties

$$\mathcal{R}_{i,j|k,\ell}(0, \Delta, \Delta) = \xi^2(0)\xi(\Delta)\xi(-\Delta)\, \mathcal{P}_{i,j|k,\ell}, \qquad (3.3)$$

$$\mathcal{R}_{i,j|k,\ell}(u, \Delta_{ij}, \Delta_{k\ell})\mathcal{R}_{k,\ell|i,j}(-u, \Delta_{k\ell}, \Delta_{ij}) = \Xi(u, \Delta_{ij}, \Delta_{k\ell})\, \mathbf{1}, \qquad (3.4)$$

$$\mathcal{R}_{i,j|k,\ell}^{t_i t_j t_k t_\ell}(u, \Delta_{ij}, \Delta_{k\ell}) = \mathcal{R}_{k,\ell|i,j}(u, -\Delta_{k\ell}, -\Delta_{ij}), \qquad (3.5)$$

$$\mathcal{M}_{i,j}^{-1}\mathcal{R}_{i,j|k,\ell}(u, \Delta_{ij}, \Delta_{k\ell})\mathcal{M}_{i,j} = \mathcal{M}_{k,\ell}\mathcal{R}_{i,j|k,\ell}(u, \Delta_{ij}, \Delta_{k\ell})\mathcal{M}_{k,\ell}^{-1}, \qquad (3.6)$$

$$\mathcal{U}_{i,j}^{-1}\mathcal{R}_{i,j|k,\ell}(u, \Delta_{ij}, \Delta_{k\ell})\mathcal{U}_{i,j} = \mathcal{U}_{k,\ell}\mathcal{R}_{i,j|k,\ell}(u, \Delta_{ij}, \Delta_{k\ell})\mathcal{U}_{k,\ell}^{-1}, \qquad (3.7)$$

$$\mathcal{R}_{i,j|k,\ell}(u + \mathrm{p}, \Delta_{ij}, \Delta_{k\ell}) = \mathcal{U}_{i,j}\mathcal{R}_{i,j|k\ell}(u, \Delta_{ij}, \Delta_{k\ell})\mathcal{U}_{i,j}^{-1}, \qquad (3.8)$$

and

$$\mathcal{R}_{i,j|k,\ell}^{t_i t_j}(u, \Delta_{ij}, \Delta_{k\ell})\mathcal{M}_{i,j}\mathcal{R}_{i,j|k,\ell}^{t_k t_\ell}(-u - 2\eta, -\Delta_{ij}, -\Delta_{k\ell})\mathcal{M}_{i,j}^{-1} = \Xi(u + \eta, \Delta_{ij}, \Delta_{k\ell})\, \mathbf{1}. \quad (3.9)$$

The equation (3.3) is a regularity property (with a different normalization) where $\mathcal{P}_{i,j|k,\ell}$ is the enlarged permutation operator acting on the vector $(a \otimes b) \otimes (c \otimes d) \in (\mathcal{V}_i \otimes \mathcal{V}_j) \otimes (\mathcal{V}_k \otimes \mathcal{V}_\ell)$

as

$$\mathcal{P}_{i,j|k,\ell}(a \otimes b) \otimes (c \otimes d) = (c \otimes d) \otimes (a \otimes b).$$

The equation (3.4) is a unitarity condition where the proportionality constant reads as

$$\Xi(u, \Delta_{ij}, \Delta_{k\ell}) = \xi(u + \Delta_{ij})\xi(-u - \Delta_{ij})\xi(u + \Delta_{ij} - \Delta_{k\ell})\xi(-u - \Delta_{ij} + \Delta_{k\ell})$$
$$\times \xi(u)\xi(-u)\xi(u - \Delta_{k\ell})\xi(-u + \Delta_{k\ell}).$$

The third property (3.5) is a *generalized* PT-symmetry. Note the sign difference of the parameters in $\mathcal{R}$ on the right and left-hand side. This can be traced back to a reordering caused by the transposition:

$$\mathcal{R}_{i,j|k,\ell}^{t_i t_j t_k t_\ell}(u, \Delta_{ij}, \Delta_{k\ell}) = (R_{i,\ell}(u + \Delta_{ij})R_{i,k}(u + \Delta_{ij} - \Delta_{k\ell})R_{j,\ell}(u)R_{j,k}(u - \Delta_{k\ell}))^{t_i t_j t_k t_\ell}$$
$$= R_{j,k}^{t_j t_k}(u - \Delta_{k\ell})R_{i,k}^{t_i t_k}(u + \Delta_{ij} - \Delta_{k\ell})R_{j,\ell}^{t_j t_\ell}(u)R_{i,\ell}^{t_i t_\ell}(u + \Delta_{ij})$$
$$= R_{k,j}(u - \Delta_{k\ell})R_{k,i}(u + \Delta_{ij} - \Delta_{k\ell})R_{\ell,j}(u)R_{\ell,i}(u + \Delta_{ij})$$
$$= \mathcal{R}_{k,\ell|i,j}(u, -\Delta_{k\ell}, -\Delta_{ij}).$$

As the PT-symmetry is related to the crossing unitary, the $\mathcal{R}$-matrix also satisfies a *generalized* crossing unitarity given in the equation (3.9) where $\mathcal{M}_{i,j} = M_i M_j$.

Finally, also the quasi-periodicity (2.106) and the symmetry relations can be directly transferred to the $\mathcal{R}$-matrix, yielding equations (3.6)-(3.8) where $\mathcal{U}_{i,j} = U_i U_j$.

3.2 STAGGERED VERTEX MODELS WITH PERIODIC BCS

Let us now construct $\mathbb{Z}_2$-staggered models with periodic BCs. Here, we show how the formulations in terms of the elementary and the composite R-matrices are related.

Consider the transfer matrix (2.110) with $2L$ sites ($L \in \mathbb{N}$) and periodic BCs. Further, let us choose on the even sites δ_1 and on the odd sites δ_2 as the inhomogeneities. In addition to this staggering, we also induce a staggering in the auxiliary direction by multiplying two transfer matrices with different shifted spectral parameters $u + \delta_0, u + \delta_{\bar{0}}$ together. This defines the composite transfer matrix $\mathbb{T}^{\text{pbc}}$ (0 and $\bar{0}$ label different auxiliary spaces)

$$\mathbb{T}^{\text{pbc}}(u, \{\delta_0, \delta_{\bar{0}}, \delta_1, \delta_2\}) = \mathfrak{t}^{\text{pbc}}(u + \delta_0, \{\delta_1, \delta_2\}) \, \mathfrak{t}^{\text{pbc}}(u + \delta_{\bar{0}}, \{\delta_1, \delta_2\}) \qquad (3.10)$$

$$= \text{Tr}_0 \bigg(R_{0,2L}(u + \delta_0 + \delta_1)R_{0,2L-1}(u + \delta_0 + \delta_2) \dots R_{0,1}(u + \delta_0 + \delta_2) \bigg)$$

$$\times \text{Tr}_{\bar{0}} \bigg(R_{\bar{0},2L}(u + \delta_{\bar{0}} + \delta_1)R_{\bar{0},2L-1}(u + \delta_{\bar{0}} + \delta_2) \dots R_{\bar{0},1}(u + \delta_{\bar{0}} + \delta_2) \bigg).$$

We can combine the two traces into one over an enlarged auxiliary space. By this and reordering the R-matrices, we obtain

$$\mathbb{T}^{\text{pbc}}(u, \{\delta_0, \delta_{\bar{0}}, \delta_1, \delta_2\}) =$$

$$\text{Tr}_{0\bar{0}} \bigg(R_{0,2L}(u + \delta_0 + \delta_1)R_{\bar{0},2L}(u + \delta_{\bar{0}} + \delta_1)R_{0,2L-1}(u + \delta_0 + \delta_2)R_{\bar{0},2L-1}(u + \delta_{\bar{0}} + \delta_2) \dots$$

$$\dots R_{0,2}(u + \delta_0 + \delta_1)R_{\bar{0},1}(u + \delta_{\bar{0}} + \delta_2)R_{0,1}(u + \delta_0 + \delta_2)R_{\bar{0},1}(u + \delta_{\bar{0}} + \delta_2) \bigg).$$

The products of four R-matrices appearing in each row can be expressed in terms of the composite $\mathcal{R}$-matrix (3.1). By shifting the spectral parameter as $u \to u - \delta_{\bar{0}} - \delta_1$, we obtain a *homogeneous* transfer matrix

$$\mathbb{T}^{\mathrm{pbc}}(u, \{\Delta_{0\bar{0}}, \Delta_{12}\}) = \mathrm{Tr}_{0\bar{0}}\left(\mathcal{R}_{0,\bar{0}|2L-1,2L}(u, \Delta_{0\bar{0}}, \Delta_{12}) \ldots \mathcal{R}_{0,\bar{0}|1,2}(u, \Delta_{0\bar{0}}, \Delta_{12})\right). \quad (3.11)$$

For the physical interpretation as a lattice model with finite range interactions, additional conditions need to be satisfied. Typically, locality can be derived from the regularity property of the R-matrix, i.e. it becomes a permutation operator at a shift point $u = u_0$. In the case at hand, (3.3), we have $u_0 = 0$ and we need to tune the staggering parameters such that

$$\Delta_{0\bar{0}} = \Delta_{12} \equiv \Delta. \quad (3.12)$$

With this constraint, and under the assumption that R is differentiable at $\pm\Delta$, a Hamiltonian which couples the degrees of freedom from nearest neighbour quantum spaces $\mathscr{V} \otimes \mathscr{V}$ is obtained by

$$\mathbb{H}^{\mathrm{pbc}} \propto \left. \frac{\partial}{\partial u} \log(\mathbb{T}^{\mathrm{pbc}}(u, \Delta, \Delta)) \right|_{u=0}. \quad (3.13)$$

The staggering in the auxiliary direction allows one to construct another generating function of commuting operators: instead of (3.10) we can consider the quotient of single row transfer matrices

$$\frac{\mathbb{t}^{\mathrm{pbc}}(u + \delta_{\bar{0}}, \{\delta_1, \delta_2\})}{\mathbb{t}^{\mathrm{pbc}}(u + \delta_0, \{\delta_1, \delta_2\})}.$$

As done for the product of transfer matrices, we shift the spectral parameter $u \to u - \delta_{\bar{0}} - \delta_1$, leading to

$$\frac{\mathbb{t}^{\mathrm{pbc}}(u - \delta_1, \{\delta_1, \delta_2\})}{\mathbb{t}^{\mathrm{pbc}}(u + \Delta_{0\bar{0}} - \delta_1, \{\delta_1, \delta_2\})}. \quad (3.14)$$

Restricting the staggering parameters $\delta_1, \delta_2, \delta_0$ and $\delta_{\bar{0}}$ to be compatible with (3.12) and taking the logarithm of this operator at the shift point, $u_0 = 0$, we obtain the so-called quasi-momentum operator

$$\mathbb{B}^{\mathrm{pbc}} = \log\left[\frac{\mathbb{t}^{\mathrm{pbc}}(-\delta_1, \{\delta_1, \delta_2\})}{\mathbb{t}^{\mathrm{pbc}}(-\delta_2, \{\delta_1, \delta_2\})}\right]. \quad (3.15)$$

This operator has proven to be essential for the characterization of the low energy effective behaviour of several staggered vertex models, see for example [24, 53, 54, 108, 31], and further has found recent application as a Floquet Hamiltonian [109].

We now want to generate the quasi-momentum from an operator constructed from the composite $\mathcal{R}$-matrix (3.1). For that, let us resolve the inverse of the single row transfer matrix (2.110) in (3.15). By using the regularity and unitarity of the R-matrix we obtain

$$\left(\mathbb{t}^{\mathrm{pbc}}(-\delta_2, \{\delta_1, \delta_2\})\right)^{-1} \propto \mathrm{Tr}_0\left(R_{1,0}(0)R_{2,0}(-\Delta) \ldots R_{2L-1,0}(0)R_{2L,0}(-\Delta)\right). \quad (3.16)$$

By defining

$$\mathbb{K}^{\text{pbc}}(u) = \text{Tr}_0 \left(R_{1,0}(-u)R_{2,0}(-u-\Delta)\,...\,R_{2L-1,0}(-u)R_{2L,0}(-u-\Delta) \right)$$
$$\times \text{Tr}_{\overline{0}} \left(R_{\overline{0},2L}(u)R_{\overline{0},2L-1}(u-\Delta)\,...\,R_{\overline{0},2}(u)R_{\overline{0},1}(u-\Delta) \right) ,$$

we obtain a *product* of R-matrices depending on a spectral parameter which, after taking the logarithm, becomes (3.15) at the shift point up to a different normalisation. Using the crossing symmetry (2.104) and expressing the result in terms of the composite $\mathcal{R}$-matrices we find:

$$
\begin{aligned}
\mathbb{K}^{\text{pbc}}(u) &= \text{Tr}_{0\overline{0}} \big(R_{0,2L}(u+\Delta-\eta)R_{0,2L-1}(u-\eta)\,...\,R_{0,2}(u+\Delta-\eta)R_{0,1}(u-\eta) \\
&\qquad\quad \times R_{\overline{0},2L}(u)R_{\overline{0},2L-1}(u-\Delta)\,...\,R_{\overline{0},2}(u)R_{\overline{0},1}(u-\Delta) \big) \\
&= \text{Tr}_{0\overline{0}} \Big(\mathcal{R}_{0,\overline{0}|2L-1,2L}(u,\Delta-\eta,\Delta)\,...\,\mathcal{R}_{0,\overline{0}|1,2}(u,\Delta-\eta,\Delta) \Big) \\
&= \mathbb{T}^{\text{pbc}} \left(u, \{\Delta-\eta,\Delta\} \right) .
\end{aligned}
\tag{3.17}
$$

Note that this becomes the product of two single row transfer matrices with arguments differing by the crossing parameter η in the homogeneous limit, $\Delta \to 0$,

$$\lim_{\Delta\to 0} \mathbb{K}^{\text{pbc}}(u) = \text{Tr}_{0\overline{0}} \big(R_{0,2L}(u-\eta)R_{\overline{0},2L}(u)\,...\,R_{0,1}(u-\eta)R_{\overline{0},1}(u) \big) = \mathfrak{t}^{\text{pbc}}(u-\eta)\,\mathfrak{t}^{\text{pbc}}(u) .$$
$$\tag{3.18}$$

This product can be related to the higher-spin transfer matrices through the T-system bilinear functional relations [110].

In summary, the transfer matrices

$$\mathbb{T}^{\text{pbc}}(u, \{\theta,\Delta\}) = \text{Tr}_{0\overline{0}} \Big(\mathcal{R}_{0,\overline{0}|2L-1,2L}(u,\theta,\Delta)\,...\,\mathcal{R}_{0,\overline{0}|1,2}(u,\theta,\Delta) \Big) \tag{3.19}$$

provide a unified framework generating both local integrals of motion such as the Hamiltonian under the locality condition (3.12), i.e. $\theta = \Delta$, and the quasi-momentum (3.15) for $\theta = \Delta - \eta$. Note that the third argument of all $\mathcal{R}$-matrices in (3.19) coincide. Therefore, the generalized YBE (3.2) ensure commutativity of $\mathbb{T}^{\text{pbc}}(u, \{\theta,\Delta\})$ for different u and θ (which includes $\mathbb{K}^{\text{pbc}}(u)$).

3.3 COMPOSITE PICTURE FOR OPEN MODELS

We now want to address the question to which extent this procedure can be applied to construct staggered models with open BCs. The strategy is the same: we begin by considering the product of two transfer matrices (2.122) built out of generic R and K-matrices satisfying the Yang-Baxter and reflection equations, respectively, i.e.

$$
\begin{aligned}
\mathbb{T}(u, \{\delta_0, \delta_{\overline{0}}, \delta_1, \delta_2\}) &= \text{Tr}_0 \Big(X_0(u+\delta_0) \Big) \text{Tr}_{\overline{0}} \Big(Y_{\overline{0}}(u+\delta_{\overline{0}}) \Big) \\
&= \text{Tr}_{0\overline{0}} \Big(X_0(u+\delta_0) Y_{\overline{0}}^{t_{\overline{0}}}(u+\delta_{\overline{0}}) \Big) ,
\end{aligned}
\tag{3.20}
$$
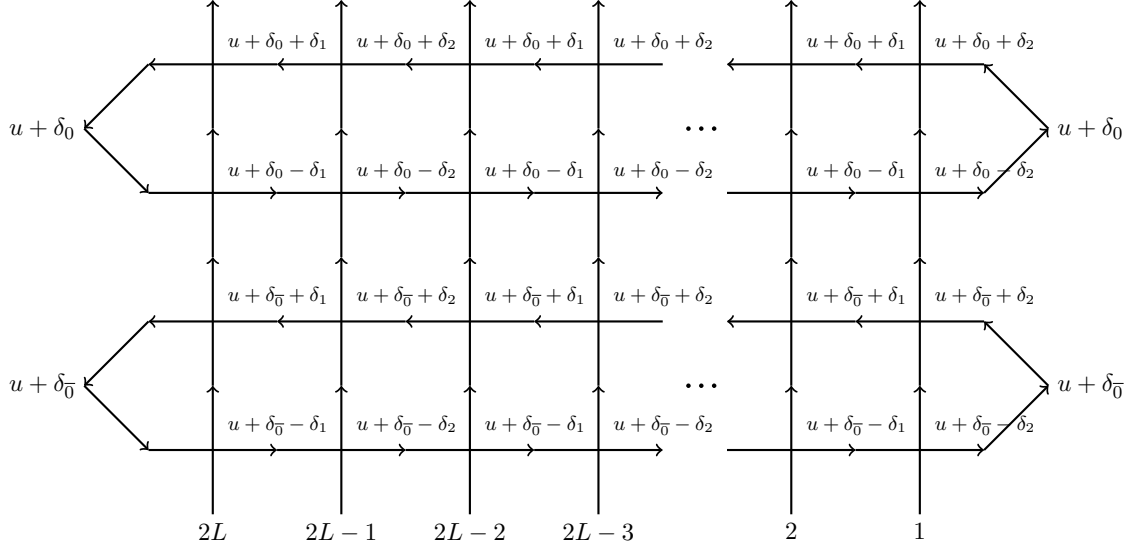
Figure 3.2: Graphical representation of the product (3.20) of two transfer matrices with arbitrary $\mathbb{Z}_2$ staggering by using the conventions defined in Figures 2.3 and 2.5.

where for presentational reasons, we have defined

$$X_0(u) \equiv K_0^L(u)T_0(u, \{\delta_1, \delta_2\})K_0^R(u)T_0^{-1}(-u, \{\delta_1, \delta_2\}),$$
$$Y_{\overline{0}}(u) \equiv T_{\overline{0}}(u, \{\delta_1, \delta_2\})K_{\overline{0}}^R(u)T_{\overline{0}}^{-1}(-u, \{\delta_1, \delta_2\})K_{\overline{0}}^L(u).$$
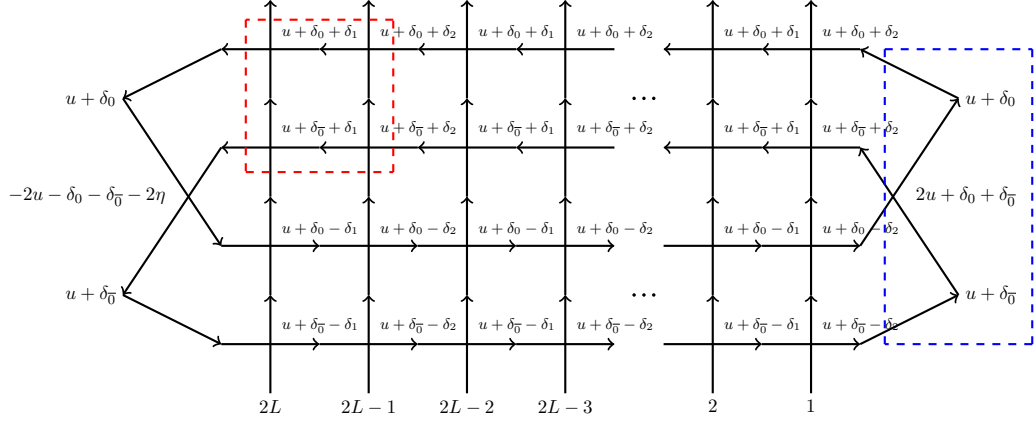
For a graphical representation of $\mathbb{T}(u)$, see Figure 3.2. Inserting a crossing unitarity (2.105), using the cyclicity of the trace and applying the PT-symmetry, we obtain

$$\mathbb{T}(u, \{\delta_0, \delta_{\overline{0}}, \delta_1, \delta_2\})\xi(2u + \delta_0 + \delta_{\overline{0}} + \eta)\xi(-2u - \delta_0 - \delta_{\overline{0}} - \eta)$$
$$= \text{Tr}_{0\overline{0}}\bigg(M_0 R_{0,\overline{0}}(-2u - \delta_0 - \delta_{\overline{0}} - 2\eta)M_0^{-1}X_0(u + \delta_0))R_{\overline{0},0}(2u + \delta_0 + \delta_{\overline{0}})Y_{\overline{0}}(u + \delta_{\overline{0}})\bigg)$$
$$= \text{Tr}_{0\overline{0}}\bigg(M_0 R_{0,\overline{0}}(-2u - \delta_0 - \delta_{\overline{0}} - 2\eta)M_0^{-1}K_0^L(u + \delta_0)$$
$$\times T_0(u + \delta_0, \{\delta_1, \delta_2\})K_0^R(u + \delta_0)T_0^{-1}(-u - \delta_0, \{\delta_1, \delta_2\})R_{\overline{0},0}(2u + \delta_0 + \delta_{\overline{0}})$$
$$\times T_{\overline{0}}(u + \delta_{\overline{0}}, \{\delta_1, \delta_2\})K_{\overline{0}}^R(u + \delta_{\overline{0}})T_{\overline{0}}^{-1}(-u - \delta_{\overline{0}}, \{\delta_1, \delta_2\})K_{\overline{0}}^L(u + \delta_{\overline{0}})\bigg).$$

Now we use the equation (2.107b) and rearrange the K-matrices to get:

$$\mathbb{T}(u, \{\delta_0, \delta_{\overline{0}}, \delta_1, \delta_2\}) = \text{Tr}_{0\overline{0}}\bigg(K_{\overline{0}}^L(u + \delta_{\overline{0}})M_0 R_{0,\overline{0}}(-2u - \delta_0 - \delta_{\overline{0}} - 2\eta)M_0^{-1}K_0^L(u + \delta_0)$$
$$\times T_0(u + \delta_0, \{\delta_1, \delta_2\})T_{\overline{0}}(u + \delta_{\overline{0}}, \{\delta_1, \delta_2\})$$
$$\times K_0^R(u + \delta_0)R_{\overline{0},0}(2u + \delta_0 + \delta_{\overline{0}})K_{\overline{0}}^R(u + \delta_{\overline{0}})$$
$$\times T_0^{-1}(-u - \delta_0, \{\delta_1, \delta_2\})T_{\overline{0}}^{-1}(-u - \delta_{\overline{0}}, \{\delta_1, \delta_2\})\bigg)$$
$$\times \xi^{-1}(2u + \delta_0 + \delta_{\overline{0}} + \eta)\xi^{-1}(-2u - \delta_0 - \delta_{\overline{0}} - \eta).$$

Figure 3.3: Graphical representation of the product of transfer matrix (3.21) after the merging procedure. The composite $\mathcal{R}$-matrix here is given by four vertices as in Figure 3.1 as indicated as an example by the red box. Further, we see we obtain some enlarged boundary matrices, as emphasized by the blue box.

Finally, using the expression for the monodromy matrices in terms of the elementary R-matrices, this transfer matrix can be represented graphically as shown in Figure 3.3 (up to a scalar factor). Clearly, this can be expressed in terms of the composite $\mathcal{R}$-matrices (3.1) giving

$$
\begin{aligned}
\mathbb{T}(u, \{\delta_0, \delta_{\overline{0}}, \delta_1, \delta_2\}) = {}& c_\tau(u + \delta_0, \{\delta_1, \delta_2\}) c_\tau(u + \delta_{\overline{0}}, \{\delta_1, \delta_2\}) \\
& \times \xi^{-1}(-2u - \delta_0 - \delta_{\overline{0}} - \eta) \xi^{-1}(2u + \delta_0 + \delta_{\overline{0}} + \eta) \\
& \times \mathrm{Tr}_{0\overline{0}}\bigg(K_{\overline{0}}^L(u + \delta_{\overline{0}}) M_0 R_{0,\overline{0}}(-2u - \delta_0 - \delta_{\overline{0}} - 2\eta) M_0^{-1} K_0^L(u + \delta_0) \\
& \qquad \times \mathcal{R}_{0,\overline{0}|2L-12L}(u + \delta_{\overline{0}} + \delta_1, \Delta_{0\overline{0}}, \Delta_{12}) ... \mathcal{R}_{0,\overline{0}|1,2}(u + \delta_{\overline{0}} + \delta_1, \Delta_{0\overline{0}}, \Delta_{12}) \\
& \qquad \times K_0^R(u + \delta_0) R_{\overline{0},0}(2u + \delta_0 + \delta_{\overline{0}}) K_{\overline{0}}^R(u + \delta_{\overline{0}}) \\
& \qquad \times \mathcal{R}_{1,2|\overline{0},0}(u + \delta_0 - \delta_1, \Delta_{12}, \Delta_{0\overline{0}}) ... \mathcal{R}_{2L-1,2L|\overline{0},0}(u + \delta_0 - \delta_1, \Delta_{12}, \Delta_{0\overline{0}}) \bigg),
\end{aligned}
\tag{3.21}
$$

where the scalar function c_τ originates from resolving the inverse of the monodromy matrix. It reads

$$
c_\tau(u, \{\delta_1, \delta_2\}) = [\xi(-u + \delta_1)\xi(-u + \delta_2)\xi(u - \delta_1)\xi(u - \delta_2)]^{-L} .
\tag{3.22}
$$

3.3.1 Local interactions I: alternating staggering

As for periodic BCs, the staggering parameters $\{\delta_0, \delta_{\overline{0}}, \delta_1, \delta_2\}$ have to satisfy constraints to generate local interactions from this open boundary transfer matrix. Nearest neighbour interactions between the composite degrees of freedom of the staggered model are obtained by taking the derivative (assuming all quantities to be differentiable at the corresponding points) of $\mathbb{T}(u)$ with respect to the spectral parameter [72]

$$
\mathbb{H} \propto \frac{\partial}{\partial u} \mathbb{T}\left(u, \{\delta_0, \delta_{\overline{0}}, \delta_1, \delta_2\}\right)\bigg|_{u=u_0} .
\tag{3.23}
$$
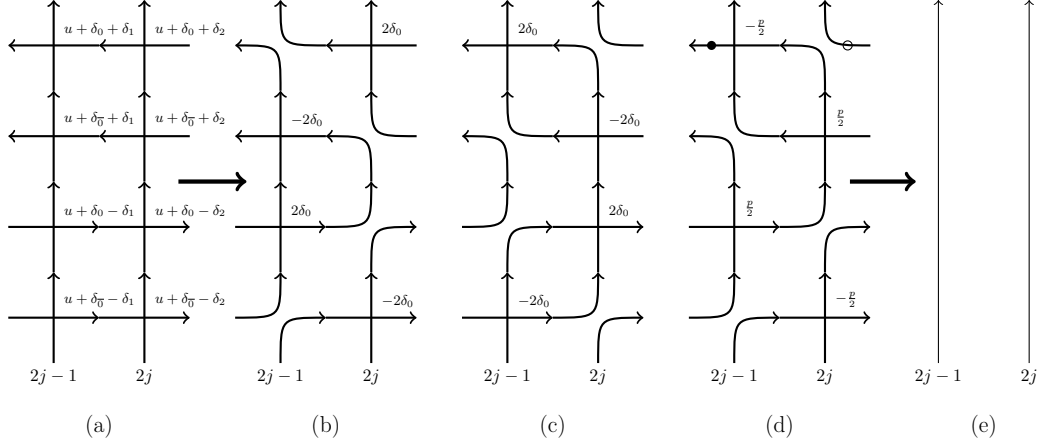
Figure 3.4: (a) To establish bulk locality at $u = 0$ the parameters $\delta_0, \delta_{\overline{0}}, \delta_1, \delta_2$ have to be fine-tuned such that the conditions i)-iii) hold. The diagrammatic schemes of the bulk elementary cells at the shift point $u = 0$ for all possible non-trivial choices of staggering are displayed in (b) & (c) (alternating case (3.24)) and (d) (quasi-periodic case (3.30)). Using the regularity (2.101), unitarity (2.102), and in (d) quasi-periodicity (2.106) of the elementary R-matrix gives the identity (e) in the bulk.

Again, locality derives from the regularity of $\mathcal{R}$. To make use of (3.3) three conditions need to be met:

i) The $\mathcal{R}$-matrices in (3.21) need to act on the same auxiliary space e.g. $\mathscr{V}_0 \otimes \mathscr{V}_{\overline{0}}$.

ii) As in the periodic case, the staggering parameters have to satisfy the constraint (3.12).

iii) The staggering parameters have to be chosen such that *all* $\mathcal{R}$ in (3.21) can simultaneously be evaluated at the shift point $u_0 = 0$.

For i) we use the identity $\mathcal{R}_{i,j|\overline{0},0} = P_{0,\overline{0}}\mathcal{R}_{i,j|0,\overline{0}}P_{0,\overline{0}}$. Conditions ii) and iii) are achieved by choosing the staggering parameters to be opposite and equal in both the horizontal and the vertical direction, i.e.

$$\delta_0 = -\delta_{\overline{0}} = \delta_1 = -\delta_2 \tag{3.24}$$

(depicted in Figure 3.4c) or the equivalent choice of parameters obtained by changing $\delta_0 \to -\delta_0$ (see Figure 3.4b). These constraints on the staggering parameters imply $\Delta_{0\overline{0}} = \Delta_{12} = 2\delta_0$ with δ_0 remaining as a *free* parameter. The resulting transfer matrix is

$$\mathbb{T}(u, \{\delta_0, -\delta_0, \delta_0, -\delta_0\}) = c_\tau(u + \delta_0, \{\delta_0, -\delta_0\})c_\tau(u - \delta_0, \{\delta_0, -\delta_0\})$$

$$\mathrm{Tr}_{0\overline{0}}\Big(\mathcal{K}_{0,\overline{0}}^L(u, 2\delta_0)\mathcal{R}_{0,\overline{0}|2L-1,2L}(u, 2\delta_0, 2\delta_0) \dots \mathcal{R}_{0,\overline{0}|1,2}(u, 2\delta_0, 2\delta_0)$$

$$\times \mathcal{K}_{0,\overline{0}}^R(u, 2\delta_0)\mathcal{R}_{1,2|0,\overline{0}}(u, 2\delta_0, 2\delta_0) \dots \mathcal{R}_{2L-1,2L|0,\overline{0}}(u, 2\delta_0, 2\delta_0)\Big),$$

where we have introduced

$$\mathcal{K}_{i,j}^R(u, 2\delta_0) = P_{i,j} K_j^R(u + \delta_0) R_{i,j}(2u) K_i^R(u - \delta_0) \,, \tag{3.25a}$$

$$\mathcal{K}_{i,j}^L(u, 2\delta_0) = \frac{1}{\xi(2u + \eta)\xi(-2u - \eta)} P_{i,j} K_j^L(u - \delta_0) M_i R_{i,j}(-2u - 2\eta) M_i^{-1} K_i^L(u + \delta_0) \,. \tag{3.25b}$$

In terms of the monodromy matrix built from the composite $\mathcal{R}$-matrices,

$$\mathcal{T}_{0,\bar{0}}(u, \Delta_{0\bar{0}}, \Delta_{12}) = \mathcal{R}_{0,\bar{0}|2L-1,2L}(u, \Delta_{0\bar{0}}, \Delta_{12}) \dots \mathcal{R}_{0,\bar{0}|1,2}(u, \Delta_{0\bar{0}}, \Delta_{12}) \,, \tag{3.26}$$

the transfer matrix for alternating staggering (3.24) is brought into its standard form (2.122)[1]

$$\begin{aligned}
\mathbb{T}^{\text{alt}}(u, 2\delta_0) &\equiv \mathbb{T}(u, \{\delta_0, -\delta_0, \delta_0, -\delta_0) \\
&= \text{Tr}_{0\bar{0}}\left(\mathcal{K}_{0,\bar{0}}^L(u, 2\delta_0) \mathcal{T}_{0,\bar{0}}(u, 2\delta_0, 2\delta_0) \mathcal{K}_{0,\bar{0}}^R(u, 2\delta_0) \mathcal{T}_{0,\bar{0}}^{-1}(-u, 2\delta_0, 2\delta_0) \right) \,.
\end{aligned} \tag{3.27}$$

Remarkably, if the $\mathcal{R}$-matrix is also quasi-periodic, the above transfer matrix possesses the following duality transformation[2]. If, we send $2\delta_0 \mapsto \mathsf{p} - 2\delta_0$, then it can be shown that $\mathbb{T}^{\text{alt}}$ is similar to itself, i.e.

$$\mathbb{T}^{\text{alt}}(u, \mathsf{p} - 2\delta_0) = \mathscr{D}\mathbb{T}^{\text{alt}}(u, 2\delta_0)\mathscr{D}^{-1} \tag{3.28}$$

with

$$\mathscr{D} = \prod_{i=1}^{L} U_{2i} \prod_{i=1}^{L} P_{2i-1,2i} R_{2i-1,2i}(2\delta_0) \,. \tag{3.29}$$

Hence, if we adjust $2\delta_0 = \frac{\mathsf{p}}{2}$, we obtain an extra symmetry as then the transfer matrix is left invariant under the action of $\mathscr{D}$. We will call this the self-dual point.

3.3.2 LOCAL INTERACTIONS II: QUASI-PERIODIC STAGGERING

Interestingly, there exists a second choice of the staggering parameters leading to a local Hamiltonian (3.23) when the elementary R-matrix is quasi-periodic (2.106), namely

$$\delta_0 = \frac{\mathsf{p}}{2}\,, \quad \delta_{\bar{0}} = 0\,, \quad \delta_1 = 0\,, \quad \delta_2 = \frac{\mathsf{p}}{2}\,, \tag{3.30}$$

which is displayed in Figure 3.4d. Again, we have to implement the same three steps to bring the transfer matrix into a form generating a local Hamiltonian: for step i), i.e. switching the auxiliary space $\mathscr{V}_{\bar{0}} \otimes \mathscr{V}_0$ to $\mathscr{V}_0 \otimes \mathscr{V}_{\bar{0}}$, we use the Yang-Baxter equation (2.100) for $v = -\mathsf{p}/2$ giving

$$\mathcal{R}_{i,j|\bar{0},0}\left(u + \frac{\mathsf{p}}{2}, -\frac{\mathsf{p}}{2}, \frac{\mathsf{p}}{2}\right) R_{0,\bar{0}}\left(-\frac{\mathsf{p}}{2}\right) = R_{0,\bar{0}}\left(-\frac{\mathsf{p}}{2}\right) \mathcal{R}_{i,j|0,\bar{0}}\left(u, -\frac{\mathsf{p}}{2}, -\frac{\mathsf{p}}{2}\right) \,. \tag{3.31}$$

---

[1]If one drops the constraint (3.24), a shift in the spectral parameter in (3.21) leads to a transfer matrix with a moving boundary [106]. This transfer matrix does not lead in general, however, to a local Hamiltonian.

[2]The same can be shown to hold true in the periodic case.

For step ii), i.e. preparing $\mathcal{R}$ such that the regularity (3.3) can be exploited, we use the quasi-periodicity of R which implies

$$\mathcal{R}_{0,\bar{0}|i,j}\left(u,\frac{\mathrm{p}}{2},-\frac{\mathrm{p}}{2}\right) = U_0\,\mathcal{R}_{0,\bar{0}|i,j}\left(u,-\frac{\mathrm{p}}{2},-\frac{\mathrm{p}}{2}\right)U_0^{-1}\,. \tag{3.32}$$

Together with the unitarity condition $R_{0,\bar{0}}(-\frac{\mathrm{p}}{2})R_{\bar{0},0}(\frac{\mathrm{p}}{2}) = \xi(\frac{\mathrm{p}}{2})\xi(-\frac{\mathrm{p}}{2})\mathbf{1}$ these identities allow us to rewrite the transfer matrix (3.21) such that also condition iii) is satisfied, i.e.

$$\mathbb{T}\left(u,\left\{\frac{\mathrm{P}}{2},0,0,\frac{\mathrm{P}}{2}\right\}\right) = c_\tau\left((u+\frac{\mathrm{P}}{2},\left\{0,\frac{\mathrm{P}}{2}\right\}\right)c_\tau\left(u,\left\{0,\frac{\mathrm{P}}{2}\right\}\right)\xi^{-1}\left(\frac{\mathrm{P}}{2}\right)\xi^{-1}\left(-\frac{\mathrm{P}}{2}\right)$$

$$\mathrm{Tr}_{0\bar{0}}\Big(\overline{\mathcal{K}}_{0,\bar{0}}^L(u,-\frac{\mathrm{P}}{2})\mathcal{R}_{0,\bar{0}|2L-1,2L}(u,-\frac{\mathrm{P}}{2},-\frac{\mathrm{P}}{2})\,...\,\mathcal{R}_{0,\bar{0}|1,2}(u,-\frac{\mathrm{P}}{2},-\frac{\mathrm{P}}{2}) \tag{3.33}$$

$$\times\overline{\mathcal{K}}_{0,\bar{0}}^R(u,-\frac{\mathrm{P}}{2})\mathcal{R}_{1,2|0,\bar{0}}(u,-\frac{\mathrm{P}}{2},-\frac{\mathrm{P}}{2})\,...\,\mathcal{R}_{2L-1,2L|0,\bar{0}}(u,-\frac{\mathrm{P}}{2},-\frac{\mathrm{P}}{2})\Big),$$

with

$$\overline{\mathcal{K}}_{i,j}^R\left(u,-\frac{\mathrm{p}}{2}\right) = U_i^{-1}K_i^R\left(u+\frac{\mathrm{p}}{2}\right)R_{j,i}\left(2u+\frac{\mathrm{p}}{2}\right)K_j^R(u)R_{i,j}\left(-\frac{\mathrm{p}}{2}\right)\,, \tag{3.34a}$$

$$\overline{\mathcal{K}}_{i,j}^L\left(u,-\frac{\mathrm{p}}{2}\right) = R_{j,i}\left(\frac{\mathrm{p}}{2}\right)K_j^L(u)M_iR_{i,j}\left(-2u-\frac{\mathrm{p}}{2}-2\eta\right)M_i^{-1}K_i^L\left(u+\frac{\mathrm{p}}{2}\right)U_i \tag{3.34b}$$

$$\times\frac{1}{\xi\left(2u+\frac{\mathrm{p}}{2}+\eta\right)}\frac{1}{\xi\left(-2u-\frac{\mathrm{p}}{2}-\eta\right)}\,.$$

Using the monodromy matrix (3.26) for the composite $\mathcal{R}$-matrices the transfer matrix for the quasi-periodic staggering (3.30) can be written as

$$\mathbb{T}^{\mathrm{qp}}(u,-\frac{\mathrm{p}}{2}) \equiv \mathbb{T}(u,\{-\frac{\mathrm{p}}{2},0,0,-\frac{\mathrm{p}}{2}\})$$

$$= \mathrm{Tr}_{0\bar{0}}\Big(\overline{\mathcal{K}}_{0,\bar{0}}^L(u,-\frac{\mathrm{p}}{2})\mathcal{T}_{0,\bar{0}}(u,-\frac{\mathrm{p}}{2},-\frac{\mathrm{p}}{2})\overline{\mathcal{K}}_{0,\bar{0}}^R(u,-\frac{\mathrm{p}}{2})\mathcal{T}_{0,\bar{0}}^{-1}(u,-\frac{\mathrm{p}}{2},-\frac{\mathrm{p}}{2})\Big) \tag{3.35}$$

$$\times\xi^{-1}\left(\frac{\mathrm{p}}{2}\right)\xi^{-1}\left(-\frac{\mathrm{p}}{2}\right)\,.$$

Note that the composite monodromy matrix $\mathcal{T}$ (3.26) enters in the transfer matrices (3.27) and (3.35) with identical arguments for the particular choice of $2\delta_0 = -\frac{\mathrm{p}}{2}$. Hence, the bulk of these models coincides while the reflection matrices $\mathcal{K}$ (3.25) and $\overline{\mathcal{K}}$ (3.34) correspond to different BCs.[3] This has been discussed recently in the context of a staggered six-vertex (or $A_1^{(1)}$) model [26, 106, 107]: for $2\delta_0 = -\frac{\mathrm{p}}{2}$ the resulting composite model is a vertex model based on the twisted affine Lie algebra $D_2^{(2)}$. The $D_2^{(2)}$ boundary matrices corresponding to $\mathcal{K}$ and $\overline{\mathcal{K}}$ were known previously [111] and can be factorized into objects of the six-vertex model subject to $U_q(\mathfrak{sl}(2))$ BCs.

3.3.3 ASSOCIATED REFLECTION ALGEBRAS AND COMPOSITE $\mathcal{K}$-MATRICES

We are left to prove that the reflection matrices (3.25) and (3.34) are indeed representations of a reflection algebra associated with the $\mathcal{R}$-matrix. We define the following *generalized*

---

[3]This does not lead to different models in the case of periodic BCs where different choices of the horizontal staggering can be related by a shift in the spectral parameter (see Figure 3.5).

(a)

(b)
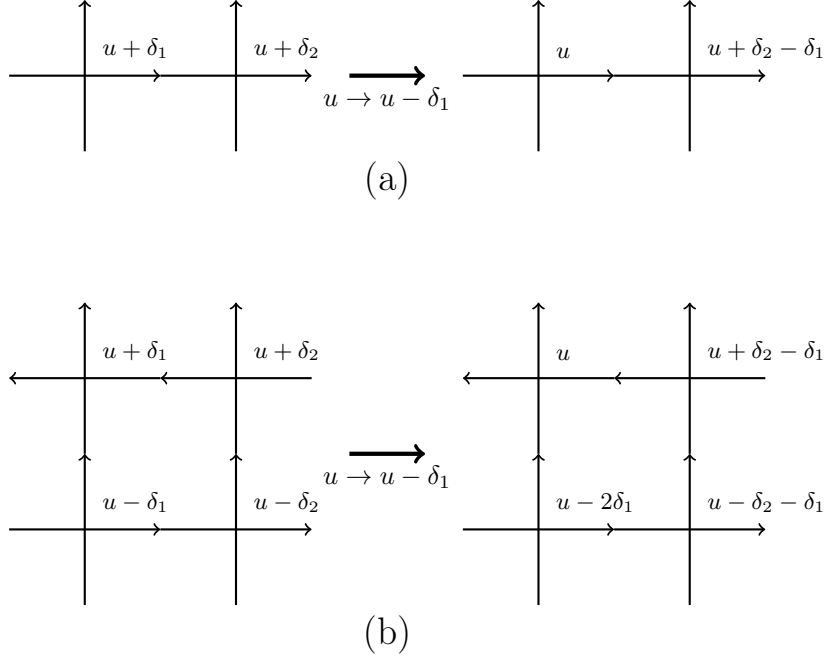
Figure 3.5: In the periodic case (a) a shift in the spectral parameter allows to adjust one inhomogeneity to zero e.g. $\delta_1 = 0$. This is not possible in the open case (b) where each inhomogeneity appears twice with different signs.

reflection algebras:

$$\mathcal{R}_{i,j|k,\ell}(u-v,\theta,\theta)\mathcal{K}^R_{i,j}(u,\theta)\mathcal{R}_{k,\ell|i,j}(u+v,\theta,\theta)\mathcal{K}^R_{k,\ell}(v,\theta) \tag{3.36a}$$
$$= \mathcal{K}^R_{k,\ell}(v,\theta)\mathcal{R}_{i,j|k,\ell}(u+v,\theta,\theta)\mathcal{K}^R_{i,j}(u,\theta)\mathcal{R}_{k,\ell|i,j}(u-v,\theta,\theta)$$

and

$$\mathcal{R}_{i,j|k,\ell}(-u+v,-\theta,-\theta)\mathcal{K}^{L,t_{i,j}}_{i,j}(u,\theta)\mathcal{M}^{-1}_{i,j}\mathcal{R}_{k,\ell|i,j}(-u-v-2\eta,-\theta,-\theta)\mathcal{M}_{i,j}\mathcal{K}^{L,t_{k,\ell}}_{k,\ell}(v,\theta) =$$
$$\mathcal{K}^{L,t_{k,\ell}}_{k,\ell}(v,\theta)\mathcal{M}_{i,j}\mathcal{R}_{i,j|k,\ell}(-u-v-2\eta,-\theta,-\theta)\mathcal{M}^{-1}_{i,j}\mathcal{K}^{L,t_{i,j}}_{i,j}(u,\theta)\mathcal{R}_{k,\ell|i,j}(-u+v,-\theta,-\theta)\,. \tag{3.36b}$$

Note that the sign of the free parameter θ in the arguments of the composite $\mathcal{R}$-matrices differs between (3.36a) and (3.36b). One of the main results is that for given $K^{R,L}$ satisfying equations (2.115-2.116) the matrices $\mathcal{K}$ (3.25) and $\overline{\mathcal{K}}$ (3.34) obey the equations (3.36) with the composite $\mathcal{R}$-matrix $\mathcal{R}(u,\theta,\theta)$ for $\theta = 2\delta_0$, δ_0 arbitrary, and $\theta = -\frac{p}{2}$, respectively. The proof for (3.25b) is given in Appendix B. The one for (3.25a) works along the same lines, for (3.34), one needs to use multiple times the quasi-periodicity in addition.

Based on the reflection algebra, it is straightforward to show the commutativity of the transfer matrices for both alternating and quasi-periodic BCs.

3.3.4 Boundary terms in the Hamiltonian

Above, we have identified two types of staggering, (3.24) and (3.30), allowing for the construction of a local bulk Hamiltonian from the corresponding transfer matrix of the

composite model. For a compact presentation, we define

$$\mathfrak{R}_{i,j|k,\ell}(u,\mathbf{s}) = \begin{cases} \mathcal{R}_{i,j|k,\ell}(u, -\frac{\mathrm{p}}{2}, -\frac{\mathrm{p}}{2}), & \mathbf{s} = 0 \\ \mathcal{R}_{i,j|k,\ell}(u, 2\delta_0, 2\delta_0), & \mathbf{s} = 1 \end{cases}, \qquad \mathfrak{K}_{i,j}^{L,R}(u,\mathbf{s}) = \begin{cases} \overline{\mathcal{K}}_{i,j}^{L,R}(u, -\frac{\mathrm{p}}{2}), & \mathbf{s} = 0 \\ \mathcal{K}_{i,j}^{L,R}(u, 2\delta_0), & \mathbf{s} = 1 \end{cases}$$

(3.37)

where $\mathbf{s} = 1$ (0) corresponds to the alternating (3.27) and the quasi-periodic staggering (3.35), respectively. Note that $\mathfrak{K}^R(0,\mathbf{s}) \propto \mathbf{1}$ by (2.118) for $\mathbf{s} = 1$ and by (2.120) for $\mathbf{s} = 0$. Hence, we obtain a local[4] Hamiltonian [72] via (3.23) whose bulk contribution is found to be

$$H_{\mathrm{bulk}}^{\mathbf{s}} = \frac{2}{\xi(\Delta)\xi(-\Delta)} \sum_{j=1}^{L-1} \mathcal{P}_{2j,2j-1|2j+2,2j+1} \mathfrak{R}'_{2j,2j-1|2j+2,2j+1}(0,\mathbf{s}).$$

(3.38)

Here and in the following, the prime indicates the derivative with respect to the first argument, where we assume that all quantities are differentiable at the corresponding points. The boundary contributions read as

$$H_{\mathrm{left}}^{\mathbf{s}} = \frac{\mathrm{Tr}_{0\overline{0}}\Big(\mathfrak{K}_{0,\overline{0}}^{'L}(0,\mathbf{s})\Big)}{\mathrm{Tr}_{0\overline{0}}\Big(\mathfrak{K}_{0,\overline{0}}^{L}(0,\mathbf{s})\Big)} + \frac{2\mathrm{Tr}_{0\overline{0}}\Big(\mathfrak{K}_{0,\overline{0}}^{L}(0,\mathbf{s})\mathcal{P}_{0,\overline{0}|2L-1,2L}\mathfrak{R}'_{0,\overline{0}|2L-1,2L}(0,\mathbf{s})\Big)}{\mathrm{Tr}_{0\overline{0}}\Big(\mathfrak{K}_{0,\overline{0}}^{L}(0,\mathbf{s})\Big)\xi(\Delta)\xi(-\Delta)},$$

(3.39)

$$H_{\mathrm{right}}^{\mathbf{s}} = \frac{\mathfrak{K}_{1,2}^{R'}(0,\mathbf{s})}{\mathfrak{K}_{1,2}^{R}(0,\mathbf{s})}.$$

Note that to obtain the spectrum of the above Hamiltonians, it is sufficient to use the Bethe ansatz for the *single* double row transfer matrix $\mathtt{t}(u)$ (2.122). Knowing the eigenvalue $t(u)$ of $\mathtt{t}(u)$, the energies can be calculated via equations (3.20) and (3.23) with operators replaced by their eigenvalues.

3.4 QUASI-MOMENTUM FOR OPEN SYSTEMS

As pointed out for the periodic case above, there exist two families of conserved quantities for the staggered models considered in this section: in addition to the ones generated by the product of elementary transfer matrices (3.20) (or equations (3.27) and (3.35) for the two cases discussed above), one can consider operators such as the quasi-momentum generated from the *quotient* of elementary transfer matrices. For the staggered model with open BCs built from arbitrary elementary R- and K-matrices, we replace (3.15) by

$$\mathbb{B} = \log\left[\frac{\mathtt{t}(-\delta_1, \{\delta_1, \delta_2\})}{\mathtt{t}(-\delta_2, \{\delta_1, \delta_2\})}\right].$$

(3.40)

To express this operator in the composite picture, we adopt the idea from the periodic case: we look for a generating function built out of a *product* of transfer matrices, giving (3.40) as the leading term.

---

[4]It is noteworthy that for $K^R(0) \not\propto \mathbf{1}$, inducing an alternating staggering is sufficient to define a local Hamiltonian. See also [112] for a similar approach.
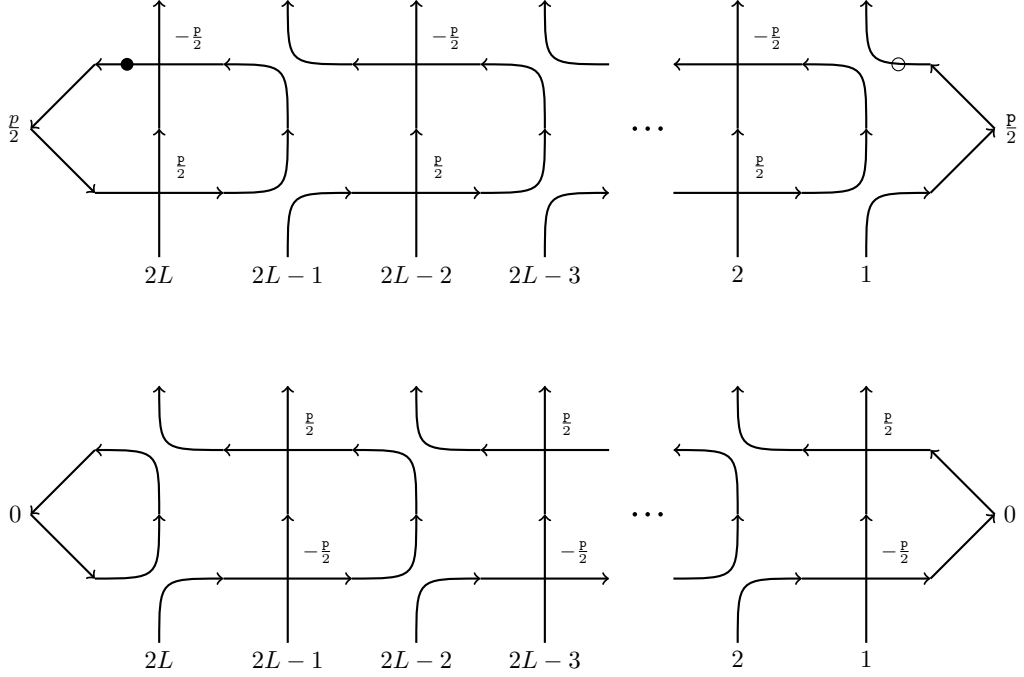
Figure 3.6: Here the two double row transfer matrices defining the quasi-momentum as in (3.40) for quasi-periodic staggering evaluated at the shift point are shown. We see that both at their own become trivial in the bulk, and if one assumes that $K^R(0), K^R\left(\frac{\mathrm{p}}{2}\right) \propto \mathbf{1}$ then the whole transfer matrices become essentially the identity leading to a trivial quasi-momentum.

3.4.1 Quasi-periodic staggering

For the quasi-periodic staggering, the single ingredients $\mathrm{t}(-\frac{\mathrm{p}}{2}, \{0, \frac{\mathrm{p}}{2}\})$ and $\mathrm{t}(0, \{0, \frac{\mathrm{p}}{2}\})$ become trivial in the bulk, see Figure 3.6. Hence, under the assumptions (2.120), the quasi-momentum operator is trivial

$$\mathbb{B}^{\mathrm{qp}} \propto \mathbf{1}. \tag{3.41}$$

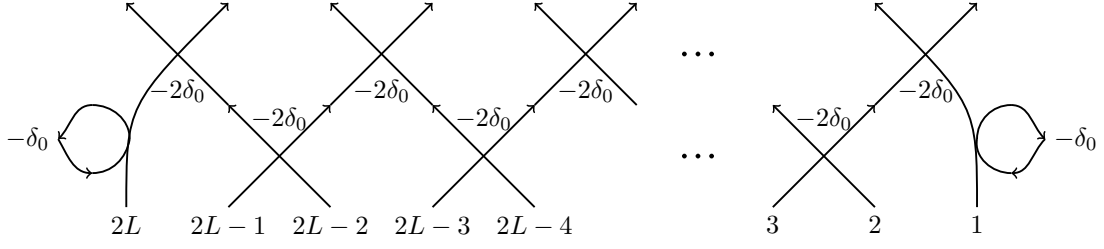We will come back to this when we consider the specific example of the six-vertex model in section 4.3.

3.4.2 Alternating staggering

For the alternating staggering case, the quasi-momentum operator can be directly related (up to an additive constant) to a single double row-transfer matrix

$$\mathbb{B}^{\mathrm{alt}} = \log\left(\mathrm{t}^2(-\delta_0, \{\delta_0, -\delta_0\})\right). \tag{3.42}$$

In this case, the quasi-momentum can be represented in the rotated geometry as displayed in Figure 3.7. Starting from $\mathrm{t}^2(u - \delta_0, \{\delta_0, -\delta_0\})$ and repeating the steps in section 3.3 to reach (3.21) and then applying the manipulations i)-ii) in section 3.3.1, we obtain another generating functional for the quasi-momentum operator:

$$\mathbb{K}(u) = \mathrm{Tr}_{0\bar{0}}\left(\mathscr{K}^L_{0,\bar{0}}(u, 2\delta_0)\mathcal{T}_{0,\bar{0}}(u, 0, 2\delta_0)\mathscr{K}^R_{0,\bar{0}}(u, 2\delta_0)\mathcal{T}^{-1}_{0,\bar{0}}(-(u - 2\delta_0), 0, 2\delta_0)\right), \tag{3.43}$$

Figure 3.7: We have graphically represented the quasi-momentum operator for alternating staggering in the rotated geometry. One can see that the quasi-momentum operator is acting non-locally. The loops at the right and left endings are due to the influences of the boundary matrices.

where the $\mathscr{K}$-matrices

$$\mathscr{K}_{i,j}^{R}(u, 2\delta_0) = P_{i,j} K_j^R(u - \delta_0) R_{i,j}(2u - 2\delta_0) K_i^R(u - \delta_0), \tag{3.44a}$$

$$\mathscr{K}_{i,j}^{L}(u, 2\delta_0) = P_{i,j} K_j^L(u - \delta_0) M_i R_{i,j}(-2u + 2\delta_0 - 2\eta) M_i^{-1} K_i^L(u - \delta_0) \tag{3.44b}$$

$$\times \frac{1}{\xi(2u - 2\delta_0 + \eta)\xi(-2u + 2\delta_0 - \eta)}$$

obey the reflection algebras

$$\mathcal{R}_{i,j|k,\ell}(u - v, 0, 0)\mathscr{K}_{i,j}^{R}(u, 2\delta_0)\mathcal{R}_{k,\ell|i,j}(u + v - 2\delta_0, 0, 0)\mathscr{K}_{k,\ell}^{R}(v, 2\delta_0) =$$
$$\mathscr{K}_{k,\ell}^{R}(v, 2\delta_0)\mathcal{R}_{i,j|k,\ell}(u + v - 2\delta_0, 0, 0)\mathscr{K}_{i,j}^{R}(u, 2\delta_0)\mathcal{R}_{k,\ell|i,j}(u - v, 0, 0) \tag{3.45a}$$

and

$$\mathcal{R}_{i,j|k,\ell}(-u + v, 0, 0)\mathscr{K}_{i,j}^{L,t_{i,j}}(u, 2\delta_0)\mathcal{M}_{i,j}^{-1}\mathcal{R}_{k,\ell|i,j}(-u - v + 2\delta_0 - 2\eta, 0, 0)\mathcal{M}_{i,j}\mathscr{K}_{k,\ell}^{L,t_{k,\ell}}(v, 2\delta_0) =$$
$$\mathscr{K}_{k,\ell}^{L,t_{k,\ell}}(v, 2\delta_0)\mathcal{M}_{i,j}\mathcal{R}_{i,j|k,\ell}(-u - v + 2\delta_0 - 2\eta, 0, 0)\mathcal{M}_{i,j}^{-1}\mathscr{K}_{i,j}^{L,t_{i,j}}(u, 2\delta_0)\mathcal{R}_{k,\ell|i,j}(-u + v, 0, 0), \tag{3.45b}$$

respectively. Again, the proof is analogous to the one shown in appendix B for $\mathcal{K}^L$. Reflection algebras of this type were introduced by Nepomechie and Retore [113, 106]: they describe a moving boundary where the reflection of a particle at the boundary not only changes the sign of its rapidity but also leads to a shift by $2\delta_0$ in the argument of the $\mathcal{R}$-matrix containing the sum of $u + v$.

These reflection algebras, together with the generalized YBE (3.2), ensure the commutativity of $\mathbb{K}$ with itself for different arguments. Finally, we need to prove the commutativity with the transfer matrix (3.27) in the composite picture. For the open chain with alternating staggering, this is not obvious because the boundary matrices $\mathcal{K}^{L,R}$ and $\mathscr{K}^{L,R}$ are representations of *different* reflection algebras. Remarkably, it turns out that they are intertwined by the following relations

$$\mathcal{R}_{i,j|k,\ell}(u - v, 0, -2\delta_0)\mathscr{K}_{i,j}^{R}(u, 2\delta_0)\mathcal{R}_{k,\ell|i,j}(u + v - 2\delta_0, 2\delta_0, 0)\mathcal{K}_{k,\ell}^{R}(v, 2\delta_0) =$$
$$\mathcal{K}_{k,\ell}^{R}(v, 2\delta_0)\mathcal{R}_{i,j|k,\ell}(u + v, 0, -2\delta_0)\mathscr{K}_{i,j}^{R}(u, 2\delta_0)\mathcal{R}_{k,\ell|i,j}(u - v - 2\delta_0, 2\delta_0, 0), \tag{3.46a}$$

and

$$
\begin{aligned}
&\mathcal{R}_{i,j|k,\ell}(-u+v,0,2\delta_0)\mathscr{K}_{i,j}^{L,t_{i,j}}(u,2\delta_0)\mathcal{M}_{i,j}^{-1}\mathcal{R}_{k,\ell|i,j}(-u-v+2\delta_0-2\eta,-2\delta_0,0)\\
&\times \mathcal{M}_{i,j}\mathcal{K}_{k,\ell}^{L,t_{k,\ell}}(v,2\delta_0) = \mathcal{K}_{k,\ell}^{L,t_{k,\ell}}(v,2\delta_0)\mathcal{M}_{i,j}\mathcal{R}_{i,j|k,\ell}(-u-v-2\eta,0,2\delta_0) &\text{(3.46b)}\\
&\times \mathcal{M}_{i,j}^{-1}\mathscr{K}_{i,j}^{L,t_{i,j}}(u,2\delta_0)\mathcal{R}_{k,\ell|i,j}(-u+v+2\delta_0,-2\delta_0,0)\,.
\end{aligned}
$$

Again, this can be proven as shown in appendix B. Using these algebras, one can show on the composite level that

$$
\mathbb{K}(u)\mathbb{T}^{\text{alt}}(v,2\delta_0) = \mathbb{T}^{\text{alt}}(v,2\delta_0)\mathbb{K}(u)\,. \tag{3.47}
$$

We want to stress that the intertwining relations (3.46) ensure the commutativity of transfer matrices with *different* boundary matrices. It would be interesting to address whether similar relations exist between other already-known boundary matrices.

3.5 CHAPTER SUMMARY

Starting from an elementary solution R of the YBE (2.100), we have constructed the composite $\mathcal{R}$-matrix (3.1). In addition to the spectral parameter, the composite matrix depends on two free parameters related to the staggering of the elementary vertices (see Figure 3.1). PT-symmetry, unitarity, regularity and crossing unitarity are inherited from the elementary R-matrix. Most importantly, the composite $\mathcal{R}$-matrix obeys a generalized YBE (3.2). In this picture, the commuting transfer matrices of arbitrary $\mathbb{Z}_2$-staggered models can be rewritten as homogeneous ones where the staggering parameters enter through the additional arguments of the composite $\mathcal{R}$-matrices (and reflection matrices in the case of open BCs). Integrals of motion, including the quasi-momentum operator, whose natural definition relies on the staggering of the model, have been described in the *homogeneous* picture based on the composite $\mathcal{R}$-matrix. In the case of open BCs, the Hamiltonian and the quasi-momentum are defined in terms of *different* representations of the reflection algebra intertwined by (3.46). This construction may provide insights into a definition of this operator in homogeneous models which may lack a known factorization of the transfer matrix. This is of particular interest for models featuring a continuous component of the conformal spectrum at criticality [23, 114, 115, 116]. Knowing the quasi-momentum operator in these models is expected to foster the identification of the CFT describing the low-energy regime.

Demanding locality in the Hamiltonian limit leads to constraints on the staggering parameters: in the case of periodic BCs, they have to be tuned to satisfy (3.12). For open BCs, the staggering has to satisfy equation (3.24) for 'alternating staggering'. Moreover, for quasi-periodic R- (and $\mathcal{R}$-) matrices, the inequivalent choice of 'quasi-periodic staggering' (3.30) leads to a different Hamiltonian with local interactions. For both cases, we have identified the corresponding composite boundary matrices, which generalise the findings of the factorization [107] for the $D_2^{(2)}$ boundary matrices [117, 118, 111] to arbitrary algebras.

4 | THE STAGGERED SIX-VERTEX MODEL WITH $U_q\big(\mathfrak{sl}(2)\big)$ BCs

In this chapter, which is based on the author's works [31, 32, 34], we want to apply our findings and investigate further the special case of the staggered six-vertex model (2.126) with so-called $U_q(\mathfrak{sl}(2))$ invariant BCs. This corresponds to setting the right K-matrix to be

$$K^R(u) = \begin{pmatrix} \mathrm{e}^u & 0 \\ 0 & \mathrm{e}^{-u} \end{pmatrix}, \tag{4.1}$$

where we assumed the R-matrix to be of the form (2.126),(2.127), and we use for the left K-matrix the isomorphic one (2.117). The above K-matrix can be obtained from the most general one (2.131) by setting $s_1 = s_2 = 0$ and sending[1] $\xi^R \to \infty$. However, for technical reasons, it is better to consider first the one-parameter[2] family (2.131) with $s_1 = s_2 = 0$ but finite ξ^R, and then recover the case of interest — the $U_q\big(\mathfrak{sl}(2)\big)$ invariant case — by taking the limit $\xi^R \to \infty$. Moreover, for the sake of generality and a coherent presentation, it is useful to discuss the more general model with arbitrary inhomogeneities $\{\delta_J\}$.

Let us proceed by defining the more general model. As discussed in the preliminaries, for the systematic extraction of the Bethe roots in the Q-operator approach — which will be of great importance later — it is advantageous to directly use the multiplicative spectral parameter ζ and arrange the definitions such that the matrix elements of both $\mathsf{t}(\zeta)$ and $\mathbb{Q}(\zeta)$ are manifestly polynomials in ζ. Therefore, we use

$$R(\zeta) = \begin{pmatrix} q - q^{-1}\zeta & 0 & 0 & 0 \\ 0 & 1 - \zeta & q - q^{-1} & 0 \\ 0 & (q - q^{-1})\zeta & 1 - \zeta & 0 \\ 0 & 0 & 0 & q - q^{-1}\zeta \end{pmatrix}, \tag{4.2}$$

instead of (2.126) in this section. Then the transfer matrix reads as

$$\mathsf{t}(\zeta q^{-1}) = q^{-2L}\,\mathrm{tr}_0\Big(K_0^L(\zeta)\,R_{0,2L}(\zeta\,\eta_{2L}^{-1})\,...\,R_{0,1}(\zeta\,\eta_1^{-1})\,K_0^R(\zeta)\,R_{1,0}(\zeta\,\eta_1)\,...\,R_{2L,0}(\zeta\,\eta_{2L})\Big), \tag{4.3}$$

where $K^{R,L}$ take the form

$$K^R(\zeta) = \begin{pmatrix} 1 + \zeta\epsilon & 0 \\ 0 & \zeta^2 + \zeta\epsilon \end{pmatrix}, \qquad K^L(\zeta) = \begin{pmatrix} q^{-2}\zeta + \epsilon & 0 \\ 0 & \zeta^{-1} + q^{-2}\epsilon \end{pmatrix}. \tag{4.4}$$

---

[1]This limit requires a regularisation factor of $\mathrm{e}^{-\xi_R}$.

[2]To get in this limit the $U_q(\mathfrak{sl}(2))$ invariant case, we need to set the other free parameter of the left K-matrix to be $\xi^L = -\xi^R$. The negative sign originates from the sign change of the isomorphism (2.117).

Here, the rational notation[3] is connected to the ones in the preliminaries in equations (2.126), (2.127) and (2.131) via the identifications

$$\zeta = \mathrm{e}^{-2u}, \qquad q = \mathrm{e}^{\mathrm{i}\gamma}, \qquad \eta_J = \mathrm{e}^{2\delta_J}, \qquad \epsilon = -\mathrm{e}^{-2\xi^R}. \tag{4.6}$$

Let us consider the case when the extra boundary parameter ϵ is set to zero (i.e. $\xi^R \to \infty$)

$$\mathbb{t}^{(0)}(\zeta) \equiv \mathbb{t}(\zeta)\big|_{\epsilon=0}. \tag{4.7}$$

A special feature of such a choice of boundary terms is that the model possesses $U_q\big(\mathfrak{sl}(2)\big)$ symmetry. This means that $\mathbb{t}^{(0)}(\zeta)$ commutes with the z-projection of the total spin operator:

$$\mathbb{S}^z = \frac{1}{2} \sum_{J=1}^{2L} \sigma_J^z, \tag{4.8}$$

and with

$$\mathbb{S}_q^\pm = \sum_{J=1}^{2L} \left(\prod_{\ell=J+1}^{2L} q^{-\frac{\sigma_\ell^z}{2}} \right) \eta_J^{\mp 1} \sigma_J^\pm \left(\prod_{\ell=1}^{J-1} q^{+\frac{\sigma_\ell^z}{2}} \right), \tag{4.9}$$

which satisfy the defining relations of the $U_q\big(\mathfrak{sl}(2)\big)$ algebra:

$$\big[\mathbb{S}^z, \mathbb{S}_q^\pm\big] = \pm\mathbb{S}_q^\pm, \qquad\qquad \big[\mathbb{S}_q^+, \mathbb{S}_q^-\big] = \frac{q^{2\mathbb{S}^z} - q^{-2\mathbb{S}^z}}{q - q^{-1}}. \tag{4.10}$$

Hence, the eigenstates of the transfer matrix form irreducible representations of this algebra, i.e. the states come in multiplets $\mathcal{M}_\mathcal{S}$. These are characterised by the Casimir operator,

$$2\mathbb{C} = (q + q^{-1})\,[\mathbb{S}^z]_q^2 + \mathbb{S}_q^+\,\mathbb{S}_q^- + \mathbb{S}_q^-\,\mathbb{S}_q^+. \tag{4.11}$$

The eigenvalues of $\mathbb{C}$ are given by $[\mathcal{S}]_q\,[\mathcal{S}+1]_q$ with integer $\mathcal{S} = 0, 1, 2, \ldots, L$. The subscript q on the bracket indicates the so-called q-bracket which is given by

$$[m]_q = (q^m - q^{-m})/(q - q^{-1}). \tag{4.12}$$

It is important to emphasise that the presence of the $U_q\big(\mathfrak{sl}(2)\big)$ symmetry simplifies the diagonalisation problem. Namely, since each multiplet has a representative in the sector $S^z = 0$, it is sufficient to consider the $(2L)!/(L!)^2$ dimensional nullspace of the operator $\mathbb{S}^z$.

The rest of this chapter is structured as follows: in the next section, we state the Q-operator of the more general model and describe how the Q-operator for the $U_q\big(\mathfrak{sl}(2)\big)$ invariant case can be obtained in the limit $\epsilon \to 0$.

Then, we investigate the scaling limit of the model with alternating staggering. First, we study the model's Hamiltonian for small system sizes by exact diagonalisation. We identify

---

[3]In fact, the transfer-matrix as defined in formula (4.3) for arbitrary inhomogeneities η_J is related to (2.122) with (2.126) and (2.131) (for $s_1 = s_2 = 0$) via a similarity transformation by a diagonal matrix and an overall multiplicative factor. Namely,

$$\mathbb{t}(\zeta) = 2^{4L}\mathrm{e}^{-4Lu-2u}\,\mathcal{U}\,\mathbb{t}(u)\mathcal{U}^{-1}. \tag{4.5}$$

Here $\mathcal{U} = G_1(\delta_1) \otimes \ldots \otimes G_{2L}(\delta_{2L})$ with $G(u) = \mathrm{diag}(1, \mathrm{e}^{-u})$, while the parameters $u, \gamma, \delta_J, \xi^R$ need to be identified with $\zeta, q, \eta_J, \epsilon$ as in (4.6). Note that the K-matrices must also be identified appropriately.
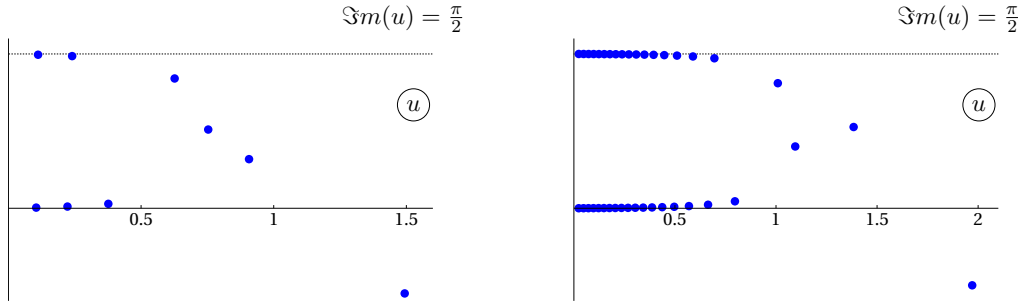
Figure 4.1: Displayed is the pattern of Bethe roots in the complex $u = -\frac{1}{2}\log(\zeta)$ plane for a low energy Bethe state that was generically chosen. For the left panel, $L = 10$ was selected, and the set $\{\zeta_m\}$ has been obtained from the eigenvalue of the Q-operator computed on the state. On the right panel, the Bethe roots for the corresponding state with $L = 40$ are shown. The trajectory is labeled by $\mathcal{S} = 1$, while the anisotropy parameter was taken to be $q = e^{\frac{10\pi i}{49}}$.

one particular class of states that partly describes the low-energy spectrum of the spin chain. We analyse this class of states in the scaling limit using analytical techniques, such as the root density approach. By means of a Wiener-Hopf analysis and numerical data of the finite-size spectrum, we conclude that a non-compact degree of freedom emerges in the scaling limit. The quasi-momentum operator parametrises this degree of freedom on the lattice. While the quasi-momentum for the considered class of states is real, we find that other states exist with purely imaginary values of the quasi-momentum. It turns out that these describe the so-called 'discrete' states. The found effective scaling dimensions mimic the ones of the conformal primaries of the Black Hole CFT introduced in the preliminaries.

After this, we generalize the study to any low-energy state for the self-dual model, applying the ODE/IQFT approach. This leads to the formulation of a so-called 'quantization condition' for the permitted values of the quasi-momentum operator, which allows us to characterise the model's scaling limit fully. This analysis yields the density of states and the discrete characters, which classify the continuous and discrete parts of the spectrum of conformal dimensions, respectively. We also calculate the partition function in the scaling limit.

Finally, we study the model with quasi-periodic staggering by an integrable spectral flow to the model with alternating staggering.

4.1 THE Q-OPERATOR

To find the Bethe roots of the model at hand systematically, we will use the introduced technique based on the notion of the Baxter Q-operator $\mathbb{Q}(\zeta)$ discussed in section 2.4.3. In the following, we present an explicit formula for the Q-operator. It was obtained based on the results of work [119] (see also [120, 121, 122]). Of particular interest is the following result: they give $\mathbb{Q}(\zeta)$ as a trace of a monodromy matrix over a q-oscillator representation for models associated with the rational [120] and trigonometric [121, 122] R-matrix for $\mathfrak{sl}(2)$. The considered BCs are essentially given by (2.131) with $s_1 = s_2 = 0$ and ξ^R, ξ^L are the free parameters. The matrix elements of $\mathbb{Q}(\zeta)$ are expressed in [119] as infinite sums, which converge only in a parametric domain not applicable to the model with $U_q\big(\mathfrak{sl}(2)\big)$

invariant BCs. Hence, it was necessary to analyze the expression in order to adapt it to a form that is directly applicable to our case.

We start by noting that the transfer matrix (4.3) of the more general model is a polynomial of order $4L + 2$ in the spectral parameter and satisfies the conditions

$$\mathbb{t}(0) = \epsilon \left(q^{2\mathbb{S}^z} + q^{-2\mathbb{S}^z} \right), \qquad\qquad \mathbb{t}(\zeta^{-1}) = \zeta^{-4L-2} \, \mathbb{t}(\zeta). \qquad (4.13)$$

As discussed below equation (4.11), for the study of the $U_q(\mathfrak{sl}(2))$ invariant case, it is sufficient to focus for $\mathbb{t}$ on the sector where the eigenvalue of the z-projection of the total spin operator is zero[4]. Denote by the tuples $(a_1 a_2 \dots a_{2L})$ and $(b_1 b_2 \dots b_{2L})$ with $a_J, b_J = \pm$ the input and output indices for the space $\left(\mathbb{C}^2\right)^{\otimes 2L}$ respectively. To state the formula for the Q-operator, we introduce the matrices

$$\begin{pmatrix} \left[A(\zeta;m)\right]^+_+ & \left[A(\zeta;m)\right]^-_+ \\ \left[A(\zeta;m)\right]^+_- & \left[A(\zeta;m)\right]^-_- \end{pmatrix} = \begin{pmatrix} q^m & q^m \\ \zeta q^{-m+1} & q^{-m} \end{pmatrix}, \qquad (4.14)$$

$$\begin{pmatrix} \left[\widetilde{A}(\zeta;m)\right]^+_+ & \left[\widetilde{A}(\zeta;m)\right]^-_+ \\ \left[\widetilde{A}(\zeta;m)\right]^+_- & \left[\widetilde{A}(\zeta;m)\right]^-_- \end{pmatrix} = \begin{pmatrix} q^m & \zeta q^{m+2} \\ q^{-m-1} & q^{-m} \end{pmatrix}. \qquad (4.15)$$

The matrix elements of $\mathbb{Q}(\zeta)$, valid in the sector $S^z = 0$, then read

$$\left[\mathbb{Q}(\zeta)\right]^{b_1 \dots b_{2L}}_{a_1 \dots a_{2L}} = \sum_{c_1 \cdot c_{2L} = \pm} q^{(S^z_c)^2} (\epsilon q^2 \zeta)^{S^z_c} \prod_{J=1}^{2L} \left[A(\zeta \eta_J^{-1}, m_{b,J})\right]^{b_J}_{c_J} \left[\widetilde{A}(\zeta \eta_J, m_{a,J+1})\right]^{c_J}_{a_J}. \quad (4.16)$$

The symbol S^z_c, which should not be confused with the eigenvalue of $\mathbb{S}^z$, is defined as

$$S^z_\mathrm{c} = \frac{1}{2} \sum_{J=1}^{2L} c_J. \qquad (4.17)$$

It provides a grading for the sum over c_J in (4.16). The internal indices $\{m_{a,J}, m_{b,J}\}$ originate from the product over the auxiliary space. They are completely fixed to be

$$m_{x,J} = \frac{1}{2} \sum_{\ell=J}^{2L} (x_\ell - c_\ell) \qquad (J = 1, \dots, 2L+1; \; x = a, b), \qquad (4.18)$$

by the ice-rule. Despite the factor $\zeta^{S^z_\mathrm{c}}$ in formula (4.16), where the exponent can take negative values, the matrix elements of $\mathbb{Q}(\zeta)$ turn out to be polynomials in ζ of degree $2L$. Further, one can show that they satisfy:

$$\mathbb{Q}(\zeta^{-1}) = \zeta^{-2L} \, \mathbb{Q}(\zeta), \qquad\qquad \mathbb{Q}(0) = \mathbf{1}. \qquad (4.19)$$

The Q-operator obeys (2.140) as well as the TQ-relation

$$
\begin{aligned}
\left(1 - \zeta^2\right) \mathbb{Q}(\zeta) \, \mathbb{t}(\zeta) \;=\; & \left(\epsilon + q^{+1} \zeta\right) \left(1 + \zeta \, q^{+1} \, \epsilon\right) f(q^{-1} \zeta) \, \mathbb{Q}(\zeta \, q^{+2}) && (4.20) \\
+ \; & \left(\epsilon + q^{-1} \zeta\right) \left(1 + \zeta \, q^{-1} \, \epsilon\right) f(q^{+1} \zeta) \, \mathbb{Q}(\zeta \, q^{-2}) && (S^z = 0),
\end{aligned}
$$

---

[4]Note, that $\mathbb{S}^z$ is defined independently of ϵ.

where

$$f(\zeta) = (1 - \zeta^2) \prod_{J=1}^{2L} \left(\zeta - \eta_J^{-1}\right)\left(\zeta - \eta_J\right).$$ (4.21)

The TQ-relation allows the application of the analytic Bethe ansatz as discussed in section 2.4.3: one considers both sides of equation (4.20) evaluated on a common eigenvector of $\mathbb{t}$ and $\mathbb{Q}$. In regards to (4.19), the eigenvalues of $\mathbb{Q}(\zeta)$ take the form

$$Q(\zeta) = \prod_{j=1}^{L} \left(1 - \zeta/\zeta_j\right)\left(1 - \zeta\zeta_j\right).$$ (4.22)

Combining this with (4.20) and setting $\zeta = \zeta_m$ into that formula, one arrives at the BAE:

$$\prod_{J=1}^{2L} \frac{\left(\zeta_m q^{+1} - \eta_J^{-1}\right)\left(\zeta_m q^{+1} - \eta_J\right)}{\left(\zeta_m q^{-1} - \eta_J^{-1}\right)\left(\zeta_m q^{-1} - \eta_J\right)} = \frac{\left(\epsilon + q^{+1}\zeta_m\right)\left(q^{+1}\epsilon + \zeta_m^{-1}\right)}{\left(\epsilon + q^{-1}\zeta_m\right)\left(q^{-1}\epsilon + \zeta_m^{-1}\right)}$$ (4.23)

$$\times \quad q^2 \prod_{\substack{j=1 \\ j \neq m}}^{L} \frac{\left(\zeta_j - q^{+2}\zeta_m\right)\left(1 - q^{+2}\zeta_m\zeta_j\right)}{\left(\zeta_j - q^{-2}\zeta_m\right)\left(1 - q^{-2}\zeta_m\zeta_j\right)} \qquad (S^z = 0).$$

These are equivalent to the BAE obtained in the original work [72], in the sector $S^z = 0$ and with $\xi^+ = -\xi^-$ under the identifications $(q, \eta_J, \epsilon) \mapsto (\mathrm{e}^\eta, \mathrm{e}^{-2u_J}, -\mathrm{e}^{2\xi^\pm})$, while $\zeta_m \mapsto \mathrm{e}^{-2v_m}$.

The limit $\epsilon \to 0$ of the Q-operator requires careful handling. It is apparent from the explicit formula (4.16) that the matrix elements of $\mathbb{Q}(\zeta)$ generically diverge due to the presence of the factor $\epsilon^{S_{\bar{c}}^z}$, where the exponent may be negative. This is a manifestation of the $U_q\big(\mathfrak{sl}(2)\big)$ invariance arising at the point $\epsilon = 0$, so that states of different sectors of S^z combine into multiplets of the symmetry group that have the same eigenvalue of $\mathbb{Q}(\zeta)$. In reference [123], a similar phenomenon was studied in the context of the XXX spin chain with twisted BCs controlled by the parameter ϕ. At $\phi = 0$, the model possesses a global $\mathfrak{su}(2)$ symmetry and the matrix elements of the Q-operator become infinite. The authors explain how to take the limit $\phi \to 0$ of $\mathbb{Q}(\zeta)$ so that one obtains a well-defined result. The discussion is readily adapted to the present case.

Define $\mathcal{S}$ to be an operator, which for an eigenstate of the quadratic Casimir (4.11) with eigenvalue $[\mathcal{S}]_q[\mathcal{S}+1]_q$ gives back the non-negative integer $\mathcal{S} \geq 0$. Then, following [123], it turns out that the limit

$$\mathbb{Q}^{(0)}(\zeta) = \lim_{\epsilon \to 0} \epsilon^{\frac{\mathcal{S}}{2}} \, \mathbb{Q}(\zeta; \epsilon) \, \epsilon^{\frac{\mathcal{S}}{2}}$$ (4.24)

exists and yields the Q-operator for the inhomogeneous six-vertex model with $U_q\big(\mathfrak{sl}(2)\big)$ invariant BCs for $S^z = 0$. The commutativity condition (2.140) and the TQ-relation (4.20) with the substitutions $\big(\mathbb{Q}, \mathbb{t}\big) \mapsto \big(\mathbb{Q}^{(0)}, \mathbb{t}^{(0)}\big)$ and in the latter, $\epsilon = 0$, are satisfied. However, the normalisation as in (4.19) no longer holds true. Instead,

$$\mathbb{Q}^{(0)}(\zeta)|\Psi_L\rangle = C\,\zeta^{\mathcal{S}} \prod_{j=1}^{L-\mathcal{S}} \left(1 - \zeta/\zeta_j\right)\left(1 - \zeta\zeta_j\right)|\Psi_L\rangle,$$ (4.25)

where C is a constant which depends only on q and $\mathcal{S}$.

The TQ-relation for $\epsilon = 0$ leads with (4.25) to the Bethe ansatz equations:

$$\prod_{J=1}^{2L} \frac{\left(\zeta_m q^{+1} - \eta_J^{-1}\right)\left(\zeta_m q^{+1} - \eta_J\right)}{\left(\zeta_m q^{-1} - \eta_J^{-1}\right)\left(\zeta_m q^{-1} - \eta_J\right)} = q^{4+4\mathcal{S}} \prod_{\substack{j=1 \\ j \neq m}}^{L-\mathcal{S}} \frac{\left(\zeta_j - q^{+2}\zeta_m\right)\left(1 - q^{+2}\zeta_m\zeta_j\right)}{\left(\zeta_j - q^{-2}\zeta_m\right)\left(1 - q^{-2}\zeta_m\zeta_j\right)} . \tag{4.26}$$

Notice that (4.26) also follows from (4.23) by taking $\epsilon \to 0$ and assuming that $\mathcal{S}$ roots ζ_j with $j \neq m$ tend to zero in this limit.

The eigenvalue of the transfer matrix $\mathbb{t}^{(0)}(\zeta)$ can be expressed in terms of the roots ζ_j:

$$t^{(0)}(\zeta) = \frac{q^{+1} - q^{-1}\zeta^2}{\zeta^{-1} - \zeta} \prod_{J=1}^{2L} \left(q^{-1}\zeta - \eta_J^{-1}\right)\left(q^{-1}\zeta - \eta_J\right) \prod_{j=1}^{L-\mathcal{S}} \frac{\left(1 - q^{+2}\zeta/\zeta_j\right)\left(1 - q^{+2}\zeta\zeta_j\right)}{\left(1 - \zeta/\zeta_j\right)\left(1 - \zeta\zeta_j\right)}$$
$$+ \frac{q^{-1} - q^{+1}\zeta^2}{\zeta^{-1} - \zeta} \prod_{J=1}^{2L} \left(q^{+1}\zeta - \eta_J^{-1}\right)\left(q^{+1}\zeta - \eta_J\right) \prod_{j=1}^{L-\mathcal{S}} \frac{\left(1 - q^{-2}\zeta/\zeta_j\right)\left(1 - q^{-2}\zeta\zeta_j\right)}{\left(1 - \zeta/\zeta_j\right)\left(1 - \zeta\zeta_j\right)} . \tag{4.27}$$

The eigenvalues and Bethe ansatz equations can also be obtained by the algebraic Bethe ansatz, see [124]. This work uses the trigonometric notation (4.6) which we also use from time to time when it simplifies the presentation. Hence, for the reader's convenience, we translate the Bethe equations and the transfer matrix eigenvalue in the trigonometric notation. With $t_c^{(0)} = 2^{4L}\mathrm{e}^{-4Lu-2u}$, they read

$$\begin{aligned}
t^{(0)}(u)/t_c^{(0)} = & \frac{\sinh(2u + \mathrm{i}\gamma)}{\sinh(2u)} \prod_{J=1}^{2L} \sinh(u - \delta_J - \tfrac{\mathrm{i}\gamma}{2})\sinh(u + \delta_J - \tfrac{\mathrm{i}\gamma}{2}) \\
& \times \prod_{m=1}^{L-\mathcal{S}} \frac{\sinh(u - u_m - \mathrm{i}\gamma)\sinh(u + u_m - \mathrm{i}\gamma)}{\sinh(u - u_m)\sinh(u + u_m)} \\
& + \frac{\sinh(2u - \mathrm{i}\gamma)}{\sinh(2u)} \prod_{J=1}^{2L} \sinh(u + \delta_J + \tfrac{\mathrm{i}\gamma}{2})\sinh(u + \delta_J + \tfrac{\mathrm{i}\gamma}{2}) \\
& \times \prod_{m=1}^{L-\mathcal{S}} \frac{\sinh(u - u_m + \mathrm{i}\gamma)\sinh(u + u_m + \mathrm{i}\gamma)}{\sinh(u - u_m)\sinh(u + u_m)}
\end{aligned} \tag{4.28}$$

and

$$\prod_{J=1}^{2L} \frac{\sinh(u_m - \delta_J + \tfrac{\mathrm{i}\gamma}{2})\sinh(u_m + \delta_J + \tfrac{\mathrm{i}\gamma}{2})}{\sinh(u_m + \delta_J - \tfrac{\mathrm{i}\gamma}{2})\sinh(u_m + \delta_J - \tfrac{\mathrm{i}\gamma}{2})} = \prod_{k=1 \neq m}^{L-\mathcal{S}} \frac{\sinh(u_m - u_k + \mathrm{i}\gamma)\sinh(u_m + u_k + \mathrm{i}\gamma)}{\sinh(u_m - u_k - \mathrm{i}\gamma)\sinh(u_m + u_k - \mathrm{i}\gamma)} . \tag{4.29}$$

From our discussion in section 3.3, we know that only the alternating or quasi-periodic staggering leads to a local Hamiltonian. In the next sections, we will now consider the scaling limit of these models.

4.2 SCALING LIMIT OF THE ALTERNATING CASE

The Hamiltonian given by (3.38) and (3.39) for alternating staggering (s = 0, see also (3.24)) can be written as

$$
\mathbb{H} = -\frac{2}{\sin(\gamma)} \sum_{j=1}^{2L-1} e_{j,j+1} + \frac{\sin(\alpha)}{\sin(\gamma)\sin^2(\alpha+\gamma)} \sum_{j=2}^{2L-1} \left(\sin(\alpha + (-1)^{j+1}\gamma)\, e_{j,j+1}\, e_{j-1,j} \right.
$$
$$
\left. + \sin(\alpha + (-1)^j \gamma)\, e_{j-1,j}\, e_{j,j+1} \right) \tag{4.30}
$$

where we introduced — to use the same notation as the literature [54] — the so-called staggering parameter $i\alpha = 2\delta_0$ and have defined $e_{j,j+1}$ to be

$$
e_{j,j+1} = \frac{1}{2} \left(\sigma_j^x \sigma_{j+1}^x + \sigma_j^y \sigma_{j+1}^y + \cos(\gamma)(\sigma_j^z \sigma_{j+1}^z - \mathbf{1}) + \mathrm{i}\sin(\gamma)(\sigma_j^z - \sigma_{j+1}^z) \right). \tag{4.31}
$$

In fact, the above $e_{j,j+1}$ are the vertex representation of the generators of the Temperely-algebra whose defining relations read

$$
\begin{aligned}
e_{j,j+1}e_{j+1,j+2}e_{j,j+1} &= e_{j,j+1}, & e_{j,j+1}e_{j,j+1} &= -2\cos(\gamma)e_{j,j+1}, \\
e_{j+1,j+2}e_{j,j+1}e_{j+1,j+2} &= e_{j+1,j+2}, & e_{k,k+1}e_{j,j+1} &= e_{j,j+1}e_{k,k+1}, & |k-j| > 1.
\end{aligned} \tag{4.32}
$$

Inserting the RHS of (4.31) in (4.30) for $e_{j,j+1}$ leads to a Hamiltonian purely expressed in Pauli matrices. For notational clarity, we have exiled it to appendix C. Note that the Hamiltonian is non-hermitian. We order its eigenvalues by their real parts. Along our study of the scaling limit, we will see that the imaginary parts will decrease to zero as $L \to \infty$.

Let us consider some limiting cases of the Hamiltonian (4.30). For $\alpha \to 0$ it becomes — as expected — the homogeneous XXZ chain with $U_q(\mathfrak{sl}(2))$ invariant BCs. A more subtle limit is $\gamma \to 0$. In this case, the Hamiltonian becomes

$$
\begin{aligned}
\lim_{\gamma \to 0} \sin(\gamma)\mathbb{H} = &-\frac{1}{2} \sum_{j=1}^{2L-2} \sigma_j^z \sigma_{j+2}^z + 2(\sigma_j^+ \sigma_{j+2}^- + \sigma_j^- \sigma_{j+2}^+) \\
&-\frac{1}{2} \left(\sigma_1^z \sigma_2^z + 2\left(\sigma_1^+ \sigma_2^- + \sigma_1^- \sigma_2^+ \right) \right) \\
&-\frac{1}{2} \left(\sigma_{2L-1}^z \sigma_{2L}^z + 2\left(\sigma_{2L-1}^+ \sigma_{2L}^- + \sigma_{2L-1}^- \sigma_{2L}^+ \right) \right) \\
&+ L,
\end{aligned} \tag{4.33}
$$

which agrees with the one of the *ferromagnetic* XXX chain with *periodic* BCs.

The quasi-momentum operator (3.42) takes up to a normalization[5] the form (see also Figure 3.7)

$$
\mathbb{B} = \log \left[\left(\prod_{i=1}^{L} P_{2i-1,2i} R_{2i-1,2i}(-\mathrm{i}\alpha) \right) e^{-\mathrm{i}\alpha\sigma_1^z/2} \left(\prod_{i=1}^{L-1} P_{2i,2i+1} R_{2i,2i+1}(-\mathrm{i}\alpha) \right) e^{\mathrm{i}\alpha\sigma_{2L}^z/2} \right].
$$
$$
\tag{4.34}
$$

---

[5]We have shifted it by an additive constant which is given by $\log\left[\frac{\sin(2\gamma-\alpha)}{\sin(2\gamma+\alpha)} \right] + (2L-1)\log\left[\frac{\sin(\gamma-\alpha)}{\sin(\gamma+\alpha)} \right]$. Further, we divided by a factor of 2.

The energies and quasi-momenta have a simple form in terms of the Bethe roots $\{u_j\}$ solving (4.29) where in the latter we set the inhomogeneities to $\pm\frac{\mathrm{i}\alpha}{2}$ on $(-)$ even and $(+)$ odd sites

$$E = \sum_{j=1}^{L-\mathcal{S}} \epsilon_0(u_j)\,, \qquad B = \sum_{i=1}^{L-\mathcal{S}} k_0(u_i)\,. \tag{4.35}$$

Here, the bare quantities ϵ_0 and k_0 read in trigonometric notation

$$\epsilon_0(u) = -\frac{2\sin(\alpha-\gamma)}{\cosh(2u)-\cos(\alpha-\gamma)} + \frac{2\sin(\alpha+\gamma)}{\cosh(2u)-\cos(\alpha+\gamma)}\,, \tag{4.36}$$

$$k_0(u) = \log\left[\frac{\cosh(2u)-\cos(\alpha+\gamma)}{\cosh(2u)-\cos(\alpha-\gamma)}\right]\,. \tag{4.37}$$

Further, we choose the branch of the logarithm in the definition of the quasi-momentum such that

$$-\pi < \Im m\big(B\big) \le \pi\,. \tag{4.38}$$

The reason why (4.38) was chosen will be explained later in the discussion around (4.80). Moreover, recall that the transfer matrix possesses the duality transformation (3.28). This can also be seen on the level of the Bethe equations (4.29). If we perform the duality transformation and the following redefinition of the Bethe roots

$$\alpha \to \pi - \alpha\,, \qquad u_k \to u_k + \frac{\mathrm{i}\pi}{2}\,, \tag{4.39}$$

solutions of (4.29) are mapped to solutions of (4.29). In view of (4.35), one can see that the energy E is invariant under (4.39) while the quasi-momentum changes the sign $B \to -B$.

### 4.2.1 NUMERICAL STUDY OF SMALL NUMBER OF LATTICE SITES

As a basis for our study of the finite-size spectrum of the staggered six-vertex model using its Bethe ansatz solution, we have numerically diagonalised the Hamiltonian (4.30) and the quasi-momentum (4.34) for small lattices in the parametric domain (to which we will restrict in the following)

$$\gamma < \alpha < \pi - \gamma\,, \qquad 0 < \gamma < \frac{\pi}{2}\,, \qquad 0 < \alpha < \pi. \tag{4.40}$$

In Figure 4.2, we present the real parts of the energies as a function of the anisotropy γ for $L = 3$ and 4 and different values of the staggering parameter α.

Surprisingly, we find the spin of the model's ground state depends on the anisotropy parameter: ground state crossings are observed at certain rational fractions of γ/π. For the small lattices which are accessible to the numerical diagonalization, we find as an approximate rule that the ground state has $U_q(\mathfrak{sl}(2))$-spin $\mathcal{S}$ for anisotropies γ in the interval

$$\frac{\pi}{2(\mathcal{S}^{GS}+1)} \lesssim \gamma \lesssim \frac{\pi}{2\mathcal{S}^{GS}}\,. \tag{4.41}$$

67
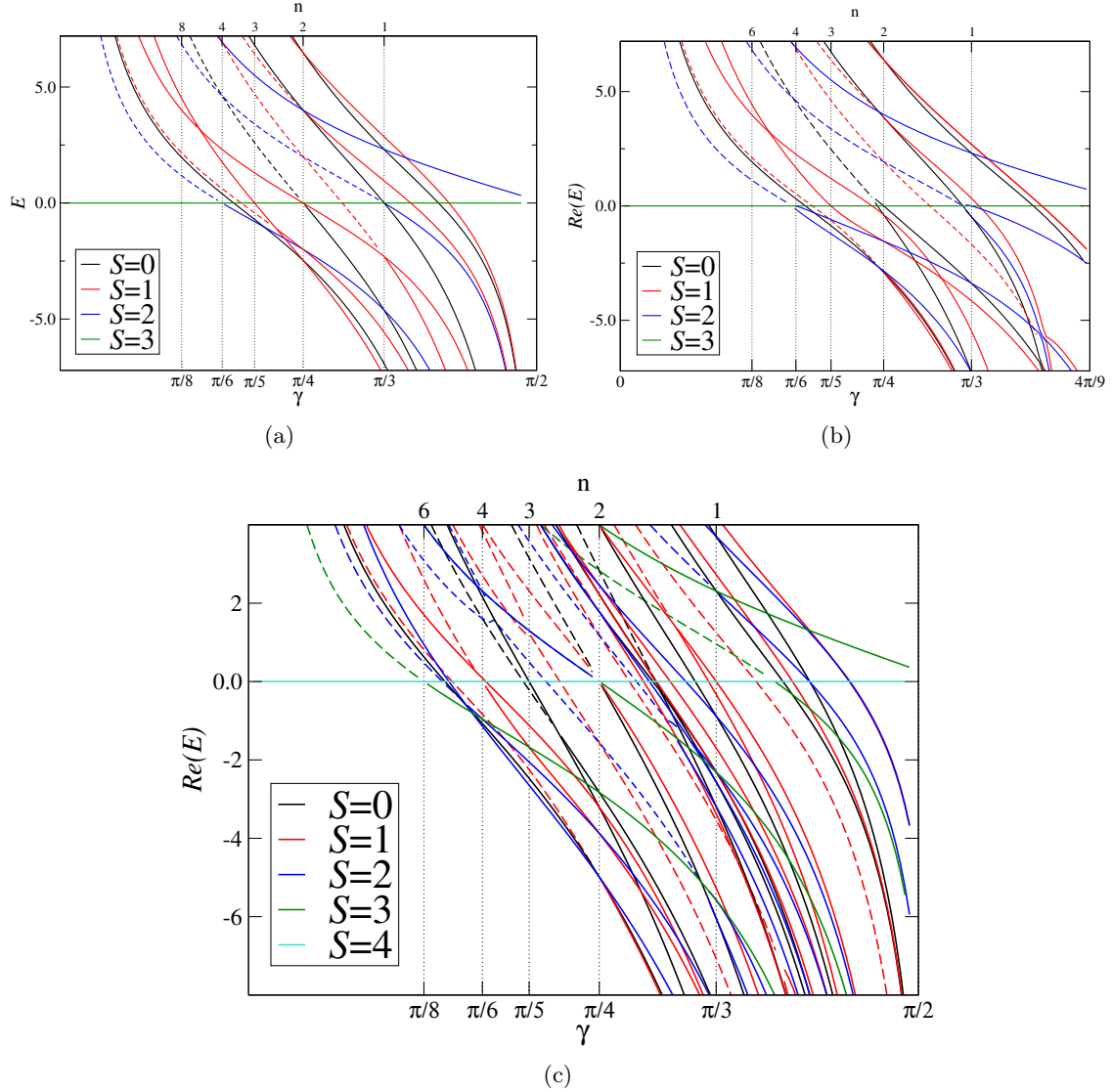
Figure 4.2: For the reader's convenience, we have displayed both conventions $q = \mathrm{e}^{\mathrm{i}\gamma}$ and the later to be introduced $q = \mathrm{e}^{\frac{\mathrm{i}\pi}{n+2}}$: (a) We illustrate the spectrum of the Hamiltonian for $L = 3$ and $\alpha = \pi/2$, which is completely real for this choice of parameters. The solid lines indicate levels with real quasi-momentum, while the dashed ones represent a purely imaginary quasi-momentum. The colours indicate the quantum number $\mathcal{S}$. (b) Depicted is the real part of the spectrum of the model with staggering $\alpha = 4\pi/9$ and $L = 3$. (c) Shown is the real part of the spectrum of the self-dual model $\alpha = \pi/2$ for $L = 4$. We see a new ground state crossing appears at $\gamma = \pi/8$, ($n = 6$) in comparison to the $L = 3$ case.

We will confirm that these inequalities become exact for larger systems through our Bethe ansatz analysis below. For $0 \leq \gamma \lesssim \pi/2L$ the ground state is in the sector with maximum $\mathcal{S}^{GS} = L$, matching our observation that the Hamiltonian (4.30) becomes that of the *ferromagnetic* Heisenberg chain in the limit $\gamma \to 0$. Hence, the $U_q(\mathfrak{sl}(2))$ symmetry is maximal spontaneously broken in this range of γ. This is different from the periodic model, where the ground state is a unique state with total $S^z = 0$ for all anisotropies [20].

Furthermore, we find that the eigenvalues of the quasi-momentum operator may transmute from real into purely imaginary ones when the anisotropy γ is lowered. The lower γ, the more energy levels acquire a purely imaginary quasi-momentum. Such a transmutation has been found to be related to the appearance of discrete states in the spectrum of conformal weights of a staggered superspin chain based on a deformation of the algebra $sl(2|1)$ [108].

The above analysis has been carried out for small lattice sizes only. However, we will see how the same results appear when using the root density formalism valid for all lattice sizes.

4.2.2 The root density approach for the ground state

To proceed with our studies, we have to identify the Bethe root configurations in the regime (4.40) describing the low energy states. We find that the Bethe states parameterised by $M = L - \mathcal{S}$ Bethe roots always realise the highest-weight state in a given $\mathcal{S}$ spin multiplet.

Moreover, we find in the regime of anisotropies $0 < \gamma < \pi/2$ that the root configurations of the ground state consist of two types of Bethe roots, either completely real or with an imaginary part $\pi/2$:

$$u_m^0 = x_m \, , \qquad m = 1, 2, 3, \ldots, M^0 \, , \qquad u_n^{\frac{\pi}{2}} = y_n + \frac{\mathrm{i}\pi}{2} \, , \qquad n = 1, 2, 3, \ldots, M^{\frac{\pi}{2}} \, . \quad (4.42)$$

This observation enables us to study the model further in the introduced root density formalism, see the discussion around (2.155). By taking the logarithm, we obtain the following logarithmic equations for real parts, x_m and y_n

$$2\pi I_m^x = -2L\phi\left(x_m, \frac{\gamma - \alpha}{2}\right) - 2L\phi\left(x_m, \frac{\alpha + \gamma}{2}\right) + \sum_{k=1,\neq m}^{M^0} \phi\left(x_m - x_k, \gamma\right)$$

$$+ \sum_{k=1,\neq m}^{M^0} \phi\left(x_m + x_k, \gamma\right) - \sum_{k=1}^{M^{\frac{\pi}{2}}} \psi\left(x_m - y_k, \gamma\right) - \sum_{k=1}^{M^{\frac{\pi}{2}}} \psi\left(x_m + y_k, \gamma\right) \, , \quad m = 1, \ldots, M^0 \, ,$$

$$2\pi I_n^y = 2L\psi\left(y_n, \frac{\gamma - \alpha}{2}\right) + 2L\psi\left(y_n, \frac{\alpha + \gamma}{2}\right) - \sum_{k=1}^{M^0} \psi\left(y_n - x_k, \gamma\right)$$

$$- \sum_{k=1}^{M^0} \psi\left(y_n + x_k, \gamma\right) + \sum_{k=1,\neq m}^{M^{\frac{\pi}{2}}} \phi\left(y_n - y_k, \gamma\right) + \sum_{k=1,\neq m}^{M^{\frac{\pi}{2}}} \phi\left(y_n + y_k, \gamma\right) \, , \quad n = 1, \ldots, M^{\frac{\pi}{2}} \, .$$

$$(4.43)$$

Here, we have introduced $I_m^{x;y} \in \mathbb{N}$ characterizing the different branches of the logarithm and further have defined

$$\phi(x, y) = 2\arctan\left(\tanh(x)\cot(y)\right) \, , \qquad (4.44)$$

$$\psi(x, y) = 2\arctan\left(\tanh(x)\tan(y)\right) \, . \qquad (4.45)$$

The solutions of these equations become dense on the whole real lines in the thermodynamic limit $L \to \infty$ with $M^{0,\frac{\pi}{2}}/L$ fixed. This allows us to describe the distributions of the Bethe roots for the ground state by two densities, i.e. see (2.155). The coupled linear integral

equations fixing these densities can be derived by the doubling procedure of the Bethe roots (see, e.g. [125]) and are given by

$$\rho^x(x) = \sigma_0^x(x) + \frac{\tau_0^x(x)}{L} + \int_{-\infty}^{\infty} dx' K_0(x-x')\rho^x(x') + \int_{-\infty}^{\infty} dx' K_1(x-x')\rho^y(x') + \mathcal{O}\left(\frac{1}{L^2}\right),$$
$$\rho^y(x) = \sigma_0^y(x) + \frac{\tau_0^y(x)}{L} + \int_{-\infty}^{\infty} dx' K_1(x-x')\rho^x(x') + \int_{-\infty}^{\infty} dx' K_0(x-x')\rho^y(x') + \mathcal{O}\left(\frac{1}{L^2}\right).$$
(4.46)

The driving terms and the integral kernels are given by the following expressions, where the prime denotes the derivative with respect to the first argument:

$$\sigma_0^x(x) = -\frac{1}{\pi}\phi'\left(x, \frac{\gamma-\alpha}{2}\right) - \frac{1}{\pi}\phi'\left(x, \frac{\alpha+\gamma}{2}\right),$$
$$\sigma_0^y(x) = \frac{1}{\pi}\psi'\left(y, \frac{\gamma-\alpha}{2}\right) + \frac{1}{\pi}\psi'\left(y, \frac{\alpha+\gamma}{2}\right),$$
$$\tau_0^x(x) = -\frac{1}{\pi}\phi'(2x, \gamma) - \frac{1}{2\pi}\phi'(x, \gamma) + \frac{1}{2\pi}\psi'(x, \gamma),$$
$$\tau_0^y(x) = -\frac{1}{\pi}\phi'(2x, \gamma) - \frac{1}{2\pi}\phi'(x, \gamma) + \frac{1}{2\pi}\psi'(x, \gamma),$$
$$K_0(x) = \frac{1}{2\pi}\phi'(x, \gamma), \quad K_1(x) = -\frac{1}{2\pi}\psi'(x, \gamma).$$
(4.47)

Note that for $\alpha = \pi/2$, the driving terms coincide, reflecting the self-duality of the model for this value of the staggering parameter. The integral equations can be solved order by order in $1/L$ by Fourier transformation. We obtain the results for the first two orders:

$$\sigma^x(x) = \frac{2\sin\left(\frac{\pi(\alpha-\gamma)}{\pi-2\gamma}\right)}{\pi-2\gamma} \frac{1}{\cosh\left(\frac{2\pi x}{\pi-2\gamma}\right) - \cos\left(\frac{\pi(\alpha-\gamma)}{\pi-2\gamma}\right)},$$
$$\sigma^y(x) = \frac{2\sin\left(\frac{\pi(\alpha-\gamma)}{\pi-2\gamma}\right)}{\pi-2\gamma} \frac{1}{\cosh\left(\frac{2\pi x}{\pi-2\gamma}\right) + \cos\left(\frac{\pi(\alpha-\gamma)}{\pi-2\gamma}\right)},$$
$$\tau^x(x) = \tau^y(x) = \frac{1}{4\pi}\int_{-\infty}^{\infty} d\omega\, e^{i\omega x} \frac{\sinh\left(\frac{3\gamma-\pi}{4}\omega\right)}{\sinh\left(\frac{\gamma\omega}{4}\right)\cosh\left(\frac{2\gamma-\pi}{4}\omega\right)}.$$
(4.48)

Note that $\sigma^x(x) \leftrightarrow \sigma^y(x)$ under the duality transformation $\alpha \to \pi - \alpha$, see (4.39). Furthermore, the bulk densities are positive in the considered interval (4.40). From these densities, we compute the number of Bethe roots of the different types describing the ground state and obtain

$$\frac{2M_{GS}^0 + 1}{L} = 2 \cdot \frac{\pi - \alpha - \gamma}{\pi - 2\gamma} + \frac{1}{L}\left(\frac{3}{2} - \frac{\pi}{2\gamma}\right) + \mathcal{O}\left(\frac{1}{L^2}\right),$$
$$\frac{2M_{GS}^{\frac{\pi}{2}} + 1}{L} = 2 \cdot \frac{\alpha - \gamma}{\pi - 2\gamma} + \frac{1}{L}\left(\frac{3}{2} - \frac{\pi}{2\gamma}\right) + \mathcal{O}\left(\frac{1}{L^2}\right).$$
(4.49)

The individual numbers of Bethe roots are α and γ dependent. With the above expression and the fact that all Bethe states are highest weight states, we can compute the sector $\mathcal{S}$ in which the ground state is realized. The surface contribution would imply a non-zero spin

$-\frac{1}{2} + \frac{\pi}{2\gamma}$ of the ground state, which is independent of the staggering α but is a non-integer due to the explicit γ dependence. This can be resolved by rounding the number of Bethe roots (4.49) and the resulting ground state spin $\mathcal{S}^{GS}$ to the nearest integer number, giving

$$\mathcal{S}^{GS} = \left\lfloor -\frac{1}{2} + \frac{\pi}{2\gamma} \right\rceil . \tag{4.50}$$

Here, the brackets $\lfloor...\rceil$ indicate the rounding to the nearest integer. Inverting this relation, we obtain a range of anisotropies γ for which the ground state is realized in the sector with spin $\mathcal{S}^{GS}$:

$$\frac{\pi}{2\mathcal{S}^{GS} + 2} < \gamma < \frac{\pi}{2\mathcal{S}^{GS}}. \tag{4.51}$$

This formula refines the approximate rule (4.41), which we have conjectured based on our numerical investigations of small systems above. The minor differences between (4.51) and the numerical observations for small lattices can be interpreted as a result of the excessive influence of the boundary terms for small L. Note that (4.50) tends to infinity as $\gamma \to 0$ reflecting the relation (4.33) to the ferromagnetic XXX chain in this limit. This generalises our findings regarding the spontaneously broken $U_q(\mathfrak{sl}(2))$ symmetry from small system sizes to general L.

While the spin $\mathcal{S}^{GS} = L - (M_{GS}^0 + M_{GS}^{\frac{\pi}{2}})$ of the ground state is independent of α, the difference or the ratio of the numbers $M_{GS}^{0,\frac{\pi}{2}}$ of the corresponding Bethe roots depend on the staggering parameter: from the bulk contributions to (4.49) we obtain

$$dN_{GS} = M_{GS}^0 - M_{GS}^{\frac{\pi}{2}} = L\frac{\pi - 2\alpha}{\pi - 2\gamma} , \tag{4.52}$$

$$\frac{2M_{GS}^0 + 1}{2M_{GS}^{\frac{\pi}{2}} + 1} = \frac{\pi - \alpha - \gamma}{\alpha - \gamma} + \mathcal{O}\left(\frac{1}{L}\right) . \tag{4.53}$$

Hence, by varying α, crossings between different $\mathcal{S}$ states may be induced. To realise the corresponding root configurations on a given lattice, the numbers of roots should be commensurate with L, i.e. have a rational ratio and a simple scaling of the difference of the number of Bethe roots for the bulk contribution. This is achieved by fixing α as

$$\alpha = \frac{r_1\gamma + r_2(\pi - \gamma)}{r_1 + r_2}, \tag{4.54}$$

where r_1 and r_2 are positive integers and relatively prime to each other [54]. With that condition, one would obtain the following expression for the ratio and difference between the two types of roots:

$$\frac{2M_{GS}^0 + 1}{2M_{GS}^{\frac{\pi}{2}} + 1} = \frac{r_1}{r_2} + \mathcal{O}\left(\frac{1}{L}\right) ,$$
$$M_{GS}^0 - M_{GS}^{\frac{\pi}{2}} = L\frac{r_1 - r_2}{r_1 + r_2} . \tag{4.55}$$

Note that by setting $r_1 = r_2 = 1$, which corresponds to the self-dual case $\alpha = \pi/2$, the numbers of the two types of Bethe roots become the same for all γ, corresponding to the additional degeneracy of the spectrum.

Knowing the ground state densities (4.48), the bulk and boundary contributions to the expectation values of the conserved quantities in the thermodynamic limit can be calculated. The bulk and surface energy densities are given by

$$e_\infty = -2 \int_{-\infty}^{\infty} d\omega \frac{\sinh(\frac{\gamma\omega}{2}) \left(\sinh\left(\frac{\pi\omega}{2} - \frac{\omega\gamma}{2}\right)\cosh(\frac{\omega\pi}{2} - \alpha\omega) - \sinh(\frac{\gamma\omega}{2})\right)}{\sinh(\frac{\omega\pi}{2})\sinh((\frac{\pi-2\gamma}{2})\omega)} , \tag{4.56}$$

$$f_\infty = -\int_{-\infty}^{\infty} d\omega \frac{\cosh\left(\frac{1}{4}(\pi - 2\alpha)\omega\right)\sinh\left(\frac{1}{4}(3\gamma - \pi)\omega\right)\cosh\left(\frac{\gamma\omega}{4}\right)}{\cosh\left(\frac{1}{4}(\pi - 2\gamma)\omega\right)\sinh\left(\frac{\pi\omega}{4}\right)} - \frac{4\sin(2\gamma)}{\cos(2\alpha) - \cos(2\gamma)}. \tag{4.57}$$

The Fermi velocity reads

$$v_{\mathrm{F}} = \frac{2\pi}{\pi - 2\gamma} . \tag{4.58}$$

Similarly, we obtain an expression for the value of the quasi-momentum of the ground state in the thermodynamic limit

$$B_{\mathrm{thermo}} = Lk_\infty + k_s, \tag{4.59}$$

where the bulk k_∞ and surface k_s contributions read

$$k_\infty = 2 \int_{-\infty}^{\infty} d\omega \frac{\sinh(\frac{\omega\gamma}{2})\sinh(\frac{\pi\omega}{2} - \alpha\omega)\sinh(\frac{\pi-\gamma}{2}\omega)}{\omega \sinh(\frac{\omega\pi}{2})\sinh(\frac{\pi-2\gamma}{2}\omega)} , \tag{4.60}$$

$$k_s = \int_{-\infty}^{\infty} d\omega \frac{\sinh(\frac{3\gamma-\pi}{4}\omega)\cosh(\frac{\gamma\omega}{4})\sinh(\frac{\pi-2\alpha}{4}\omega)}{\omega \sinh(\frac{\omega\pi}{4})\cosh(\frac{2\gamma-\pi}{4}\omega)} - \log\left(\frac{\sin(\gamma + \alpha)}{\sin(\gamma - \alpha)}\right) . \tag{4.61}$$

Having these explicit expressions, we can start to characterise the effective field theory describing the low-energy regime of the spin chain for large system sizes by studying the finite-size spectrum. Due to the criticality of the model and the open BCs, we expect that the field theory is a BCFT. Hence, we expect (2.97) to hold. In the following, it is useful to introduce the following parameterisation of the anisotropy parameter

$$\gamma = \frac{\pi}{n + 2} \qquad (n > 0) . \tag{4.62}$$

By studying the asymptotic behaviour of energy of the ground state of the lattice model, which is realized in the sector with spin $\mathcal{S} = \mathcal{S}^{GS}(\gamma)$, (see equation (4.50)), we can extract the effective central charge [27]

$$c_{\mathrm{eff}} = -24\, X_{\mathrm{eff}}^{GS} \tag{4.63}$$

$$= 2 - \frac{24}{n + 2} \left(\mathrm{frac}\left(1 + \frac{n}{2}\right) - \frac{1}{2}\right)^2 , \tag{4.64}$$

where $\mathrm{frac}\left(1 + \frac{n}{2}\right)$ denotes the fractional part of $1 + \frac{n}{2}$. The cusps are, due to the fractional part of the effective central charge, a consequence of the ground state crossings occurring at integer values of $1 + \frac{n}{2}$ in the staggered six-vertex model, see Figure 4.3.
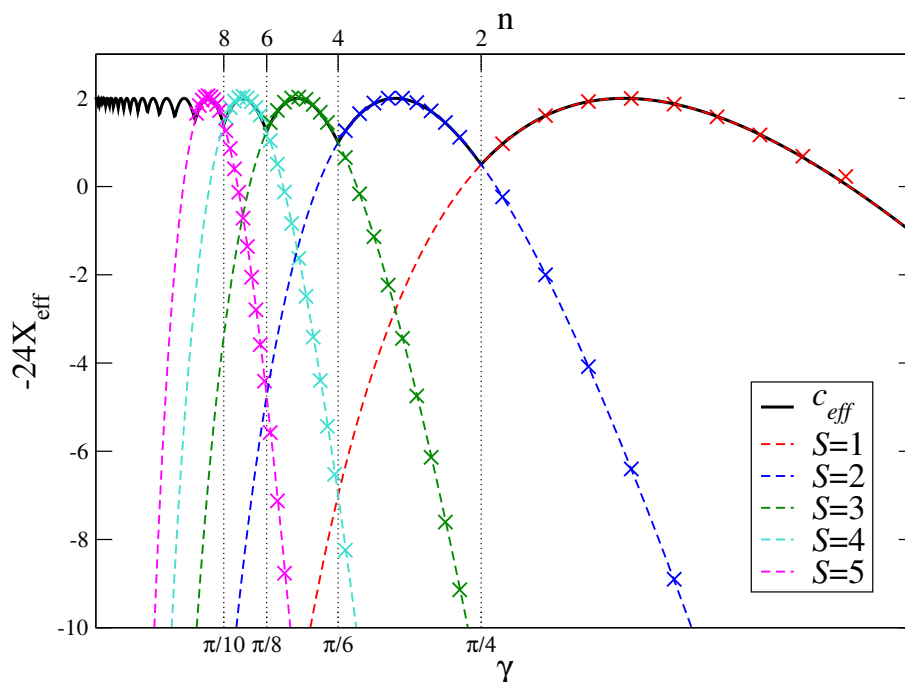
Figure 4.3: The effective central charge (4.64) of the staggered spin chain as a function of the anisotropy is represented as the solid black line. The dashed coloured lines are plots of (4.63) in sectors with given spin $\mathcal{S}$, crosses represent the effective central charges c_{eff} obtained from the Bethe ansatz solutions for large L. The vertical dotted lines represent the ground state crossings.

4.2.3 Analysis of one class of states

To determine the (effective) scaling dimensions, one needs to take low-lying excitations above the ground state into account. We find that a particular class of states has Bethe root configurations that are still given by (4.42) but with different quantum numbers $\mathcal{S}$ and dN as compared to the ground state (4.51), (4.52), see Figure 4.4 for an illustration. Hence, these states can be analogous to the ground state described in the framework of the root density formalism. However, the integral boundaries of the linear integral equations for the excited states will differ from those of the ground state representing the different values of quantum numbers $\mathcal{S}$, dN.

For two branches of excitations with the same Fermi velocity, the resulting finite-size energies can be expressed in terms of the above quantum numbers as [126, 127, 128, 129] (for the particular case of open BCs see [125, 62])

$$E(L) \asymp Le_{\infty} + f_{\infty} + \frac{\pi v_{\text{F}}}{L} \left\{ \frac{1}{2} \Delta \vec{M}^T \left(Z Z^{\top} \right)^{-1} \Delta \vec{M} \right\}, \tag{4.65}$$

where

$$\Delta \vec{M} = \begin{pmatrix} M^0 - M_{GS}^0 \\ M^{\frac{\pi}{2}} - M_{GS}^{\frac{\pi}{2}} \end{pmatrix}, \qquad Z = \lim_{x \to \infty} \begin{pmatrix} \xi_{11}(x) & \xi_{12}(x) \\ \xi_{21}(x) & \xi_{22}(x) \end{pmatrix}.$$
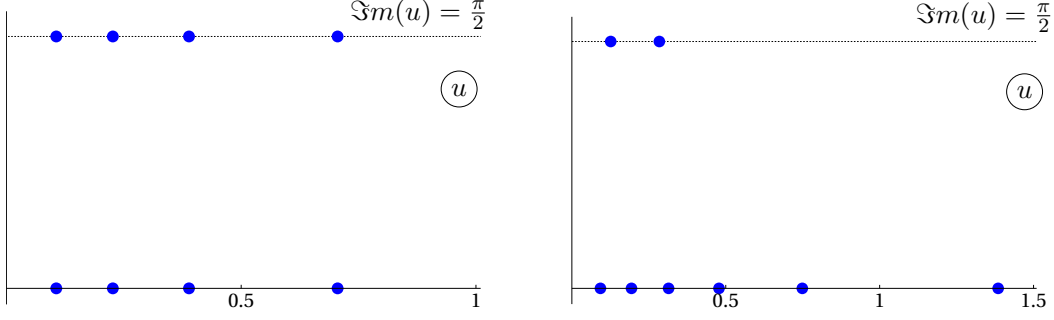
Figure 4.4: The left and right panels display the Bethe roots in the complex $u = -\frac{1}{2}\log(\zeta)$ plane for the ground state and an excited state, respectively, of the spin chain with $L = 10$. The excitation is built by disbalancing the number of roots on the two lines with respect to the ground state pattern. The states have total $U_q\big(\mathfrak{sl}(2)\big)$ spin $\mathcal{S} = 2$ while $n = 2.9$ ($\gamma = 0.64114$).

We recall that $\mathcal{S} = L - M^0 - M^{\frac{\pi}{2}}$ and the difference in the numbers of Bethe roots of the two different types (4.42) is $dN = M^0 - M^{\frac{\pi}{2}}$. Z is the so-called dressed charge matrix defined by linear integral equations similar to (4.46):

$$\begin{aligned}
\xi_{11}(x) &= 1+ \int_{-\infty}^{\infty} \mathrm{d}x' \, K_0(x-x')\xi_{11}(x') + \int_{-\infty}^{\infty} \mathrm{d}x' \, K_1(x-x')\xi_{21}(x') \,, \\
\xi_{21}(x) &= \int_{-\infty}^{\infty} \mathrm{d}x' \, K_1(x-x')\xi_{11}(x') + \int_{-\infty}^{\infty} \mathrm{d}x' \, K_0(x-x')\xi_{21}(x') \,, \\
\xi_{12}(x) &= \int_{-\infty}^{\infty} \mathrm{d}x' \, K_0(x-x')\xi_{12}(x') + \int_{-\infty}^{\infty} \mathrm{d}x' \, K_1(x-x')\xi_{22}(x') \,, \\
\xi_{22}(x) &= 1+ \int_{-\infty}^{\infty} \mathrm{d}x' \, K_1(x-x')\xi_{12}(x') + \int_{-\infty}^{\infty} \mathrm{d}x' \, K_0(x-x')\xi_{22}(x') \,.
\end{aligned} \tag{4.66}$$

By means of the Wiener-Hopf method one finds that [129]

$$\left(ZZ^{\top}\right) = \begin{pmatrix} 1 - \int_{-\infty}^{\infty} \mathrm{d}x \, K_0(x) & -\int_{-\infty}^{\infty} \mathrm{d}x \, K_1(x) \\ -\int_{-\infty}^{\infty} \mathrm{d}x \, K_1(x) & 1 - \int_{-\infty}^{\infty} \mathrm{d}x \, K_0(x) \end{pmatrix}^{-1}$$

giving

$$E(L) \asymp Le_{\infty} + f_{\infty} + \frac{\pi v_{\mathrm{F}}}{L}\left(-\frac{1}{12} + \frac{p^2}{n+2} + \frac{1}{4}\frac{(dN - dN_{GS})^2}{\tilde{Z}_D^2}\right), \tag{4.67}$$
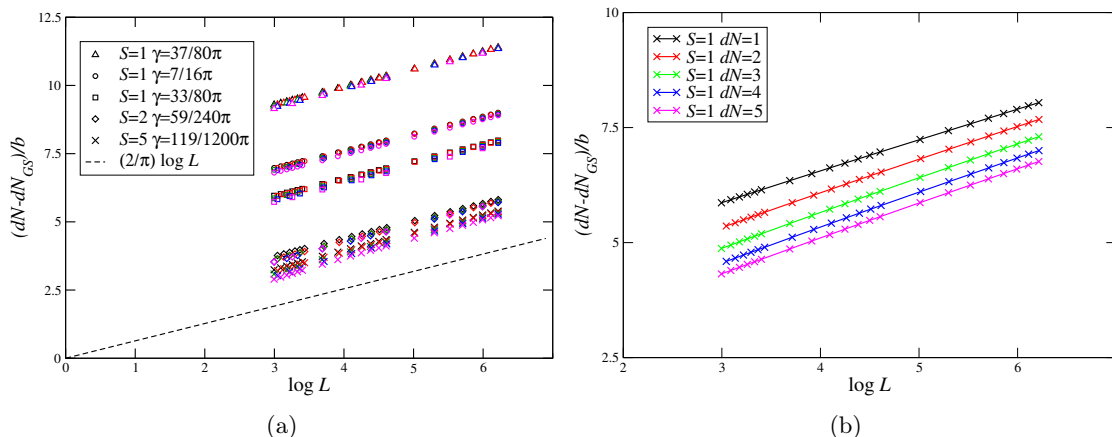
The term p is shorthand for the expression

$$p = \frac{1}{2}\left(2\mathcal{S} + 1 + \mathtt{w}\,(n+2)\right) \qquad \text{with} \qquad \mathtt{w} = -1 \,, \tag{4.68}$$

and we have defined

$$\tilde{Z}_D = \lim_{\omega \to 0}\left(1 - \int_{-\infty}^{\infty} \mathrm{d}x \, \mathrm{e}^{\mathrm{i}\omega x}\,(K_0(x) - K_1(x))\right)^{-1}.$$

We note that $\tilde{Z}_D$ diverges in the limit $\omega \to 0$ as a consequence of the degeneracy of the integral kernel in (4.66). This is a characteristic feature in several lattice models with a

Figure 4.5: $(dN - dN_{GS})/b$ vs. $\log(L)$ on the self-dual line $\alpha = \pi/2$. Different symbols indicate different combinations of $\mathcal{S}$ and γ as labelled in the legend. (a) Collapse of data for spin-$\mathcal{S}$ states and anisotropies $\gamma \lesssim \pi/2\mathcal{S}$ corresponding to the continuous part of the conformal spectrum with different dN (encoded by colouring: black $dN = 1$, red $dN = 2$, green $dN = 3$, blue $dN = 4$ and magenta $dN = 5$). (b) Lifting of this degeneracy w.r.t. dN for the states in the $\mathcal{S} = 1$-continuum for anisotropy $\gamma = 23\pi/80 \gtrsim \pi/4$, where the ground state crosses into the $\mathcal{S} = 2$ sector.

.

continuous spectrum of scaling dimensions emerging in the continuum limit, see e.g. [18, 20, 21]: as a consequence of this singularity, the penultimate term in (4.67) does not contribute to the finite-size scaling for any finite $dN - dN_{GS}$ in the limit $L \to \infty$. For large but finite L one finds that the energy gaps between states with different $dN - dN_{GS}$ vanish as $1/L(\log L)^2$. As in the periodic model, we find that these logarithmic corrections are determined in terms of the eigenvalues of the quasi-momentum operator: to bring the logarithmic corrections in the scaling dimensions under control we introduce the quantum number b based on the difference between the quasi-momentum of the RG trajectory and the one of the thermodynamic ground state

$$b = \frac{n}{2\pi}\Big(B - B_{\text{thermo}}\Big). \tag{4.69}$$

The variable b can be related to the deviation of dN from the one of the ground state dN_{GS} (note that b is real for root configurations (4.42)). One finds that it satisfies the large L asymptotic behaviour [31]

$$b_{dN}(L) = \frac{\pi dN}{2\log(L)} + O\big(1/(\log L)^2\big) \qquad (dN - \text{fixed}). \tag{4.70}$$

We checked this asymptotic behaviour numerically for levels in the spin sectors with several $\mathcal{S}$ and corresponding anisotropies γ from equation (4.51) on the self-dual line. For $\gamma \lesssim \pi/2\mathcal{S}$, i.e. close to the *right* boundary of these intervals, we find that the quotient $(dN - dN_{GS})/b$ for different dN (and L) collapse to a single line $\propto \log L$ with a slope of $2/\pi$ independent of γ, as predicted by (4.70), see Figure 4.5(a). On the other hand, for values of $\gamma \gtrsim \pi/(2\mathcal{S} + 2)$, i.e. close to the transition $\mathcal{S}^{GS} \to \mathcal{S}^{GS} + 1$, we observe a splitting

75

into lines for different values of dN, although still with a slope of $2/\pi$ for sufficiently large system sizes L, see Figure 4.5(b). We emphasise, however, that this does not affect the quality of the parameterization of the logarithmic corrections of the continuous part of the spectrum; see Figures 4.6 and 4.7 below.

Using the quantum number b, we find numerically that

$$E \asymp L\,e_\infty + f_\infty + \frac{\pi v_F}{L}\left(\frac{p^2}{n+2} + \frac{b^2}{n} - \frac{1}{12} + \mathtt{d}\right). \tag{4.71}$$

with $\mathtt{d} = 0$. When assigning an L dependence $|\Psi_L\rangle$ to the class of states discussed above, it is tempting to keep the integer dN fixed. Then, in view of formula (4.70), the value of $b(L)$ would go to zero as $L \to \infty$. However, there is another way of organizing the RG flow. One may increase dN as $\sim \log(L)$ so that the value of $b(L)$ tends to a finite, non zero limit as $L \to \infty$. Such an RG trajectory would be characterized by

$$s = \operatorname*{slim}_{L\to\infty} b(L), \tag{4.72}$$

which can be arranged to be an arbitrary real number as argued in the following: From (4.70) is it clear that as L becomes large, $\Delta b_{dN}(L) = b_{dN+2}(L) - b_{dN}(L) \propto 1/\log L$, so that the values of $b_{dN}(L)$ are densely distributed in some segment of the real line. The latter is given by $(-b_{dN_{\max}}, +b_{dN_{\max}})$, where $dN_{\max}(L) \ll L$ is the maximum value of the integer dN such that the state with Bethe roots (4.42) is still of low energy. Assuming that $dN_{\max}$ grows faster than $\log(L)$ as $L \to \infty$, this segment becomes the entire real line in the scaling limit. Hence, the limiting value s in (4.72) can be arranged to take any real value and we have, in view of (2.97),

$$X_{\mathrm{eff}} = \frac{p^2}{n+2} + \frac{s^2}{n} - \frac{1}{12}. \tag{4.73}$$

Thus, we conclude that the spectrum of scaling dimensions develops a continuous component labeled by the parameter $s \in \mathbb{R}$. Some part of the numerical data used for the above analysis is shown in Figures 4.6 and 4.7. Displayed is the finite-size estimate $X_{\mathrm{eff}}(L)$ of effective conformal weights for fixed dN, once obtained by the finite-size energies (2.168) and also calculated by the Bethe ansatz results for b from (4.71) for various anisotropies γ and staggering α in the spin sector containing the ground state. Extrapolation of the finite-size data to $L \to \infty$ by means of a rational function of $1/\log L$ shows that various levels with $dN \neq dN_{GS}$ converge to the bottom of the corresponding continuum (given by the Bethe state with $dN = dN_{GS}$). Note that (4.73) is the same as the effective scaling dimension for the conformal primaries obtained from the Euclidean Black Hole CFT (2.99) if we make the identification

$$k = n+2 \qquad \left(k = \tfrac{\pi}{\gamma}\right). \tag{4.74}$$

Transmutation: continuous to discrete

In the Euclidean Black Hole CFT, besides the continuous part of the conformal dimensions considered above, there also exists a set of conformal weights with discrete values; see equation (2.83). From the latter and (4.74), we expect that a discrete state with fixed J is
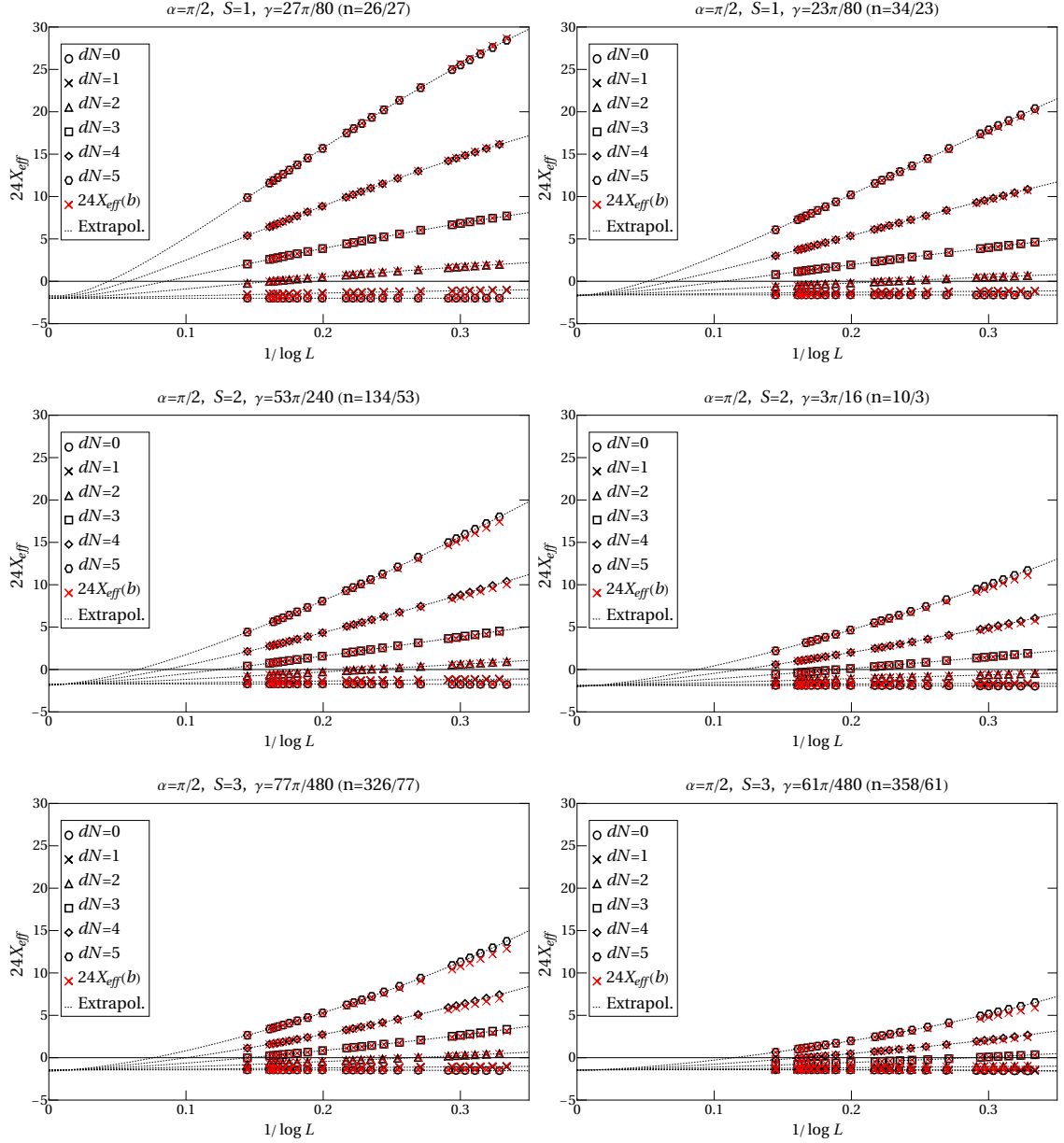
Figure 4.6: Spectrum of conformal weights for the self-dual model (i.e. $dN_{GS} = 0$): for each $\mathcal{S} = 1, 2, 3$ we have chosen two values of the anisotropy in the intervals (4.51) for which $\mathcal{S}$ is the spin of the ground state. The black symbols are the finite-size estimate of the effective scaling dimensions using the finite-size energies obtained from the solution of the Bethe equations. Red symbols represent the scaling dimensions obtained from (4.71) using the Bethe ansatz results for the quasi-momentum. Note that the latter provides an excellent parameterization of the logarithmic corrections via the continuous variable b for all γ values considered (e.g. in the top-right figure for the parameters used in Figure 4.5(b) showing the lifting of the degeneracy of (4.70) w.r.t. dN).
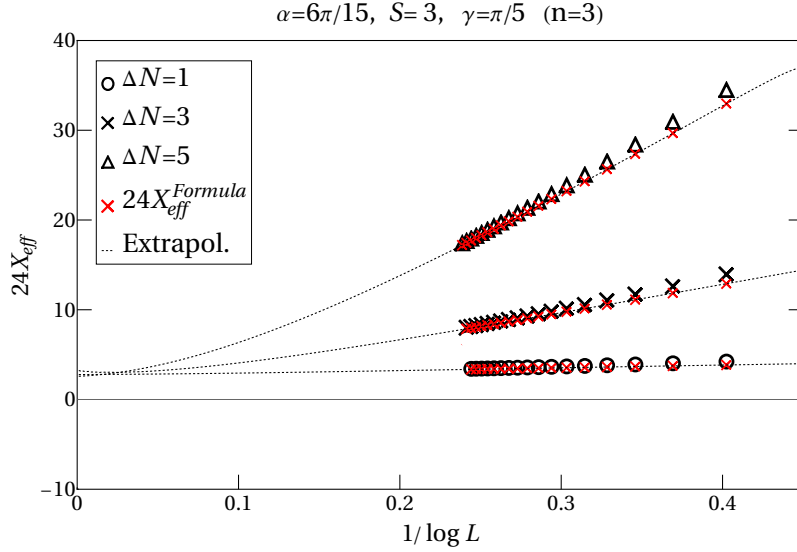
Figure 4.7: Similar as Figure 4.6 but for values of α away from the self-dual point ($\Delta N = dN - dN_{GS}$).

realised in the spin-chain spectrum for n ranging from ∞ to some root integer. Specifically, a discrete state with given J may be realised for

$$0 < \gamma < \frac{\pi}{2J+1}\,, \qquad \left(J < \frac{n+1}{2}\right).\tag{4.75}$$

The discrete CFT states and their realisation conditions can also be related to the quasi-momentum of the Bethe state. In our study of the continuous part of the spectrum above, we found that the Bethe states are parameterised by root configurations (4.42), resulting in real eigenvalues for the quasi-momentum. However, as seen in the study of small lattice sizes, the quasi-momentum can also change from real values to purely imaginary ones when the anisotropy γ is lowered see Figure 4.2.

On the level of Bethe roots, this translates into a root pattern changing from (4.42) to more complicated complex configurations: the real parts (in the u-plane) of one or more of the roots diverge as the anisotropy approaches from above certain rational multiples of π. Reducing the anisotropy further these roots reappear in the finite domain with different imaginary parts. Depending on the state considered this process may be repeated several times until the root configuration acquires the following remarkable pattern: for states parameterised by an even number M of Bethe roots they come in pairs $u_j, \bar{u}_j$ mirrored at the line $\mathrm{i}\pi/4$

$$\begin{aligned} u_j &= x_j + \mathrm{i}y_j\,, \qquad \bar{u}_j = x_j + \mathrm{i}\left(\frac{\pi}{2} - y_j\right) \\ &\text{with} \quad x_j, y_j \geq 0 \qquad j = 1, 2, \ldots, \frac{M}{2}\,. \end{aligned}\tag{4.76}$$

If the number M of Bethe roots is odd there appears an additional root with imaginary
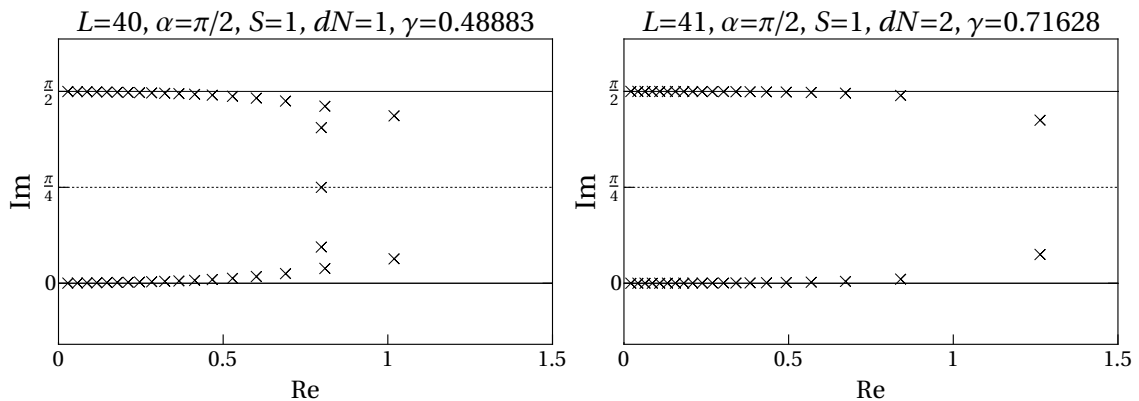
Figure 4.8: Displayed is a typical pattern of Bethe roots leading to an imaginary quasi-momentum. The configurations are obtained from the configurations given in (4.42), with dN as indicated, by lowering the anisotropy. On the left ($n = 4.42676$), we have an odd number of Bethe roots, and so one root lies on the line $\mathrm{i}\pi/4$, while the rest is paired. On the right ($n = 2.38598$), we have an even number of roots, hence, the pairing works.

part $\pi/4$, i.e.

$$u_j = x_j + \mathrm{i}y_j\,, \quad \bar{u}_j = x_j + \mathrm{i}\left(\frac{\pi}{2} - u_j\right)\,, \quad u_M = x + \frac{\mathrm{i}\pi}{4}$$
$$\text{with} \quad x_j, y_j, x \geq 0\,, \qquad j = 1, 2, \ldots, \frac{M-1}{2}\,. \tag{4.77}$$

Examples of such root configurations for spin-1 states on lattices with $L = 40$ (41) sites, i.e. $M = 39$, $M = 40$, evolving from (4.42) with $dN = M^0 - M^{\frac{\pi}{2}} = 1$ and 2, respectively, as γ is lowered are shown in Figures 4.8 and 4.11.

By following the transmutation of configurations (4.42) to (4.76), (4.77) under the variation of γ for small values of dN we are able to observe what happens to the scaling dimensions when the quasi-momentum changes from real to imaginary: as discussed above, the scaling dimensions corresponding to spin-1 states are in the continuous part of the spectrum (4.71) for anisotropies $\pi/4 < \gamma < \pi/2$ where they are separated by finite-size gaps $\sim (dN/\log L)^2$.[6] As γ is reduced further, the lowest levels approach the lower bound of the $\mathcal{S} = 1$ continuum, leaving it when the quasi-momentum becomes purely imaginary, see Figure 4.9 for the lowest states in this spin sector. Specifically we find that the finite-size energies of the states with $dN = 1, 2$ ($dN = 3, 4$), realized for even and odd lattice sizes L respectively, lead to the conformal weights (2.99) of the Black Hole CFT with $J = (k-3)/2$ (($k-5)/2$) in the regime where $s \in \mathrm{i}\mathbb{R}$. It turns out that the finite-size formula (4.73) continues to hold for purely imaginary s: in this case, $J = \frac{1}{2} + \mathrm{i}s$ has to be an element of the discrete set (2.83). This leads to the following condition on the allowed imaginary values of s to which $b(L)$ tends in the scaling limit

$$s = \pm\mathrm{i}\left(-p - \frac{1}{2} - a\right) \qquad \text{with} \qquad a = 0, 1, 2, \ldots < -p - \tfrac{1}{2} \qquad (\mathtt{d} = 0)\,. \tag{4.78}$$

---

[6]In the limit $\gamma \to \pi/2$, one observes a crossover to a linear dependence on $1/\log L$. This can be understood from the fact that the staggered six-vertex model at $\gamma = \pi/2$ coincides with the integrable $OSp(2|2)$ model, which is in a different universality class [130, 131].
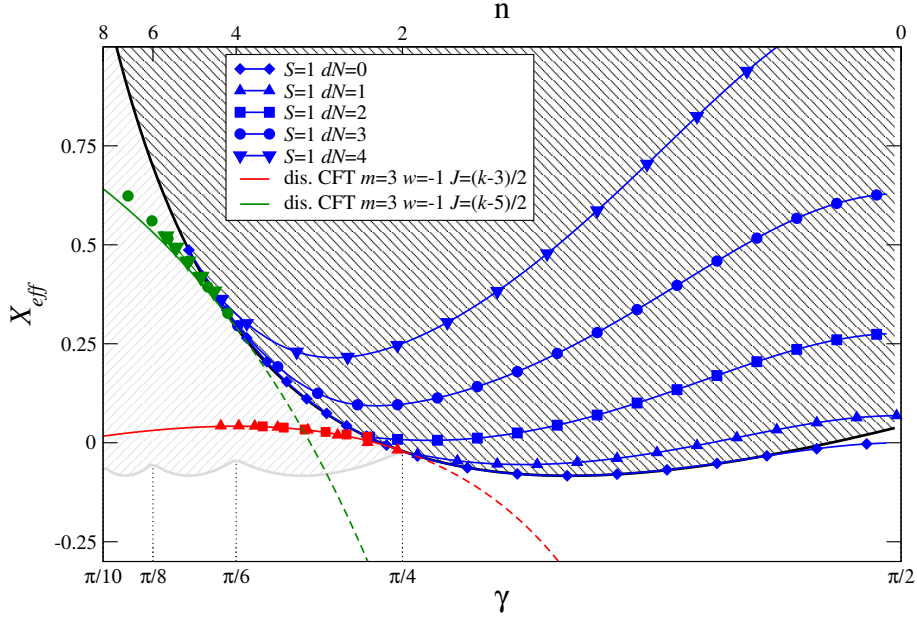
Figure 4.9: Effective scaling dimensions vs. anisotropy γ (n) for the self-dual model, $\alpha = \pi/2$, of size $L = 40, 41$ derived for the lowest states in the $\mathcal{S} = 1$ sector, showing the transmutations of continuous states into discrete ones. The black shaded area represents the continuum of levels starting at the spin-$\mathcal{S}^{GS} = 1$ ground state. Grey shading indicates the continua in the spin $\mathcal{S}^{GS} > 1$ sectors, which overlap with each other and the spin-$\mathcal{S}^{GS} = 1$ one. The lower edge of the continua corresponds to c_{eff} (4.64) up to a factor of -24. Blue symbols denote the effective scaling dimensions obtained from finite-size data corresponding to weights from the continuous part with $\mathcal{S} = 1$ of the CFT spectrum given in terms of root configurations (4.42) with different dN. Red and green symbols depict the continuation of the corresponding states (same symbol shape) to anisotropies where the Bethe root patterns change to (4.76) or (4.77) and the quasi-momentum b becomes imaginary. Red (green) solid lines are the effective scaling dimensions (2.82), (2.83), (2.99) of the primary fields with $m = 3, w = -1$ and $J = (k-3)/2$ $((k-5)/2)$ for $k = \pi/\gamma, (n+2)$. Dashed lines are their continuation to anisotropies $\gamma > \pi/(2J+1), (n+1 < 2J)$ where the corresponding operators in the CFT become non-normalizable.

Note that this implies that the thresholds for the appearance of discrete levels of the Black Hole CFT resulting from the unitarity condition (2.83) coincide with the anisotropies (4.51) where the spin of the ground state in the lattice model changes. This prediction can be compared with our numerical findings for the $\mathcal{S} = 1$ states with $J = (k-3)/2 - a$, $a = 0, 1$, considered in Figure 4.9. Their quasi-momentum $b(L)$, once it becomes imaginary, is expected to match[7] the condition for s above for $a = 0, 1$, i.e.

$$
\begin{aligned}
s_{a=0} &= \pm \mathrm{i}\left(\frac{n}{2} - 1\right) &&\text{for } 2 < n\,, \\
s_{a=1} &= \pm \mathrm{i}\left(\frac{n}{2} - 2\right) &&\text{for } 4 < n\,.
\end{aligned}
\tag{4.79}
$$

Our numerical data show that the change from real to imaginary quasi-momentum takes

---

[7]Note that, as the states are then discreet, we expect that the $b(L) \to s$ very fast, such that one can set $b(L) \sim s$ already for immediate system sizes such as $L \sim 40$.
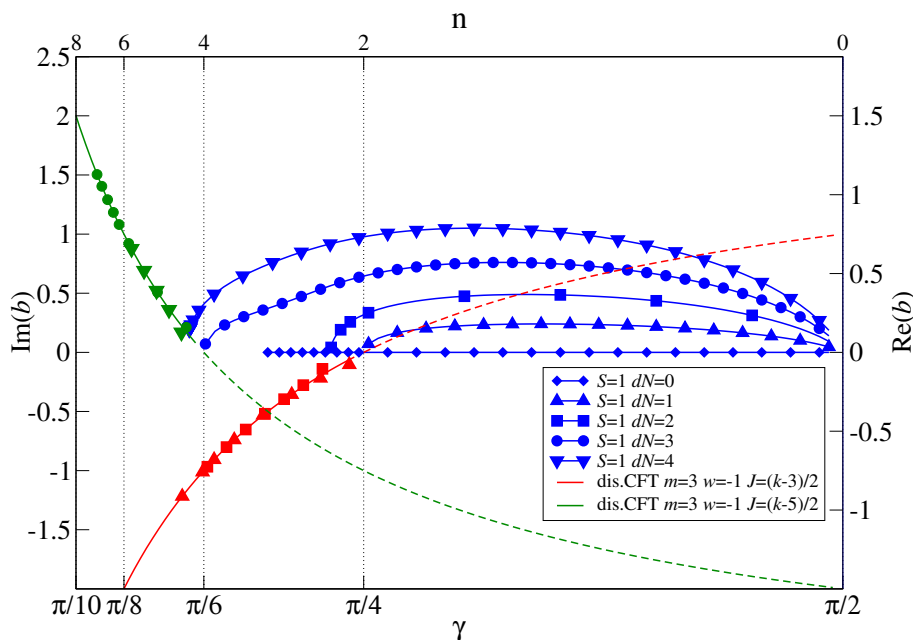
Figure 4.10: Real (blue symbols) and imaginary (red and green symbols) part of the quasi-momentum b vs. anisotropy γ (n) for the spin $\mathcal{S} = 1$ states considered in Figure 4.9. The solid red and green lines depict the CFT predictions s via (4.79). Dashed lines are obtained by continuation of the CFT data into the region where the unitarity condition (2.83) is violated. Note that $b \equiv 0$ for the $dN = 0$ state.

place at or slightly below these values of γ. Overall, i.e. up to finite-size corrections near these thresholds, equations (4.79) match our results for the quantum number b obtained for system sizes $L = 40$ and 41, see Figure 4.10.

To end this section, let us briefly comment on the the choice of the branch for the logarithm in the expression (4.38) which induces

$$ -\frac{n}{2} < \Im m\big(b(L)\big) \leq \frac{n}{2} \,. \tag{4.80} $$

For all the trajectories — also in the later analysis — we constructed, it turned out that consistency with the asymptotic formula for the energy (4.71) requires this particular choice of the branch. The question of which of the boundaries $\Im m\big(b(L)\big) = \pm\frac{n}{2}$ to include in the domain of $b(L)$ does not matter for the following reason. The only RG trajectories, e.g. see Figure 4.11, of the spin chain which were observed such that $\Im m\big(b(L)\big) \to \pm\frac{in}{2}$ as $L \to \infty$ had vanishing real part in the scaling limit. In this case, one notes that the asymptotic formula for the energy (4.71) yields the same result for $\lim_{L\to\infty} L\left(E - Le_\infty - f_\infty\right)$ regardless of whether $\lim_{L\to\infty} b(L)$ coincides with $-\frac{in}{2}$ or $+\frac{in}{2}$.

Let us briefly summarise the key results obtained so far. Firstly, the model possesses a spontaneously broken $U_q(\mathfrak{sl}(2))$-symmetry. Secondly, we have seen the presence of state-dependent strong logarithmic corrections in the spectrum of effective scaling dimensions. We have found that the quasi-momentum operator parameterises these corrections. This led to the expression (4.71) for the effective scaling dimensions, which is consistent with the continuous spectrum of the $\mathrm{SL}(2,\mathbb{R})/U(1)$ sigma model at level k via the identification
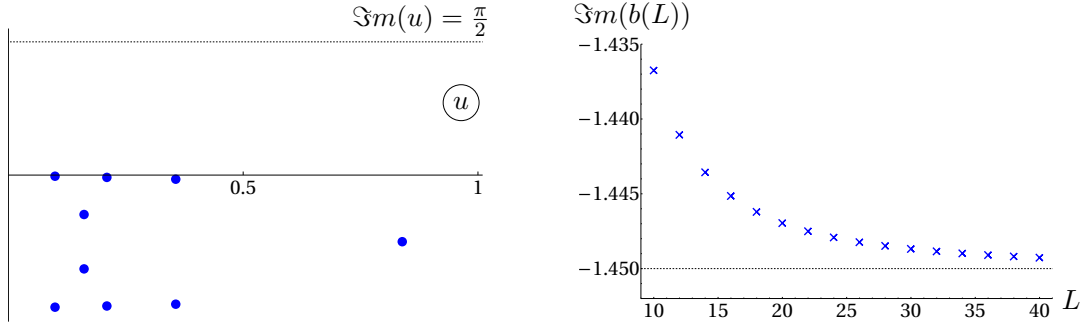
Figure 4.11: Displayed is numerical data for a RG trajectory where $b(L)$ tends to $-\frac{\mathrm{i}n}{2}$. The left panel depicts the pattern of Bethe roots in the complex $u = -\frac{1}{2}\log(\zeta)$ plane for the state $|\Psi_L\rangle$ with $L = 10$. The right panel is a plot of $b(L)$ as a function of L, where the dashed line represents its limiting value. Here $\mathcal{S} = 1$ and n, which parameterizes q as in (4.62), is given by $n = 2.9$ ($\gamma = 0.64114$).

(4.74). Further, we have seen that states with purely imaginary quasi-momentum yield the same effective scaling dimensions as states in the cigar with the discrete value of J (2.83). The results hold for the entire regime $\gamma < \alpha < \pi - \gamma$ of the staggering parameter α. Only non-universal quantities, such as the energy densities or the bulk quasi-momentum, depend on α. Hence, regarding the universality class, we conclude that $\alpha \in (\gamma, \pi - \gamma)$ is an irrelevant deformation from the self-dual case $\alpha = \pi/2$, similar as observed in the periodic model [54].

However, we should stress that we have only considered certain classes of states yielding conformal primaries until now. A full classification of the scaling limit of the self-dual model — including the space of state and, in particular, the density of states— is the subject of the next sections using the powerful approach of the ODE/IQFT correspondence. As briefly discussed in the preliminaries the central element is the scaling limit of the Q-operator, hence, we change from here to the rational notation. For the reader's convenience, we write out the energies and quasi-momentum operator eigenvalues in the rational notation for the self-dual case:

$$E = \sum_{m=1}^{L-\mathcal{S}} \frac{4\mathrm{i}\left(q^2 - q^{-2}\right)}{\zeta_m^2 + \zeta_m^{-2} + q^2 + q^{-2}}\,, \tag{4.81}$$

$$B = \sum_{m=1}^{L-\mathcal{S}} \log\left[\frac{\left(\zeta_m + \mathrm{i}q^{-1}\right)\left(\zeta_m - \mathrm{i}q\right)}{\left(\zeta_m - \mathrm{i}q^{-1}\right)\left(\zeta_m + \mathrm{i}q\right)}\right]\,. \tag{4.82}$$

4.2.4 ODE/IQFT CORRESPONDENCE

Mathematical techniques that are more sophisticated than those used in the last section are needed to fully characterize the scaling limit of a lattice model whose spectrum of scaling dimensions possesses a continuous component. A suitable approach to the study of the scaling limit is based on the ODE/IQFT correspondence [132, 28, 29, 30]. We found that the ODEs which govern the scaling limit of the staggered[8] six-vertex model with $U_q\big(\mathfrak{sl}(2)\big)$ invariant BCs fall within the same class of ODEs which describe the model for twisted BCs

---

[8]We mean here the case at hand, the alternating staggering.

[91, 25]. This allowed us to transfer over many previous results in regard to the differential equations.

Let us recall that the primary Bethe states, i.e., the RG trajectories whose energy obeys the asymptotic (4.71) with $\mathtt{d} = 0$, are labelled by the $U_q\big(\mathfrak{sl}(2)\big)$ spin $\mathcal{S}$ and the RG invariant s which is defined in equation (4.72). The ODE/IQFT correspondence implies a relation between the scaling limit of the eigenvalue of the Q-operator for $|\Psi_L\rangle$ and the spectral determinant of the ODE:

$$\left[-\frac{\mathrm{d}^2}{\mathrm{d}z^2} + \frac{p^2 - \frac{1}{4}}{z^2} + \frac{2\mathrm{i}s}{z} + 1 + \mu^{-2-n}\, z^n \right] \psi = 0 \; . \tag{4.83}$$

Here, recall that p is given in terms of $\mathcal{S}$ as in equation (4.68), $n > 0$ parameterizes the anisotropy of the spin chain, see (4.62), while μ is the scaled version of the spectral parameter ζ (see (2.201) for the homogeneous XXZ chain). The spectral determinant $D(\mu\,|\,p, s)$ is defined similarly to section 2.4.4. One specifies a solution to the differential equation by its behaviour in the vicinity of the singular point $z = 0$:

$$\psi_p(z) \to z^{\frac{1}{2}+p} \qquad \text{as} \qquad z \to 0 \; . \tag{4.84}$$

For large z, the term $\mu^{-2-n}\, z^n$ in (4.83) becomes dominant and one can define another solution through the $z \to +\infty$ asymptotic:

$$\Xi(z) \asymp \left(\frac{z}{\mu}\right)^{-\frac{n}{4}} \exp\left[-\frac{2}{n+2} \left(\frac{z}{\mu}\right)^{\frac{n}{2}+1} {}_2F_1\left(-\frac{1}{2}, -\frac{n+2}{2n}, \frac{n-2}{2n} \,\big|\, -\mu^{n+2}\, z^{-n}\right) + o(1) \right] \tag{4.85}$$

where ${}_2F_1(a, b, c|z)$ is the Gauss hypergeometric function, and we make the technical assumption that $\mu > 0$ and[9]

$$n \neq \frac{2}{2k-1} \qquad k = 1, 2, \dots \; . \tag{4.86}$$

The spectral determinant $D(\mu) = D(\mu\,|\,p, s)$ is given by

$$D(\mu) = \sqrt{\pi}\, (n+2)^{-\frac{2p}{n+2}-\frac{1}{2}}\, \mu^{-p+\frac{1}{2}}\, \frac{W[\psi_p, \Xi]}{\Gamma(1 + \frac{2p}{n+2})} \; , \tag{4.87}$$

where we recall the Wronskian $W[\psi_p, \Xi] = \Xi\, \partial_z \psi_p - \psi_p\, \partial_z \Xi$. The normalisation has been chosen such that

$$D(0) = 1 \; . \tag{4.88}$$

It is worth mentioning that the procedure for computing the spectral determinant based on formula (4.87) with the solutions ψ_p and Ξ obtained via numerical integration of the ODE (4.83) works only for $\Re e(p) \geq 0$. Nevertheless $D(\mu\,|\,p, s)$ turns out to be a meromorphic function of p and can be analytically continued to generic complex values.

Instead of considering the eigenvalue of $\mathbb{Q}^{(0)}(\zeta)$ (4.25) for a primary Bethe state, we consider the scaling limit of

$$A(\zeta) = \prod_{j=1}^{L-\mathcal{S}} (1 - \zeta/\zeta_j)\, (1 - \zeta\zeta_j) \; . \tag{4.89}$$

---

[9]For the delicate case of $n = \frac{2}{3k-2}$ we refer the reader to [25].

The advantage is that it does not involve the overall factor $\zeta^{\mathcal{S}}$, and the normalization yields $A(0) = 1$ (compare with (4.88)). Then, the scaling relation between $A(\zeta)$ and the spectral determinant is given by

$$\operatorname*{slim}_{\substack{L \to \infty \\ b(L) \to s}} G^{(L)}\!\left(-\mu^2 \Big| \tfrac{2}{n+2}\right) A\!\left((L/L_0)^{-\frac{n}{n+2}} \, \mathrm{i}\mu\right) = D(\mu) \,. \tag{4.90}$$

Here, the function G has been chosen to ensure the convergence of the limit for all values of the anisotropy and is given by[10]

$$G^{(L)}(E \,|\, g) = \exp\left(\sum_{m=1}^{\left[\frac{1}{2(1-g)}\right]} \frac{(-1)^m \, L}{m \cos(\pi m g)} \left(\frac{L}{L_0}\right)^{2m(g-1)} E^m\right), \tag{4.91}$$

where the brackets $[\dots]$ stand for the integer part, while

$$L_0 = \frac{\sqrt{\pi}\,\Gamma\!\left(1 + \tfrac{1}{n}\right)}{4\Gamma\!\left(\tfrac{3}{2} + \tfrac{1}{n}\right)} \,. \tag{4.92}$$

For the RG trajectories with $\mathsf{d} \neq 0$ entering into the asymptotic formula for the energy (4.71), the scaling relation (4.90) needs to be modified as follows. The LHS remains the same, while for the RHS one takes $D(\mu)$ to be the spectral determinant for the differential equation:

$$\left[-\frac{\mathrm{d}^2}{\mathrm{d}z^2} + \frac{p^2 - \tfrac{1}{4}}{z^2} + \frac{2\mathrm{i}s}{z} + 1 + \sum_{a=1}^{\mathsf{d}}\left(\frac{2}{(z-w_a)^2} + \frac{n}{z(z-w_a)}\right) + \mu^{-2-n}\, z^n\right]\psi = 0. \tag{4.93}$$

Here,

$$\boldsymbol{w} = (w_1, \dots, w_{\mathsf{d}}) \tag{4.94}$$

are not arbitrary parameters. They are restricted by the condition that any solution $\psi(z)$ of the differential equation must be single-valued in the vicinity of $z = w_a$. This leads to the coupled algebraic system:

$$\begin{aligned}
0 \;=\; & 4n\,w_a^2 + 8\mathrm{i}s\,(n+1)\,w_a - (n+2)\left((n+1)^2 - 4p^2\right) \tag{4.95} \\
& + 4\sum_{b \neq a}^{\mathsf{d}} \frac{w_a\left((n+2)^2\,w_a^2 - n(2n+5)\,w_a w_b + n(n+1)\,w_b^2\right)}{(w_a - w_b)^3} \qquad (a = 1, \dots, \mathsf{d})\,.
\end{aligned}$$

For generic n, s and p the number of solutions $\boldsymbol{w} = \{w_a\}_{a=1}^{\mathsf{d}}$, up to permutations of the w_a's, is given by $\mathrm{par}_2(\mathsf{d})$ – the number of bipartitions of d. The generating function for this combinatorial quantity reads as

$$\sum_{\mathsf{d}=0}^{\infty} \mathrm{par}_2(\mathsf{d})\, \mathsf{q}^{\mathsf{d}} = \prod_{j=1}^{\infty} \frac{1}{(1 - \mathsf{q}^j)^2} \,. \tag{4.96}$$

For applications to the staggered six-vertex model with $U_q\big(\mathfrak{sl}(2)\big)$ invariant BCs p is not generic, but should be taken as in (4.68), i.e., $2p = 2\mathcal{S} + 1 - (n+2)$. Then, it turns out

---

[10]This can be compared with formula (5.48) in the work [25].

that the number of solutions of the coupled equations (4.95) is typically less than $\mathrm{par}_2(\mathsf{d})$. To explain this phenomenon, let's replace p with $p_\varepsilon = p + \varepsilon^{2\mathcal{S}+1}$ where $0 < \varepsilon \ll 1$. Of the $\mathrm{par}_2(\mathsf{d})$ solution sets of (4.95) with $p \mapsto p_\varepsilon$ there exists those where

$$w_a = O(\varepsilon) \qquad \text{for} \qquad a = 1, 2, \ldots, 2\mathcal{S} + 1 \ . \qquad (4.97)$$

The other variables $\{w_a\}_{a=2\mathcal{S}+2}^{\mathsf{d}}$ tend to a finite, non-vanishing limit as $\varepsilon \to 0$. Their limiting values obey (4.95) with the replacements $p \mapsto \mathcal{S} + \frac{1}{2} + \frac{1}{2}(n+2)$ and $\mathsf{d} \mapsto \mathsf{d} - 2\mathcal{S} - 1$. In counting the solution sets of the algebraic system on w_a with $2p = 2\mathcal{S} + 1 - (n+2)$ we only consider those to be admissible where none of the w_a are zero. It is easy to see that

$$N(\mathsf{d} \,|\, \mathcal{S}) := \# \left\{ \text{solution sets of (4.95) with } p \text{ as in (4.68)} \right\} = \mathrm{par}_2(\mathsf{d}) - \mathrm{par}_2(\mathsf{d} - 2\mathcal{S} - 1) \qquad (4.98)$$

Note that $\mathrm{par}_2(\mathsf{d}) = 0$ when its argument is a negative integer.

We suppose that for a given trajectory $\{|\Psi_L\rangle\}$ with RG invariants $\mathcal{S}$, s and d, there exists a solution set $\boldsymbol{w}$ of (4.95) such that the scaling relation (4.90) holds true with $D(\mu) = D(\mu \,|\, \boldsymbol{w}, p, s)$ being the spectral determinant[11] for the differential equation (4.93).

Unfortunately, we cannot rigorously prove the above statement. We checked it numerically for a variety of cases using the method of sum rules, which we have explained around (2.204). The analysis is not included here as it is essentially the same as that presented in section 11 of the work [25] concerning the staggered six-vertex model with twisted BCs. However, one particular scaling relation involving the products over the Bethe roots

$$\Pi_\pm = \prod_{m=1}^{L-\mathcal{S}} q \left(\zeta_m \pm \mathrm{i} q^{-1} \right) \left(\zeta_m^{-1} \pm \mathrm{i} q^{-1} \right), \qquad (4.99)$$

is worth mentioning as it will become important later. It reads

$$\Pi_\pm \asymp \frac{C}{2\cos(\frac{\pi}{n+2})} \, \mathrm{e}^{\pm \frac{\pi}{n} s} \, \mathfrak{C}_{p,s}^{(\pm)}(\boldsymbol{w}) \left(\frac{L}{L_0} \right)^{-\frac{np}{n+2} \pm \mathrm{i} s} \left(\frac{4n}{n+2} \right)^L \left(1 + O(L^{-\epsilon}) \right) . \qquad (4.100)$$

Let us now discuss its ingredients. The coefficients $\mathfrak{C}_{p,s}^{(\pm)} = \mathfrak{C}_{p,s}^{(\pm)}(\boldsymbol{w})$, are related to the asymptotic expansion of $D(\mu)$ in μ:

$$D(\mu \,|\, \boldsymbol{w}, p, s) \asymp \mathfrak{C}_{p,s}^{(\pm)}(\boldsymbol{w}) \, (\pm\mu)^{\pm \frac{\mathrm{i}(n+2)s}{n} - p} \exp\left(\frac{2L_0}{\cos(\frac{\pi}{n})} (\pm\mu)^{\frac{n+2}{n}} + o(1) \right) \quad \text{for} \quad \Re e(\pm\mu) > 0 . \qquad (4.101)$$

For the case when $\mathsf{d} = 0$, the coefficients are given by

$$\mathfrak{C}_{p,s}^{(0,\pm)} = \sqrt{\frac{2\pi}{n+2}} \ \ 2^{-p \pm \frac{\mathrm{i}(n+2)s}{n}} \ (n+2)^{-\frac{2p}{n+2}} \ \frac{\Gamma(1+2p)}{\Gamma(1+\frac{2p}{n+2})\,\Gamma(\frac{1}{2}+p\pm\mathrm{i}s)} \ . \qquad (4.102)$$

In general,

$$\mathfrak{C}_{p,s}^{(\pm)}(\boldsymbol{w}) = \mathfrak{C}_{p,s}^{(0,\pm)} \, \check{\mathfrak{C}}_{p,s}^{(\pm)}(\boldsymbol{w}), \qquad (4.103)$$

---

[11]Note that eqs. (4.84)-(4.87) for the definition of $D(\mu)$ still remain valid since the inclusion of the extra sum in the ODE has no impact on the leading asymptotics of ψ_p and Ξ.

where $\check{\mathfrak{C}}^{(\pm)}$ are normalized to be one for $\mathtt{d} = 0$. A closed form expression for $\check{\mathfrak{C}}^{(\pm)}$ for general $\mathtt{d} = 0, 1, 2, \ldots$ was obtained in [133] and is quoted in appendix D.

In (4.100), C is a non-universal constant which is given by

$$C = \exp\left(2 \int_{-\infty}^{\infty} \mathrm{d}\omega \left(\frac{\hat{\tau}(\omega)}{\omega} \left(\Im m\left[\mathrm{e}^{\frac{2\mathrm{i}\pi}{n+2}} \, \Phi\!\left(\mathrm{e}^{-\frac{\mathrm{i}n\pi}{n+2}} , 1 , 1 - \tfrac{\mathrm{i}\omega}{4} \right) \right] - \frac{\pi}{n+2} - \frac{2}{\omega} \right) - \frac{n-1}{2\pi\omega^2} \right) \right) . \tag{4.104}$$

We recall that $\tau(\omega)$ is Fourier transform of the surface density (see (4.48)) i.e. in the notation (4.62) given by

$$\hat{\tau}(\omega) = -\frac{1}{4\pi} \, \frac{\sinh(\frac{\pi(n-1)}{4(n+2)}\,\omega)}{\sinh(\frac{\pi\omega}{4(n+2)})\cosh(\frac{n\pi\omega}{4(n+2)})} \tag{4.105}$$

and $\Phi(z, s, a)$ is the standard Lerch transcendent function

$$\Phi(z, s, a) = \sum_{m=0}^{\infty} \frac{z^m}{(m+a)^s} . \tag{4.106}$$

Finally, we mean by the notation $O(L^{-\epsilon})$ with some $\epsilon > 0$ that the correction terms fall off faster than any power of the logarithm of L. The asymptotic formula (4.100) is the analogue for the lattice system with open $U_q\big(\mathfrak{sl}(2)\big)$ invariant BCs of a product rule presented in [25], see (11.19) therein.

4.2.5 Quantization condition

In the next section, a full description of the space of states $\mathcal{H}$ appearing in the scaling limit will be given. Among other things, this includes the admissible values of pure imaginary s as well as the density of states characterizing the continuous spectrum. The results are based on an analysis of the so-called 'quantization condition' for $b(L)$, which we shall obtain below.

The key observation is that the eigenvalue of the quasi-momentum operator (4.82), used in the computation of $b(L)$ (4.69), may be expressed as

$$\exp B = (-1)^{L-\mathcal{S}} \, \frac{\Pi_+}{\Pi_-} . \tag{4.107}$$

Here $\Pi_{\pm}$ stand for the products over the Bethe roots defined in (4.99). Let us substitute these products for their asymptotics (4.100) with s replaced by the 'running coupling' $b(L)$. Upon rearranging and making use of eq. (4.69), one finds

$$\left(\frac{L}{L_0} \right)^{2\mathrm{i}s} \mathrm{e}^{\frac{\mathrm{i}}{2}\delta(\boldsymbol{w},p,s)} \bigg|_{s=b(L)} = \sigma + O(L^{-\epsilon}) \tag{4.108a}$$

$$\mathrm{e}^{\frac{\mathrm{i}}{2}\delta(\boldsymbol{w},p,s)} = \frac{\mathfrak{C}_{p,s}^{(+)}(\boldsymbol{w})}{\mathfrak{C}_{p,s}^{(-)}(\boldsymbol{w})} \tag{4.108b}$$

$$\sigma = (-1)^{L-\mathcal{S}} . \tag{4.108c}$$

The above relation given in (4.108), which will be henceforth referred to as the quantization condition, is interpreted in the following way. Given an RG trajectory $\{|\Psi_L\rangle\}$ one computes p from the value of the $U_q\big(\mathfrak{sl}(2)\big)$ spin $\mathcal{S}$ via the definition (4.68) as well as the sign factor $\sigma = (-1)^{L-\mathcal{S}}$. The latter is kept fixed along the RG trajectory $\{|\Psi_L\rangle\}$. Then $b(L)$, computed from the Bethe roots according to equations (4.82) and (4.69), obeys (4.108a) for some solution set $\boldsymbol{w} = \{w_a\}_{a=1}^{\mathtt{d}}$ of the algebraic system (4.95) with s replaced by $b(L)$. The 'phase shift' δ is given in terms of the coefficients $\mathfrak{C}_{p,s}^{(\pm)}(\boldsymbol{w})$ (4.103), which were introduced in the previous subsection. For the primary Bethe states with $\mathtt{d} = 0$, one has

$$\mathrm{e}^{\frac{\mathrm{i}}{2}\delta(\emptyset,p,s)} = 2^{\frac{2\mathrm{i}(n+2)s}{n}}\,\frac{\Gamma(\frac{1}{2} + p - \mathrm{i}s)}{\Gamma(\frac{1}{2} + p + \mathrm{i}s)} \qquad\qquad (\mathtt{d} = 0)\,. \qquad (4.109)$$

For $\mathtt{d} = 1, 2, 3, \ldots$ one must make use of eqs. (4.102), (4.103) together with the explicit formula for $\breve{\mathfrak{C}}_{p,s}^{(\pm)}(\boldsymbol{w})$ which is contained in appendix D.

Let's take a moment to discuss the quantization condition (4.108) for the primary Bethe states in the context of the results in the last section, see also [27]. We start with the asymptotic (4.70) for $b(L)$ that was observed for a class of RG trajectories labelled by the integer dN. In this case, it is useful to take the logarithm of both sides of formula (4.108a) with the phase shift as in (4.109) and write it in the form:

$$2b_{dN}\log\left(\frac{L}{L_0}\right) - \mathrm{i}\log\left[2^{\frac{2\mathrm{i}(n+2)b_{dN}}{n}}\,\frac{\Gamma(\frac{1}{2} + p - \mathrm{i}b_{dN})}{\Gamma(\frac{1}{2} + p + \mathrm{i}b_{dN})}\right] = \pi dN + O(L^{-\epsilon})\,. \qquad (4.110)$$

For the class of states, we are considering $b_{dN}(L)$ goes to zero as $L \to \infty$. As a result, the second term in the LHS of the above relation containing the Γ-functions also tends to zero and, to a first approximation, can be ignored. This way, one obtains (4.70). The formula (4.110) provides a refinement to the large L asymptotic behaviour of $b_{dN}(L)$ which takes into account all power-law corrections in $1/\log(L)$. To demonstrate its accuracy, some numerical data obtained from the Bethe roots for a primary Bethe state $|\Psi_L\rangle$ is compared with the predictions coming from the quantization condition in Figure 4.12.

Another possibility of how (4.108a) could be satisfied for $L \gg 1$ is if $b(L)$ approaches a singularity of the phase shift. The explicit formula (4.109), valid for $\mathtt{d} = 0$, shows that these occur for pure imaginary s when $\frac{1}{2} + p \pm \mathrm{i}s$ is a positive integer. If the imaginary part of $b(L)$ is positive, then the vanishing of the first term in the LHS of (4.108a) may be compensated if $b(L)$ tends to a pole of $\mathrm{e}^{\frac{\mathrm{i}}{2}\delta}$, i.e.,

$$\mathop{\mathrm{slim}}\limits_{L\to\infty} b(L) = s \qquad \text{with} \qquad s = \mathrm{i}\big(-p - \tfrac{1}{2} - \ell\big) \qquad \big(\Im m(b(L)) > 0\big) \qquad (4.111)$$

and $\ell = 0, 1, 2, \ldots$. This is the same as eq. (4.78) with the sign factor chosen to be '+'. The upper bound on ℓ in that equation ensures the condition $\Im m(b(L)) > 0$. The minus version of the relation is deduced from (4.108a) by means of similar arguments.

A verification of the quantization condition (4.108) was carried out using numerical data obtained from the lattice model with $L = 10$. The spin chain Hamiltonian was constructed, and the first few hundred lowest energy Bethe states were found via a direct diagonalization procedure. Note that, because of the $U_q\big(\mathfrak{sl}(2)\big)$ symmetry, it was sufficient to focus on the
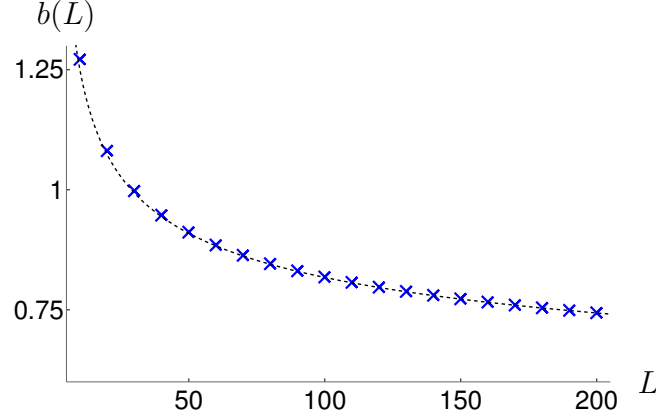
Figure 4.12: The numerical data of $b(L)$ for an RG trajectory $\{|\Psi_L\rangle\}$ is depicted. The representative state for $L = 10$ is the one whose pattern of Bethe roots is displayed on the right panel of Figure 4.4. In particular, it has $\mathtt{d} = 0$, total $U_q(\mathfrak{sl}(2))$ spin $\mathcal{S} = 2$ and the integer dN — the difference between the number of roots lying on the real line and the line $\Im m(u) = \frac{\pi}{2}$ in the complex u plane — is held fixed along the flow to be $dN = 4$. The crosses depict the numerical values of $b(L) = b_{dN}(L)$ for different L which were computed from the Bethe roots corresponding to $|\Psi_L\rangle$ via formulae (4.69) and (4.82). The dashed line gives the predictions coming from the quantization condition (4.110) with $dN = 4$ and the correction terms ignored. Note that the branch of the logarithm was fixed by requiring that the LHS of (4.110) is a continuous function for real b_{dN} which vanishes at $b_{dN} = 0$.

sector with $S^z = 0$ as there is always one state $|\Psi_L\rangle$ from the $U_q(\mathfrak{sl}(2))$ multiplet $\mathcal{M}_{\mathcal{S}}$ lying in this sector. For each Bethe state, apart from the energy, the eigenvalue of the quasi-momentum operator was computed from which we extracted b. The numerical data for $b(L)$ was compared with $b_*(L)$ — the predictions coming from the quantization condition. The latter was obtained by considering (4.108) as an equation from which $b_*(L)$ could be determined numerically (in (4.108a) we ignore the correction term $O(L^{-\epsilon})$ and set $L = 10$). Note that the phase shift $\mathrm{e}^{\frac{\mathrm{i}}{2}\delta}$ therein depends on b transcendentally via the Γ-functions as in (4.109) and algebraically through the set $\boldsymbol{w}$, which solves the coupled system (4.95) with $s \mapsto b$. For given $\mathtt{d} \leq 3$ we took the $\mathrm{par}_2(\mathtt{d}) - \mathrm{par}_2(\mathtt{d} - 2\mathcal{S} - 1)$ equations which are obtained from the quantization condition by specializing the phase shift $\delta = \delta(\boldsymbol{w}, p, s)$ to different solution sets $\boldsymbol{w} = \{w_a\}_{a=1}^{\mathtt{d}}$ of (4.95). For each of them we found all possible solutions $b_*(L)$ that lie in a suitably chosen finite portion of the strip $\left|\Im m(b_*)\right| < \frac{n}{2} + \varepsilon$ with $0 < \varepsilon \ll 1$ of the complex b plane. Some of the results for the comparison of $b(L)$ and $b_*(L)$ for $L = 10$ are presented in Figure 4.13. They motivated us to make the following conjecture.

Conjecture: For any RG trajectory $\{|\Psi_L\rangle\}$ labelled by $\mathcal{S}$, $\mathtt{d}$ and a solution set $\boldsymbol{w} = \{w_a\}_{a=1}^{\mathtt{d}}$ of equation (4.95) the corresponding value[12] of $b(L) = \frac{n}{2\pi}B$, with B computed according to formula (4.82), obeys the quantization condition (4.108). Conversely, let $b_*(L) : -\frac{n}{2} < \Im m\big(b_*(L)\big) \leq \frac{n}{2}$ be a solution of the relation (4.108a) with the correction terms ignored. Then, there exists a unique $U_q(\mathfrak{sl}(2))$ multiplet $\mathcal{M}_{\mathcal{S}}$ for which B obtained from $|\Psi_L\rangle \in \mathcal{M}_{\mathcal{S}}$ is such that $\exp(B) - \exp\big(\frac{2\pi}{n}b_*(L)\big)$ tends to zero faster than any power of the logarithm of L.

---

[12]Note that for the self-dual case $\alpha = \pi/2$ the term B_{thermo} vanishes in (4.69).
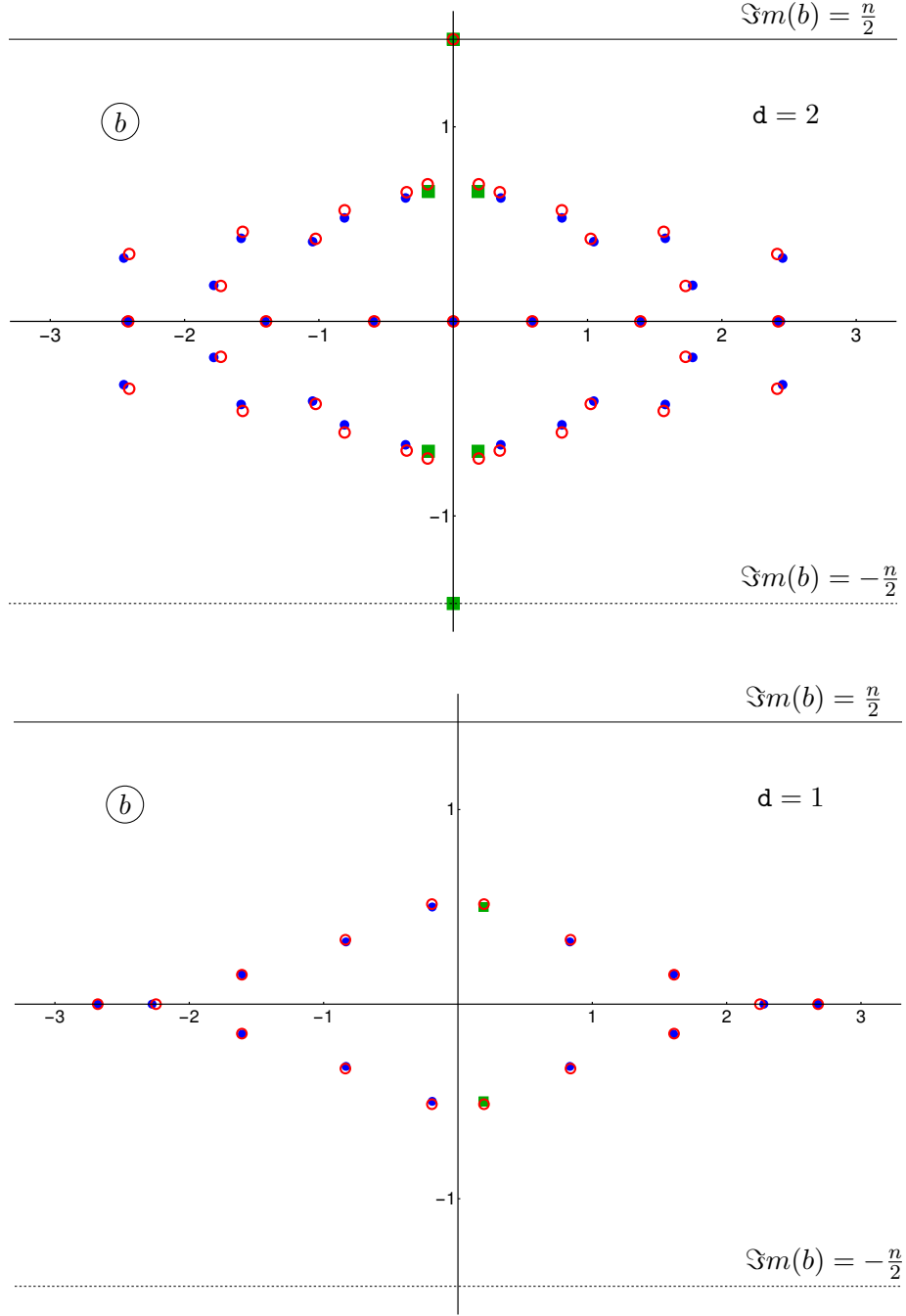
Figure 4.13: Numerical data for $b(L)$ and $b_*(L)$ is plotted in the complex b plane for the lattice system with $L = 10$. Out of the few hundred states that were considered, only those with $\mathtt{d} = 2$ (top panel), $\mathtt{d} = 1$ (bottom panel) and $U_q\big(\mathfrak{sl}(2)\big)$ spin $\mathcal{S} = 2$ were used to produce the figure. The open circles correspond to $b(L)$ that was extracted from the Bethe roots by means of eqs. (4.82), (4.69). The filled shapes represent $b_*(L)$ obtained from an analysis of the quantization condition (4.108). The green squares and blue circles are used to distinguish whether $b_*(L)$ becomes a pure imaginary number or a real number, respectively, in the scaling limit. The two green squares in the top panel for which $\mathrm{slim}_{L \to \infty} b_*(L) = \pm \frac{\mathrm{i}n}{2}$ correspond to the same state. It seems interesting to note that the agreement between $b(L)$ and $b_*(L)$ is better than in the case of the lattice model with twisted BCs imposed. To see that, compare the above figures with the ones contained in appendix C of the work [25]. The anisotropy parameter was taken to be $n = 2.9$ ($\gamma = 0.641141$).

4.2.6 Space of states in the scaling limit

Continuous and discrete spectrum

A key result is the above conjecture which was motivated by our numerical work. It describes a certain one-to-one relation between $b(L)$ and $b_*(L)$. The former is computed via the Bethe roots corresponding to a state $|\Psi_L\rangle$ in a multiplet $\mathcal{M}_\mathcal{S}$, labeled by $2p = 2\mathcal{S} + 1 - (n+2)$, the non-negative integer $\mathtt{d}$ and one of the $N(\mathtt{d} \,|\, \mathcal{S}) = \mathrm{par}_2(\mathtt{d}) - \mathrm{par}_2(\mathtt{d} - 2\mathcal{S} - 1)$ solution sets $\boldsymbol{w} = \{w_a\}_{a=1}^{\mathtt{d}}$ of the algebraic system (4.95). The notation $b_*(L)$ stands for a solution of the quantization condition (4.108) treated as an equation for $b(L)$ with the correction terms ignored.

Accepting the conjecture to be true, one can determine the spectrum of $b(L)$ for the low energy states at large L via a study of the quantization condition. In turn, the results allow one to fully characterize the spectrum of conformal dimensions as well as the space of low energy states in the scaling limit.

Consider the quantization condition (4.108) and suppose that the phase shift $\delta(\boldsymbol{w}, p, s)|_{s \mapsto b(L)}$ is significantly smaller than $\log(L)$. Then, the first term dominates, and one can obtain an asymptotic expansion for $b(L)$ in $1/\log(L)$. The leading and subleading asymptotic behaviour are given by

$$b_{dN}(L) = \frac{2\pi dN - \delta_0}{4\log\left(\mathrm{e}^{\frac{1}{4}\delta_0'} L/L_0\right)} + O\left((\log L)^{-3}\right) \qquad \left(L \gg 1,\ dN - \text{fixed}\right). \qquad (4.112)$$

Here, we have introduced the notation

$$\delta_0 = \delta|_{s=0}, \qquad\qquad \delta_0' = \partial_s \delta|_{s=0}, \qquad\qquad (4.113)$$

while dN, which labels[13] the different $b(L)$ obeying the quantization condition comes about as a result of taking the logarithm of (4.108a) and is an even or odd integer for $\sigma = +1$ or $\sigma = -1$, respectively.

Formula (4.112) shows that, in general, $b_{dN}(L)$ is a complex number since δ_0 and δ_0' are generically complex. However, while $\Im m\left(b_{dN}(L)\right) \sim 1/\log(L) \to 0$ as $L \to \infty$ the magnitude of the real part is controlled by the integer dN which, for the low energy states, may take any values up to some $dN_{\max} \ll L$. Numerical work leads us to suppose that $\lim_{L \to \infty} b_{dN_{\max}} = \infty$.

Let $\mathcal{H}_{L|\mathcal{S}}^{(\text{cont})}$ denote the set of low energy states $|\Psi_L\rangle$ with fixed value of the $U_q\left(\mathfrak{sl}(2)\right)$ spin $\mathcal{S} = 0, 1, 2, \ldots$ such that $\Im m\left(b(L)\right) \to 0$ as $L \to \infty$. Recall that the states come in multiplets $\mathcal{M}_\mathcal{S}$ and one can choose a basis for that multiplet in which $\mathbb{S}^z = \frac{1}{2}\sum_{J=1}^{2L} \sigma_J^z$, is diagonal. This yields the refinement

$$\mathcal{H}_{L|\mathcal{S}}^{(\text{cont})} = \bigcup_{S^z=-\mathcal{S}}^{\mathcal{S}} \mathcal{H}_{L|\mathcal{S}, S^z}^{(\text{cont})}. \qquad\qquad (4.114)$$

---

[13]We intentionally used the same letter as the one which is associated to the class of states (4.42). For those states, these numbers 'coincide'. However, for general complex Bethe roots the definition of dN is — from the perspective of the root pattern — subtle.

Each low energy Bethe state in $\mathcal{H}_{L|\mathcal{S},S^z}^{(\mathrm{cont})}$ is uniquely specified by the non-negative integer d, a solution set $\boldsymbol{w} = \{w_a\}_{a=1}^{\mathsf{d}}$ of the algebraic system (4.95) with $s \mapsto b(L)$, as well as the even or odd integer dN that enters into the asymptotics (4.112). For $L \gg 1$, the value of $b_{dN}(L)$ becomes densely distributed in the segment $(-b_{dN_{\max}}(L), +b_{dN_{\max}}(L))$. The density of states is obtained from the quantization condition (4.108) written in logarithmic form:

$$\big[4s \log(L/L_0) + \delta(\boldsymbol{w}, p, s) \big]\big|_{s \mapsto b_{dN}(L)} = 2\pi dN + O(L^{-\epsilon}) . \tag{4.115}$$

Here, the branch of the logarithm needed to define δ from (4.108b) is taken such that the phase shift is a continuous function of s in the strip $|\Im m(s)| < \varepsilon$ for some $\varepsilon > 0$ (it is being assumed that $\mathrm{e}^{\frac{\mathrm{i}}{2}\delta}$ contains no zeroes or poles for real s). The term in the square brackets on the LHS of (4.115) is a monotonic function of s for L sufficiently large. This way one concludes that the number of states in $\mathcal{H}_{L|\mathcal{S},S^z}^{(\mathrm{cont})}$ with fixed d such that $\Re e\big(b(L)\big)$ lies in the interval $(s, s + \Delta s) \in (-b_{dN_{\max}}(L), +b_{dN_{\max}}(L))$ is given by $\rho_p^{(\mathsf{d})}(s) \, \Delta s$ with[14]

$$\rho_p^{(\mathsf{d})}(s) = \frac{1}{\pi} \, N(\mathsf{d}\,|\,\mathcal{S}) \log \left(2^{\frac{n+2}{n}} \frac{L}{L_0} \right) + \frac{1}{2\pi\mathrm{i}} \, \partial_s \log \left[\left(\frac{\Gamma(\frac{1}{2} + p - \mathrm{i}s)}{\Gamma(\frac{1}{2} + p + \mathrm{i}s)} \right)^{N(\mathsf{d}\,|\,\mathcal{S})} \prod_{\substack{\boldsymbol{w} \\ \mathsf{d}-\mathrm{fixed}}} \frac{\check{\mathfrak{C}}_{p,s}^{(+)}(\boldsymbol{w})}{\check{\mathfrak{C}}_{p,s}^{(-)}(\boldsymbol{w})} \right] \tag{4.116}$$

up to corrections which vanish as $L \to \infty$. The product over $\boldsymbol{w}$ appearing in the RHS goes over all the $N(\mathsf{d}\,|\,\mathcal{S})$ (4.98) solution sets of the algebraic system (4.95) with d fixed. Also, recall that $2p = 2\mathcal{S} + 1 - (n + 2)$.

In [133] a formula is presented for a product over $\boldsymbol{w}$ similar to the one appearing in the RHS of (4.116) (see also Appendix B of [25]). It is valid for the case of generic p and n when the number of solution sets $\boldsymbol{w}$ of (4.95) is $\mathrm{par}_2(\mathsf{d})$. Based on this, one can derive the result:

$$\prod_{\substack{\boldsymbol{w} \\ \mathsf{d}-\mathrm{fixed}}} \frac{\check{\mathfrak{C}}_{p,s}^{(+)}(\boldsymbol{w})}{\check{\mathfrak{C}}_{p,s}^{(-)}(\boldsymbol{w})} = (-1)^{\mathrm{par}_2(\mathsf{d}-2\mathcal{S}-1)} \prod_{a=0}^{\mathsf{d}-1} \left(\frac{\frac{1}{2} + a + p - \mathrm{i}s}{\frac{1}{2} + a + p + \mathrm{i}s} \right)^{N(\mathsf{d}\,|\,\mathcal{S}) - N_a^+(\mathsf{d}\,|\,\mathcal{S})}$$

$$\times \prod_{a=0}^{\mathsf{d}-1} \left(\frac{\frac{1}{2} + a - p - \mathrm{i}s}{\frac{1}{2} + a - p + \mathrm{i}s} \right)^{N(\mathsf{d}\,|\,\mathcal{S}) - N_a^-(\mathsf{d}\,|\,\mathcal{S})} \tag{4.117}$$

with the integers $N_a^{\pm}$ being defined through their generating function as

$$\sum_{\mathsf{d}=0}^{\infty} N_a^{\pm}(\mathsf{d}\,|\,\mathcal{S}) \, \mathsf{q}^{\mathsf{d}} = \left(\prod_{j=1}^{\infty} (1 - \mathsf{q}^j)^{-2} \right) \sum_{m=0}^{\infty} (-1)^m \left(1 - \mathsf{q}^{(1\pm m)(2\mathcal{S}+1)} \right) \mathsf{q}^{ma + \frac{m(m+1)}{2}} . \tag{4.118}$$

Notice that

$$N_a^+(\mathsf{d}\,|\,\mathcal{S}) = N(\mathsf{d}\,|\,\mathcal{S}) - N_{-a-1}^-(\mathsf{d}\,|\,\mathcal{S}) . \tag{4.119}$$

---

[14]This line of arguments is analogous to the standard derivation in the root density approach. One introduces a monotonic increasing counting function which evaluates to (half-)integers at the Bethe roots similar to the LHS of (4.115) evaluates to odd/even integers dN multiplied by π when s is swapped for $b_{dN}(L)$ and $L \gg 1$. Differentiating the counting function in the root density approach yields the root density, while we obtain the density of states (4.116) by differentiating (4.115) and dividing by 4π.

The scaling limit of the RG trajectory $L \mapsto |\Psi_L\rangle \in \mathcal{H}_{L|\mathcal{S}}^{(\text{cont})}$ labelled by real s, the integers $\mathcal{S}$, S^z, $\mathtt{d}$ and the solution set $\boldsymbol{w}$ yields

$$\operatorname*{slim}_{L \to \infty} |\Psi_L\rangle = |\psi_{p,s}^{(S^z)}(\boldsymbol{w})\rangle \; . \tag{4.120}$$

One can define the linear span $\mathcal{H}_{\mathcal{S}}^{(\text{cont})}$ of all such possible states with fixed $\mathcal{S}$. The above discussion implies that this linear space admits the decomposition

$$\mathcal{H}_{\mathcal{S}}^{(\text{cont})} = \bigoplus_{S^z=-\mathcal{S}}^{\mathcal{S}} \mathcal{H}_{\mathcal{S},S^z}^{(\text{cont})} \; , \tag{4.121}$$

where each of the spaces $\mathcal{H}_{\mathcal{S},S^z}^{(\text{cont})}$ is isomorphic to $\mathcal{H}_{\mathcal{S},\mathcal{S}}^{(\text{cont})}$ and

$$\mathcal{H}_{\mathcal{S},\mathcal{S}}^{(\text{cont})} = \int_{\mathbb{R}}^{\oplus} \mathrm{d}s \bigoplus_{\mathtt{d}=0}^{\infty} \mathcal{H}_{p,s}^{(\text{cont},\mathtt{d})} \qquad \left(2p = 2\mathcal{S}+1-n-2 \right) . \tag{4.122}$$

The components appearing inside the direct sum are finite dimensional such that

$$\dim \left(\mathcal{H}_{p,s}^{(\text{cont},\mathtt{d})} \right) = N(\mathtt{d} \,|\, \mathcal{S}) \; . \tag{4.123}$$

For the low energy states where the value of $\Im m\big(b(L)\big)$ is non-vanishing in the limit $L \to \infty$ so that they do not belong to $\mathcal{H}_{L|\mathcal{S}}^{(\text{cont})}$, one may repeat a similar analysis to the one in [25] in the context of the staggered six-vertex model with twisted BCs (see appendix B therein). Let us denote by $\mathcal{H}_{L|\mathcal{S},S^z}^{(\text{disc})}$ the set of such states $|\Psi_L\rangle$ with given quantum numbers $\mathcal{S}$ and S^z. The quantization condition (4.108) implies that the set $\boldsymbol{w}$ and $s = \operatorname{slim}_{L \to \infty} b(L)$ labelling the RG trajectory $\{|\Psi_L\rangle\}$ must be such that

$$\mathrm{e}^{-\frac{\mathrm{i}}{2}\delta(\boldsymbol{w},p,s)} = 0 \qquad \text{if} \qquad \Im m(s) > 0 \,, \qquad \mathrm{e}^{+\frac{\mathrm{i}}{2}\delta(\boldsymbol{w},p,s)} = 0 \qquad \text{if} \qquad \Im m(s) < 0 \,. \tag{4.124}$$

We supplement this with the additional constraint

$$-\frac{n}{2} < \Im m(s) \leq \frac{n}{2} \tag{4.125}$$

on the imaginary part of s. It originates from the inequality (4.38), while the line $\Im m(s) = -\frac{\mathrm{i}n}{2}$ was excluded from the interval in order to avoid double counting states with $\operatorname{slim}_{L \to \infty} b(L) = \pm\frac{\mathrm{i}n}{2}$. It turns out that the phase shift satisfies:

$$\mathrm{e}^{\frac{\mathrm{i}}{2}\delta(\boldsymbol{w},p,s)} = \mathrm{e}^{-\frac{\mathrm{i}}{2}\delta(-\boldsymbol{w},p,-s)} \; . \tag{4.126}$$

Here, $-\boldsymbol{w}$ denotes the set $\{-w_a\}_{a=1}^{\mathtt{d}}$ where, if $\boldsymbol{w}$ obeys the algebraic system (4.95), then $-\boldsymbol{w}$ obeys the same set of equations with $s \mapsto -s$. This allows one to focus on the case with $0 < \Im m(s) \leq \frac{n}{2}$ while results for $-\frac{n}{2} < \Im m(s) < 0$ follow by simply flipping the sign $s \mapsto -s$.

The analysis of (4.124) is greatly facilitated by the relation

$$\prod_{\substack{\boldsymbol{w} \\ \mathtt{d}-\text{fixed}}} \mathrm{e}^{\frac{\mathrm{i}}{2}\delta(\boldsymbol{w},p,s)} = \left(2^{(2n+4)\frac{\mathrm{i}s}{n}} \frac{\Gamma(\frac{1}{2}+p-\mathrm{i}s)}{\Gamma(\frac{1}{2}+p+\mathrm{i}s)} \right)^{N(\mathtt{d}\,|\,\mathcal{S})} \prod_{\substack{\boldsymbol{w} \\ \mathtt{d}-\text{fixed}}} \frac{\check{\mathfrak{C}}_{p,s}^{(+)}(\boldsymbol{w})}{\check{\mathfrak{C}}_{p,s}^{(-)}(\boldsymbol{w})} \tag{4.127}$$

with the last term in the RHS being given by the product (4.117). It follows from the definitions (4.108b), (4.102) and (4.103). Also, we will need the following assumptions on the positions of the poles and zeroes of the function $e^{\frac{i}{2}\delta(\boldsymbol{w},p,s)}$, which were verified numerically for small $\mathtt{d} \leq 3$:

(i) The points where $e^{\frac{i}{2}\delta(\boldsymbol{w},p,s)}$ is singular do not coincide with the location of any zero of $e^{\frac{i}{2}\delta(\boldsymbol{w}',p,s)}$ with $\boldsymbol{w}'$ being some other solution set of (4.95).

(ii) All singularities of $e^{\frac{i}{2}\delta(\boldsymbol{w},p,s)}$ in the complex s plane are simple poles. Notice that, in view of eq. (4.126), this implies that all of its zeroes are simple as well.

From assumption (i), any pole or zero of $e^{\frac{i}{2}\delta(\boldsymbol{w},p,s)}$ must appear as a pole/zero in the RHS of (4.127). This way, one finds that the values of s for which the first condition in (4.124) is obeyed are $s = \pm s_a$, with (see also our earlier analysis (4.78))

$$s_a = \mathrm{i}\left(-p - \tfrac{1}{2} - a\right) = \mathrm{i}\left(\tfrac{n}{2} - \mathcal{S} - a\right) \qquad \text{and} \qquad 0 \leq a + \mathcal{S} < \tfrac{n}{2}, \quad a \in \mathbb{Z}, \qquad (4.128)$$

where the bound on $a + \mathcal{S}$ comes from (4.125). Moreover, due to (ii), one can determine the number of solution sets $\boldsymbol{w}$ with (4.124) being satisfied at $s = s_a$ by reading off the multiplicity of that pole/zero from eqs. (4.127) and (4.117). This would coincide with the dimension of the linear space $\mathcal{H}_{p,s}^{(\mathrm{disc},\mathtt{d})}$ which is the span of all states of the form $|\psi_{p,s}^{(S^z)}(\boldsymbol{w})\rangle$ having fixed $\mathcal{S}, S^z$, $\mathtt{d}$ and s with $\Im m(s) \neq 0$. One finds the number of such $\boldsymbol{w}$ to be $N_a^+(\mathtt{d})$.

Define the space $\mathcal{H}_{\mathcal{S},S^z}^{(\mathrm{disc})}$ as the linear span of all the states that appear in the scaling limit of $\mathcal{H}_{L|\mathcal{S},S^z}^{(\mathrm{disc})}$. These are isomorphic to $\mathcal{H}_{\mathcal{S},\mathcal{S}}^{(\mathrm{disc})}$ and the analysis of the quantization condition performed above implies that:

$$\mathcal{H}_{\mathcal{S},\mathcal{S}}^{(\mathrm{disc})} = \bigoplus_{s \in \Sigma^+ \cup \Sigma^-} \bigoplus_{\mathtt{d}=0}^{\infty} \mathcal{H}_{p,s}^{(\mathrm{disc},\mathtt{d})} \ . \qquad (4.129)$$

Here $\Sigma^{(\pm)}$ denote the finite sets of pure imaginary numbers:

$$\Sigma^+ = \left\{s \ : \ \tfrac{n}{2} + \mathrm{i}s \in \mathbb{Z}, \ \Im m(s) \in (0, \tfrac{n}{2}]\right\}, \quad \Sigma^- = \left\{s \ : \ \tfrac{n}{2} - \mathrm{i}s \in \mathbb{Z}, \ \Im m(s) \in (-\tfrac{n}{2}, 0)\right\}, \qquad (4.130)$$

which incorporate the bound on the imaginary part of s (4.125). Each component $\mathcal{H}_{p,s}^{(\mathtt{d})}$ is finite dimensional and

$$\dim\left(\mathcal{H}_{p,s}^{(\mathrm{disc},\mathtt{d})}\right) = N_a^+(\mathtt{d}\,|\,\mathcal{S}) \qquad \text{with} \qquad a = \tfrac{n}{2} - \mathcal{S} \pm \mathrm{i}s \in \mathbb{Z} \qquad (4.131)$$

Here and below, when a condition involving $\pm \mathrm{i}s$ appears, we mean it is to be satisfied for some choice of the sign $+$ or $-$.

The following comment is in order here. For the case $a < 0$, the integers $N_a^+(\mathtt{d}\,|\,\mathcal{S})$ (4.118) are all zero for $\mathtt{d} = 0$:

$$N_a^+(0\,|\,\mathcal{S}) = 0 \qquad \text{for} \qquad a = -1, -2, -3, \ldots \ . \qquad (4.132)$$

As a result, for the primary Bethe states, the limiting values of $\Im m\big(b(L)\big)$ are given by $s = \pm s_a$ (4.128) with the extra condition imposed that $a \geq 0$. Thus, one recovers the

formula (4.78). Of course, RG trajectories exist for the spin chain, which are not primary Bethe states that are labelled by $s = \pm s_a$ with $a < 0$.

We conjecture that any RG trajectory of the lattice model with given $U_q\big(\mathfrak{sl}(2)\big)$ spin $\mathcal{S}$ and eigenvalue of the z-projection of the total spin operator S^z belongs either to $\mathcal{H}^{(\text{cont})}_{L|\mathcal{S},S^z}$ or $\mathcal{H}^{(\text{disc})}_{L|\mathcal{S},S^z}$. Thus, the full space of low energy states of the lattice system in the scaling limit becomes the linear space

$$\mathcal{H} = \mathcal{H}^{(\text{cont})} \oplus \mathcal{H}^{(\text{disc})} \tag{4.133}$$

with

$$\mathcal{H}^{(\text{cont})} = \bigoplus_{\mathcal{S}=0}^{\infty} \bigoplus_{S^z=-\mathcal{S}}^{\mathcal{S}} \mathcal{H}^{(\text{cont})}_{\mathcal{S},S^z}, \qquad \mathcal{H}^{(\text{disc})} = \bigoplus_{\mathcal{S}=0}^{\infty} \bigoplus_{S^z=-\mathcal{S}}^{\mathcal{S}} \mathcal{H}^{(\text{disc})}_{\mathcal{S},S^z}. \tag{4.134}$$

We call $\mathcal{H}^{(\text{cont})}$ the 'continuous spectrum' due to the presence of a direct integral over s in its decomposition, see (4.122). The space $\mathcal{H}^{(\text{disc})}$ will be referred to as the 'discrete spectrum'.

$\mathcal{W}_\infty$ algebra

In the scaling limit, the critical lattice system possesses extended conformal symmetry. The corresponding algebra is expected to be the $\mathcal{W}_\infty$ algebra from reference [134] with central charge $c < 2$. This is the same one that appears in the scaling limit of the staggered six-vertex model with twisted BCs [91, 25]. Among other things, such a statement implies that the graded linear spaces

$$\bigoplus_{\mathsf{d}=0}^{\infty} \mathcal{H}^{(\mathsf{d})}_{p,s}, \qquad \mathcal{H}^{(\mathsf{d})}_{p,s} = \begin{cases} \mathcal{H}^{(\text{cont},\mathsf{d})}_{p,s} & \text{for} \quad s \in \mathbb{R} \\ \mathcal{H}^{(\text{disc},\mathsf{d})}_{p,s} & \text{for} \quad p + \frac{1}{2} \pm \mathrm{i}s \in \mathbb{Z} \end{cases} \tag{4.135}$$

are isomorphic to a (irreducible) representation of $\mathcal{W}_\infty$. Then formulae (4.134), (4.122) and (4.129) would provide a classification of the space of states $\mathcal{H}$ occurring in the scaling limit of the lattice model in terms of irreducible representations (irreps) of the algebra of extended conformal symmetry. In order to demonstrate this, we briefly mention some details concerning the $\mathcal{W}_\infty$ algebra and its representations while referring the reader to section 16 of reference [25] for further discussion.

The $\mathcal{W}_\infty$ algebra is generated by a set of currents $W_j(u)$ of Lorentz spin $j = 2, 3, \ldots$. These satisfy an infinite system of operator product expansions (OPEs). Its first few

members can be chosen to be

$$W_2(u)\,W_2(0) \;=\; \frac{c}{2u^4} - \frac{2}{u^2}\,W_2(0) - \frac{1}{u}\,\partial W_2(0) + O(1)\,,$$

$$W_2(u)\,W_3(0) \;=\; -\frac{3}{u^2}\,W_3(0) - \frac{1}{u}\,\partial W_3(0) + O(1)\,, \tag{4.136}$$

$$W_3(u)\,W_3(0) \;=\; -\frac{c(c+7)(2c-1)}{9(c-2)u^6} + \frac{(c+7)(2c-1)}{3(c-2)u^4}\,\big(W_2(u)+W_2(0)\big) - \frac{1}{u^2}\,\Big(W_4(u)$$

$$+\; W_4(0) + W_2^2(u) + W_2^2(0) + \frac{2c^2+22c-25}{30(c-2)}\,\big(\partial^2 W_2(u)+\partial^2 W_2(0)\big)\Big)$$

$$+\; O(1)\,,$$

where in the last line W_2^2 is a composite field which coincides with the first regular term in the OPE $W_2(u)W_2(0)$. Notice that there is some ambiguity in the definition of W_j for $j \geq 3$. Apart from the freedom in the overall multiplicative normalization, $W_j \mapsto CW_j$, it is possible to add to W_j any differential polynomial of Lorentz spin j involving the lower spin currents W_k with $k < j$. Here, the W_3 current was fixed by the requirement that it is a primary field of spin three, so that its OPE with W_2 takes the form of the second line in formula (4.136). As for W_4, one cannot arrange for it to be a primary field by adding linear combinations of W_2^2, ∂W_3 and $\partial^2 W_2$. Defined such that it appears in the OPE of $W_3(u)W_3(0)$ as above, it turns out that $W_2(u)W_4(0)$ takes a simpler form,

$$W_2(u)\,W_4(0) = \frac{(c+10)(17c+2)}{15(c-2)\,u^4}\,W_2(0) - \frac{4}{u^2}\,W_4(0) - \frac{1}{u}\,\partial W_4(0) + O(1)\,, \tag{4.137}$$

where the singular terms $\propto u^{-6}$ and $\propto u^{-3}$ are not present.

For the study of the $\mathcal{W}_\infty$ algebra it is useful that it admits a realization in terms of two independent chiral Bose fields. We normalize them as

$$\partial\vartheta(u)\,\partial\vartheta(0) = -\frac{1}{2u^2} + O(1)\,, \qquad\qquad \partial\varphi(u)\,\partial\varphi(0) = -\frac{1}{2u^2} + O(1)\,, \tag{4.138}$$

while $\partial\varphi(u)\partial\vartheta(0) = O(1)$. One can check that as a consequence of the free field OPEs, the currents

$$W_2 \;=\; (\partial\vartheta)^2 + (\partial\varphi)^2 + \frac{\mathrm{i}}{\sqrt{n+2}}\,\partial^2\varphi\,, \tag{4.139}$$

$$W_3 \;=\; \frac{6n+8}{3n+6}\,(\partial\vartheta)^3 + 2\,(\partial\varphi)^2\partial\vartheta + \mathrm{i}\sqrt{n+2}\,\partial^2\varphi\,\partial\vartheta - \frac{\mathrm{i}n}{\sqrt{n+2}}\,\partial\varphi\,\partial^2\vartheta + \frac{n}{6(n+2)}\,\partial^3\vartheta$$

obey the algebra (4.136). The parameter n entering above is related to the central charge c as

$$c = \frac{2(n-1)}{n+2}\,. \tag{4.140}$$

Hence, if n is real and positive, the central charge c is smaller than two. Notice that, while an expression for W_4 in terms of $\partial\vartheta$ and $\partial\varphi$ has not been stated, it can be deduced from the OPEs (4.136) and the formula (4.139) for W_2 and W_3. One computes $W_3(u)W_3(0)$

with W_3 written in terms of free fields and compares the coefficient $\propto u^{-2}$ with the one appearing in the last two lines of eq. (4.136). It turns out that the higher spin currents always appear in the OPEs involving the lower spin ones. This way, starting from (4.139) and recursively computing OPEs, one can determine the full realization of W_j in terms of the free fields $\partial\varphi$ and $\partial\vartheta$ for any $j = 4, 5, 6, \ldots$.

A stepping stone for the construction of highest weight irreducible representations of the $\mathcal{W}_\infty$ algebra is the Verma module construction, which we have introduced around equation (2.40). There, we mentioned the possibility of nullstates. Let us now discuss them for the $\mathcal{W}_\infty$ algebra.

The Verma module is defined using the Fourier modes of $W_j(u)$, which we assume to be periodic functions of the variable $u \sim u + 2\pi$:

$$W_j = -\frac{c}{24}\,\delta_{j,2} + \sum_{m=-\infty}^{\infty} \widetilde{W}_j(m)\,\mathrm{e}^{-\mathrm{i}mu}\,. \tag{4.141}$$

We introduce the highest weight state $|\boldsymbol{\omega}\rangle$, which is specified by the conditions

$$\widetilde{W}_j(m)\,|\boldsymbol{\omega}\rangle = 0 \qquad (\forall m > 0)\,, \qquad \widetilde{W}_j(0)\,|\boldsymbol{\omega}\rangle = \omega_j\,|\boldsymbol{\omega}\rangle \tag{4.142}$$

with $j = 2, 3$. The highest weight is given by $\boldsymbol{\omega} = (\omega_2, \omega_3)$, where the component ω_2 is equal to the conformal dimension of the highest state, while ω_3 is the eigenvalue of $\widetilde{W}_3(0)$, which commutes with $\widetilde{W}_2(0)$. The Verma module is spanned by the states that are obtained by acting with the 'creation modes' of the spin 2 and spin 3 currents on the highest state:

$$\widetilde{W}_2(-\ell_1)\ldots\widetilde{W}_2(-\ell_m)\,\widetilde{W}_3(-\ell_1')\ldots\widetilde{W}_3(-\ell_{m'}')|\boldsymbol{\omega}\rangle \tag{4.143}$$

with $\ell_j, \ell_{j'}' \geq 1$. It possesses a natural grading given by

$$\mathtt{d} = \sum_{j=1}^{m} \ell_j + \sum_{j=1}^{m'} \ell_j'\,, \tag{4.144}$$

and the dimensions of its level subspace with fixed $\mathtt{d}$ is the number of bi-partitions of $\mathtt{d}$, i.e., $\mathrm{par}_2(\mathtt{d})$ (4.96). In what follows, we will parameterize the highest weight for the Verma module $\mathcal{V}_{\rho,\nu}$ as

$$\omega_2 = \frac{\rho^2 - \frac{1}{4}}{n+2} + \frac{\nu^2}{n}\,, \tag{4.145}$$

$$\omega_3 = \frac{2\nu}{\sqrt{n}} \left(\frac{\rho^2}{n+2} + \frac{(3n+4)\,\nu^2}{3n\,(n+2)} - \frac{2n+3}{12\,(n+2)} \right)\,.$$

This is motivated by the free field realization (4.139). Supposing that the highest state is an eigenvector of the operators $\int \mathrm{d}u\,\partial\vartheta(u)$ and $\int \mathrm{d}u\,\partial\varphi(u)$ with eigenvalues $\frac{\nu}{\sqrt{n}}$ and $\frac{\rho}{\sqrt{n+2}}$, respectively, formula (4.145) follows from (4.139). The highest weight is an even function of ρ. As a result, the spaces $\mathcal{V}_{\rho,\nu}$ and $\mathcal{V}_{-\rho,\nu}$ should be identified. In the parameterization (4.145), the conformal dimensions of a state in the Verma module at level $\mathtt{d}$ is such that

$$\widetilde{W}_2(0) - \frac{c}{24} = \frac{\rho^2}{n+2} + \frac{\nu^2}{n} - \frac{1}{12} + \mathtt{d}\,, \tag{4.146}$$

which should be compared with eq. (4.73).

For generic complex values of ρ and ν the Verma module $\mathcal{V}_{\rho,\nu}$ is an irreducible representation of the $\mathcal{W}_\infty$ algebra. However, with ρ, ν obeying certain constraints, the Verma module contains nullstates. Then the highest weight irrep $\mathcal{W}_{\rho,\nu}$ can be obtained from $\mathcal{V}_{\rho,\nu}$ by factoring out all of the invariant subspace(s) generated by the nullstate(s). In view of applications to the scaling limit of the lattice model of particular interest is when ρ takes the values $\rho = \pm\frac{1}{2}\big(r - m(n+2)\big)$ with $r, m = 1, 2, \ldots$. In this case, a nullvector appears at level $\mathtt{d} = mr$ and the Verma module splits into the direct sum of two representations, which are irreducible for generic n and ν:

$$\mathcal{V}_{\rho,\nu} = \mathcal{W}_{\rho,\nu} \oplus \mathcal{W}_{\rho',\nu} \qquad \text{with} \qquad \begin{aligned} \rho &= \tfrac{1}{2}\left(r - m\left(n+2\right)\right) & (n,\,\nu - \text{generic}) \\ \rho' &= \tfrac{1}{2}\left(r + m\left(n+2\right)\right) & (r, m = 1, 2, \ldots) \end{aligned} \;. \tag{4.147}$$

The space $\mathcal{W}_{\rho',\nu}$ is isomorphic to the Verma module and the dimensions of its level subspaces is $\mathrm{par}_2(\mathtt{d})$, while for $\mathcal{W}_{\rho,\nu}$, the level subspaces are $\mathrm{par}_2(\mathtt{d}) - \mathrm{par}_2(\mathtt{d} - mr)$ dimensional. Consider again the components $\mathcal{H}_{p,s}^{(\mathrm{cont},\mathtt{d})}$, which appear in the decomposition of the continuous spectrum of the space of states occurring in the scaling limit of the spin chain. Taking into account formulae (4.123) and (4.98), it is clear that

$$\mathcal{W}_{p,s} \cong \bigoplus_{\mathtt{d}=0}^{\infty} \mathcal{H}_{p,s}^{(\mathrm{cont},\mathtt{d})} \qquad \left(2p = 2\mathcal{S} + 1 - (n+2),\; s \in \mathbb{R}\right). \tag{4.148}$$

To describe the discrete spectrum in terms of irreps of the $\mathcal{W}_\infty$ algebra, it is necessary to analyze the case when ν is such that $\rho + \frac{1}{2} \pm \mathrm{i}\nu$ is an integer for some choice of the sign $\pm$. As explained in, e.g., section 16.2 of [25] the Verma module with $\rho + \frac{1}{2} + \mathrm{i}\nu = -a_+ = 0, \pm 1, \pm 2, \ldots$ contains a nullvector at level $|a_+ + \frac{1}{2}| + \frac{1}{2}$, while for $-\rho + \frac{1}{2} + \mathrm{i}\nu = -a_- = 0, \pm 1, \pm 2, \ldots$ there is a nullvector at level $|a_- + \frac{1}{2}| + \frac{1}{2}$. Assuming ρ is generic for now, the character of the irreducible representation,

$$\mathrm{ch}_{\rho,\nu}(\mathtt{q}) \equiv \mathrm{Tr}_{\mathcal{W}_{\rho,\nu}}\left[\mathtt{q}^{\widetilde{W}_2(0) - \frac{c}{24}}\right], \tag{4.149}$$

is given by [135] (see also [136, 137])

$$\mathrm{ch}_{\rho,\nu}(\mathtt{q}) = \mathtt{q}^{-\frac{1}{12} + \frac{\nu^2}{n} + \frac{\rho^2}{n+2}} \left(\prod_{m=1}^{\infty} \frac{1}{(1-\mathtt{q}^m)^2}\right) \sum_{m=0}^{\infty} (-1)^m \, \mathtt{q}^{m|a+\frac{1}{2}| + \frac{m^2}{2}} \tag{4.150}$$

where n, ρ are generic and $\rho + \frac{1}{2} \pm \mathrm{i}\nu = -a \in \mathbb{Z}$. If, in addition to ν being constrained as above, $\rho \to \frac{1}{2}(2\mathcal{S} - n - 1)$ then $\mathcal{W}_{\rho,\nu}$ further breaks up into two irreducible representations. One of them is generated by the nullvector which appears at level $2\mathcal{S} + 1$ and has highest weights (ρ',ν) with $\rho' = \frac{1}{2}(2\mathcal{S} + n + 3)$. Its character is given by (4.150) with ρ replaced by ρ' and $a \mapsto a' = -2(\mathcal{S}+1) - a$. Taking the difference $\mathrm{ch}_{\rho,\nu}(\mathtt{q}) - \mathrm{ch}_{\rho',\nu}(\mathtt{q})$ with $\rho \to \frac{1}{2}(2\mathcal{S} - n - 1)$ and $\rho' \to \frac{1}{2}(2\mathcal{S} + n + 3)$ yields for the character of the irreducible representation $\mathcal{W}_{\rho,\nu}$

$$\mathrm{ch}_{\rho,\nu} = \mathtt{q}^{-\frac{1}{12} + \frac{\nu^2}{n} + \frac{\rho^2}{n+2}} \left(\prod_{j=1}^{\infty} \frac{1}{(1-\mathtt{q}^j)^2}\right) \sum_{m=0}^{\infty} (-1)^m \, q^{\frac{m^2}{2}} \left(q^{m|a+\frac{1}{2}|} - q^{2\mathcal{S}+1+m|2\mathcal{S}+a+\frac{3}{2}|}\right) \tag{4.151}$$

with

$$\rho + \tfrac{1}{2} \pm \mathrm{i}\nu = -a \in \mathbb{Z} \qquad \text{and} \qquad 2\rho = 2\mathcal{S} - n - 1 \,. \qquad (4.152)$$

For the case $a \geq 0$ the above expression, apart from the overall factor $\mathsf{q}^{-\frac{1}{12} + \frac{\nu^2}{n} + \frac{\rho^2}{n+2}}$, coincides with the generating function (4.118) for the integers $N_a^+(\mathsf{d}\,|\,\mathcal{S})$. This way, one concludes

$$\mathcal{W}_{p,s} \cong \bigoplus_{\mathsf{d}=0}^{\infty} \mathcal{H}_{p,s}^{(\mathrm{disc},\mathsf{d})} \qquad \left(p = \mathcal{S} + \tfrac{1}{2} - \tfrac{1}{2}(n+2), \ \tfrac{n}{2} - \mathcal{S} \pm \mathrm{i}s = a \in \mathbb{Z}_{\geq 0} \right). \qquad (4.153)$$

The remaining case to be considered is when $-\mathcal{S} \leq a < 0$. The lower bound comes from the condition $s \in (-\tfrac{n}{2}, \tfrac{n}{2}]$ which induces that $\pm \mathrm{i}s = \tfrac{n}{2} - \mathcal{S} - a \leq \tfrac{n}{2}$. From the definition of the integers $N_a^+(\mathsf{d}\,|\,\mathcal{S})$ (4.118), which give the dimensions of the level subspaces $\mathcal{H}_{p,s}^{(\mathrm{disc},\mathsf{d})} \subset \mathcal{H}^{(\mathrm{disc})}$, one finds

$$\dim \left(\mathcal{H}_{p,s}^{(\mathsf{d})} \right) = 0 \qquad \text{for} \qquad \mathsf{d} = 0, 1, \ldots, |a| - 1 \qquad \left(-p - \tfrac{1}{2} \pm \mathrm{i}s = a \in \mathbb{Z}, \ -\mathcal{S} \leq a < 0 \right). \qquad (4.154)$$

Thus, the corresponding irrep (4.135) has a highest state whose conformal dimension is given by:

$$\Delta = \frac{p^2}{n+2} + \frac{s^2}{n} + |a| \qquad \left(-\mathcal{S} \leq a < 0 \right). \qquad (4.155)$$

This turns out to be an irreducible representation of the $\mathcal{W}_\infty$ algebra,

$$\mathcal{W}_{\rho,\nu} = \bigoplus_{\mathsf{d}=0}^{\infty} \mathcal{H}_{p,s}^{(\mathsf{d})}\,, \qquad (4.156)$$

with the highest weight parameterized as in (4.145), where

$$\rho = \mathcal{S} + \frac{1}{2}\,, \qquad \nu = \begin{cases} s - \frac{\mathrm{i}n}{2} & \text{for} \quad (-\mathrm{i}s) > 0 \\ s + \frac{\mathrm{i}n}{2} & \text{for} \quad (-\mathrm{i}s) < 0 \end{cases} \qquad \left(\tfrac{n}{2} - \mathcal{S} \pm \mathrm{i}s = a \in \mathbb{Z}_{<0}\,, \ -\mathcal{S} \leq a < 0 \right).$$

Assuming n is irrational, the character of such a representation is given by

$$\mathrm{ch}_{\rho,\nu}(\mathsf{q}) = \mathsf{q}^{-\frac{1}{12} + \frac{\nu^2}{n} + \frac{\rho^2}{n+2}} \prod_{m=1}^{\infty} \frac{1}{(1 - \mathsf{q}^m)^2} \sum_{m=0}^{\infty} (-1)^m \, \mathsf{q}^{\frac{m^2}{2}} \left(\mathsf{q}^{m|\,|\rho| - |\nu|\,|} - \mathsf{q}^{(m+1)(|\rho| + |\nu| + 1) - \frac{1}{2}} \right). \qquad (4.157)$$

One can check that the dimensions of the level subspaces, obtained by expanding $\mathrm{ch}_{\rho,\nu}(\mathsf{q})$ in a series in q, coincides with the integers $N_a^+(\mathsf{d}|\mathcal{S})$ with $-\mathcal{S} \leq a < 0$ and $\mathsf{d} = |a|, |a| + 1, |a| + 2, \ldots$.

Finally, we mention that the states $|\psi_{p,s}^{(S^z)}(\boldsymbol{w})\rangle \in \mathcal{W}_{\rho,\nu}$ appearing in the scaling limit of the Bethe states, see eq.(4.120), have an important interpretation. They are the simultaneous eigenstates of the so-called quantum AKNS integrable structure [138, 139]. The function $\mathrm{e}^{\frac{\mathrm{i}}{2}\delta}$ (4.108b) entering into the quantization condition coincides with the eigenvalue of a certain so-called reflection operator [140] computed on $|\psi_{p,s}^{(S^z)}(\boldsymbol{w})\rangle$, see reference [133] for details.

4.2.7 PARTITION FUNCTION IN THE SCALING LIMIT

In the case of the lattice model with twisted BCs, it was proposed [24] and then verified numerically [25] that the partition function appearing in the scaling limit of the lattice system, $Z^{(\mathrm{scl})}$, coincides with twice the partition function of the 2D Euclidean Black Hole CFT. Recall that, the latter was constructed in refs. [51, 49] by computing a functional integral with the worldsheet being taken to be a torus. The results presented in the previous section allow one to easily compute $Z^{(\mathrm{scl})}$ for the staggered six-vertex model subject to $U_q\big(\mathfrak{sl}(2)\big)$ invariant open BCs. One may expect $\frac{1}{2}\,Z^{(\mathrm{scl})}$ to coincide with the partition function for 2D Euclidean Black Hole CFT on the open segment $x \in (0, R)$, with certain conditions imposed on the fields at $x = 0, R$.

Consider the lattice partition function

$$Z_L^{(\mathrm{lattice})} = \mathrm{Tr}_{\mathscr{H}}\big[\mathrm{e}^{-M\,\mathbb{H}}\big]\,, \tag{4.158}$$

where the Hamiltonian $\mathbb{H}$ is given by (4.30) with $\alpha = \frac{\pi}{2}$ and $\gamma = \frac{\pi}{n+2}$ and $n \geq 0$, while the trace is taken over the 2^{2L} dimensional space of states: $\mathscr{H} = \mathbb{C}_{2L}^2 \otimes \mathbb{C}_{2L-1}^2 \otimes \ldots \otimes \mathbb{C}_1^2$. Keeping the ratio

$$\tau = \frac{v_{\mathrm{F}} M}{2L} \tag{4.159}$$

fixed as $L \to \infty$, one finds that the large L behaviour of the lattice partition function is given by

$$Z_L^{(\mathrm{lattice})} \asymp \mathrm{e}^{-MLe_\infty - Mf_\infty}\, Z^{(\mathrm{scl})}\,. \tag{4.160}$$

Here $Z^{(\mathrm{scl})}$ takes the form of a trace over the space of states $\mathcal{H}$ appearing in the scaling limit of the lattice model:

$$Z^{(\mathrm{scl})} = \mathrm{Tr}_{\mathcal{H}}\Big(\mathsf{q}^{\hat{H}_{\mathrm{CFT}}}\Big) \qquad \text{with} \qquad \mathsf{q} = \mathrm{e}^{-2\pi\tau}\,. \tag{4.161}$$

It involves the 'CFT Hamiltonian' $\hat{H}_{\mathrm{CFT}}$ which when restricted to the finite-dimensional spaces $\mathcal{H}_{p,s}^{(\mathrm{cont},\mathsf{d})}$ or $\mathcal{H}_{p,s}^{(\mathrm{disc},\mathsf{d})}$ appearing in the decomposition of $\mathcal{H}$ is diagonal with

$$E_{\mathrm{CFT}} = \frac{p^2}{n+2} + \frac{s^2}{n} - \frac{1}{12} + \mathsf{d}\,. \tag{4.162}$$

Notice that the asymptotic formula for the energy (4.71) can be re-written as the formal relation

$$\hat{H}_{\mathrm{CFT}} = \operatorname*{slim}_{L\to\infty} \frac{L}{\pi v_{\mathrm{F}}}\left(\mathbb{H} - L\,e_\infty - f_\infty\right)\,. \tag{4.163}$$

In subsection 4.2.6, the space of states $\mathcal{H}$ was expressed as a direct sum of the continuous spectrum $\mathcal{H}^{(\mathrm{cont})}$ and the discrete one $\mathcal{H}^{(\mathrm{disc})}$, see formula (4.133). The contribution of the states to the trace in eq. (4.161) for each of these spaces will be denoted as $Z^{(\mathrm{cont})}$ and $Z^{(\mathrm{disc})}$, respectively, so that

$$Z^{(\mathrm{scl})} = Z^{(\mathrm{cont})} + Z^{(\mathrm{disc})}\,, \tag{4.164}$$

where

$$Z^{(\mathrm{disc})} = \mathrm{Tr}_{\mathcal{H}^{(\mathrm{disc})}}\Big(\mathsf{q}^{\hat{H}_{\mathrm{CFT}}}\Big)\,, \qquad\qquad Z^{(\mathrm{cont})} = \mathrm{Tr}_{\mathcal{H}^{(\mathrm{cont})}}\Big(\mathsf{q}^{\hat{H}_{\mathrm{CFT}}}\Big)\,. \tag{4.165}$$

Let us focus on the computation of $Z^{(\text{disc})}$. The space $\mathcal{H}^{(\text{disc})}$ is made up of the components $\mathcal{H}^{(\text{disc})}_{\mathcal{S},\mathcal{S}^z} \cong \mathcal{H}^{(\text{disc})}_{\mathcal{S},\mathcal{S}}$, which admit the decomposition (4.129) into finite dimensional spaces. We introduce the notation

$$\chi_{a,\mathcal{S}}(\mathsf{q}) = \mathsf{q}^{-\frac{(\frac{n}{2}-\mathcal{S}-a)^2}{n}+\frac{p^2}{n+2}-\frac{1}{12}} \prod_{j=1}^{\infty}(1-\mathsf{q}^j)^{-2} \sum_{m=0}^{\infty}(-1)^m \left(1-\mathsf{q}^{(1+m)(2\mathcal{S}+1)}\right)\mathsf{q}^{ma+\frac{m(m+1)}{2}},$$
(4.166)

where, aside from the prefactor, the function $\chi_{a,\mathcal{S}}(\mathsf{q})$ coincides with the generating function for the dimensions of the level subspaces $\mathcal{H}^{(\text{disc,d})}_{\mathcal{S},\mathcal{S}}$, see eqs. (4.131) and (4.118). Then, the contribution of the discrete spectrum to the partition function reads as:

$$Z^{(\text{disc})} = \sum_{\mathcal{S}\geq 0}(2\mathcal{S}+1)\left(\chi_{-\mathcal{S},\mathcal{S}}(\mathsf{q}) + 2\sum_{\substack{a\in\mathbb{Z} \\ 0<a+\mathcal{S}<\frac{n}{2}}} \chi_{a,\mathcal{S}}(\mathsf{q})\right).$$
(4.167)

Each term in the sum over $\mathcal{S}$ has multiplicity $(2\mathcal{S}+1)$ as a result of the $U_q\big(\mathfrak{sl}(2)\big)$ symmetry of the lattice model. Also, for every state with given $s = s_a$ (4.128) there exists another one with $s = -s_a$ which yields the same contribution to the partition function, except for the case when $s = \pm\frac{in}{2}$, where they are identified as the same state. This explains why the functions $\chi_{a,\mathcal{S}}(\mathsf{q})$ come with a factor of two except the one with $a = -\mathcal{S}$ (recall that $s_a = \mathrm{i}(\frac{n}{2}-\mathcal{S}-a)$ and hence $s_a = \frac{in}{2}$ for $a = -\mathcal{S}$).

The contribution of the continuous spectrum to the partition function is given by

$$Z^{(\text{cont})} = \sum_{\mathcal{S}\geq 0}(2\mathcal{S}+1)\int_{-\infty}^{\infty}\mathrm{d}s\sum_{\mathsf{d}\geq 0}\rho_p^{(\mathsf{d})}(s)\,\mathsf{q}^{\frac{s^2}{n}+\frac{p^2}{n+2}-\frac{1}{12}+\mathsf{d}}.$$
(4.168)

Here $\rho_p^{(\mathsf{d})}(s)$ is the density of states defined in formulae (4.116) and (4.117), while we recall that $2p = 2\mathcal{S}+1-(n+2)$. Notice that $Z^{(\text{cont})}$ becomes singular as $L \to \infty$:

$$Z^{(\text{cont})} = Z^{(\text{sing})} + O(1),$$
(4.169)

where the singular part is given by

$$Z^{(\text{sing})} = \sqrt{\frac{n}{2\tau}}\,\frac{\log\left(2^{\frac{n+2}{n}}L/L_0\right)}{\pi\,\mathsf{q}^{\frac{1}{24}}\prod_{m=1}^{\infty}(1-\mathsf{q}^m)}\sum_{\mathcal{S}=0}^{\infty}(2\mathcal{S}+1)\,\mathsf{q}^{-\frac{1}{24}+\frac{p^2}{n+2}}\,\frac{1-\mathsf{q}^{2\mathcal{S}+1}}{\prod_{m=1}^{\infty}(1-\mathsf{q}^m)}.$$
(4.170)

The factor out the front of the sum is easily recognised to be the partition function of a boson taking values in the segment $\sim \log(L)$ with Neumann BCs imposed at the endpoints of the field at $x = 0, R$ (see also (2.58)). As for the remaining term,

$$Z_2^{(\text{sing})} = \sum_{\mathcal{S}=0}^{\infty}(2\mathcal{S}+1)\,\mathsf{q}^{-\frac{1}{24}+\frac{p^2}{n+2}}\,\frac{1-\mathsf{q}^{2\mathcal{S}+1}}{\prod_{m=1}^{\infty}(1-\mathsf{q}^m)},$$
(4.171)

in all likelihood, $Z_2^{(\text{sing})}$ corresponds to a boundary state, which is a superposition of Ishibashi states associated with a degenerate representation of the Virasoro algebra with generic central charge c (see reference [141] for the $c = 1$ case). Note that $Z_2^{(\text{sing})}$ also appears in the scaling limit of the XXZ spin-$\frac{1}{2}$ chain with open $U_q\big(\mathfrak{sl}(2)\big)$ invariant BCs imposed [142].

Formulae (4.167) and (4.168) do not seem to correspond to the published results in the literature concerning branes in the 2D Euclidean Black Hole CFT, in particular, reference [48]. As such, a separate investigation is required in order to establish the relation between the partition function $Z^{(\mathrm{scl})} = Z^{(\mathrm{cont})} + Z^{(\mathrm{disc})}$ and that of the Black Hole CFTs in the presence of boundaries.

4.3 Spectral flow to the quasi-periodic model

In the last section, we have discussed the scaling limit of the $U_q(\mathfrak{sl}(2))$ invariant self-dual six-vertex model with *alternating* staggering in depth. Recall that there also exists the case of quasi-periodic staggering (3.30). The Hamiltonian for quasi-periodic staggering coincides with the one of the model with alternating staggering at the self-dual point up to boundary terms

$$\mathbb{H}^{\mathrm{qper}} = \mathbb{H}^{\mathrm{alt}}\left(\frac{\mathrm{i}\pi}{2}\right) + \frac{2}{\sin(2\gamma)\cos(\gamma)}\left(e_{1,2} + e_{2L-1,2L}\right), \qquad (4.172)$$

where we recall that

$$\mathbb{H}^{\mathrm{alt}}\left(\frac{\mathrm{i}\pi}{2}\right) = -\frac{2}{\sin(2\gamma)}\left(2\cos(\gamma)\sum_{j=1}^{2L-1} e_{j,j+1} + \sum_{j=2}^{2L-1} e_{j,j+1}e_{j-1,j} + e_{j-1,j}e_{j,j+1}\right). \quad (4.173)$$

Remarkably, this choice of BCs, i.e. the presence of the additional term in (4.172), has a profound influence on the low energy properties of the staggered models. Namely, by studying the antiferromagnetic Potts model[15], Robertson *et al.* found that the continuum limit of the model (4.172) does not contain a continuous component [26]. Further, a boundary RG flow between these two critical fixed points has been studied. It has been concluded that the fixed points corresponding to (4.173) and (4.172) are unstable and stable, respectively [27]. The numerical investigation was based on finite-size estimates of the gap between the ground state and the lowest excitation when the amplitude of the boundary term in (4.172) is varied between the two integrable points. However, simply varying the amplitude of the boundary terms in (4.172), yields a *non-integrable* boundary RG Flow.

In the setting of the composite $\mathcal{R}$-matrix, both (4.173) and (4.172) originate from a staggered vertex model. This allows us to study the spectral flow between (4.173) and (4.172) in an *integrable* setting with a fixed choice of the boundary matrices under the variation of the bulk inhomogeneities. The price to pay for integrability is giving up the locality of the Hamiltonian at the intermediate points. Using the same staggering in the vertical and horizontal directions of the vertex model discussed in chapter 3, i.e. $\{\delta_0, \delta_{\bar{0}}\} = \{\delta_1, \delta_2\}$, we can tune δ_1 and δ_2 to interpolate between the integrable models with local interactions. We choose the following normalization of the non-local 'Hamiltonian' obtained from the transfer matrix (3.20) (with R given by (2.126),(2.127) and K-matrices

---

[15]The antiferromagnetic Potts model has been shown to be equivalent to the case at hand for suitable BCs. We do not go into detail here, but discuss this point at the beginning of chapter 6.

given by (4.1))

$$
\mathbb{H} = \frac{q \det\left(T\left(-\delta_1 - \frac{i\gamma}{2}\right)\right) q \det\left(T\left(-\delta_2 - \frac{i\gamma}{2}\right)\right)}{2 i f(\delta_1) f(\delta_2)}
$$
$$
\times \left(\left.\frac{d}{du}\right|_{u=0} \mathbb{T}(u, \{\delta_1, \delta_2, \delta_1, \delta_2\}) - \left.\frac{d}{du}\right|_{u=0} f(u+\delta_1) f(u+\delta_2) \right)
$$

(4.174)

with

$$
f(u) = \frac{\sinh(2u + 2i\gamma)}{\sinh(2u + i\gamma)} \sinh^L(u - \delta_1 + i\gamma) \sinh^L(u - \delta_2 + i\gamma)
$$
$$
\times \sinh^L(u + \delta_1 + i\gamma) \sinh^L(u + \delta_2 + i\gamma),
$$
$$
q \det(T(u)) = \sinh^L\left(u + \delta_1 - \frac{i\gamma}{2}\right) \sinh^L\left(u + \delta_1 + \frac{3i\gamma}{2}\right)
$$
$$
\times \sinh^L\left(u + \delta_2 - \frac{i\gamma}{2}\right) \sinh^L\left(u + \delta_2 + \frac{3i\gamma}{2}\right).
$$

Specifically, we choose the parameterization

$$
\delta_1 = \frac{i\vartheta}{2} + \frac{i\pi}{4}, \qquad \delta_2 = \frac{i\vartheta}{2} - \frac{i\pi}{4}, \qquad -\frac{\pi}{2} \leq \vartheta \leq 0,
$$

(4.175)

for the remaining inhomogeneities resulting in alternating and quasi-periodic staggering for $\vartheta = 0$ and $-\pi/2$, respectively.

The eigenvalues of the 'Hamiltonian' (4.174) in this parameterization are given in terms of the Bethe roots $\{u_m\}$ solving the BAE (4.29) whereby we substitute (4.175). We get

$$
E = \left(-4L \cot(2\gamma) + L \frac{2\sin(2\vartheta)}{\sin(2\gamma)\sin(2(\gamma+\vartheta))} - \frac{2\sin(\vartheta)}{\cos(\gamma)\cos(\gamma+\vartheta)} + \frac{2\sin(\vartheta)}{\cos(2\gamma)\cos(2\gamma+\vartheta)} \right.
$$
$$
\left. + \frac{2\tan(\gamma)}{\cos(2\gamma)} \right) \times \left(\prod_{m=1}^{M} \frac{\cos(2(\gamma-\vartheta)) + \cosh(4u_m)}{\cos(2(\gamma+\vartheta)) + \cosh(4u_m)} - 1 \right)
$$
$$
- 4\sin(2\gamma) \sum_{k=1}^{M} \left\{ \frac{\cos(2\gamma) + \cos(\vartheta)\cosh(4u_k)}{(\cos(2(\gamma+\vartheta)) + \cosh(4u_k))^2} \right\} \times \prod_{\substack{m=1 \\ m \neq k}}^{M} \frac{\cos(2(\gamma-\vartheta)) + \cosh(4u_m)}{\cos(2(\gamma+\vartheta)) + \cosh(4u_m)}.
$$

(4.176)

As expected, this expression reduces to a sum of bare quasi-particle energies $\epsilon_0(u_m)$ for $\vartheta = 0, \pm\pi/2$ where the Hamiltonian becomes local. Away from these points, the normalization of (4.176) leads to singularities at particular values of the flow parameter: the one at $\vartheta = \frac{\pi}{2} - 2\gamma$ can be removed by multiplying the Hamiltonian by the ϑ-dependent factor $\cos(2\gamma + \vartheta)$ while $\vartheta = \frac{\pi}{2} - \gamma > 0$ does not lie on the spectral flow (4.175). The remaining singularity at $\vartheta_{c1} = -\gamma$ depends on the state considered. In terms of the corresponding Bethe root configuration this can be related to the low energy root configurations of the quasi-periodic model (4.172). These consists of pairs of complex conjugate roots with imaginary part $\pm\frac{\pi}{4}$ and an additional root at $\frac{i\pi}{4}$ for M^{qper} odd [26]:

$$
u^{\mathrm{qper}} \in \left\{ x_m + \frac{i\pi}{4}, x_m - \frac{i\pi}{4} \,\middle|\, x_m \in \mathbb{R}_{>0}, m = 1, \ldots, \left\lfloor \frac{M^{\mathrm{qper}}}{2} \right\rfloor \right\} \cup \left\{ \frac{i\pi}{4} \right\}.
$$

(4.177)

Here $\lfloor ... \rfloor$ denotes the Gaussian bracket. Exact diagonalization of the Hamiltonian for small systems together with the determination of the corresponding Bethe roots shows that root patterns of this type persist throughout the interval $\vartheta = -\pi/2 ... \vartheta_{c1}$. At ϑ_{c1}, however, several roots become purely imaginary, $u_m = i\pi/4$, changing the order of the pole in (4.176). This singularity can be removed by renormalization of the spectrum by a factor $\sin^\nu(\vartheta + \gamma)$ with an appropriate choice of an integer ν.

The spectral flow starting from the alternating model (4.173), $\vartheta = 0$, can be studied in a similar way. We recall the class of low energy states (including the ground state) is given by (4.42). Configurations of this type exist in the interval $\vartheta_{c2} < \vartheta < 0$ where roots with vanishing real parts appear for $\vartheta_{c2} = \gamma - \pi/2$. These do not, however, lead to singularities in the eigenvalues of (4.176).

Both at ϑ_{c1} and ϑ_{c2} the appearance of purely imaginary Bethe roots leads to degeneracies involving many states. This is illustrated in Figure 4.14 for a spin chain with $2L = 8$ sites and anisotropy $\gamma = 0.9$ for the sector $\mathcal{S} = 2$. Under the spectral flow, low energy states of the local Hamiltonian (4.173) are mapped to high energy ones for (4.172) and vice versa. The crossing of a large number of levels indicates the presence of first-order transitions when the flow parameter is ϑ_{c1} or ϑ_{c2}.

Support for this interpretation can be obtained by studying the *spectral flow* within the root density formalism. In the thermodynamic limit, the densities of roots in the configuration (4.42) of the alternating model are found to be

$$\rho^a(v) = \sigma^a(v) + \frac{1}{L}\tau^a(v)\,, \quad a = x, y\,, \tag{4.178}$$

with bulk and surface contributions

$$\sigma^x(v) = \sigma^y(v) = \frac{\cos\left(\frac{\pi\,\vartheta}{\pi - 2\gamma}\right)}{\pi - 2\gamma}\left[\frac{1}{\cosh\left(\frac{2\pi v}{\pi - 2\gamma}\right) + \sin\left(\frac{\pi\,\vartheta}{\pi - 2\gamma}\right)} + \frac{1}{\cosh\left(\frac{2\pi v}{\pi - 2\gamma}\right) - \sin\left(\frac{\pi\,\vartheta}{\pi - 2\gamma}\right)}\right]\,,$$

$$\tau^x(v) = \tau^y(v) = \frac{1}{4\pi}\int_{-\infty}^{\infty} d\omega\, e^{i\omega v}\,\frac{\sinh\left(\frac{3\gamma - \pi}{4}\omega\right)}{\sinh\left(\frac{\gamma\omega}{4}\right)\cosh\left(\frac{2\gamma - \pi}{4}\omega\right)}\,.$$

Similarly, the density $\bar\rho(x)$ of root configurations (4.177) of the quasi-periodic model is found to be

$$\bar\sigma(x) = \frac{4}{\pi - 2\gamma}\frac{\cos\left(\frac{\pi}{2}\frac{\pi + 2\vartheta}{\pi - 2\gamma}\right)\cosh\left(\frac{2\pi x}{\pi - 2\gamma}\right)}{\cosh\left(\frac{4\pi x}{\pi - 2\gamma}\right) + \cos\left(\pi\frac{\pi + 2\vartheta}{\pi - 2\gamma}\right)}\,, \quad \bar\tau(x) = \frac{1}{\pi - 2\gamma}\frac{1}{\cosh\left(\frac{2\pi x}{\pi - 2\gamma}\right)}\,. \tag{4.179}$$
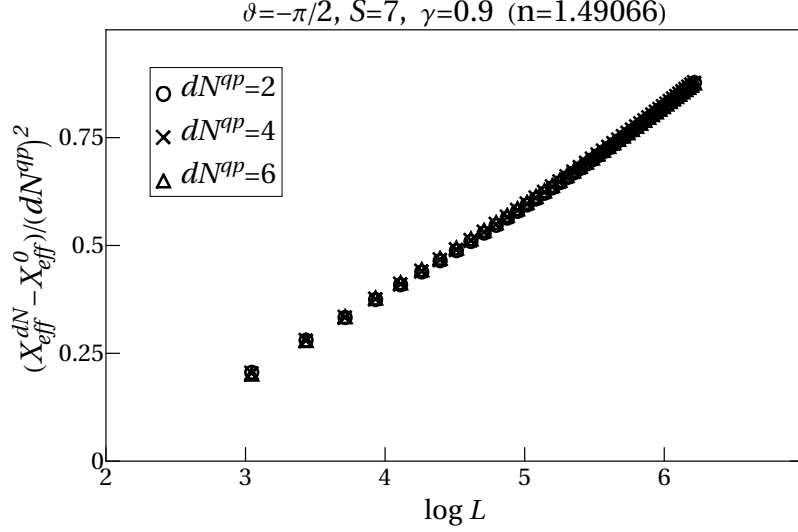
That the bulk densities $\sigma^{x,y}(v)$ $(\bar\sigma(x))$ vanish at ϑ_{c2} (ϑ_{c1}), indicates a transition into a different state in accordance with our results for small system sizes.
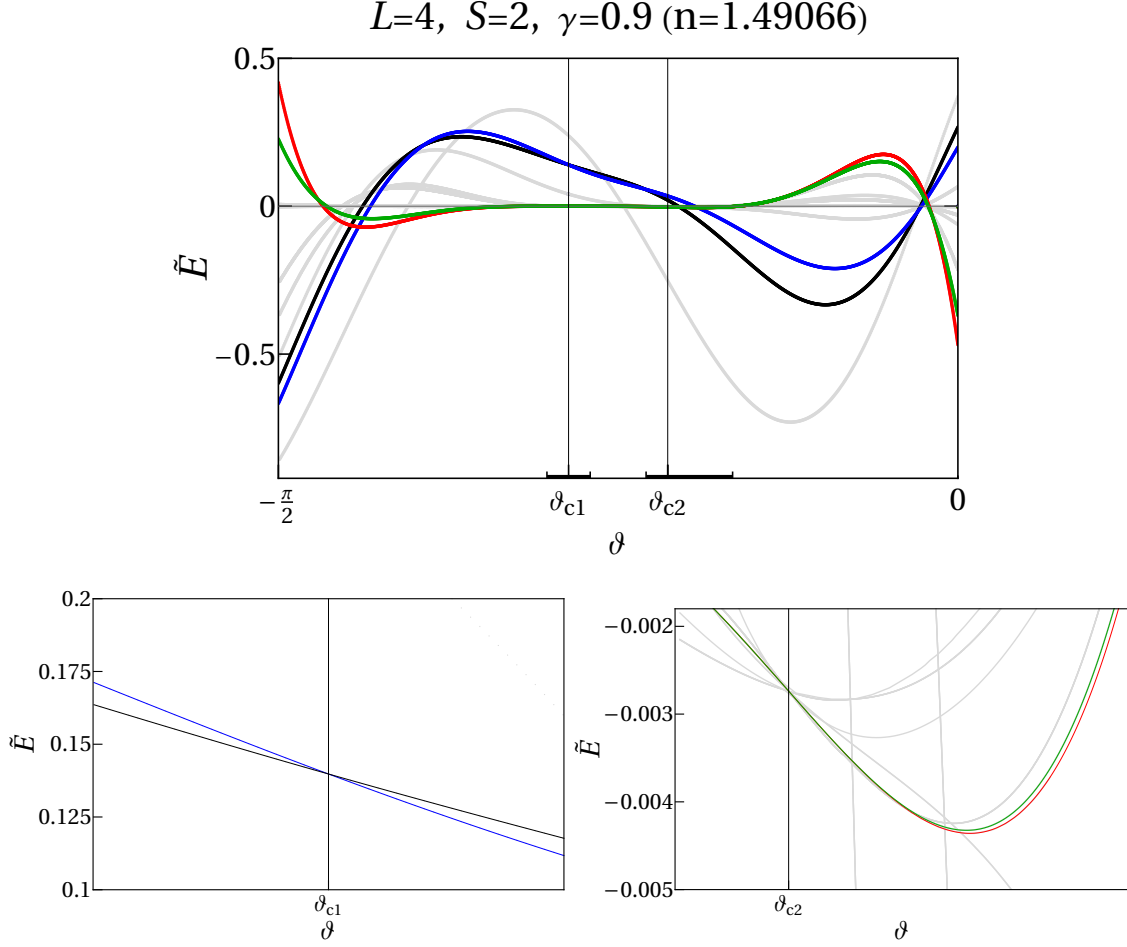
Figure 4.14: Rescaled real parts $\tilde{E}$ of the eigenvalues of the staggered six-vertex Hamiltonian with $2L = 8$ sites, anisotropy $\gamma = 0.9$, ($n = 1.49066$) for the charge sector $\mathcal{S} = 2$ for the spectral flow (4.175). Energies have been multiplied with $-\cos(\vartheta + 2\gamma)\sin^5(\vartheta + \gamma)$ to regularize the singularities as described in the main text. The mapping between low and high-energy states in the local models is clearly seen. In the lower plots, the level crossings at $\vartheta = \vartheta_{c1}, \vartheta_{c2}$ of low-lying states evolving from the respective ground states are resolved within the ϑ-intervals indicated in the upper image details.

As discussed in the previous sections, e.g. 4.2.3, the continuum limit of the alternating model (4.173) possesses a continuum of scaling dimensions. Recall that the underlying mechanism on the level of the Bethe configurations (4.42) is based on the difference $dN^{\text{alt}} = M^0 - M^{\frac{i\pi}{2}}$. Motivated by this, for the quasi-periodic model we consider the scaling behaviour of states with Bethe configurations (4.177) with different numbers $M^{\pm \frac{i\pi}{4}}$ of roots on the lines $\Im m(u_m) = \pm\frac{\pi}{4}$. The bulk energies e_∞^{qp}, f_∞^{qp} and Fermi velocity of the quasi-periodic model can be calculated in the root density formalism using (4.179) with $\vartheta = -\frac{\pi}{2}$. We obtain

$$e_\infty^{\text{qp}} = 2f_\infty^{\text{qp}} = -\frac{1}{2}\int_{-\infty}^{\infty} d\omega \, \frac{\sinh\left(\frac{\gamma\omega}{2}\right)}{\sinh\left(\frac{\pi\omega}{4}\right)\cosh\left(\frac{1}{4}(\pi - 2\gamma)\omega\right)}, \qquad v_F^{\text{qp}} = \frac{2\pi}{\pi - 2\gamma}. \qquad (4.180)$$

Figure 4.15: Scaling of energy gaps of the quasi-periodic chain in the sector $\mathcal{S} = 7$ weighted by $1/(dN^{\text{qp}})^2$ obtained by solving the Bethe ansatz equations for various dN^{qp} and L and fixed $\gamma = 0.9$, ($n = 1.49066$) . We see that the scaling dimensions of those states depend on $(dN^{\text{qp}})^2$ and display a clear logarithmic divergence as $L \to \infty$. While solving the Bethe equations numerically, we found that the dN^{qp} needs to be smaller than $\mathcal{S}$ for numerical convergence.

Using the Bethe ansatz we have calculated the finite-sizes estimate $X_{\text{eff}}(L)$ for states with various $dN^{\text{qp}} = M^{-\frac{i\pi}{4}} - M^{\frac{i\pi}{4}}$. Parts of our numerical results are displayed in Figure 4.15. Differing from the alternating model, we see that the $X_{\text{eff}}(L)$ *diverge* logarithmically with an amplitude proportional to $(dN^{\text{qp}})^2$. We interpret these diverging scaling dimensions in the quasi-periodic case in the manner that states with $dN^{\text{qp}} \neq 0$ disappear from the low energy sector in the thermodynamic limit. Only states with $dN^{\text{qp}} = 0$ stay in the low energy regime as L tends to infinity which have been extensively studied in [26].

We have investigated whether the logarithmic divergent corrections can be parameterised by a conserved quantity. A natural candidate would be the quasi-momentum operator. However, for the case at hand, it is trivial (see (3.41)). Hence, we have considered the next leading term, i.e.

$$\overline{\mathbb{B}}^{\text{qp}} \propto \frac{\mathrm{d}}{\mathrm{d}u} \frac{\mathbb{t}(u, \{0, \frac{\mathbb{P}}{2}\})}{\mathbb{t}(u - \frac{\mathbb{P}}{2}, \{0, \frac{\mathbb{P}}{2}\})}\bigg|_{u=0} , \tag{4.181}$$

This operator can be expressed in terms of Pauli matrices as given in appendix (C.3). It turns out to be a sum of local operators in contrast to the alternating case; see Figure 3.7. A normalization can be chosen such that its eigenvalue $\overline{B}^{\text{qp}}$ can be expressed in a simple form in terms of the Bethe roots:

$$\overline{B}^{\text{qp}} = \sum_j k_0(u_j) \quad \text{with} \quad k_0(u) = \frac{16i \sin(\gamma) \cosh(2u)}{\cosh(4u) - \cos(2\gamma)} . \tag{4.182}$$

105
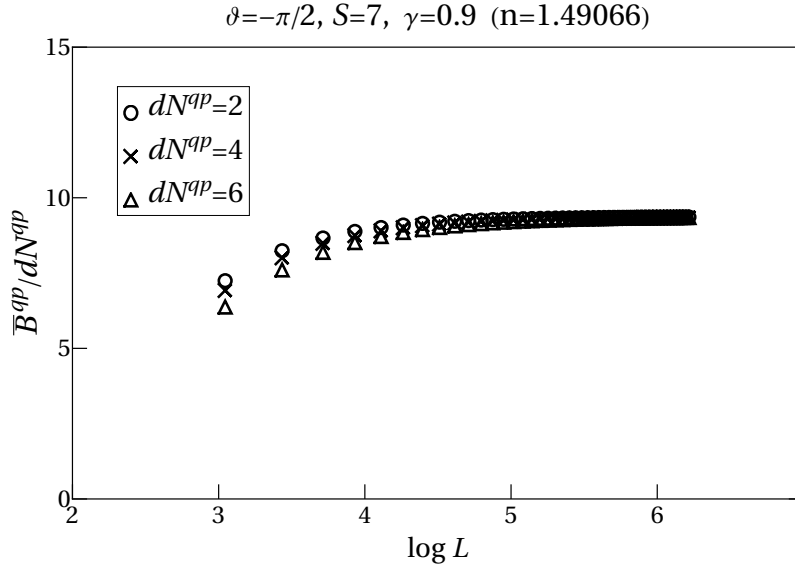
Figure 4.16: The quasi-momentum of Bethe states having a non-vanishing quantum number dN^{qp}.

Note that $\overline{B}^{\mathrm{qp}}$ measures the difference of the number of Bethe roots on the lines $\pm\frac{\mathrm{i}\pi}{4}$:

$$k_0\left(x+\frac{\mathrm{i}\pi}{4}\right) = -k_0\left(x-\frac{\mathrm{i}\pi}{4}\right). \tag{4.183}$$

This is similar to the role of (3.42) in the alternating case. In the present case, however, $\overline{B}^{\mathrm{qp}} \propto dN^{\mathrm{qp}}$ as $L \to \infty$, see Figure 4.16. Hence, $\overline{B}^{\mathrm{qp}}$ does not capture the L-dependence observed in Figure 4.15.

4.4 CHAPTER SUMMARY

In this chapter, we have considered the concrete example of the staggered six-vertex model with quantum group invariant BCs ($U_q(\mathfrak{sl}(2))$ symmetry). We have described how the $U_q(\mathfrak{sl}(2))$ case can be obtained from a limiting procedure $\epsilon \to 0$ of the more general model with two anti-parallel boundary magnetic fields of strength ϵ. We presented a formula for the Q-operator of the latter, valid in the sector $S^z = 0$. The main advantage of (4.16), as opposed to the expressions for $\mathbb{Q}(\zeta)$ appearing in the literature [119, 120, 121, 122], is that it contains no infinite sums and works literally for any (generic) complex values of q, ϵ. Further, it can be programmed efficiently on the computer.

The TQ-relation allowed us to solve the model via the analytic Bethe ansatz. The limit $\epsilon \to 0$ yields the known — from the algebraic Bethe ansatz — solution of the $U_q(\mathfrak{sl}(2))$ invariant case.

We analysed the special case of the model with alternating staggering. We found that the $U_q(\mathfrak{sl}(2))$-symmetry is spontaneously broken: in contrast to the periodic chain where the lowest state is always in the sector with $S^z = 0$, the ground state of the open chain has non-zero spin depending on the anisotropy γ. It becomes completely polarised for sufficiently small γ ($\gamma \to 0$ in the thermodynamic limit).

An analysis of the finite-size spectrum based on the Bethe hypothesis (4.42) showed the presence of strong logarithmic corrections to scaling. Further, we observed the existence of 'discrete states', for which there are no logarithmic corrections. As in previous studies of the periodic model [24, 53, 54] the eigenvalues of the quasi-momentum operator $\mathbb{B}$ (4.34) play an important role: On the one hand, they determine the amplitudes $b(L)$ of the strong logarithmic corrections of the states leading to a continuous degree of freedom in the scaling limit, $s = \mathrm{slim}_{L \to \infty} b(L) \in \mathbb{R}$. On the other hand, a pure imaginary eigenvalue of the quasi-momentum serves as a good indication that the corresponding state will become part of the discrete spectrum in the scaling limit. These results led to the working hypothesis that the scaling limit is related to the $SL(2,\mathbb{R})/U(1)$ sigma model where the level is determined from the anisotropy of the model via (4.74). Further, we show that tuning the value of the staggering parameter α in the regime (4.40) away from the self-dual point is an irrelevant deformation, similar as found in the periodic case [54].

After this, we focused on the self-dual model with $\alpha = \frac{\pi}{2}$. For this particular case, we carried out a full characterisation of the scaling limit. The powerful analytic technique crucial to our investigation is the ODE/IQFT approach to studying the scaling limit of integrable, critical lattice systems. While it was developed for the case of twisted BCs, we found it to be applicable for $U_q\big(\mathfrak{sl}(2)\big)$ invariant open BCs as well. This points to the versatility of the ODE/IQFT approach, where the analysis for one set of BCs can be readily carried over to another.

One of the key results is the explicit formula for the density of states $\rho^{(\mathsf{d})}(s)$ (4.116), (4.117), which characterises the continuous spectrum. In addition, we studied the RG trajectories $\{|\Psi_L\rangle\}$, where s becomes a pure imaginary number in the scaling limit. Building on our previous analysis, the discrete set $\Sigma \equiv \Sigma^+ \cup \Sigma^-$ (4.130) of all admissible values of pure imaginary s was found. We also determined the dimension of the linear span of states occurring in the scaling limit of $|\Psi_L\rangle$ with given $s \in \Sigma$ and conformal dimensions Δ (4.73).

Our work includes a full characterisation of the linear space $\mathcal{H}$ appearing in the scaling limit of the space of low energy states of the lattice system. To describe it, $\mathcal{H}$ was decomposed into a direct sum of the 'continuous spectrum' $\mathcal{H}^{(\mathrm{cont})}$ and the 'discrete spectrum' $\mathcal{H}^{(\mathrm{disc})}$. The former, when expressed in terms of finite-dimensional spaces, involves a direct integral over s, see equation (4.134), (4.121), (4.122), while the latter contains a direct sum (4.129). We explained how the graded linear spaces $\oplus_{\mathsf{d}=0}^\infty \mathcal{H}_{p,s}^{(\mathrm{cont},\mathsf{d})}$ and $\oplus_{\mathsf{d}=0}^\infty \mathcal{H}_{p,s}^{(\mathrm{disc},\mathsf{d})}$ are irreps of the $\mathcal{W}_\infty$ algebra — the algebra of extended conformal symmetry of the model.

Perhaps the most interesting question is the relation between the scaling limit of the lattice system and the 2D Euclidean/Lorentzian Black Hole CFTs introduced in the preliminaries. We believe that the formula for the partition function $Z^{(\mathrm{scl})}$ provided in sec. 4.2.7 may be of help. Unfortunately, it does not seem to correspond to known results in the literature on branes in the 2D Black Hole CFTs. Progress in this direction would likely require further research.

Finally, we have studied the spectral flow between the alternating and quasi-periodic models. Following this flow along a line of integrable models, we find that the endpoints are separated by two first-order transitions, consistent with the different properties of the corresponding spectra observed previously.

5 | ANTIDIAGONAL BCs

Let us now study the influence of antidiagonal BCs (the second expression in (2.129)) on the staggered six-vertex model. The transfer matrix can be depicted as shown in Figure 5.1. The corresponding Hamiltonian takes the form (4.30) except that the upper and lower bounds in the sum are 1 and $2L$ respectively and we identify operators according to (2.114). The latter generates terms such as $\sim \sigma^x \sigma^y$, when expressed in the Pauli matrices using (4.31). These terms break the usual $U(1)$ symmetry of the model with periodic or twisted BCs. Left are only two discrete $\mathbb{Z}_2$ symmetries. They take the form

$$\mathbb{G} = \prod_{j=1}^{2L} \sigma_j^z, \qquad \mathbb{C} = \prod_{j=1}^{2L} \sigma_j^x. \tag{5.1}$$

Using the exact solution via the analytical Bethe ansatz presented in section 2.4.3, we obtain for the energy and the eigenvalues of the quasi-momentum operator

$$E = \sum_{k=1}^{2L} \frac{\sin\left(\frac{\gamma}{2}\right)}{\cosh(u_k - \frac{i\alpha}{2}) - \cos(\frac{\gamma}{2})} + \frac{\sin\left(\frac{\gamma}{2}\right)}{\cosh(u_k + \frac{i\alpha}{2}) - \cos(\frac{\gamma}{2})}, \tag{5.2}$$

$$B = \log\left(\frac{\sin(\gamma + \alpha)}{\sin(\gamma - \alpha)}\right)^L + \sum_{k=1}^{2L} \log\left(\frac{\cosh(u_k) - \cos\left(\frac{\alpha-\gamma}{2}\right)}{\cosh(u_k) - \cos\left(\frac{\alpha+\gamma}{2}\right)}\right). \tag{5.3}$$

Here, $\{u_k\}$ are the Bethe roots solving (2.153). The following comment is in order here. Consider the duality transformation (3.28) where $\alpha \to \pi - \alpha$. If we simultaneously perform $\gamma \mapsto \pi - \gamma$ we interchange the high energy and low energy spectra

$$\mathbb{H}\big|_{\substack{\alpha \mapsto \pi - \alpha \\ \gamma \mapsto \pi - \gamma}} = -\mathbb{H}. \tag{5.4}$$
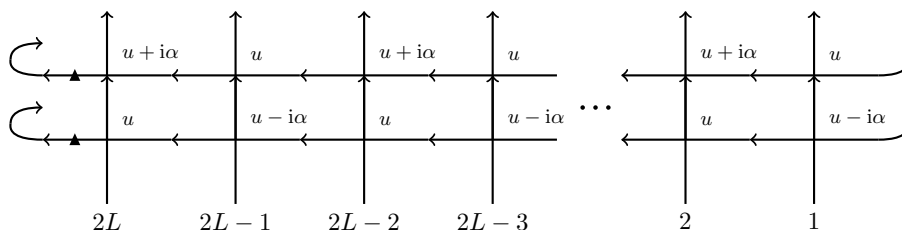
Figure 5.1: Graphical representation of transfer matrices with antidiagonal BCs represented by triangular-shaped operator insertions.

108
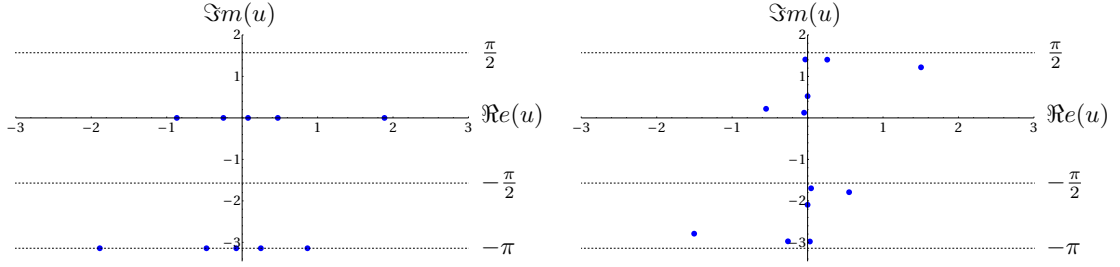
Figure 5.2: The left (right) plot displays the dual Bethe-root configuration for the regime I in the complex u-plane of the ground state for $2L = 10$, $(2L = 12)$, $\gamma = \pi/6$ and $\alpha = \pi/2$.

Note that we can compensate for the influence of this transformation on the Hamiltonian by adding an additional minus sign. The eigenvalue of the Q-operator will change under the transformation. This leads to the fact that there exist two interchangeable sets of Bethe roots describing the spectrum of $\mathbb{H}$. We have found that the root patterns of the duality-transformed roots are slightly more convenient for further study. Hence, we always use these 'dual' root configurations in the following. Note that this phenomenon is special to antidiagonal BCs due to the factor of $\frac{1}{2}$ in the hyperbolic functions on the LHS of (2.153). For twisted BCs the BAE are left invariant under the transformation see (2.136).

In the following, we study the low energy spectrum of the lattice theory in the limit of infinite system size to extract information about the effective field theory arising in its scaling limit. We investigate two regimes given by

- Regime I: $\quad \gamma < \alpha < \pi - \gamma$.

- Regime II: $\quad \gamma > \alpha > \pi - \gamma$.

5.1 REGIME I

For regime I, we find that the analysis of small system sizes, which is used to formulate a Bethe hypothesis for the ground state and the low energy excitations, is problematic. Namely, it is plagued by level crossings and the appearance of complex energies when the anisotropy γ or system size L is changed. Hence, from the study of small system sizes $L \sim 6$ one cannot obtain reliable support for a Bethe hypothesis, e.g. see Figure 5.2 for the drastic change in the root configurations for the ground state from $L = 5$ to $L = 6$ and Figure 5.3 for the appearance of complex energies under the variation of the anisotropy. By using parallel computing on a compute cluster, we have pushed our results from direct diagonalization to intermediate system sizes $2L \leq 28$ to study these crossings. By considering their behaviour, we conjecture that the bulk part of the Bethe roots should align on the following four lines in the thermodynamic limit $(x_k, y_k, z_k \in \mathbb{R})$

$$u_k^{(1)} = x_k \,, \qquad u_k^{(2)} = y_k - \mathrm{i}\pi \,, \qquad u_k^{(3)} = z_k \pm \frac{\mathrm{i}\pi}{2} \,. \tag{5.5}$$

Note that the third 'type of roots' are two-strings. By inserting the above form of roots into the logarithmic form of the Bethe equations, we obtain the following counting functions for
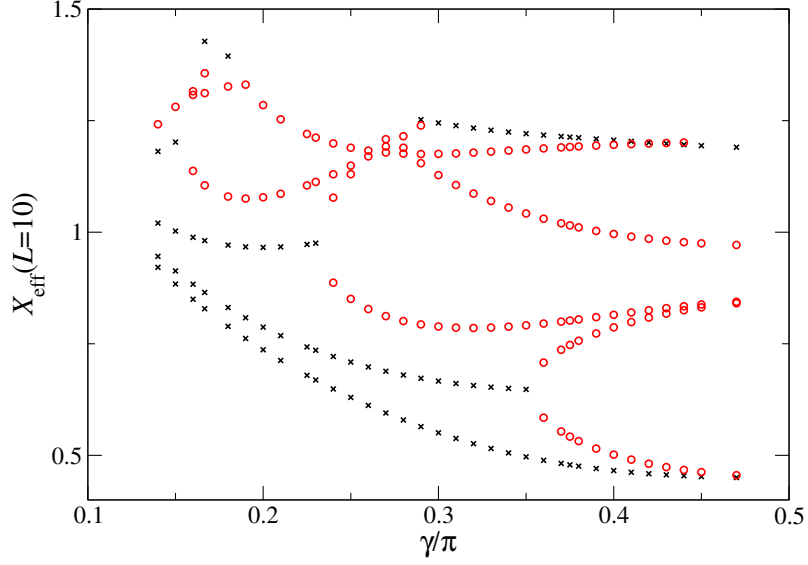
Figure 5.3: Lowest finite size estimate of the scaling dimensions in regime I: While the red circles are derived from the lowest real energies for $L = 10$, i.e. 20 lattice sites, the black crosses resemble the real part of complex eigenvalues.

real parts x_k, y_k and z_k

$$c^x(x) = -L\,\psi(x, \tfrac{\alpha-\gamma}{2}) + L\,\psi\left(x, \tfrac{\alpha+\gamma}{2}\right) - \sum_{m=1}^{M_x} \psi\left(\tfrac{1}{2}(x - x_m), \tfrac{\gamma}{2}\right)$$

$$+ \sum_{m=1}^{M_y} \phi\left(\tfrac{1}{2}(x - y_m), \tfrac{\gamma}{2}\right) - \sum_{m=1}^{M_z} \psi\left(x - z_m, \gamma\right),$$

$$c^y(x) = -L\,\psi(x, \tfrac{\alpha-\gamma}{2}) + L\,\psi\left(x, \tfrac{\alpha+\gamma}{2}\right) + \sum_{m=1}^{M_x} \phi\left(\tfrac{1}{2}(x - x_m), \tfrac{\gamma}{2}\right)$$

$$- \sum_{m=1}^{M_y} \psi\left(\tfrac{1}{2}(x - y_m), \tfrac{\gamma}{2}\right) - \sum_{m=1}^{M_z} \psi\left(x - z_m, \gamma\right),$$

$$c^z(x) = -L\,\psi(x, \tfrac{\alpha-\gamma}{2}) + L\,\psi\left(x, \tfrac{\alpha+\gamma}{2}\right) - \sum_{m=1}^{M_x} \psi\left(\tfrac{1}{2}(x - x_m), \tfrac{\gamma}{2}\right)$$

$$+ \sum_{m=1}^{M_y} \phi\left(\tfrac{1}{2}(x - y_m), \tfrac{\gamma}{2}\right) - \sum_{m=1}^{M_z} \psi\left(x - z_m, \gamma\right). \tag{5.6}$$

In terms of these, the Bethe equations become

$$c^x(x_k) = 2\pi I_k^x, \quad c^y(y_k) = 2\pi I_k^y, \quad c^z(z_k) = 2\pi I_k^z. \tag{5.7}$$

In the above formula, the numbers of roots are constrained to sum up to $2L$, and we recall (4.44). The corresponding root densities — defined as usual as the derivative of the counting functions — resemble the bulk densities given in (4.48): the density of the real centres of the two-strings is given by σ^y, the densities of the real parts of the type one $u^{(1)}$ and type
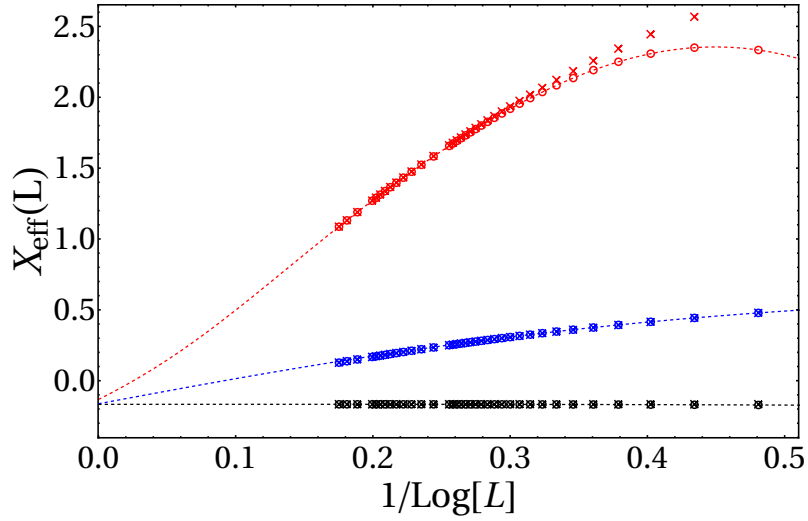
Figure 5.4: The circles display the finite-size estimates of effective scaling dimensions obtained from the energies of the states whose Bethe roots solve (5.7) for a symmetric filling and imbalances of the numbers of two-strings: 0 (black), 2 (blue) and 4 (red). The crosses display the formula $-\frac{1}{6} - \frac{2\gamma b(L)^2}{\pi - 2\gamma}$ where $b(L)$ is calculated from the quasi-momentum operator. The dashed lines are a rational extrapolation. The anisotropy is given by $\gamma = \pi/6$, and the staggering parameter is $\alpha = \pi/2$.

two roots $u^{(2)}$ turns out to be the same as σ^x. Due to the latter fact, we expect that the type $u^{(1)}$ and $u^{(2)}$ roots combine in the thermodynamic limit into two-strings. Further, the energy density also turns out to be identical to the one given in (4.56). As the leading term in the energy expansion is not susceptible to BCs, the recovery of the bulk energy density is expected and supports the Bethe hypothesis formulated in (5.5).

Now, one may solve the logarithmic equations (5.7) directly. By considering a symmetric filling around zero of the Bethe integers I_k^i, we obtain that one can generate an infinite tower of excitations by disbalancing the numbers of two-strings. It seems that all of these states flow to the same scaling dimension in the limit $L \to \infty$, see Figure 5.4. For finite system sizes, this degeneracy is lifted by logarithmic corrections, which behave as $\sim \log(L)^{-2}$. As seen in the previous chapter, the quasi-momentum (5.3) parameterises these logarithmic corrections.

Despite the above underpinning evidence, the following problem arises: it seems that only states with non-symmetric Bethe integers I_k^x, I_k^y are realised on the lattice, e.g. see the shifted Bethe root configuration in Figure 5.2. We found in our analysis of small-to-intermediate system sizes no fully symmetric states of the type (5.5).

We have investigated the scaling behaviour of the realised states on the lattice, where the integers are unsymmetrical or shifted against each other, e.g. the ground state displayed in Figure 5.5 for $L = 8$ and its extension to $L = 100$. They all show logarithmic *increasing* or complex scaling dimensions see Figure 5.6. These two facts lead to a negative result. We have not been able to extract any information about the scaling limit in this regime. Based on this, we conclude that the antidiagonal BCs seem to be incompatible with the emergence of a non-compact degree of freedom.
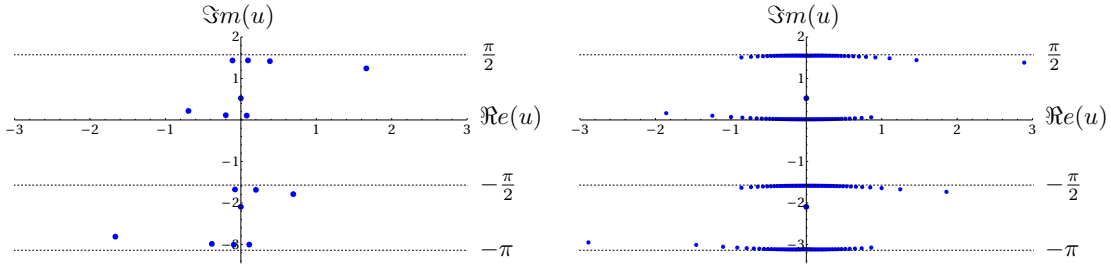
Figure 5.5: The left (right) plot displays the dual Bethe-root configuration for the regime I in the complex u-plane of the ground state for $2L = 16$ ($2L = 200$). Here, $\gamma = \pi/6$, $\alpha = \pi/2$.
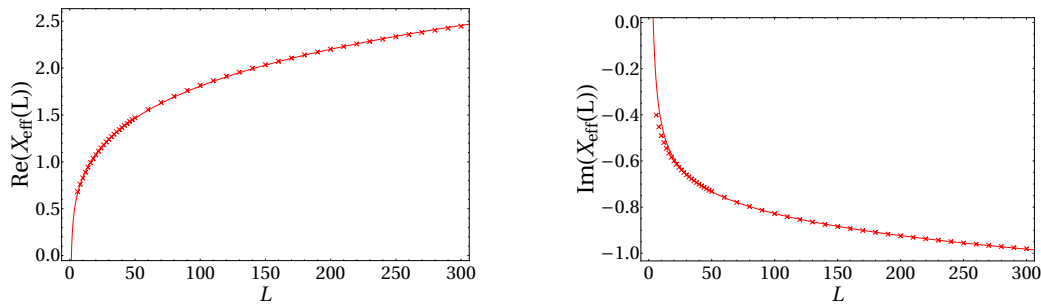
Figure 5.6: The left (right) plot displays the real (imaginary) part of the effective scaling dimensions of the ground state configuration displayed in Figure 5.5. The fits are chosen of the form $a_1 + a_2 \log^2(L) + a_3 L^{-1}$. The other parameters are $\gamma = \pi/6$ and $\alpha = \pi/2$.

5.2 REGIME II

In contrast to the previous parameter domain, in regime II, there are no ground state crossings with increasing system sizes. Thus, the study of small system sizes $L \geq 8$ provides reliable results about the root patterns of the low energy states. It is found that the Bethe roots for the ground state resemble the following pattern for even L:

$$u_k^{(1)} = x_k \pm \frac{\mathrm{i}(\pi + \alpha)}{2}, \qquad u_k^{(2)} = y_k \pm \frac{\mathrm{i}(\pi - \alpha)}{2} \qquad k = 1, \ldots, L - 1 \qquad (5.8)$$

plus two additional roots on the real axis. Excitations above the ground state are generated by removing roots from the lines of the ground state pattern and placing them in the complex plane either as single roots or as complexes such as strings. The Bethe root configuration of the ground state and for one excited state is depicted in the left and right panel of Figure 5.7 respectively.

Using the regular pattern of the ground state's Bethe roots, the energy density can be extracted via the root density approach. It is equal to that of the periodic case ([143])

$$e_\infty = -\frac{\sin(\gamma)}{\pi - \gamma} \int_{-\infty}^{\infty} \mathrm{d}x \, \frac{1}{\cosh(\frac{\pi x}{2\pi - 2\gamma})} \left(\frac{1}{\cosh(x) + \cos(\gamma)} + \frac{1}{\cosh(x - 2\mathrm{i}\alpha) + \cos(\gamma)} \right). \quad (5.9)$$
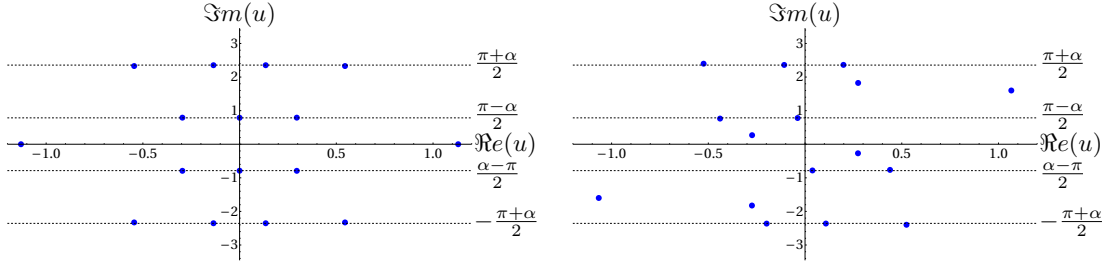
Figure 5.7: The left (right) plot displays the dual Bethe-root configuration for the regime II in the complex u-plane of the ground state (excited state) for $2L = 16$, $\gamma = 4\pi/6$ and $\alpha = \pi/2$.

The Fermi velocity is given by

$$v_{\mathrm{F}} = \frac{\pi}{\pi - \gamma}\,. \tag{5.10}$$

We find the following finite-size spectrum

$$X_{\mathrm{eff}}(k) = \frac{1}{12} + \frac{k}{2}, \qquad k = 0, 1, 2, \ldots \tag{5.11}$$

while the degeneracy $\deg(k)$ of an effective scaling dimension $X_{\mathrm{eff}}(k)$ is consistent with the generating function

$$\sum_{k=0}^{\infty} \deg(k)\, \mathsf{q}^{\frac{1}{12} + \frac{k}{2}} = \mathsf{q}^{\frac{1}{12}} \prod_{m=0}^{\infty} \left(1 - \mathsf{q}^{m+\frac{1}{2}}\right)^{-4}$$
$$= \mathsf{q}^{\frac{1}{12}} + 4\mathsf{q}^{\frac{7}{12}} + 10\mathsf{q}^{\frac{13}{12}} + 24\mathsf{q}^{\frac{23}{12}} + \ldots \tag{5.12}$$

5.2.1 Conjectured CFT

We propose that the scaling limit of the lattice in regime II is governed by a CFT constructed from two $U(1)$ twisted Kac-Moody algebras [144], leading to $c = 2$.

For two copies of the $U(1)$ twisted Kac-Moody algebra CFT, the zero mode of the Virasoro algebra takes the form [144]

$$L_0 = 2 \sum_{\mu \in \mathbb{N} + \frac{1}{2}} \mu\, a_\mu^\dagger\, a_\mu + 2 \sum_{\nu \in \mathbb{N} + \frac{1}{2}} \nu\, b_\nu^\dagger\, b_\nu + \frac{2}{16}\,. \tag{5.13}$$

Hereby, the operators a_m, b_m with $m \in \mathbb{Z} + \frac{1}{2}$ form two independent Heisenberg algebras. In fact, all operators commute among each other except for

$$\left[a_k^\dagger, a_p\right] = \left[b_k^\dagger, b_p\right] = \frac{k}{2}\, \delta_{k,p}\,. \tag{5.14}$$

The space of states can then be described as a Fock space (see discussion around (2.40)) originating from one vacuum with weight $\frac{2}{16}$. After taking the other chirality into account,

the degeneracy of each Fock space level is given by (5.12). One can also decompose the Fock Space into a direct sum of representations of the Virasoro algebra as presented in [144].

Further, we have checked consistency with the results of the homogeneous chain [145], which is described by one $U(1)$ twisted Kac-Moody algebra. In [145], it was found (see equation (16) therein) that the energy levels of the lattice have fixed combinations of the eigenvalues of the operators $\mathbb{C}^{\text{hom}}, \mathbb{G}^{\text{hom}}$. For the case at hand, the splitting of the Hilbert space in the eigenvalues of the symmetry operators $\mathbb{C}$, $\mathbb{G}$ is consistent with the results of a homogeneous chain in the following way: consider a lattice state which flows to a conformal state. The corresponding conformal weight can be split into two weights, each corresponding to one weight of the homogeneous chain. We can identify the corresponding eigenvalues of $\mathbb{C}^{\text{hom}}$ and $\mathbb{G}^{\text{hom}}$ with the help of equation (16) in [145]. The eigenvalues of $\mathbb{C}$, $\mathbb{G}$ are then obtained by simply taking the product for the corresponding eigenvalues $\mathbb{C}^{\text{hom}}, \mathbb{G}^{\text{hom}}$ for the two copies of the homogeneous chain. So we conclude that the staggering is, in this regime, an irrelevant deformation of the homogeneous case up to doubling of the underlying CFT.

5.3 Chapter summary

In this chapter, we have studied the influence of the antidiagonal BCs on the staggered six-vertex model. The antidiagonal BCs reduce the symmetry of the model to two discrete symmetries given by (5.1). We have investigated two parametric domains.

In the first one, in which for the case of twisted [54] or $U_q(\mathfrak{sl}(2))$ invariant BCs, a continuous component in the spectrum of scaling dimensions has been identified, we could not obtain any insights about the model's scaling limit. This is due to complex and logarithmically *divergent* — even for the ground state — effective scaling dimensions. We conclude that this phase is incompatible with antidiagonal BCs.

For the second regime, we conjecture that the CFT governing the scaling limit is constructed from two $U(1)$ twisted Kac-Moody algebras. We have checked compatibility with the homogeneous model by the discrete $\mathbb{Z}_2$ symmetries.

6 | To higher rank: $D_3^{(2)}$

This chapter is based on the author's work [33].

Let us one last time recall the composite $\mathcal{R}$ matrix given in (3.1). Depending on the choice of the parameters, the $\mathcal{R}$-matrix may have an extended symmetry; for instance, this might be the case at the self-dual point (3.28). This has been discussed recently in the work [26] in which it has been shown that the antiferromagnetic Potts model — in particular with open BCs — can be mapped to an integrable model based on the affine $D_2^{(2)}$ Lie algebra. The homogeneous transfer matrix of the latter has been shown [113] to factorize — the same way as presented in chapter 3 — into the self-dual staggered six-vertex model[1], see also [22]. Such a factorization is not known for the higher-rank models based on $D_n^{(2)}$. Nevertheless, obvious questions to ask are whether these, too, give rise to a series of non-compact CFTs; what is the number of compact and non-compact degrees of freedom; and finally, what is the operator content of the CFTs describing the low energy spectrum in the scaling limit.

In this chapter, we investigate this question for the simplest case beyond the staggered six-vertex model, i.e. the $D_3^{(2)}$ spin chain. The chapter is organised as follows: in section 6.1 we construct the transfer matrix of the model subject to generic diagonal twisted BCs. Also, we identify some of its symmetries. Generalising the analytical Bethe ansatz for the periodic case [146], we obtain the eigenvalues of the transfer matrix and the resulting Hamiltonian with local, i.e. nearest-neighbour interactions. In section 6.4, we identify the root configurations of the low-lying states. This is used in section 6.5 to compute the ground state energy density in the thermodynamic limit and in section 6.6 to construct the renormalisation group trajectories for the ground state and excitations used in the finite-size scaling analysis of the spectrum. We find compact and non-compact parts in the spectrum of conformal dimensions. The flow of the compact modes under the twist resembles that of two compact bosons with compactification radii depending on the anisotropy. In addition, we observe the emergence of discrete states from the continuous parts of the spectrum of conformal weights for sufficiently large twists.

---

[1]In this context the boundary matrices (3.25), (3.34) are different representations [117, 118, 111] of the corresponding $D_2^{(2)}$ reflection algebra.

6.1 THE $D_3^{(2)}$ R-MATRIX

To make a connection to other works, we will face the following abuse of notation. We denote in the rest of this chapter by η^{cross} the crossing parameter as it is given in (2.104) and we set $4\eta = -\eta^{\text{cross}}$.

The basic ingredient of the $D_3^{(2)}$ integrable quantum spin chain is the 36×36 R-matrix obtained in [147]. We use the conventions of the work [118] given in equations (A.8-10). Namely, our R-matrix $\mathbb{R}(u)$ is related to the one of Jimbo $R_J(x)$ given in his work [147] by

$$\mathbb{R}(u) = \mathrm{e}^{-2u-6\eta} R_J(x), \qquad x = \mathrm{e}^u, \qquad k = \mathrm{e}^{2\eta}. \tag{6.1}$$

Using this normalisation, the standard characteristics (2.101)-(2.106) take the explicit form

$$\xi(u) = 4\sinh(u + 2\mathrm{i}\gamma)\sinh(u + 4\mathrm{i}\gamma), \qquad \eta^{\text{cross}} = -4\mathrm{i}\gamma, \qquad \mathtt{p} = \mathrm{i}\pi, \tag{6.2}$$

$$V = \begin{pmatrix} & & & & & \mathrm{e}^{-3\mathrm{i}\gamma} \\ & & & & \mathrm{e}^{-\mathrm{i}\gamma} & \\ & & & 1 & & \\ & & 1 & & & \\ & \mathrm{e}^{\mathrm{i}\gamma} & & & & \\ \mathrm{e}^{3\mathrm{i}\gamma} & & & & & \end{pmatrix}, \qquad U = \begin{pmatrix} 1 & & & & \\ & 1 & & & \\ & & 0 & 1 & \\ & & 1 & 0 & \\ & & & & 1 \\ & & & & & 1 \end{pmatrix}. \tag{6.3}$$

where we used $\eta = \mathrm{i}\gamma$. In addition, we have a positive sign in (2.106).

The R-matrix possesses two continuous $U(1)$ symmetries

$$[\mathbb{R}(u), (\mathbb{h}_j \otimes \mathbf{1} + \mathbf{1} \otimes \mathbb{h}_j)] = 0, \qquad j = 1, 2, \tag{6.4}$$

where we have

$$\mathbb{h}_1 = e^{(1,1)} - e^{(6,6)}, \qquad \mathbb{h}_2 = e^{(2,2)} - e^{(5,5)}, \tag{6.5}$$

and $e^{(k,l)}$ stands for the elementary 6×6 matrices with vanishing entries except for the one at position (k, l) where it is 1. Further, we have the additional $\mathbb{Z}_2$ symmetry:

$$\mathbb{R}_{12}(u) = W_1(u)\, W_2(0)\, \mathbb{R}_{12}(u)\, W_1(u)\, W_2(0), \qquad W(u) = \begin{pmatrix} & & & & \mathrm{e}^{-u} & \\ & & & & & -\mathrm{e}^{-u} \\ & & 1 & & & \\ & & & -1 & & \\ \mathrm{e}^{u} & & & & & \\ & -\mathrm{e}^{u} & & & & \end{pmatrix}. \tag{6.6}$$

Note that we have $V^2 = U^2 = W(u)^2 = \mathbf{1}$. Moreover, by exponenting (6.5) we obtain a diagonal twist matrix $\mathbb{K}$

$$\varpi = \mathrm{e}^{\sum_{j=1}^2 \mathrm{i}\phi_j\, \mathbb{h}_j} = \mathrm{diag}\left(\mathrm{e}^{\mathrm{i}\phi_1}, \mathrm{e}^{\mathrm{i}\phi_2}, 1, 1, \mathrm{e}^{-\mathrm{i}\phi_2}, \mathrm{e}^{-\mathrm{i}\phi_1}\right), \tag{6.7}$$

where ϕ_1 and ϕ_2 are the twist parameters. In the following, we only consider $\phi_{1,2} \in \mathbb{R}$. We consider the homogeneous transfer matrix $\mathtt{t}(u)$ with BCs controlled by (6.7) of length L, i.e.

$$\mathtt{t}(u) := \mathrm{tr}_0\left(\varpi_0\, \mathbb{R}_{0L}(u) \ldots \mathbb{R}_{01}(u)\right). \tag{6.8}$$

Recall from the preliminaries that the $U(1)$ symmetries (6.4) induce the following symmetries of the transfer matrix

$$\left[\mathtt{t}(u), \mathbb{h}_j^{(L)}\right] = 0, \qquad j = 1, 2, \tag{6.9}$$

where[2]

$$\mathbb{h}_j^{(L)} = \sum_{i=1}^{L} (\mathbb{h}_j)_i \,, \tag{6.10}$$

and $(\mathbb{h}_j)_i$ is the generator $\mathbb{h}_j$ (6.5) at the lattice site i, i.e.

$$(\mathbb{h}_j)_i = \mathbf{1} \otimes \cdots \otimes \mathbf{1} \otimes \underbrace{\mathbb{h}_j}_{i} \otimes \mathbf{1} \otimes \cdots \otimes \mathbf{1} \,. \tag{6.11}$$

By similar arguments, it follows that

$$\mathbb{t}^t(u; \{\phi_j\}) = \mathbb{t}(4\mathrm{i}\gamma - u; \{-\phi_j\}) \,, \tag{6.12}$$

$$\mathbb{t}(u + \mathrm{i}\pi) = \mathbb{t}(u) \,, \tag{6.13}$$

$$\mathbb{t}(u) = U^{\otimes L} \, \mathbb{t}(u) \, U^{\otimes L} \,. \tag{6.14}$$

We mention here that the $\mathbb{Z}_2$ symmetry (6.14) resembles a generalisation of the $\mathbb{Z}_2$ symmetry identified[3] for $D_2^{(2)}$ [20, 26, 106]. In addition, for generic values of the twist parameter ϕ_1, ϕ_2, one can derive the following identity

$$W(0)^{\otimes L} \, \mathbb{t}(u; \phi_1, \phi_2) \, W(0)^{\otimes L} = \mathbb{t}(u; -\phi_2, -\phi_1) \,. \tag{6.15}$$

Hence, if the twist angles are the additive inverse of each other, i.e. $\phi_1 = -\phi_2$, the transfer matrix (6.8) possesses the extra $\mathbb{Z}_2$ symmetry

$$W(0)^{\otimes L} \, \mathbb{t}(u; \phi, -\phi) \, W(0)^{\otimes L} = \mathbb{t}(u; \phi, -\phi) \,. \tag{6.16}$$

Finally, the transfer matrix is the CPT invariant

$$V^{\otimes L} \, \Pi \, \mathbb{t}^t(u; \{-\phi_j\}) \, \Pi \, V^{\otimes L} = \mathbb{t}(u; \{\phi_j\}) \,, \tag{6.17}$$

where the so-called parity operator Π reads

$$\Pi = \prod_{i=1}^{\lfloor \frac{L}{2} \rfloor} P_{i,L+1-i} \,. \tag{6.18}$$

Its conjugate action on any local operator X_j yields $\Pi \, X_j \, \Pi = X_{L+1-j}$. Proofs of the symmetries (6.12), (6.15) and (6.17) are sketched in appendix F.

---

[2]By abuse of notation, we will abbreviate $\mathbb{h}_j^{(L)}$ as $\mathbb{h}_j$ if the meaning is evident from the context.

[3]In [106], the $\mathbb{Z}_2$ symmetry of the periodic transfer matrix built from the R-matrix of the twisted affine Lie algebra $D_2^{(2)}$ is expressed, see (3.32) therein, in terms of an operator built from a matrix C (2.10), in the gauge that is specified by a matrix B (2.9), where

$$B\,C\,B = \begin{pmatrix} & & 1 \\ & \begin{smallmatrix} 0 & 1 \\ 1 & 0 \end{smallmatrix} & \\ 1 & & \end{pmatrix} \,,$$

which is clearly the lower rank case of the matrix U in (6.3).

6.2 BETHE ANSATZ

The periodic transfer matrix (6.8) with ($\phi_1 = \phi_2 = 0$) has been diagonalised by means of the analytical Bethe ansatz in the work [146]. The generalisation to the case of non-vanishing twist angles is given in appendix E. Our conventions of the Bethe-roots are related to the ones given in [146] by

$$u_j^{[1]} = 2\mathrm{i}x_j\,, \qquad u_j^{[2]} = 2\mathrm{i}y_j\,. \tag{6.19}$$

Using this convention, the eigenvalues $t(u)$ of the transfer matrix read

$$
\begin{aligned}
t(u) = {}& (4\sinh(u - 2\mathrm{i}\gamma)\sinh(u - 4\mathrm{i}\gamma))^L\, \mathrm{e}^{\mathrm{i}\phi_1}\, A(u) \\
& + (4\sinh(u - 4\mathrm{i}\gamma)\sinh u)^L \left[\mathrm{e}^{\mathrm{i}\phi_2}\, B_1(u) + B_2(u) + B_3(u) + \mathrm{e}^{-\mathrm{i}\phi_2}\, B_4(u) \right] \\
& + (4\sinh(u - 2\mathrm{i}\gamma)\sinh u)^L\, \mathrm{e}^{-\mathrm{i}\phi_1}\, C(u)\,,
\end{aligned}
\tag{6.20}
$$

where we have introduced the functions

$$
\begin{aligned}
A(u) &= \prod_{j=1}^{m_1} \frac{\sinh(u - u_j^{[1]} + \mathrm{i}\gamma)}{\sinh(u - u_j^{[1]} - \mathrm{i}\gamma)}\,, \\
B_1(u) &= \prod_{j=1}^{m_1} \frac{\sinh(u - u_j^{[1]} - 3\mathrm{i}\gamma)}{\sinh(u - u_j^{[1]} - \mathrm{i}\gamma)} \prod_{j=1}^{m_2} \frac{\sinh(u - u_j^{[2]})}{\sinh(u - u_j^{[2]} - 2\mathrm{i}\gamma)}\,, \\
B_2(u) &= \prod_{j=1}^{m_2} \frac{2\cosh\left(\frac{1}{2}\left(u - u_j^{[2]}\right)\right)\sinh\left(\frac{1}{2}\left(u - u_j^{[2]} - 4\mathrm{i}\gamma\right)\right)}{\sinh(u - u_j^{[2]} - 2\mathrm{i}\gamma)}\,, \\
C(u) &= \bar{A}(4\mathrm{i}\gamma - u)\,, \qquad B_3(u) = \bar{B}_2(4\mathrm{i}\gamma - u)\,, \qquad B_4(u) = \bar{B}_1(4\mathrm{i}\gamma - u)\,,
\end{aligned}
\tag{6.21}
$$

and where the barred quantities are obtained by the negation $u_j^{[l]} \mapsto -u_j^{[l]}$. Note that the bar resembles the complex conjugation *provided* u and $\eta = \mathrm{i}\gamma$ are real. In addition, if the latter condition is satisfied, the periodic transfer-matrix eigenvalue has the crossing symmetry

$$\bar{t}(u) = t(4\mathrm{i}\gamma - u)\,. \tag{6.22}$$

The same holds true in the XXZ model [148]. In general, (6.20) is periodic, i.e. $t(u + \mathrm{i}\pi) = t(u)$, see (6.13).

The eigenvalue $t(u)$ of the transfer matrix must be a Fourier polynomial and so an analytic function. Requiring that the residues of (6.20) at the apparent poles

$$u = u_j^{[1]} + \mathrm{i}\gamma\,, \qquad u = u_j^{[2]} + 2\mathrm{i}\gamma \tag{6.23}$$

vanish, yields the BAE (see also [146, 149])

$$
\left(\frac{\sinh\left(u_j^{[1]} - \mathrm{i}\gamma\right)}{\sinh\left(u_j^{[1]} + \mathrm{i}\gamma\right)}\right)^L = \mathrm{e}^{\mathrm{i}(\phi_2 - \phi_1)} \prod_{k \neq j}^{m_1} \frac{\sinh\left(u_j^{[1]} - u_k^{[1]} - 2\mathrm{i}\gamma\right)}{\sinh\left(u_j^{[1]} - u_k^{[1]} + 2\mathrm{i}\gamma\right)} \prod_{k=1}^{m_2} \frac{\sinh\left(u_j^{[1]} - u_k^{[2]} + \mathrm{i}\gamma\right)}{\sinh\left(u_j^{[1]} - u_k^{[2]} - \mathrm{i}\gamma\right)},
$$
$$
j = 1, \ldots, m_1,
$$
$$
\prod_{k=1}^{m_1} \frac{\sinh\left(u_j^{[2]} - u_k^{[1]} - \mathrm{i}\gamma\right)}{\sinh\left(u_j^{[2]} - u_k^{[1]} + \mathrm{i}\gamma\right)} = \mathrm{e}^{-\mathrm{i}\phi_2} \prod_{k \neq j}^{m_2} \frac{\sinh\frac{1}{2}\left(u_j^{[2]} - u_k^{[2]} - 2\mathrm{i}\gamma\right)}{\sinh\frac{1}{2}\left(u_j^{[2]} - u_k^{[2]} + 2\mathrm{i}\gamma\right)}, \quad j = 1, \ldots, m_2.
$$
$$(6.24)$$

As the BAE are invariant under the transformations $u_j^{[1]} \to u_j^{[1]} + \mathrm{i}\pi$ and $u_j^{[2]} \to u_j^{[2]} + 2\mathrm{i}\pi$, we can restrict ourselves to

$$
-\frac{\pi}{2} < \Im m(u_j^{[1]}) \leq \frac{\pi}{2}, \tag{6.25}
$$

$$
-\pi < \Im m(u_j^{[2]}) \leq \pi. \tag{6.26}
$$

Further, we are also allowed to do the mapping $u_j^{[2]} \to u_j^{[2]} + \mathrm{i}\pi$, but only if we shift *all* the Bethe-roots at the same time.

The eigenvalues h_j of the $U(1)$ charges $\mathbb{h}_j$ are related to the numbers m_1, m_2 of Bethe roots by [146]

$$
\begin{aligned}
h_1 &= L - m_1, \\
h_2 &= m_1 - m_2.
\end{aligned} \tag{6.27}
$$

As usual, the Bethe ansatz provides solutions subject to the restriction

$$
L \geq m_1 \geq m_2 \geq 0. \tag{6.28}
$$

Although an algebraic Bethe ansatz has not yet been worked out in detail, we expect that the eigenstates $|u_1^{[1]}, \ldots, u_{m_1}^{[1]}; u_1^{[2]}, \ldots, u_{m_2}^{[2]}\rangle$ of the $D_3^{(2)}$ transfer matrix (6.8) can be constructed as follows: the first level of nesting (introducing type-1 Bethe roots $u_1^{[1]}, \ldots, u_{m_1}^{[1]}$) can be accomplished following the work [150], reducing the problem to $D_2^{(2)}$. The transfer matrix for the latter factorises in a product of $A_1^{(1)}$ transfer matrices (see the construction of chapter 3 and also [106]). The latter can then be diagonalised by the usual algebraic Bethe ansatz, which leads to the type-2 Bethe roots $u_1^{[2]}, \ldots, u_{m_2}^{[2]}$. Hence, it is expected (see also (3.34) in [106] of the $D_2^{(2)}$ case) that the $\mathbb{Z}_2$ symmetry (6.14) leads to a global shift of all type-2 Bethe roots by $\mathrm{i}\pi$:

$$
U^{\otimes L} |u_1^{[1]}, \ldots, u_{m_1}^{[1]}; u_1^{[2]}, \ldots, u_{m_2}^{[2]}\rangle \propto |u_1^{[1]}, \ldots, u_{m_1}^{[1]}; u_1^{[2]} + \mathrm{i}\pi, \ldots, u_{m_2}^{[2]} + \mathrm{i}\pi\rangle. \tag{6.29}
$$

6.3 THE $D_3^{(2)}$ HAMILTONIAN

Commuting integrals of motion for the $D_3^{(2)}$ spin chain are obtained by expanding the transfer matrix (6.8) about the regular point $u = 0$. The leading term is given by

$$\mathtt{t}(0) = (4 \sinh(2\mathrm{i}\gamma) \sinh(4\mathrm{i}\gamma))^L \, \mathrm{e}^{\mathrm{i}\,\mathbb{P}} , \qquad (6.30)$$

where $e^{\mathrm{i}\,\mathbb{P}}$ is the one-site translation operator of the model with twisted BCs. Its matrix elements read

$$\left[\mathrm{e}^{\mathrm{i}\,\mathbb{P}} \right]_{a_1, \dots, a_L}^{b_1, \dots, b_L} = \exp \left\{ \mathrm{i}\phi_1 \left(\delta_1^{b_1} - \delta_6^{b_1} \right) + \mathrm{i}\phi_2 \left(\delta_2^{b_1} - \delta_5^{b_1} \right) \right\} \delta_{a_1}^{b_2} \delta_{a_2}^{b_3} \dots \delta_{a_{L-1}}^{b_L} \delta_{a_L}^{b_1} . \qquad (6.31)$$

From (6.20) we deduce that its eigenvalue $\mathrm{e}^{\mathrm{i}P}$ is

$$\mathrm{e}^{\mathrm{i}\,P} = \mathrm{e}^{\mathrm{i}\phi_1} \prod_{k=1}^{m_1} \frac{\sinh(u_k^{[1]} - \mathrm{i}\gamma)}{\sinh(u_k^{[1]} + \mathrm{i}\gamma)} . \qquad (6.32)$$

A local Hamiltonian of the $D_3^{(2)}$ spin chain can be defined as the next leading term[4]

$$\mathbb{H} = \sinh(2\mathrm{i}\gamma) \frac{\mathrm{d}}{\mathrm{d}u} \log\left(\mathtt{t}(u) \right) \Big|_{u=0} + L \sinh(2\mathrm{i}\gamma) \left[\coth(2\mathrm{i}\gamma) + \coth(4\mathrm{i}\gamma) \right] \mathbf{1}^{\otimes L} . \qquad (6.33)$$

The energies can be expressed in terms of the Bethe roots:

$$E = \sum_{k=1}^{m_1} \epsilon_0(u_k^{[1]}) = -\sum_{k=1}^{m_1} \frac{2\sinh^2(2\mathrm{i}\gamma)}{\cosh\left(2u_k^{[1]} \right) - \cosh\left(2\mathrm{i}\gamma \right)} . \qquad (6.34)$$

The Hamiltonian of course inherits the symmetry properties (6.9), (6.14), (6.16) of the transfer matrix

$$[\mathbb{H}, \mathbb{h}_j] = 0, \qquad j = 1, 2, \qquad (6.35)$$

$$\left[\mathbb{H}, U^{\otimes L} \right] = 0, \qquad (6.36)$$

$$\left[\mathbb{H}(\phi, -\phi), W(0)^{\otimes L} \right] = 0. \qquad (6.37)$$

In addition, the Hamiltonian also has a CP symmetry, i.e.

$$\left[\mathbb{H}, V^{\otimes L} \Pi \right] = 0. \qquad (6.38)$$

For details, see appendix F. We stress that this symmetry does *not* extend to the full transfer matrix.

The commutator of the $U(1)$ generators with the ones of the $\mathbb{Z}_2$ symmetry given in (6.14) is zero:

$$\left[\mathbb{h}_j, U^{\otimes L} \right] = 0, \qquad j = 1, 2. \qquad (6.39)$$

---

[4] With this sign the Hamiltonian generalizes the $D_2^{(2)}$ spin chain, which has been related to the antiferromagnetic Potts model [26] or respectively the corresponding staggered-six vertex model [106, 31].

The $U(1)$ generators transform into each other under the transformation $W(0)$ (6.6)

$$W(0)^{\otimes L}\, \mathbb{h}_1\, W(0)^{\otimes L} = -\mathbb{h}_2\,,$$
$$W(0)^{\otimes L}\, \mathbb{h}_2\, W(0)^{\otimes L} = -\mathbb{h}_1\,. \tag{6.40}$$

Under the CP symmetry, the $U(1)$ generators change sign

$$V^{\otimes L}\, \Pi\, \mathbb{h}_j\, \Pi\, V^{\otimes L} = -\mathbb{h}_j\,, \qquad j = 1\,,2\,. \tag{6.41}$$

The symmetry transformations (6.37) together with (6.38) induce degeneracies in the energy spectrum between different sectors of the $U(1)$-charges. For the analysis of the finite-size spectrum, it is sufficient to focus on one representative of a given energy level, keeping these degeneracies implicit. The symmetries (6.37), (6.38) allow one to restrict to the case $h_1 \geq |h_2|$ for suitably chosen twist angles. In addition, we found by exact diagonalization of the Hamiltonian for small system sizes that one can further restrict to

$$0 \leq h_2 \leq h_1\,. \tag{6.42}$$

Note that all the sectors specified by (6.42) can be accessed by the above Bethe ansatz; see (6.28) and (6.27). Further, we should stress that the defined Hamiltonian is non-Hermitian, which leads to complex eigenvalues. On numerical grounds, however, we find that the energies of the ground state and lowest excitations are real. In the rest of this work, we study states parameterized by the classes of Bethe root configurations listed in the following section. These states, too, turn out to have real energies.

6.4 CONSIDERED CLASS OF STATES

In the regime

$$0 < \gamma < \tfrac{\pi}{4} \tag{6.43}$$

and for small twist angles $\phi_{1,2}$, we found that the bulk of the Bethe root configurations corresponding to low energy states consists of four-strings, each containing a pair of conjugate roots on both levels centred at real x_j:

$$
\begin{aligned}
u^{[1]} &\longrightarrow & v_j^{[1]} &= x_j + \delta_j^{[1]} + \frac{\mathrm{i}\pi}{2} - \mathrm{i}\gamma - \mathrm{i}\epsilon_j^{[1]}\,, & \bar{v}_j^{[1]} &= x_j + \delta_j^{[1]} - \frac{\mathrm{i}\pi}{2} + \mathrm{i}\gamma + \mathrm{i}\epsilon_j^{[1]}\,, \\
u^{[2]} &\longrightarrow & v_j^{[2]} &= x_j + \delta_j^{[2]} + \frac{\mathrm{i}\pi}{2} + \mathrm{i}\epsilon_j^{[2]}\,, & \bar{v}_j^{[2]} &= x_j + \delta_j^{[2]} - \frac{\mathrm{i}\pi}{2} - \mathrm{i}\epsilon_j^{[2]}\,,
\end{aligned}
\tag{6.44}
$$

where $j \leq \frac{L}{2}$ and $\delta_j^{[k]}, \epsilon_j^{[k]}$ are small real deviations. For even system sizes, the ground state of the system is realised in the sector $h_1 = h_2 = 0$ with $\epsilon_j^{[2]} \equiv 0$. See Figure 6.1 for the ground state of the $L = 18$ chain. The low-energy spectrum is described by various root configurations. In this work, we focus on a particular class of states described by the following additional roots outside these four-string configurations:

i) Level-1 roots placed on the line $\frac{\mathrm{i}\pi}{2}$,

ii) Level-2 roots placed on the line $\mathrm{i}\pi$,

iii) Level-2 roots placed on the real line,

subject to the constraint (6.28).
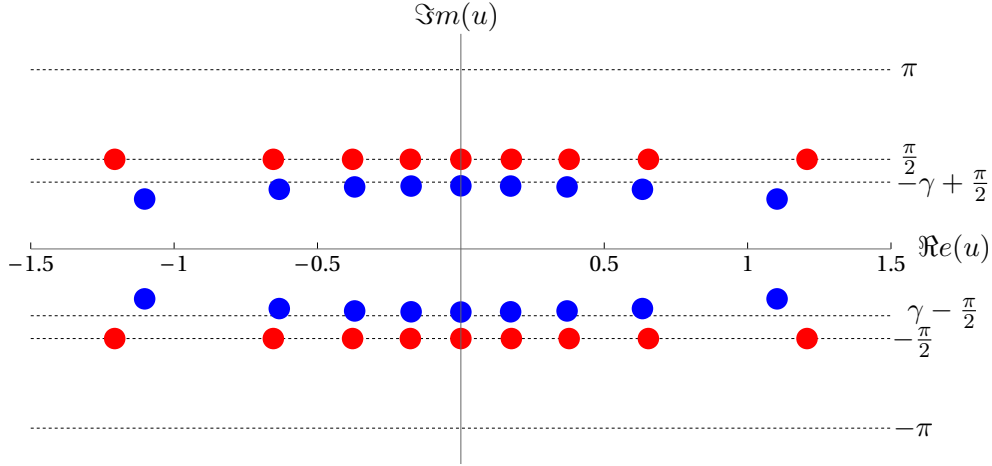
Figure 6.1: Bethe root configuration of the ground state for $L = 18$ and $\gamma = 0.4$ plotted in the complex u-plane. Blue (red) symbols denote level 1 (2) roots. One can clearly see the pattern described in (6.44).

6.5 ROOT DENSITY APPROACH FOR THE GROUND STATE

For even L, the ground state is parameterized by roots arranged in the configuration (6.44) where j runs from one to $\frac{L}{2}$ and $\epsilon_j^{[2]}$ is set to zero. Further, we find numerically that the remaining deviations $\delta_j^{[k]}, \epsilon_j^{[1]}$ in (6.44) tend to zero as $L \to \infty$. Hence, we can study the ground state in the root density approach as discussed in the preliminaries. By inserting (6.44) into the Bethe equations and taking the logarithm, one obtains the following counting function for the real centres:

$$z^x(x) = \frac{1}{2\pi}\psi(x, 2\gamma) + \frac{1}{2\pi L}\sum_{k=1}^{\frac{L}{2}} \chi(x - x_k, 4\gamma),\tag{6.45}$$

where again have

$$\chi(x,y) = 2\arctan\left(\tanh(x)\cot(y)\right), \quad \psi(x,y) = 2\arctan\left(\tanh(x)\tan(y)\right).\tag{6.46}$$

Upon differentiation, we obtain the following linear integral equation for the root density defined by $\rho^x(x) = \partial_x z^x(x)$:

$$\rho^x(x) = \frac{1}{2\pi}\psi'(x, 2\gamma) + \frac{1}{2\pi}\int_{-\infty}^{\infty} dx' \, \chi'(x - x', 4\gamma)\rho^x(x').\tag{6.47}$$

The equation is easily solved by the Fourier transform. It yields

$$\rho^x(x) = \frac{1}{2(\pi - 4\gamma)}\frac{1}{\cosh(\frac{\pi x}{\pi - 4\gamma})}.\tag{6.48}$$

The density is positive and becomes singular at $\gamma = \frac{\pi}{4}$, giving additional support to our choice of the parameter domain (6.43) for γ. Similarly, the *dressed* energy $\epsilon^x(x)$

of excitations corresponding to the removal of a four-string is obtained from the same linear integral equation as (6.47) but with the driving term ψ being replaced by $\epsilon_0^x(x) = \epsilon_0(x + \frac{i\pi}{2} - i\gamma) + \epsilon_0(x - \frac{i\pi}{2} + i\gamma)$, where ϵ_0 has been defined in (6.34). For γ in the domain (6.43), these excitations turn out to be gapless with a linear dispersion. The corresponding Fermi velocity is

$$v_{\mathrm{F}} = \frac{1}{2\pi} \lim_{\Lambda \to \infty} \frac{1}{\rho^x(\Lambda)} \frac{\mathrm{d}}{\mathrm{d}\Lambda} \epsilon^x(\Lambda) = \frac{\pi \sin(2\gamma)}{\pi - 4\gamma} \, . \tag{6.49}$$

Finally, using (6.48), we obtain the energy density e_∞ in the thermodynamic limit

$$e_\infty = -\frac{\sin(2\gamma)}{2} \int_{-\infty}^{\infty} \mathrm{d}\omega \, \frac{\sinh(2\gamma\omega)}{\sinh\left(\frac{\pi\omega}{2}\right)} \frac{1}{\cosh(\frac{1}{2}(\pi - 4\gamma)\omega)} \, . \tag{6.50}$$

6.6 ANALYSIS OF THE FINITE-SIZE SPECTRUM

As the model is critical, the spectrum of low-energy excitations can be described within the framework of a conformal field theory. One can easily show that

$$\mathrm{e}^{\mathrm{i}\mathbb{P}L} = \exp\left\{2\mathrm{i}\pi\left(\mathbb{h}_1 \frac{\phi_1}{2\pi} + \mathbb{h}_2 \frac{\phi_2}{2\pi}\right)\right\} \, . \tag{6.51}$$

The relation (2.94), suggests

$$\Delta - \bar{\Delta} = h_1 \frac{\phi_1}{2\pi} + h_2 \frac{\phi_2}{2\pi} \mod 1 \, . \tag{6.52}$$

To proceed further in our analysis, we rely on numerical methods, the results of which we present in the following sections.

6.6.1 COMPACT PART

In this section, we investigate two classes of fundamental excitation patterns. In terms of the Bethe roots, the first class is simply built from configurations following the structure (6.44) but with a non-zero h_1 in contrast to the ground state. Here, the eigenvalue h_2 of the $U(1)$-charge $\mathbb{h}_2$ is kept the same as for the ground state, i.e. $h_2 = 0$. See Figure 6.2 for an illustration.

The second class of excitations gives h_2 a non-vanishing value. This is accomplished on the level of the Bethe roots by mechanism i), i.e. by placing additional level-1 roots on the line $\frac{i\pi}{2}$. We have illustrated this type of excitation in Figure 6.3.

We start our numerical analysis by investigating the scaling behaviour of the ground state energy E_0. We obtain[5]

$$c_{\mathrm{eff}} = 4 \, . \tag{6.53}$$

Further, for periodic BCs $\phi_{1,2} = 0$, we have constructed the RG trajectories for various excited states based on the mechanisms discussed above. Exemplary plots of the numerical

---

[5]Recall the definition of the effective central charge $c_{\mathrm{eff}} = -\lim_{L \to \infty} \frac{6L}{\pi v_{\mathrm{F}}}(E_0 - Le_\infty)$
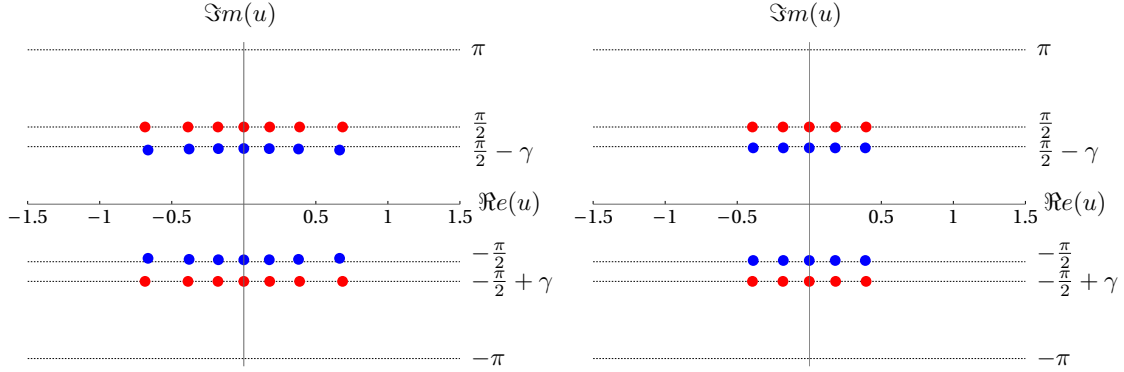
Figure 6.2: The left (right) plot displays the Bethe-root configuration in the complex u-plane of an excited state for $L = 18$, $\gamma = 0.4$, $\phi_{1,2} = 0$ in the sector $h_1 = 4$ (8). The blue (red) symbols denote level 1 (2) roots. This excitation corresponds to removing 2 (4) four-strings from the configuration of the ground state; see Figure 6.1.
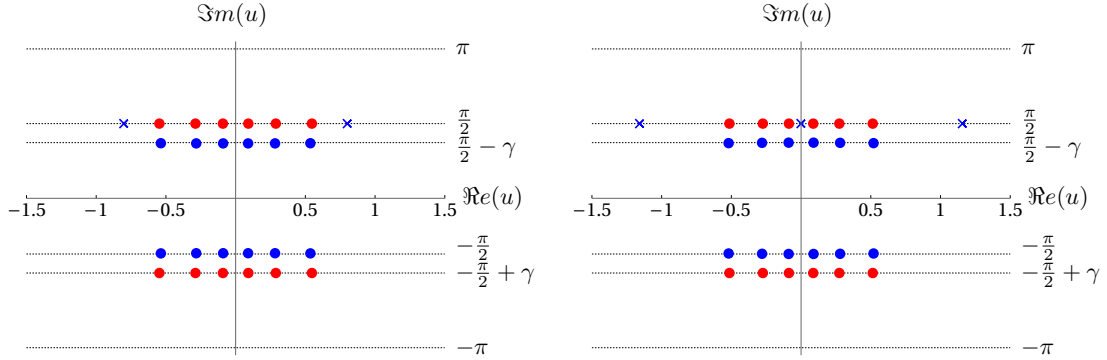

Figure 6.3: The left (right) plot displays the Bethe-root configuration in the complex plane of an excited state for $L = 18$, (19), $\gamma = 0.4$, $\phi_{1,2} = 0$ in the sector $h_1 = 4$ and $h_2 = 2$, (3). The blue (red) symbols denote level 1 (2) roots. This excitation is built by placing 2(3) level-1 roots ($\times$) on the line $\frac{\mathrm{i}\pi}{2}$ in addition to the bulk roots ($\bullet$).

data for finite L calculated by the Bethe ansatz and their extrapolations to $L \to \infty$ are given in Figure 6.4-6.5. Here, the extrapolation procedure is based on the assumption that the effective scaling dimensions are rational functions of $\frac{1}{\log(L)}$. We conclude that they flow to the following effective scaling dimensions:

$$X_{\mathrm{eff}}^{\mathrm{Com}} = -\frac{4}{12} + \frac{(h_1)^2}{2k} + \frac{(h_2)^2}{2k} \,. \tag{6.54}$$

In (6.54), the first term accounts for the effective central charge and agrees with our findings (6.53). Note the exchange symmetry of h_1 and h_2 observed in the spectrum. The parameter k specifying the amplitudes is related to the anisotropy by (recall (4.74))

$$k = \frac{\pi}{\gamma} \,. \tag{6.55}$$
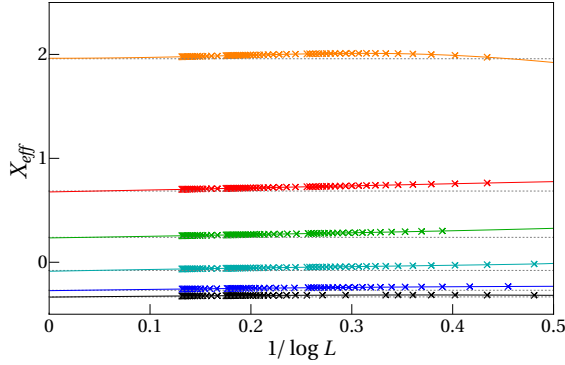
Figure 6.4: Finite-size scaling up to $L \sim$ 2000 of the ground state (black) and states with pattern (see Figure 6.2) similar to the ground state with $h_2 = 0$ but with different $U(1)$-charge $\mathbb{h}_1$, i.e., $h_1 = 1, 2, 3, 4, 6$ in increasing order from below. The crosses are the numerically obtained effective scaling dimensions. The dashed lines are given by formula (6.54) with the associated $h_{1,2}$. Solid lines are given by a rational extrapolation. Here $\gamma = 0.4$ and $\phi_{1,2} = 0$.
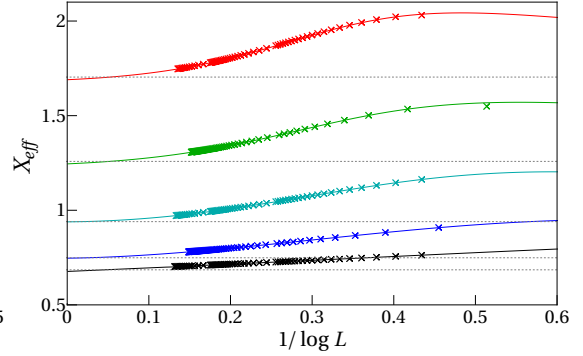
Figure 6.5: Finite-size scaling up to $L \sim$ 2000 for states with similar root configuration, as depicted in Figure 6.3. Crosses are the numerically obtained effective scaling dimensions. The $U(1)$-charges (h_1, h_2) take the values $(4,0), (4,1), (4,2), (4,3), (4,4)$ labelled from below. Dashed lines are given by equation (6.54), and the solid lines are given by a rational extrapolation. Here $\gamma = 0.4$ and $\phi_{1,2} = 0$.

Spectral flow of the compact modes under twists

We now turn to the extension of formula (6.54) to small non-vanishing twist angles. The analytic expression (6.52) and symmetry arguments suggest the following generalization

$$X_{\text{eff}}^{\text{Com}}(h_1, h_2, \phi_1, \phi_2) = -\frac{4}{12} + \frac{(h_1 + k\frac{\phi_1}{2\pi})^2}{4\,k} + \frac{(h_2 + k\frac{\phi_2}{2\pi})^2}{4\,k} + \frac{(h_1 - k\frac{\phi_1}{2\pi})^2}{4\,k} + \frac{(h_2 - k\frac{\phi_2}{2\pi})^2}{4\,k}\,. \tag{6.56}$$

We have numerically verified the above expression by using the data of the periodic model by applying the following iterative method: We start with a solution $\{u^{[1]}, u^{[2]}\}_{\phi_2^{\text{in}}}^{\phi_1^{\text{in}}}$ of the BAE (6.24) in logarithmic form with a particular initial set $(\phi_1^{\text{in}}, \phi_2^{\text{in}})$ of twist values e.g., $(\phi_1^{\text{in}}, \phi_2^{\text{in}}) = (0,0)$. We see that the maximal error using $\{u^{[1]}, u^{[2]}\}_{\phi_2^{\text{in}}}^{\phi_1^{\text{in}}}$ as an initial approximation for the BAE for new values $(\phi_1^{\text{in}} + \Delta\phi_1, \phi_2^{\text{in}} + \Delta\phi_2)$ behave as $\max\{|\Delta\phi_1|, |\Delta\phi_2 - \Delta\phi_1|\}$. Hence, by taking the steps sizes $\Delta\phi_1, \Delta\phi_2$ small enough, we can iteratively obtain the state at some $(\phi_1^{\text{end}}, \phi_2^{\text{end}})$.

Note that the above form of the effective scaling dimensions is compatible with the symmetries (6.16), (6.38). To interpret these results further, recall the conformal weights of a compact free boson given in (2.54). By comparing (2.54) and (6.56) we see that the excitations (6.56) mimic two independent twisted compact bosonic modes with the same compactification radii $R_{1,2} = \sqrt{\frac{k}{2\pi}}$ with charges $n_{1,2} = h_{1,2}$ and zero windings. Despite extensive study of root patterns of the low-lying excitations, we have not been able to identify any state with non-zero winding. Note that the functional dependence on the

compactification radii induced by non-zero twists $\phi_{1,2}$ is exactly the same as for two compact bosons, as expected from the symmetries of the model.

We want to end this section with the following important remark. The above expressions for the scaling dimensions capture the leading finite-size behaviour only. Corrections to scaling can arise, e.g., due to perturbations of the fixed-point Hamiltonian by terms involving irrelevant operators present in the lattice model (6.33) [60]. In the presence of a marginally irrelevant operator, one expects these subleading corrections to contain logarithms [151]. In the present case, we observe such corrections, see, e.g., Figures 6.4 and 6.5. However, as found in previous chapters, in the present case, these corrections are a signature of non-compact degrees of freedom in the effective theory describing the critical behaviour.
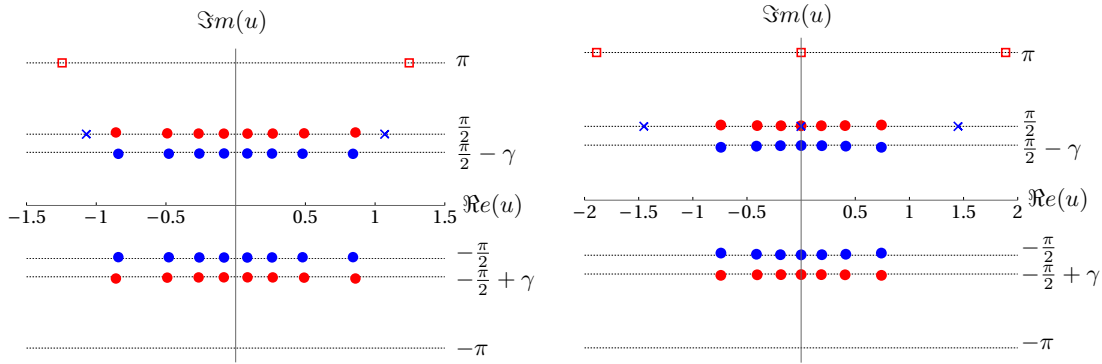
Figure 6.6: The left (right) plot displays the Bethe-root configuration in the complex plane of an excited state for $L = 19, (18)$, $\gamma = 0.4$ in the sector $h_1 = 1$ and $h_2 = 0$. The blue (red) symbols denote level 1 (2) roots. This excitation is built by placing 2(3) level 1 roots ($\times$) on the line $\frac{i\pi}{2}$ and 2,(3) level-2 roots ($\square$) on the line $i\pi$ in addition to the bulk roots ($\bullet$). Further, one (and a half four-string) has been removed with respect to the lowest energy state configuration in this sector.
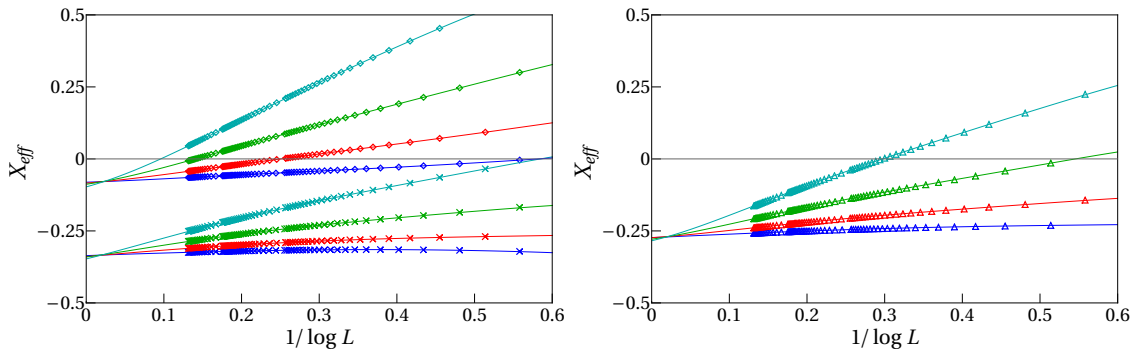
Figure 6.7: The left (right) plot displays the finite-size Scaling up to $L \sim 2000$ in the sectors (h_1, h_2): $(0,0) \times$, $(2,0) \diamond$ $((1,0) \triangle)$ for states with $M_\pi = 0, 1, 2, 3$ in increasing order from below (blue, red, green, cyan). The solid lines are rational extrapolations. One can see clearly the logarithmic dependence of the scaling dimensions. The parameters are set to $\gamma = 0.4$ and $\phi_{1,2} = 0$.

6.6.2 CONTINUOUS PART

Interestingly, there exist excitations whose scaling dimensions coincide with compact ones (6.56) up to logarithmic corrections. These excitations are characterised by the presence of roots of type ii) and iii). Consider first the ones of type ii). Examples of their root configurations are displayed in Figure 6.6. By replacing more and more four-strings by roots of type i) and ii), one generates an infinite tower of excitations labelled by the number M_π of type ii) roots. All of them flow to the same scaling dimension (6.56), see Figure 6.7.
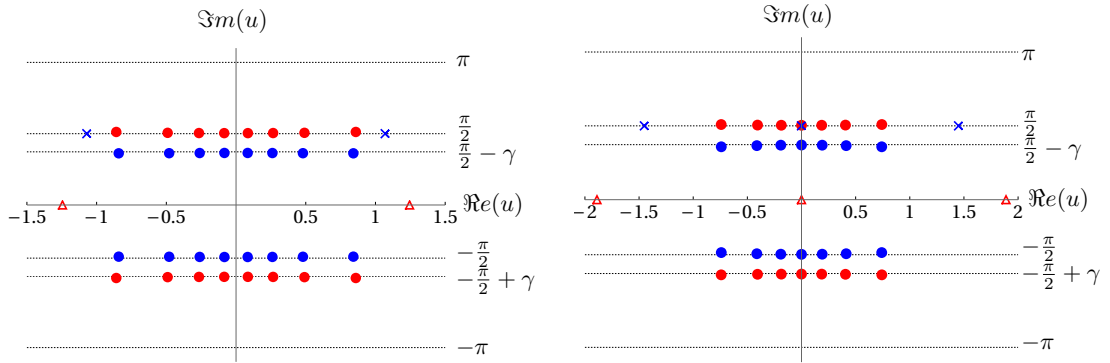
Figure 6.8: The left (right) plot displays the Bethe-root configuration in the complex plane of an excited state for $L = 19, (18)$, $\gamma = 0.4$ in the sector $h_1 = 1$ and $h_2 = 0$. The blue (red) symbols denote level 1 (2) roots. This excitation is built by placing 2(3) level-1 roots ($\times$) on the line $\frac{i\pi}{2}$ and 2,(3) level-2 roots ($\triangle$) on the real line in addition to the bulk roots ($\bullet$). Further, one (and a half four-string) has been removed with respect to the lowest energy state configuration in this sector. It is the state displayed in Figure 6.6 transformed by $u^{[2]} + i\pi$, and so it has the same energy.
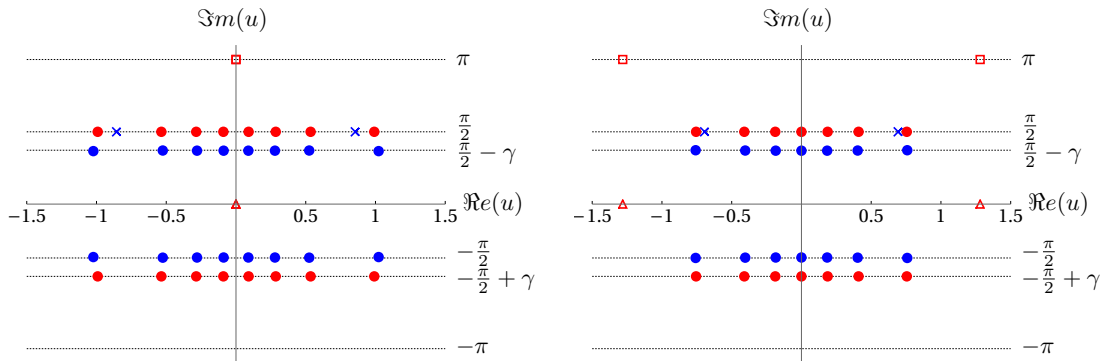
Figure 6.9: The left (right) plot displays the Bethe-root configuration in the complex plane of an excited state for $L = 18$, $\gamma = 0.4$ in the sector $h_1 = 0$ and $h_2 = 0$. The blue (red) symbols denote level 1 (2) roots. This excitation is built by placing 2(4) level-1 roots ($\times$) on the line $\frac{i\pi}{2}$ and 1,(2) level-2 roots ($\triangle$) on the real line and 1,(2) level-2 roots ($\square$) on the line $i\pi$ in addition to the bulk roots ($\bullet$). This is an excitation of both non-compact modes.
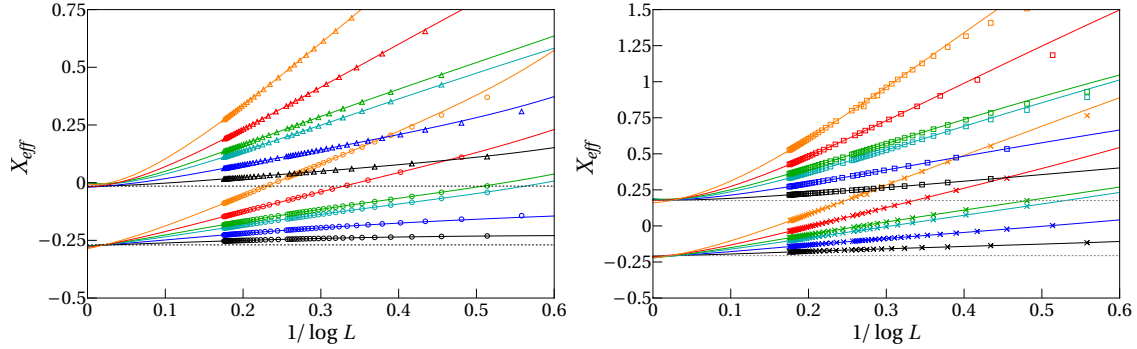
Figure 6.10: The left (right) plot displays the finite-size scaling up to $L \sim 300$ in the sectors (h_1, h_2): $(1,0)$ ○, $(2,1)$ △ $((1,1)$ ×, $(2,2)$ □) for states with $(M_0, M_\pi) = (0,0), (0,1), (1,1), (0,2), (1,2), (2,2)$ in increasing order from below (black, blue, cyan, green, red, orange). The solid lines are obtained by a rational extrapolation. The dashed lines depict the limiting value given by (6.56). One can see clearly the logarithmic dependence of the scaling dimensions. The parameters are set to $\gamma = 0.4$, $\phi_{1,2} = 0$.

Using the symmetry $u_j^{[2]} \to u_j^{[2]} + i\pi$ that exchanges the ii) and iii) types of roots, one deduces that the RG trajectories of excitations with root configuration built by mechanism iii) instead of ii), see e.g. Figure 6.8, also flow to the same scaling dimensions. Let's label them by the number M_0 of type iii) roots.

Moreover, it turns out that combinations of the two above excitation patterns are possible, see Figure 6.9 for the Bethe root configuration of a mixed state of both fundamental excitations ii) and iii). Further, see Figure 6.10 to see how such states fit in within the scaling behaviour of other states.

The obtained numerical data for various RG trajectories with different M_0, M_π can be used to extract the form of the logarithmic corrections: The rational extrapolation in Figure 6.10 suggest a general quadratic decay as $\propto \frac{1}{\log(L)^2}$. Further, the existence of two excitation mechanisms refines this ansatz to $\propto \frac{C_1}{\log(L)^2} + \frac{C_2}{\log(L)^2}$ with state-dependent constants $C_{1,2}$. As the $\mathbb{Z}_2$ symmetry interchanges these two contributions, we conclude that we must have $C_1 = C_2$. Multiplying the numerical data with $\log(L)^2$ extrapolating $L \to \infty$, we can access, by considering ratios, the dominant state dependence for each $|\Psi_L\rangle$. This numerical work reveals the following behaviour:

$$X_{\text{eff}} = X_{\text{eff}}^{\text{Com}}(h_1, h_2, 0, 0) + \frac{\mathcal{A}(\gamma)(M_0 + \frac{2}{3})^2}{\log(L/L_0)^2} + \frac{\mathcal{A}(\gamma)(M_\pi + \frac{2}{3})^2}{\log(L/L_0)^2} \,. \tag{6.57}$$

Here, L_0 is a non-universal, state-dependent constant, which we do not attempt to calculate. We are left to extract the amplitude $\mathcal{A}(\gamma)$. As it is the same for all states, we determine it by considering the effective scaling dimensions of the ground state where we expect the subleading logarithmic corrections to be the smallest:

$$X_{\text{eff}}^{GS}(L) = -\frac{4}{12} + \frac{8}{9} \frac{\mathcal{A}(\gamma)}{\log(L/L_0)^2} \,. \tag{6.58}$$
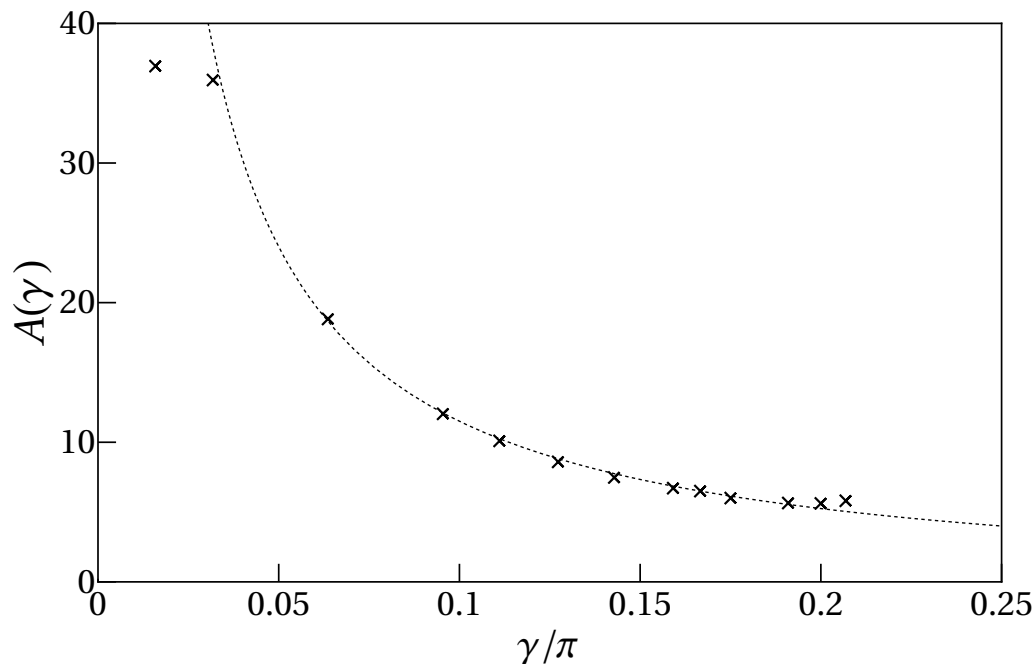
Figure 6.11: The amplitude $\mathcal{A}(\gamma)$ calculated via (6.59) for $L^1 = 2000$, $L^2 = 1000$ for various γ-values. The dashed line is the conjecture (6.60). One sees a fairly good matching. At the boundaries $\gamma \approx 0, (\frac{\pi}{4})$ one sees deviations which are assumed to be due to increasing finite-size corrections, see also [20].

Following [20], we eliminate L_0 by using data points for two system size L^1 and L^2 and get

$$\mathcal{A}(\gamma) = \frac{9}{8} \left[\frac{\log(\frac{L^1}{L^2})}{(X_{\text{eff}}^{GS}(L^1) + \frac{4}{12})^{-\frac{1}{2}} - (X_{\text{eff}}^{GS}(L^2) + \frac{4}{12})^{-\frac{1}{2}}} \right]^2 . \tag{6.59}$$

The numerical results are displayed in Figure 6.11. Based on these, we conjecture that

$$\mathcal{A}(\gamma) = \frac{5\pi - 4\gamma}{4\gamma} . \tag{6.60}$$

The mechanism of how the above leads to two continuous components in the spectrum of scaling dimensions resembles the one discussed around (4.72). We recall it here for the reader's convenience: we have defined the RG trajectories $|\Psi_L\rangle$ by keeping the numbers $M_{0,\pi}$ fixed, leading at first view to infinite degeneracies in the scaling limit. However, we can also organize the RG trajectories differently. Instead of keeping $M_{0,\pi}$ fixed, we can also let them run under the RG flow. In particular, we group states into trajectories $|\Psi_L\rangle$ such that

$$M_0 \sim \log(L), \quad M_\pi \sim \log(L) . \tag{6.61}$$

Here (6.61) is subject to the constraint $M_{0,\pi} \ll L$ such that $|\Psi_L\rangle$ is still a low energy state for any finite L, i.e. its energy obeys (2.96). This restriction is essential as RG trajectories leave the low energy spectrum once $M_{0,\pi} \sim L$. In fact, it is straightforward to show within the root density approach that the state with $M_{0,\pi} = L$ is highly excited: in comparison to

the energy Le_∞ of the ground state (6.50), its energy is of the order $\sim L$ (similar as e.g. in the staggered $sl(2|1)$ superspin chain [18]). This supports the interpretation of the findings above as evidence for the existence of continuous components in the conformal spectrum.

The redefinition (6.61) of RG trajectories enables that (6.57) can tend as $L \to \infty$ to a different scaling dimension than $X_{\text{eff}}^{\text{Com}}(h_1, h_2, 0, 0)$. In fact, by suitably arranging the concrete behaviour (6.61), the scaling dimensions can take any value larger or equal to $X_{\text{eff}}^{\text{Com}}(h_1, h_2, 0, 0)$. Note that X_{eff} for trajectories with similar $M_{0,\pi}(L)$ for fixed L become densely distributed ($\sim \frac{1}{\log(L)}$), leading to a continuous spectrum of scaling dimensions. As the two excitation mechanisms labelled by M_0 and M_π are independent of each other, we must have two continuous variables, call them $s_0 \sim \frac{M_0}{\log(L)}, s_\pi \sim \frac{M_\pi}{\log(L)}$, whose limits label the state in the scaling limit. The existence of two continua is also further supported by our finding for finite twist angles discussed below.

We want to stress that for the identification of the underlying CFT with two continuous components, a more rigorous definition of the scaling limit than in (6.61) is needed. A proper scaling limit can be defined in inhomogeneous models, where the logarithmic corrections can be parameterized by the quasi-momentum operator. However, the definition of this operator in these models relies on their inhomogeneity and is therefore not applicable to our model. An interesting further research direction could be additional investigation within the framework of chapter 3: searching for a more general algebraic structure, i.e. a *generalized* YBE (3.2) from which one could define a suitable quasi-momentum operator, e.g. see (3.19).

Spectral flow for continuum states

Having identified the finite-size spectrum for vanishing twist angles, we now turn to the question of what happens when these angles are turned on. We follow the procedure described below eq. (6.56) starting from $(\phi_1^{\text{in}}, \phi_2^{\text{in}}) = (0, 0)$ and iterating to the higher twists. This procedure can be technically involved, as certain roots of a given configuration can tend to infinity as the twists approach certain values. If these specific twist values are exceeded, then the infinite roots come back to a finite value. To avoid numerical problems caused by these infinities, it is suitable to transform to a different coordinate set. By using the rational chart $\zeta = \mathrm{e}^{-2u}$ infinitely large roots are mapped to zero.

We start by discussing the lowest states ($M_0 = M_\pi = 0$) in the two continua first. Some of our results are represented in Figure 6.12. One can see that for small twist angles, the scaling dimensions follow (6.57) but with the first term replaced by (6.56) with a non-vanishing twist. However, after critical values of the twists given by
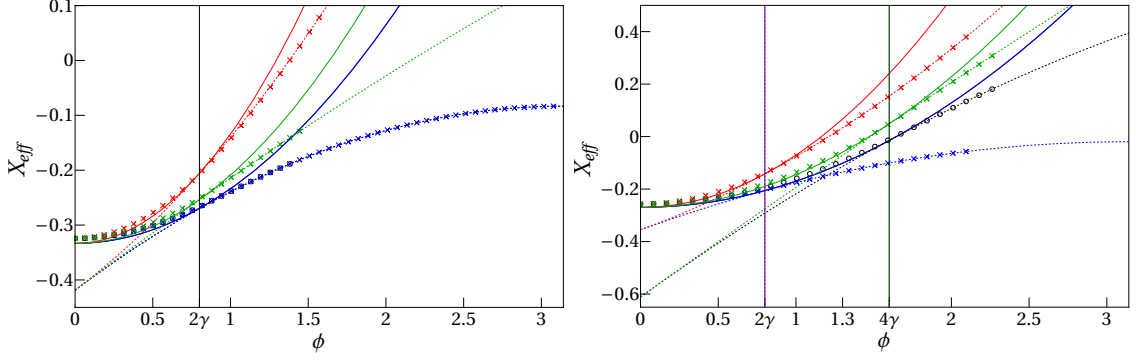
$$\phi_{1,2}^c = 2\gamma(h_{1,2} + 1) = \frac{2\pi(h_{1,2} + 1)}{k}, \tag{6.62}$$

the behaviour changes drastically to

$$X_{\text{eff}} = X_{\text{eff}}^{\text{Com}}(h_1, h_2, \phi_1, \phi_2) - \frac{(h_{1,2} + 1 - k\frac{\phi_{1,2}}{2\pi})^2}{2(k-2)}, \qquad \phi_{1,2}^c < \phi_{1,2} < \widetilde{\phi}_{1,2}^c, \tag{6.63}$$

with the *absence* of logarithmic corrections. Numerical work suggests that the choice between 1 and 2 in the above formulae seems to be taken in a way such that the second term in (6.63) always incorporates the bigger twist angle and, if both twists are equal,

Figure 6.12: The left (right) plot displays the effective scaling dimensions for the lowest state in the continuum in the sectors $(h_1, h_2) = (0,0), ((1,0))$ for $L = 2000$, (1999), under various twists $(\phi_1, \phi_2) = (\phi, 0), (0, \phi), (\phi, \phi), (\phi, \frac{1}{2}\phi)$ (Black, Blue, Red, Green). The solid lines display the expected behaviour (6.56) for small twist angles, excluding the strong logarithmic corrections. The crosses or circles display the numerical data obtained from the Bethe ansatz for twist angles as far as possible in the numerical procedure. The vertical lines designate the critical twist values, where the agreement with (6.56) breaks down. The dashed lines indicate the conjectured formula (6.63) for the scaling dimensions valid beyond the critical points. Note that the matching with the conjecture is extremely accurate. We interpret this as the emergence of discrete states having less logarithmic corrections.

minimizing the critical twist angle (see Figure 6.12). It turns out that (6.63) is valid just until the twist exceeds another critical twist angle $\widetilde{\phi}^c_{1,2}$. For example, for twisting only with ϕ_1 or ϕ_2 in the lowest sector $h_1 = h_2 = 0$, we find that

$$\widetilde{\phi}^c_{1,2}\Big|_{h_1=h_2=0} = 2\pi - \phi^c_{1,2}\Big|_{h_1=h_2=0} . \tag{6.64}$$

So far, we have considered only the lowest states in the continua. If we twist excited states, their scaling dimensions follow (6.63) but are again spoiled by decreasing logarithmic corrections. To investigate this phenomenon further, we have searched for twists for which the Bethe root configurations are again regular enough to define RG trajectories. We find that a suitable point is $(\phi_1, \phi_2) = (\pi, 0)$. Here, the Bethe roots parametrising the low-energy states consist mainly of

$$
\begin{aligned}
u^{[1]} &\longrightarrow \quad x_j + \frac{\mathrm{i}\pi}{2} - \mathrm{i}\gamma - \mathrm{i}\epsilon^{[1]}_j, \quad x_j - \frac{\mathrm{i}\pi}{2} + \mathrm{i}\gamma + \mathrm{i}\epsilon^{[1]}_j, \\
u^{[2]} &\longrightarrow \quad z_l + \frac{\mathrm{i}\pi}{2}, \quad l = 1, \ldots, M_z, \\
&\qquad\qquad w_k - \frac{\mathrm{i}\pi}{2}, \quad k = 1, \ldots, M_w.
\end{aligned}
\tag{6.65}
$$

In addition, there are level-1 roots sitting exponentially close to the following values depending on the parity of $dN := M_z - M_w$:

$$
\begin{aligned}
&\mathrm{i}\gamma, -\mathrm{i}\gamma \quad \text{if } dN \text{ even}, \\
&2\mathrm{i}\gamma, 0, -2\mathrm{i}\gamma \quad \text{if } dN \text{ odd}.
\end{aligned}
\tag{6.66}
$$
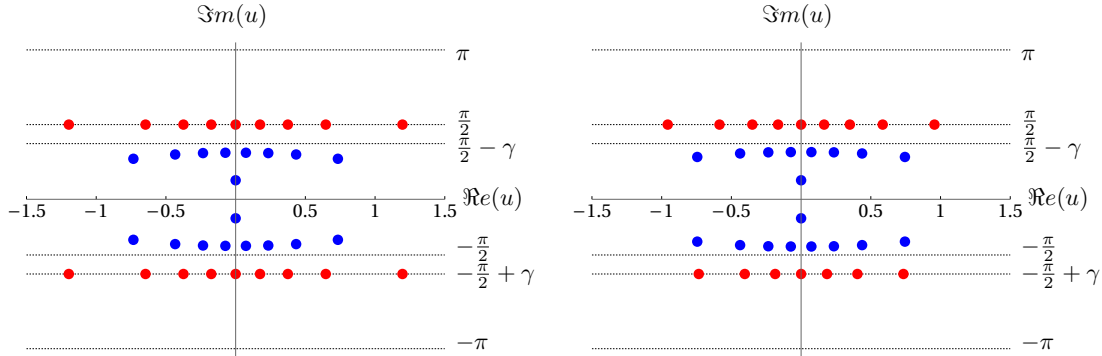
Figure 6.13: The left (right) plot displays the Bethe-root configuration in the complex u-plane of an excited state for $L = 18$, $\gamma = 0.4$, $\phi_1 = \pi$, $\phi_2 = 0$ in the sector $h_1 = 0$ and $h_2 = 0$. The blue (red) symbols denote level 1 (2) roots. The left figure shows the ground state configuration, while the right excitation is built by unbalancing, $dN = 4$, the number of level-2 on the lines $\pm\frac{i\pi}{2}$. The two level-1 roots with vanishing real parts have imaginary parts close to $\pm\gamma$.

Plots of typical configurations are shown in Figure 6.13. It turns out that states with different distributions dN of level-2 roots on the two lines $\pm\frac{i\pi}{2}$ flow to the same conformal dimensions (6.63) with $\phi_1 = \pi$ and $\phi_2 = 0$, see e.g. Figure 6.14. We find that the scaling of dimensions of excited states for $\phi_1 = \pi, \phi_2 = 0$ are given by

$$X_{\text{eff}} = X_{\text{eff}}^{\text{Com}}(h_1, h_2, \phi_1, \phi_2)\big|_{\phi_1=\pi,\phi_2=0} - \frac{(h_1 + 1 - k\frac{\phi_1}{2\pi})^2}{2(k-2)}\bigg|_{\phi_1=\pi} + \tilde{\mathcal{A}}(\gamma)\frac{dN^2}{\log(L/\tilde{L}_0)^2} \,,$$

(6.67)

where again $\tilde{L}_0$ is a non-universal constant, which we do not attempt to calculate here. Further, the above formula also holds true for small deviations around the twist angles, i.e. $\phi_1 \approx \pi$, $\phi_2 \approx 0$ with the obvious modifications. We conjecture that the amplitude $\tilde{\mathcal{A}}(\gamma)$ is given by

$$\tilde{\mathcal{A}}(\gamma) = \frac{2(2-5\gamma)\gamma}{3(1-4\gamma)^2} \,.$$

(6.68)

Recall that from the previous chapters, we have seen the possibility of the existence of discrete states that do not possess logarithmic corrections. Further, we have seen that a state belonging to a continua can become a discrete state under the variation of the lattice parameters, e.g. recall Figure 4.9. We interpret our findings in this section in an analogous way. Consider a state whose scaling limit is described by the two continuous variables s_0, s_π. Under a twist, one of the continuous variables changes its class to the discrete one, while the other remains in the continuous family. The latter still induces logarithmic corrections on the level of the lattice regularization as seen in (6.67).

Ultimately, this conjecture should imply the existence of purely discrete states (apart from the $dN = 0$ state) without any logarithmic corrections. We have checked that this is indeed the case. Starting from the twist $(\phi_1, \phi_2) = (\pi, 0)$, we turn on the second twist
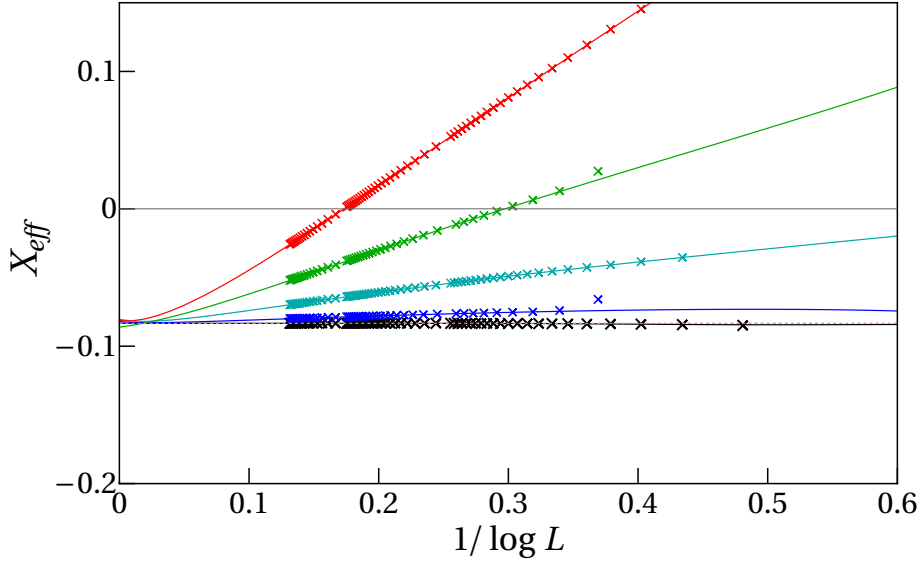
Figure 6.14: Effective scaling dimensions up to $L \sim 2000$ for $\phi_1 = \pi$, $\phi_2 = 0$, $\gamma = 0.4$ in the sector $h_1 = h_2 = 0$ for $dN = 0, 1, 2, 3, 4$ in increasing order from below (black, blue, cyan, green, red). The crosses are the numerical data obtained from the Bethe ansatz. The solid lines are rational extrapolation. Further, the dashed pink line is given by the constant limit value (6.63). In order to obtain the numerical data, we have assumed that the roots which are exponentially close to (6.66) actually sit on these values. This leads to a small offset (see the green and blue crosses on the far right) for small system sizes, as here the approximation is inducing an error.
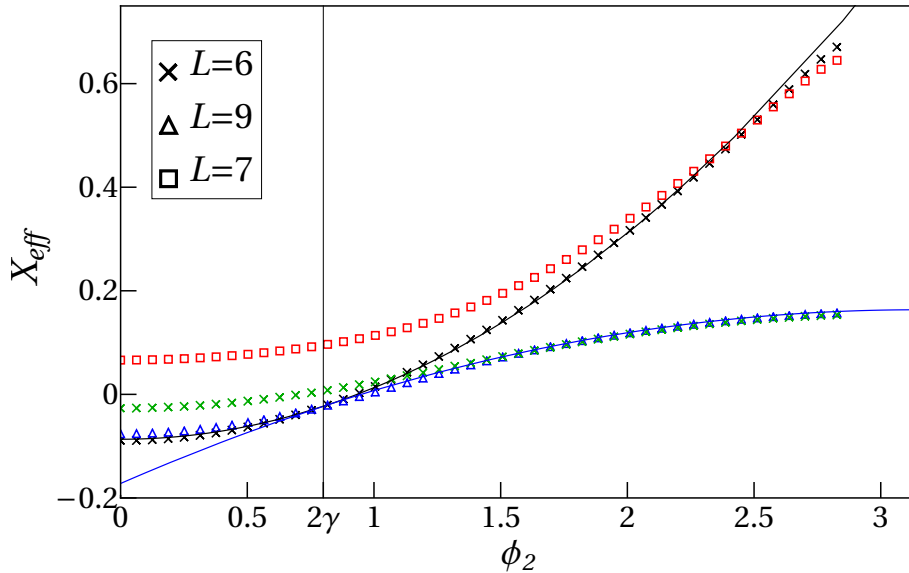
Figure 6.15: Effective scaling dimensions for small L and $\phi_1 = \frac{9\pi}{10}$, $\gamma = 0.4 + i0^+$ in the sector $h_1 = h_2 = 0$ for $dN = 0, 1, 2, 3$ (black, blue, green, red) under variation of the second twist ϕ_2. The slightly complex value of the anisotropy and offset of the first twist angle from π is due to numerical purposes. The black solid line displays $X_{\text{eff}}^{\text{Com}}(h_1, h_2, \frac{9\pi}{10}, \phi_2)$ while the blue line is given by (6.69). The black vertical line hallmarks the appearance of a purely discrete state.

significantly. The first excited states $dN = 1, 2$ in the sector $h_1 = 0 = h_2$ become purely discrete states when the second twist angle exceeds the critical value $\phi_2 = 2\gamma$. It has effective scaling dimensions

$$X_{\text{eff}} = X_{\text{eff}}^{\text{Com}}(h_1, h_2, \pi, \phi_2) - \frac{(h_1 + 1 - k\frac{\pi}{2\pi})^2}{2(k-2)} - \frac{(h_2 + 1 - k\frac{\phi_2}{2\pi})^2}{2(k-2)} \quad \text{with} \quad \phi_2 > 2\gamma. \quad (6.69)$$

Note that this check can be done on the level of small L, as we expect this state to possess no logarithmic corrections; see Figure 6.15. The purely discrete scaling dimensions (6.69) are valid for large twist angles only; however, one can analytically continue back the scaling dimensions (6.69) to zero twist. For the lowest state with $h_1 = h_2 = 0$, we obtain:

$$X_{\text{eff}} = -\frac{4}{12} + \frac{1}{k-2}. \quad (6.70)$$

Assuming that the conformal weights $\Delta, \bar{\Delta}$ vanish in this procedure as it is, for example, in the twisted staggered six-vertex model or the $A_2^{(2)}$ model [23], we obtain on very speculative grounds that the central charge is given by

$$c = 4 - \frac{12}{k-2} = 2\left(2 - \frac{6}{k-2}\right), \quad (6.71)$$

which formally coincides with two Black Hole CFTs.

6.7 CHAPTER SUMMARY

We have generalised the periodic $D_3^{(2)}$ spin chain [146] to the twisted case. The induced BCs are parameterized by two twist angles ϕ_1, ϕ_2. We have solved the twisted model by means of the analytic Bethe ansatz (6.20), (6.24). Since the rank of $D_3^{(2)}$ is two, the Bethe ansatz possesses two-level nesting.

The model has a variety of symmetry transformations, e.g. (6.14), (6.16), (6.17). The most useful result is a generalization (6.14) of the $\mathbb{Z}_2$-symmetry of the lower-rank case $D_2^{(2)}$. It originates from the quasi-periodicity of the R-matrix while on the level of the Bethe ansatz, it maps states among each other whose level-2 Bethe roots differ by the quasi-period $\mathbf{p} = i\pi$. In addition, we have found that the transfer matrix is CPT-invariant (6.17) while on the Hamiltonian level, this symmetry reduces to CP-symmetry (6.38).

Turning to the analysis of the scaling limit, we have focused on the regime of the anisotropy $\gamma \in (0, \frac{\pi}{4})$. The spin chain is found to be critical, as it possesses gapless excitations with a linear dispersion relation. Hence, the effective theory of its low-lying excitations arising in the thermodynamic limit $L \to \infty$ should be governed by a conformal field theory. We have identified certain classes of the low-lying energy states parameterized by the $U(1)$-charges. We have found that their effective scaling dimensions give rise to two compact modes in the scaling limit. More precisely, these modes mimic two compact bosons with zero winding (6.56). Indeed, despite considerable numerical effort, we did not find any non-zero winding states. Whether non-trivial winding states exist is left open for future investigation.

In addition to the two compact modes, we found two types of decreasing logarithmic corrections. The corrections are generated by the number of level-2 Bethe roots on the

real line and the line with imaginary part π. We provide evidence that these logarithmic corrections give rise to two non-compact degrees of freedom in the scaling limit. The two non-compact modes are interchanged by the $\mathbb{Z}_2$ symmetry (6.14). Furthermore, we have considered the influence of large twists. We found that some of the logarithmic corrections disappear beyond certain critical twist angles. We interpret this phenomenon as the emergence of discrete states under twists. For the case of $\phi_1 = \pi$ and small ϕ_2, one of the continua becomes purely discrete while the other persists. For the extreme case of $\phi_1 = \pi$ and large ϕ_2, we observe the existence of purely discrete states (6.69). By analytical continuation of its effective scaling dimension to zero twists and assuming that the conformal dimensions vanish there [23, 108], we can speculate about the value of the true central charge (6.71). Formally, it agrees with the sum of two Black Hole CFT central charges.

For a rigorous identification of the underlying CFT, we would need a conserved operator that parameterizes the non-compact degrees of freedom on the lattice. The search for such an operator, maybe among the lines of chapter 3, might be an interesting research direction, supporting the analysis of the scaling limit. It could help identify the space of states in the scaling limit, especially calculating the density of states of the continua as done in chapter 4.

Further, it should be possible to study the influence of open BCs for selecting certain sectors of the underlying CFT, as has been done in chapters 4, 5 for the lower rank case $D_2^{(2)}$, which is equivalent to the staggered six-vertex model. It might also be interesting to investigate the different parameter regimes $\gamma \in (\frac{\pi}{4}, \frac{\pi}{2})$.

7 | CONCLUSION

In this thesis, we considered the influence of BCs on the scaling limit of integrable lattice models. The principal example was the staggered six-vertex model, which is known to possess a non-compact degree of freedom in the scaling limit when twisted BCs are imposed. We explored the impact that different BCs for the lattice model have on the spectrum of critical dimensions.

The starting point of our study was the formulation of a uniform framework of vertex models with periodically repeating inhomogeneities (staggered models), which enables one to generalise earlier found factorisation identities [106, 107]. We showed how the basic properties of an elementary R-matrix translate to the characteristics of a composite $\mathcal{R}$-matrix. The requirement of locality of the associated Hamiltonian led, in the open case, to two inequivalent staggerings, alternating and quasi-periodic. In the latter case, the quasi-momentum operator is trivial. For the alternating staggering, it is not, and we were able to express it in the language of the composite $\mathcal{R}$-matrix. This is of interest for the following reason: in all the known cases, the fundamental definition of the quasi-momentum relies on the inhomogeneity of the model. However, the transfer matrix, when expressed in terms of the composite $\mathcal{R}$-matrix, contains *no* inhomogeneity parameters. We hope that our result facilitates the study of homogenous models with non-compact spectrum.

The two different cases of staggerings were discussed in depth using the example of the six-vertex model, in particular for the choice of $U_q(\mathfrak{sl}(2))$ invariant BCs. The name originates from the fact that, with such BCs imposed, the model possesses $U_q(\mathfrak{sl}(2))$ symmetry. Hence, all energies appear in multiplets, characterised by the Casimir operator $\mathbb{C}$ of the $U_q(\mathfrak{sl}(2))$ algebra; see (4.11). We found an expression for the Q-operator in the $S^z = 0$ sector, which enabled us to apply the analytic Bethe ansatz to solve the model (as an alternative to the earlier algebraic approach in [124]). Further, the Q-operator formula allowed us to systematically study the Bethe root configurations of the model, which forms the basis of our analysis of the scaling limit.

For the alternating case, we investigated a critical phase of the lattice model. We observed that the $U_q(\mathfrak{sl}(2))$ symmetry is spontaneously broken. In addition, strong logarithmic corrections in the finite-size spectrum for a specific class of states were found. We showed — for the first time for open BCs — that the defined quasi-momentum operator parametrises these logarithmic corrections and, in turn, the continuous degree of freedom in the scaling limit. Motivated by previous studies, we proposed that the scaling limit is related to the $\mathrm{SL}(2, \mathbb{R})/U(1)$ gauged WZW model. In the latter, discrete states also exist. When realised on the lattice, they are expected to possess no logarithmic corrections and be

characterised by a purely imaginary quasi-momentum. We indeed identified such states in the lattice model. In addition, our analysis generalized one of the main results of the work [54] concerning periodic BCs to the case of $U_q(\mathfrak{sl}(2))$ invariant BCs: the universal behaviour is the same for all values of the staggering parameter α as long as $\gamma < \alpha < \pi - \gamma$.

For further analysis, we restricted to the self-dual case. We employed the ODE/IQFT approach: based on a detailed numerical study of certain sums over the Bethe roots, we concluded that the ODEs governing the scaling limit of the lattice model fall within the same class which appears in the model with twisted BCs. This enabled us to carry over many results concerning the ODEs. We obtained a quantization condition for the quasi-momentum and checked its validity via a detailed spectroscopy study for intermediate lattice sizes. The latter was facilitated by the formula we previously obtained for the Q-operator. Using the quantization condition, the space of states in the scaling limit was fully classified. In particular, we obtained the density of states characterising the continuous spectrum of scaling dimensions, as well as all characters for discrete states. Unfortunately, the results on branes for the $\mathrm{SL}(2,\mathbb{R})/U(1)$ sigma model studied in the work [12] seem to be inapplicable to our study.

The model with quasi-periodic staggering was studied via a spectral flow to the model with alternating staggering. In contrast to the previous work [27], the flow is, by definition, integrable, as it was developed in the uniform framework of the composite $\mathcal{R}$-matrix. Hence, we were able to explicitly investigate the behaviour of the Bethe roots under the flow, where a drastic change in their pattern signals the onset of a phase transition. We found that the two models are separated by two first-order phase transitions. The intermediate phases are not of physical interest as the associated Hamiltonians are non-local. This is consistent with the different properties of the corresponding spectra observed previously (for the quasi-periodic staggering, the spectrum of critical exponents does not possess a continuous component).

For the antidiagonal BCs, which reduce the symmetry of the model to a discrete $\mathbb{Z}_2 \times \mathbb{Z}_2$ symmetry, we started our analysis by generalising[1] the well-known derivation of the Baxter Q-operator [88] to the inhomogeneous case. Thereby, we found a genuinely explicit expression of the operator's matrix elements, which does not involve any implicit matrix multiplication or inversion in contrast to [88]. This expression for the Q-operator allowed us to systematically deduce the Bethe root configuration corresponding to the low-energy states. In the Black Hole regime, the root configurations, e.g. for the ground state, significantly change when the system size is increased. Despite our efforts to study intermediate system sizes $L \sim 15$, we were not able to obtain any insights into the scaling limit of the lattice model due to the presence of logarithmically increasing scaling dimensions. Hence, we conclude that the Black Hole phase is incompatible with antidiagonal BCs. The other non-trivial phase of the lattice model is governed by a CFT constructed from two $U(1)$ twisted Kac-Moody algebras.

Our study of higher rank generalisations of the staggered six-vertex model has shown that an increase in rank can lead to multiple continuous components in the spectrum of scaling dimensions. In the $D_3^{(2)}$ model two independent continua were identified. Further,

---

[1]Note that this derivation is used as an example in the preliminaries of the thesis.

we showed the presence of purely discrete states by considering the influence of twisted BCs. The analysis was based on symmetry arguments and numerical evidence of strong logarithmic corrections. An open question is the definition of operators that parameterise the non-compact degrees of freedom directly on the lattice. Analogues of the quasi-momentum operator of the rank 1 model would drastically facilitate the identification of the scaling limit. Among other things, they would be important for computing the density of states using the ODE/IQFT correspondence.

Another exciting generalization of our results consists in consideration of different integrable BCs for the $D_3^{(2)}$ model such as given in [117] or the study of the whole higher rank family $D_n^{(2)}$, similar to [114] for the $A_n^{(2)}$ series.

There are many interesting further research directions regarding the study of the $U_q(\mathfrak{sl}(2))$ invariant staggered six-vertex model. The ODE/IQFT correspondence has only been applied to the case of alternating staggering. To fully classify the scaling limit of the model with the quasi-periodic choice of inhomogeneities, one should deduce the ODE governing the scaling limit. Moreover, one can generalise the analysis of the alternating staggering to the case of arbitrary strength ξ of the two anti-parallel boundary magnetic fields $\xi^L = -\xi^R$. Research along these directions may yield an explicit connection — which the present work did not produce — to the D0 brane and the one-parameter family of D1 branes of the Black Hole sigma model considered in [12]. Regarding the other extreme case of BCs in the staggered six-vertex model, the antidiagonal ones, the identification of the scaling limit in the 'Black hole regime' remains open.

A | EVALUATION OF THE PARTITION FUNCTION AS PATH INTEGRAL

This appendix is based on [37].

The non-compact case

The partition function of the free massless boson in two dimensions can also be evaluated in the path integral formalism. We take the world sheet to be the torus $\mathbb{C}/\mathbb{Z}_2$ generated by the two complex numbers t_1, t_2 as basis vectors such that we can impose the following periodicity condition

$$\varphi(x + n_1 t_1 + n_2 t_2) = \varphi(x) \,. \tag{A.1}$$

The partition function then takes the form

$$\mathcal{Z}(\tau) = \sqrt{A} \int_{\Phi \backslash \varphi_0} \mathcal{D}\varphi \, \exp\left[-\frac{1}{2} \int \mathrm{d}^2 x \, (\partial_{x_1}\varphi)^2 + (\partial_{x_2}\varphi)^2 \right] \tag{A.2}$$

where we integrate over all fields except the diverging contribution from the zero mode φ_0, and A is the area of the torus given by $\mathrm{Im}(t_2 t_1^*)$. We can partially integrate to obtain[1]:

$$\mathcal{Z}(\tau) = \sqrt{A} \int_{\Phi \backslash \varphi_0} \mathcal{D}\varphi \, \exp\left[\frac{1}{2} \int \mathrm{d}^2 x \, \varphi(x)\Delta\varphi(x) \right] \,. \tag{A.3}$$

To evaluate this further, we need to study the properties of the Laplacian on a torus spanned by $t_{1,2}$. Any function on the tours can be expanded in the countable set of eigenfunctions of the Laplacian, which take the form:

$$\varphi_{m_1,m_2}(x) = \exp\left[2\mathrm{i}\pi \langle x, m_1 k_1 + m_2 k_2 \rangle \right] \tag{A.4}$$

where the scalar product $\langle , \rangle$ mimics the one in $\mathbb{R}^2$ induced by the indification of $\mathbb{C} \sim \mathbb{R}^2$ and k_1 and k_2 are the dual vectors to t_1, t_2 defined by the relation

$$\langle t_i, k_j \rangle \in \mathbb{Z} \,. \tag{A.5}$$

This ensures the periodicity condition (A.1). Explicitly, we have

$$k_1 = -\frac{\mathrm{i}t_2}{A} \,, \quad k_2 = \frac{\mathrm{i}t_1}{A} \,. \tag{A.6}$$

---

[1]Note that the boundary terms vanish due to the periodicity condition

Direct computation shows that the eigenvalues $-\lambda_{m_1,m_2}$ of the Laplacian are

$$-\lambda_{m_1,m_2} = -4\pi^2 \|m_1 k_1 + m_2 k_2\|^2 . \tag{A.7}$$

Hence, we obtain for the partition function

$$\mathcal{Z}(\tau) = \prod_{m_1+m_2\neq 0} \sqrt{\frac{2\pi}{\lambda_{m_1,m_2}}} = \sqrt{A}\exp\left\{\frac{1}{2}G'(0)\right\}$$

where we defined the function

$$G(s) = \sum_{m_1+m_2\neq 0} \frac{1}{\lambda_{m_1,m_2}^s} . \tag{A.8}$$

In general, this quantity is divergent and so needs to be appropriately regularized. In the following, we sketch the method of ζ-function regularisation. First, let us introduce the modular parameter $\tau = t_2/t_1$ again which leads to

$$G(s) = \sum_{m_1+m_2\neq 0} \frac{1}{|m_2 + m_1\tau|^{2s}} \left|\frac{A}{2\pi t_1}\right|^{2s} . \tag{A.9}$$

Splitting the sum gives

$$\left|\frac{2\pi t_1}{A}\right|^{2s} G(s) = 2\zeta(2s) + \sum_{m_1\neq 0}\sum_{m_2} \frac{1}{|m_2 + m_1\tau|^{2s}} , \tag{A.10}$$

where ζ is the Riemann ζ-function. We write $\tau = \tau_1 + i\tau_2$ and assume $\tau_2 > 0$ to obtain

$$\sum_{m_2} \frac{1}{|m_2 + m_1\tau|^{2s}} = \frac{\sqrt{\pi}}{\Gamma(s)}\sum_{n\in\mathbb{Z}}\int_0^\infty dt\, t^{s-\frac{3}{2}}\exp\left(-tm_1^2\tau_2^2 + \pi^2 n^2/t - 2i\pi n m_1\tau_1\right), \tag{A.11}$$

where we have used the following identities for the Γ-function

$$\frac{1}{z^s} = \frac{1}{\Gamma(s)}\int_0^\infty dt\ t^{s-1}e^{-zt}, \quad \Gamma(s) = \int_0^\infty dt\ t^{s-1}e^{-t} . \tag{A.12}$$

Splitting the contributions of $n = 0$ from the rest, we obtain by direct calculations

$$\left|\frac{2\pi t_1}{A}\right|^{2s} G(s) = 2\zeta(2s) + 2\left(\frac{\tau_2}{\pi}\right)^{1-2s}\frac{\Gamma(1-s)}{\Gamma(s)}\zeta(2-2s)$$
$$+ \frac{\sqrt{\pi}}{\Gamma(s)}\sum_{m_1\neq 0}\sum_{n\neq 0} e^{2i\pi n m_1\tau_1}\int_0^\infty dt\left(\frac{\pi|n|}{|m_1|\tau_2}\right)^{s-\frac{1}{2}}t^{s-\frac{3}{2}}\exp\left(-|m_1 n|\pi\tau_2\left(t+\frac{1}{t}\right)\right). \tag{A.13}$$

Expanding the function $G(s)$ around $s \approx 0$, we can evaluate the integrals explicitly in the first order in s. This yields

$$G(s) \approx -1 + s\left(-2\log\left|\frac{A}{t_1}\right| + \frac{\pi\tau_2}{3} + \sum_{m_1\neq 0}\sum_{n\neq 0} e^{2i\pi n m_1\tau_1}\frac{1}{|n|}e^{-2\pi|nm_1|\tau_2}\right). \tag{A.14}$$

The double sum can be evaluated in the following way by using the definition (2.45)

$$\sum_{m_1 \neq 0} \sum_{p \neq 0} e^{2i\pi p m_1 \tau_1} \frac{1}{|p|} e^{-2\pi |p m_1| \tau_2} = \sum_{m_1, p > 0} \frac{2}{p} (q^{m_1 p} + \bar{q}^{m_1 p})$$

$$= -2 \ln \left(\prod_{m_1 > 0} (1 - q^{m_1})(1 - \bar{q}^{m_1}) \right)$$

$$= -2 \ln \left(|\eta(q)|^2 \right) - \frac{\pi \tau_2}{3} .$$

When evaluating the double sum and using the explicit values of the ζ we get

$$G(s) \approx -1 - 2s \left(\log \left| \frac{A}{t_1} \right| + \ln \left(|\eta(q)|^2 \right) \right) . \tag{A.15}$$

And so we obtain

$$G'(0) = -2 \log \left(\left| \frac{A}{t_1} \right| |\eta(q)|^2 \right) . \tag{A.16}$$

Using $\sqrt{\Im m(\tau)} = \sqrt{A}/t_1$, we get

$$\mathcal{Z} = \frac{1}{\sqrt{\Im m(\tau)} |\eta(\tau)|^2} . \tag{A.17}$$

The compact case

For the compactified boson, we have the following BCs in the path integral formalism

$$\varphi(x + n_1 t_1 + n_2 t_2) = \varphi(x) + 2\pi R(n_1 \vartheta_1 + n_2 \vartheta_2) \tag{A.18}$$

where $n_1, n_2, \vartheta_1, \vartheta_2 \in \mathbb{Z}$ and R is the compactification radius. The path integral runs over all field configurations which obey this periodicity condition. Note that since the boson is compactified, the zero mode does not contribute an infinite amount to the path integral. The integration will be done for fields with fixed $(\vartheta_1, \vartheta_2)$ and we sum over all $\vartheta_1, \vartheta_2 \in \mathbb{Z}$. In a given sector $(\vartheta_1, \vartheta_2)$, we spilt the field into two parts:

$$\varphi(z) = \varphi_{\vartheta_1, \vartheta_2}^{cl}(z) + \tilde{\varphi}(z) \tag{A.19}$$

where $\tilde{\varphi}$ is the standard periodic field and $\varphi_{\vartheta_1, \vartheta_2}^{cl}(z)$ is the solution of the classical equations of motions $\partial_\mu \partial^\mu \varphi_{\vartheta_1, \vartheta_2}^{cl}(z) = 0$ obeying (A.18). It is given by

$$\varphi_{\vartheta_1, \vartheta_2}^{cl}(z) = 2\pi R \left[\frac{z}{\omega_1} \frac{\vartheta_1 \bar{\tau} - \vartheta_2}{\bar{\tau} - \tau} - \frac{\bar{z}}{\omega_1^*} \frac{\vartheta_1 \tau - \vartheta_2}{\bar{\tau} - \tau} \right] . \tag{A.20}$$

The action is then given by the sum of the actions as the cross terms vanish by integration by parts and $\partial_\mu \partial^\mu \varphi_{\vartheta_1, \vartheta_2}^{cl}(z) = 0$:

$$S[\varphi] = S[\tilde{\varphi}] + S[\varphi_{\vartheta_1, \vartheta_2}^{cl}] \tag{A.21}$$

The integration over $\tilde{\varphi}$ can be carried out analogously to the non-compact case. The action of the other part of the field is

$$S[\varphi^{cl}_{\vartheta_1,\vartheta_2}] = \pi R^2 \frac{|\vartheta_1\tau - \vartheta_2|}{2\mathrm{Im}(\tau)} \ . \tag{A.22}$$

Hence, we obtain

$$\mathcal{Z} = \frac{R}{\sqrt{2\mathrm{Im}(\tau)}|\eta(\tau)|^2} \sum_{\vartheta_1,\vartheta_2\in\mathbb{Z}} \exp \pi R^2 \frac{|\vartheta_1\tau - \vartheta_2|}{2\mathrm{Im}(\tau)} \ . \tag{A.23}$$

Using the re-summation formula of Poisson

$$\sum_{n\in\mathbb{Z}} \exp\left(-\pi a n^2 + bn\right) = \frac{1}{\sqrt{a}} \sum_{k\in\mathbb{Z}} \exp\left(-\frac{\pi}{a}\left(k + \frac{b}{2i\pi}\right)^2\right) \tag{A.24}$$

with

$$a = \frac{R^2}{2\Im m(\tau)} \qquad b = \frac{\pi m R^2 \Re e(\tau)}{\Im m(\tau)} \ , \tag{A.25}$$

one obtains

$$\mathcal{Z}(\tau) = \sum_{n,\vartheta\in\mathbb{Z}} q^{\frac{1}{8\pi}\left(\frac{n}{R}+2\pi R\vartheta\right)^2} \bar{q}^{\frac{1}{8\pi}\left(\frac{n}{R}-2\pi R\vartheta\right)^2} \frac{1}{|\eta(\tau)|^2} \ . \tag{A.26}$$

B | PROOF OF (3.36B) FOR $\mathcal{K}^L$

This appendix is based on the author's publication [32].

Using the definitions of the composite quantities in the LHS of the reflection algebra (3.36b), we obtain (we omit the prefactor of $\mathcal{K}^L$ and set $ijk\ell = 1234$ for notational clarity):

$$
\begin{aligned}
&\mathcal{R}_{1,2|3,4}(-u+v,-\theta,-\theta)\mathcal{K}^{L,t_{1,2}}_{1,2}(u,\theta)\mathcal{M}^{-1}_{1,2}\mathcal{R}_{3,4|1,2}(-u-v-2\eta,-\theta,-\theta)\mathcal{M}_{1,2}\mathcal{K}^{L,t_{3,4}}_{3,4}(v,\theta)\\
=&R_{1,4}(-u+v-\theta)R_{1,3}(-u+v)R_{2,4}(-u+v)R_{2,3}(-u+v+\theta)\\
&\times\left(P_{1,2}K^L_2(u-\frac{\theta}{2})M_1R_{1,2}(-2u-2\eta)M^{-1}_1K^L_1(u+\frac{\theta}{2})\right)^{t_1t_2}M^{-1}_1M^{-1}_2\\
&\times R_{3,2}(-u-v-2\eta-\theta)R_{3,1}(-u-v-2\eta)R_{4,2}(-u-v-2\eta)R_{4,1}(-u-v-2\eta+\theta)\\
&\times M_1M_2\left(P_{3,4}K^L_4(v-\frac{\theta}{2})M_3R_{3,4}(-2v-2\eta)M^{-1}_3K^L_3(v+\frac{\theta}{2})\right)^{t_3t_4}.
\end{aligned}
$$

Resolving the transpositions and reordering the permutation operators gives

$$
\begin{aligned}
&\mathcal{R}_{1,2|3,4}(-u+v,-\theta,-\theta)\mathcal{K}^{L,t_{1,2}}_{1,2}(u,\theta)\mathcal{M}^{-1}_{1,2}\mathcal{R}_{3,4|1,2}(-u-v-2\eta,-\theta,-\theta)\mathcal{M}_{1,2}\mathcal{K}^{L,t_{3,4}}_{3,4}(v,\theta)\\
=&P_{3,4}R_{1,3}(-u+v-\theta)R_{1,4}(-u+v)R_{2,3}(-u+v)R_{2,4}(-u+v+\theta)\\
&\times\left(K^L_1\left(u+\frac{\theta}{2}\right)\right)^{t_1}M^{-1}_1R_{2,1}(-2u-2\eta)M_1\left(K^L_2\left(u-\frac{\theta}{2}\right)\right)^{t_2}M^{-1}_1M^{-1}_2\\
&\times R_{4,1}(-u-v-2\eta-\theta)R_{4,2}(-u-v-2\eta)R_{3,1}(-u-v-2\eta)R_{3,2}(-u-v-2\eta+\theta)\\
&\times M_1M_2\left(K^L_4\left(v+\frac{\theta}{2}\right)\right)^{t_4}M^{-1}_4R_{3,4}(-2v-2\eta)M_4\left(K^L_3\left(v-\frac{\theta}{2}\right)\right)^{t_3}P_{1,2}.
\end{aligned}
$$

From now on, we present also the graphical proof for maximal clarity:
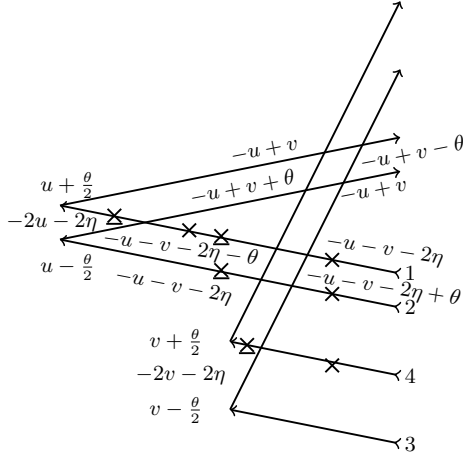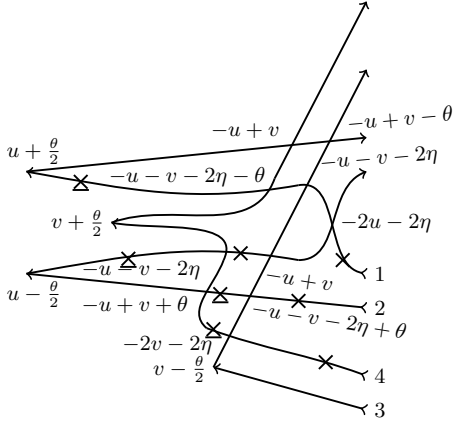
$$
\begin{aligned}
= & P_{3,4} R_{1,3}(-u+v-\theta) R_{1,4}(-u+v) R_{2,3}(-u+v) \\
& \times R_{2,4}(-u+v+\theta) \left(K_1^L \left(u+\frac{\theta}{2} \right) \right)^{t_1} M_1^{-1} \\
& \times R_{2,1}(-2u-2\eta) M_1 \left(K_2^L \left(u-\frac{\theta}{2} \right) \right)^{t_2} \\
& \times M_1^{-1} M_2^{-1} R_{4,1}(-u-v-2\eta-\theta) \\
& \times R_{4,2}(-u-v-2\eta) R_{3,1}(-u-v-2\eta) \\
& \times R_{3,2}(-u-v-2\eta+\theta) M_1 M_2 \left(K_4^L \left(v+\frac{\theta}{2} \right) \right)^{t_4} \\
& \times M_4^{-1} R_{3,4}(-2v-2\eta) M_4 \left(K_3^L \left(v-\frac{\theta}{2} \right) \right)^{t_3} P_{1,2}.
\end{aligned}
$$

Cancelling the operator insertions gives
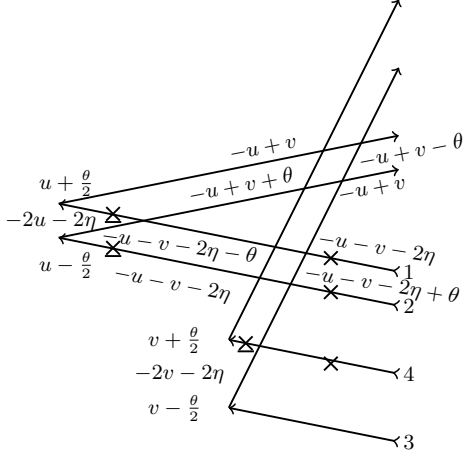
$$
\begin{aligned}
= & P_{3,4} R_{1,3}(-u+v-\theta) R_{1,4}(-u+v) R_{2,3}(-u+v) \\
& \times R_{2,4}(-u+v+\theta) \left(K_1^L \left(u+\frac{\theta}{2} \right) \right)^{t_1} M_1^{-1} \\
& \times R_{2,1}(-2u-2\eta) \left(K_2^L \left(u-\frac{\theta}{2} \right) \right)^{t_2} \\
& \times M_2^{-1} R_{4,1}(-u-v-2\eta-\theta) \\
& \times R_{4,2}(-u-v-2\eta) R_{3,1}(-u-v-2\eta) \\
& \times R_{3,2}(-u-v-2\eta+\theta) M_1 M_2 \left(K_4^L \left(v+\frac{\theta}{2} \right) \right)^{t_4} \\
& \times M_4^{-1} R_{3,4}(-2v-2\eta) M_4 \left(K_3^L \left(v-\frac{\theta}{2} \right) \right)^{t_3} P_{1,2}.
\end{aligned}
$$

Using the YBE to pass the weight $-2u-2\eta$ to the right side gives
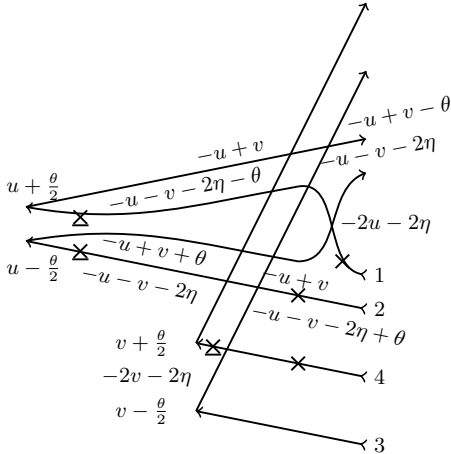
$$
\begin{aligned}
= & P_{3,4} R_{1,3}(-u+v-\theta) R_{1,4}(-u+v) \left(K_1^L (u+\frac{\theta}{2}) \right)^{t_1} \\
& \times M_1^{-1} R_{4,1}(-u-v-2\eta-\theta) R_{3,1}(-u-v-2\eta) \\
& \times R_{2,1}(-2u-2\eta) R_{2,3}(-u+v) R_{2,4}(-u+v+\theta) \\
& \times \left(K_2^L \left(u-\frac{\theta}{2} \right) \right)^{t_2} M_2^{-1} R_{4,2}(-u-v-2\eta) \\
& \times R_{3,2}(-u-v-2\eta+\theta) M_1 M_2 \left(K_4^L \left(v+\frac{\theta}{2} \right) \right)^{t_4} \\
& \times M_4^{-1} R_{3,4}(-2v-2\eta) M_4 \left(K_3^L \left(v-\frac{\theta}{2} \right) \right)^{t_3} P_{1,2}.
\end{aligned}
$$

Using the reflection algebra (2.116) and moving the K^L-matrix with weight $v+\theta/2$ upwards, we obtain:

144

$$
\begin{aligned}
= & P_{3,4}R_{1,3}(-u+v-\theta)R_{1,4}(-u+v)\left(K_1^L(u+\tfrac{\theta}{2})\right)^{t_1} \\
& \times M_1^{-1}R_{4,1}(-u-v-2\eta-\theta)R_{3,1}(-u-v-2\eta) \\
& \times R_{2,1}(-2u-2\eta)R_{2,3}(-u+v)\left(K_4^L\left(v+\tfrac{\theta}{2}\right)\right)^{t_4} \\
& \times M_2R_{2,4}(-u-v-2\eta)M_2^{-1}\left(K_2^L\left(u-\tfrac{\theta}{2}\right)\right)^{t_2} \\
& \times R_{4,2}(-u+v+\theta)M_2^{-1}R_{3,2}(-u-v-2\eta+\theta)M_1 \\
& \times M_2M_4^{-1}R_{3,4}(-2v-2\eta)M_4\left(K_3^L\left(v-\tfrac{\theta}{2}\right)\right)^{t_3}P_{1,2}\,.
\end{aligned}
$$

Using (2.116) again this yields:
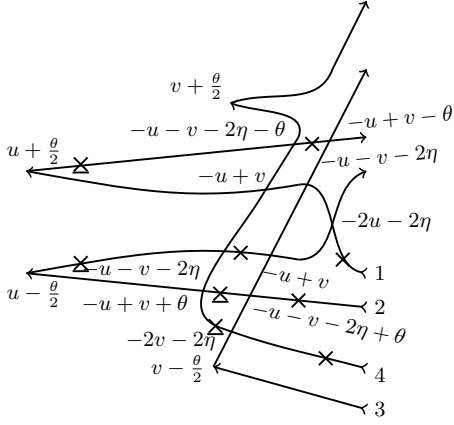
$$
\begin{aligned}
= & P_{3,4}R_{1,3}(-u+v-\theta)\left(K_4^L\left(v+\tfrac{\theta}{2}\right)\right)^{t_4}M_1 \\
& \times R_{1,4}(-u-v-2\eta-\theta)M_1^{-1}\left(K_1^L\left(u+\tfrac{\theta}{2}\right)\right)^{t_1} \\
& \times R_{4,1}(-u+v)M_1^{-1}R_{3,1}(-u-v-2\eta) \\
& \times R_{2,1}(-2u-2\eta)R_{2,3}(-u+v) \\
& \times M_2R_{2,4}(-u-v-2\eta)M_2^{-1}\left(K_2^L\left(u-\tfrac{\theta}{2}\right)\right)^{t_2} \\
& \times R_{4,2}(-u+v+\theta)M_2^{-1}R_{3,2}(-u-v-2\eta+\theta)M_1 \\
& \times M_2M_4^{-1}R_{3,4}(-2v-2\eta)M_4\left(K_3^L\left(v-\tfrac{\theta}{2}\right)\right)^{t_3}P_{1,2}\,.
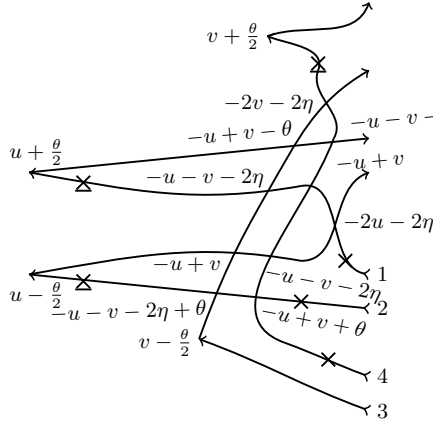\end{aligned}
$$

Reshuffling the operator insertions by using the invariance of the R-matrix under M, we get
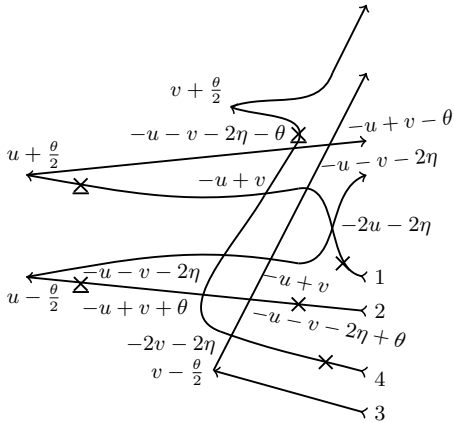
$$
\begin{aligned}
= & P_{3,4}R_{1,3}(-u+v-\theta)\left(K_4^L\left(v+\tfrac{\theta}{2}\right)\right)^{t_4}M_4^{-1} \\
& \times R_{1,4}(-u-v-2\eta-\theta)\left(K_1^L\left(u+\tfrac{\theta}{2}\right)\right)^{t_1}M_1^{-1} \\
& \times R_{4,1}(-u+v)R_{3,1}(-u-v-2\eta)R_{2,1}(-2u-2\eta) \\
& \times R_{2,3}(-u+v)R_{2,4}(-u-v-2\eta)\left(K_2^L\left(u-\tfrac{\theta}{2}\right)\right)^{t_2} \\
& \times M_2^{-1}R_{4,2}(-u+v+\theta)R_{3,2}(-u-v-2\eta+\theta) \\
& \times M_1M_2R_{3,4}(-2v-2\eta)M_4\left(K_3^L\left(v-\tfrac{\theta}{2}\right)\right)^{t_3}P_{1,2}\,.
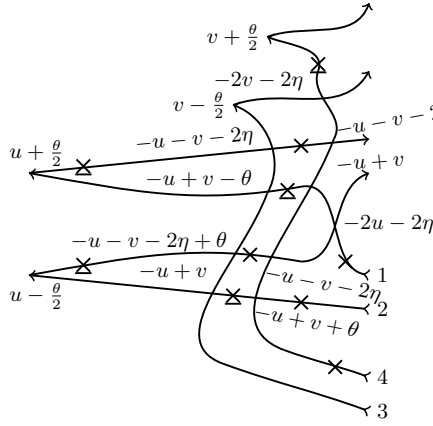\end{aligned}
$$

By using the YBE to bring the weight $-2v-2\eta$ to the top we obtain:

$$
\begin{aligned}
=P_{3,4}\left(K_4^L\left(v+\frac{\theta}{2}\right)\right)^{t_4}&M_4^{-1}R_{3,4}(-2v-2\eta)\\
\times\;& R_{1,4}(-u-v-2\eta-\theta)R_{1,3}(-u+v-\theta)\\
\times\;&\left(K_1^L(u+\frac{\theta}{2})\right)^{t_1}M_1^{-1}R_{3,1}(-u-v-2\eta)R_{4,1}(-u+v)\\
\times\;& R_{2,1}(-2u-2\eta)R_{2,4}(-u-v-2\eta)R_{2,3}(-u+v)\\
\times\;&\left(K_2^L\left(u-\frac{\theta}{2}\right)\right)^{t_2}M_2^{-1}R_{3,2}(-u-v-2\eta+\theta)\\
\times\;& R_{4,2}(-u+v+\theta)M_1M_2M_4\left(K_3^L\left(v-\frac{\theta}{2}\right)\right)^{t_3}P_{1,2}\,.
\end{aligned}
$$

Similar as above we use the reflection algebra (2.116) twice to get
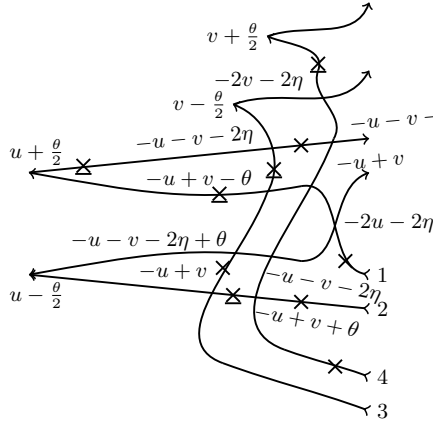

$$
\begin{aligned}
=P_{3,4}\left(K_4^L\left(v+\frac{\theta}{2}\right)\right)^{t_4}&M_4^{-1}R_{3,4}(-2v-2\eta)\\
\times\;&\left(K_3^L\left(v-\frac{\theta}{2}\right)\right)^{t_3}R_{1,4}(-u-v-2\eta-\theta)M_1\\
\times\;& R_{1,3}(-u-v-2\eta)M_1^{-1}\left(K_1^L(u+\frac{\theta}{2})\right)^{t_1}R_{3,1}(-u+v-\theta)\\
\times\;& M_1^{-1}R_{4,1}(-u+v)R_{2,1}(-2u-2\eta)R_{2,4}(-u-v-2\eta)\\
\times\;& M_2R_{2,3}(-u-v-2\eta+\theta)M_2^{-1}\left(K_2^L\left(u-\frac{\theta}{2}\right)\right)^{t_2}\\
\times\;& R_{3,2}(-u+v)M_2^{-1}R_{4,2}(-u+v+\theta)M_1M_2M_4P_{1,2}\,.
\end{aligned}
$$

We reshuffle the operator insertions again to obtain:

$$
\begin{aligned}
=P_{3,4}\left(K_4^L\left(v+\frac{\theta}{2}\right)\right)^{t_4}&M_4^{-1}R_{3,4}(-2v-2\eta)\\
\times\;&\left(K_3^L\left(v-\frac{\theta}{2}\right)\right)^{t_3}R_{1,4}(-u-v-2\eta-\theta)M_1\\
\times\;& R_{1,3}(-u-v-2\eta)M_1^{-1}\left(K_1^L\left(u+\frac{\theta}{2}\right)\right)^{t_1}M_1^{-1}\\
\times\;& M_3^{-1}R_{3,1}(-u+v-\theta)R_{4,1}(-u+v)R_{2,1}(-2u-2\eta)\\
\times\;& R_{2,4}(-u-v-2\eta)R_{2,3}(-u-v-2\eta+\theta)\\
\times\;& M_3\left(K_2^L\left(u-\frac{\theta}{2}\right)\right)^{t_2}R_{3,2}(-u+v)M_2^{-1}\\
\times\;& R_{4,2}(-u+v+\theta)M_1M_2M_4P_{1,2}\,.
\end{aligned}
$$

Now, we can use the YBE to bring the weight $-2u-2\eta$ back to the left.
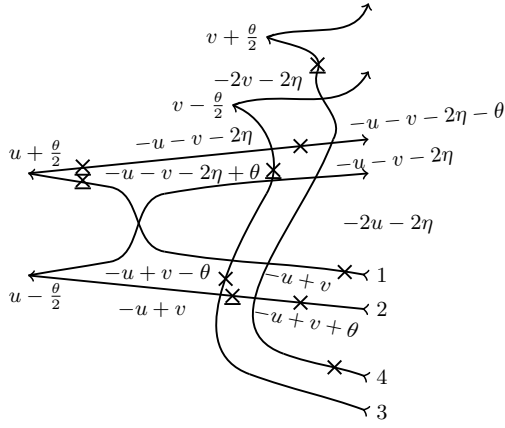
$$=P_{3,4}\left(K_4^L\left(v+\frac{\theta}{2}\right)\right)^{t_4}M_4^{-1}R_{3,4}(-2v-2\eta)$$

$$\times\left(K_3^L\left(v-\frac{\theta}{2}\right)\right)^{t_3}R_{1,4}(-u-v-2\eta-\theta)M_1$$

$$\times R_{1,3}(-u-v-2\eta)M_1^{-1}\left(K_1^L\left(u+\frac{\theta}{2}\right)\right)^{t_1}M_1^{-1}$$

$$\times M_3^{-1}R_{2,4}(-u-v-2\eta)R_{2,3}(-u-v-2\eta+\theta)$$

$$\times R_{2,1}(-2u-2\eta)R_{3,1}(-u+v-\theta)R_{4,1}(-u+v)$$

$$\times M_3\left(K_2^L\left(u-\frac{\theta}{2}\right)\right)^{t_2}R_{3,2}(-u+v)M_2^{-1}$$
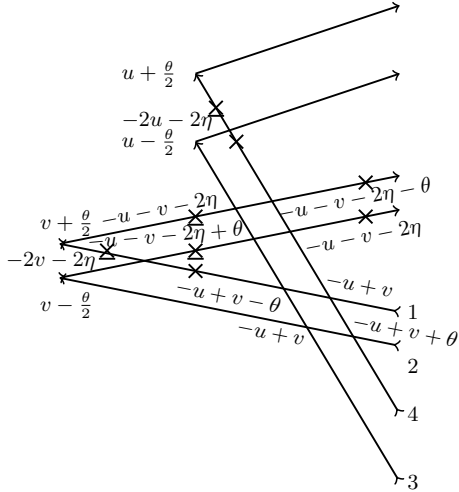
$$\times R_{4,2}(-u+v+\theta)M_1M_2M_4P_{1,2}\,.$$

Now we reshuffle the operator insertion a last time to finally obtain:

$$=P_{3,4}\left(K_4^L\left(v+\frac{\theta}{2}\right)\right)^{t_4}M_4^{-1}R_{3,4}(-2v-2\eta)M_4$$

$$\times\left(K_3^L\left(v-\frac{\theta}{2}\right)\right)^{t_3}M_1M_2R_{1,4}(-u-v-2\eta-\theta)$$

$$\times R_{1,3}(-u-v-2\eta)R_{2,4}(-u-v-2\eta)$$

$$\times R_{2,3}(-u-v-2\eta+\theta)M_1^{-1}M_2^{-1}\left(K_1^L\left(u+\frac{\theta}{2}\right)\right)^{t_1}$$

$$\times M_1^{-1}R_{2,1}(-2u-2\eta)M_1\left(K_2^L\left(u-\frac{\theta}{2}\right)\right)^{t_2}$$

$$\times R_{3,1}(-u+v-\theta)R_{4,1}(-u+v)M_3R_{3,2}(-u+v)$$

$$\times R_{4,2}(-u+v+\theta)M_1M_2M_4P_{1,2}\,.$$

Now we proceed algebraically. We reorder the permutation operators

$$\mathcal{R}_{1,2|3,4}(-u+v,-\theta,-\theta)\mathcal{K}_{1,2}^{L,t_{1,2}}(u,\theta)\mathcal{M}_{1,2}^{-1}\mathcal{R}_{3,4|1,2}(-u-v-2\eta,-\theta,-\theta)\mathcal{M}_{1,2}\mathcal{K}_{3,4}^{L,t_{3,4}}(v,\theta)$$

$$=\left(K_3^L(v+\frac{\theta}{2})\right)^{t_3}M_3^{-1}R_{4,3}(-2v-2\eta)M_3\left(K_4^L(v-\frac{\theta}{2})\right)^{t_4}P_{3,4}M_1M_2$$

$$\times R_{1,4}(-u-v-2\eta-\theta)R_{1,3}(-u-v-2\eta)R_{2,4}(-u-v-2\eta)R_{2,3}(-u-v-2\eta+\theta)$$

$$\times M_1^{-1}M_2^{-1}\left(K_1^L\left(u+\frac{\theta}{2}\right)\right)^{t_1}M_1^{-1}R_{2,1}(-2u-2\eta)M_1\left(K_2^L\left(u-\frac{\theta}{2}\right)\right)^{t_2}P_{1,2}$$

$$\times R_{3,2}(-u+v-\theta)R_{4,2}(-u+v)M_3R_{3,1}(-u+v)R_{4,1}(-u+v+\theta)M_1M_2M_4\,,$$

and reintroduce the transposition, while using (2.103) to obtain

$$\mathcal{R}_{1,2|3,4}(-u+v,-\theta,-\theta)\mathcal{K}_{1,2}^{L,t_{1,2}}(u,\theta)\mathcal{M}_{1,2}^{-1}\mathcal{R}_{3,4|1,2}(-u-v-2\eta,-\theta,-\theta)\mathcal{M}_{1,2}\mathcal{K}_{3,4}^{L,t_{3,4}}(v,\theta)$$

$$=\left(P_{3,4}K_4^L(v-\frac{\theta}{2})M_3R_{3,4}(-2v-2\eta)M_3^{-1}K_3^L(v+\frac{\theta}{2})\right)^{t_3t_4}M_1M_2$$

$$\times R_{1,4}(-u-v-2\eta-\theta)R_{1,3}(-u-v-2\eta)R_{2,4}(-u-v-2\eta)R_{2,3}(-u-v-2\eta+\theta)$$

$$\times M_1^{-1}M_2^{-1}\left(P_{1,2}K_2^L(u-\frac{\theta}{2})M_1R_{1,2}(-2u-2\eta)M_1^{-1}K_1^L(u+\frac{\theta}{2})\right)^{t_1,t_2}$$

$$\times R_{3,2}(-u+v-\theta)R_{4,2}(-u+v)M_3R_{3,1}(-u+v)R_{4,1}(-u+v+\theta)M_1M_2M_4$$

$$=\mathcal{K}_{3,4}^{L,t_{3,4}}(v,\theta)\mathcal{M}_{1,2}\mathcal{R}_{3,4|1,2}(-u-v-2\eta,-\theta,-\theta)\mathcal{M}_1^{-1}\mathcal{K}_{1,2}^{L,t_{1,2}}(u,\theta)\mathcal{R}_{1,2|3,4}(-u+v,-\theta,-\theta),$$

which completes the proof.

C | Expressions (4.30) and (4.181) in Pauli matrices

This appendix recalls some results of the author's works [31] and [32].

The expression for $\mathbb{H}$

The Hamiltonian (4.30) reads in terms of the Pauli-matrices σ_j^α:

$$
U_{\mathcal{H}}^{odd}(-\mathrm{i}\alpha)\mathbb{H}U_{\mathcal{H}}^{odd}(\mathrm{i}\alpha) = -\frac{1}{2\sin(\gamma)\xi(-\mathrm{i}\alpha)\xi(\mathrm{i}\alpha)}\Bigg\{
$$

$$
-2\sin^2(\gamma)\sum_{j=1}^{2L-1}\cos(\gamma)\sigma_j^z\sigma_{j+1}^z + 2\cos(\alpha)(\sigma_j^+\sigma_{j+1}^- + \sigma_j^-\sigma_{j+1}^+)
$$

$$
+\cos(\gamma)\sin^2(\alpha)\sum_{j=1}^{2L-2}\sigma_j^z\sigma_{j+2}^z + 2(\sigma_j^+\sigma_{j+2}^- + \sigma_j^-\sigma_{j+2}^+)
$$

$$
+\sin(\alpha)\sin(2\gamma)\sum_{j=1}^{2L-2}(-1)^{j+1}\sigma_j^z\sigma_{j+1}^+\sigma_{j+2}^- + (-1)^j\sigma_j^z\sigma_{j+1}^-\sigma_{j+2}^+
$$

$$
+\sin(\alpha)\sin(2\gamma)\sum_{j=1}^{2L-2}(-1)^{j+1}\sigma_j^+\sigma_{j+1}^-\sigma_{j+2}^z + (-1)^j\sigma_j^-\sigma_{j+1}^+\sigma_{j+2}^z
$$

$$
+\sin(\gamma)\sin(2\alpha)\sum_{j=1}^{2L-2}(-1)^{j+1}\sigma_j^-\sigma_{j+1}^z\sigma_{j+2}^+ + (-1)^j\sigma_j^+\sigma_{j+1}^z\sigma_{j+2}^-
$$

$$
+\cos(\gamma)\sin^2(\alpha)(\sigma_1^z\sigma_2^z + \sigma_{2L-1}^z\sigma_{2L}^z)
$$

$$
+\mathrm{i}(\sin(\alpha)\cos(2\gamma) - \sin(\alpha)e^{2\mathrm{i}\alpha})(\sigma_1^+\sigma_2^- + \sigma_{2L-1}^+\sigma_{2L}^-)
$$

$$
-\mathrm{i}(\sin(\alpha)\cos(2\gamma) - \sin(\alpha)e^{-2\mathrm{i}\alpha})(\sigma_1^-\sigma_2^+ + \sigma_{2L-1}^-\sigma_{2L}^+)
$$

$$
+2\mathrm{i}\xi(\mathrm{i}\alpha)\xi(-\mathrm{i}\alpha)\sin(\gamma)(\sigma_1^z - \sigma_{2L}^z)
$$

$$
+\cos(\gamma)(L\cos(2\alpha) + (1-2L)\cos(2\gamma) + L - 1)\Bigg\}
$$

$$\tag{C.1}$$

where $U_{\mathcal{H}}^{odd}(\mathrm{i}\alpha)$ is the rotation of the spin variables on the odd lattice sites by $-\mathrm{i}\alpha$ in the x,y-spin plane

$$
U_{\mathcal{H}}^{odd}(\mathrm{i}\alpha)\,\sigma_{2j-1}^\pm\,U_{\mathcal{H}}^{odd}(-\mathrm{i}\alpha) = e^{\mp\mathrm{i}\alpha}\sigma_{2j-1}^\pm, \qquad j = 1,...,L. \tag{C.2}
$$

The expression for $\bar{\bar{\mathbb{B}}}^{qp}$

The quasi-momentum (4.181) in terms of the Pauli-matrices σ_j^α reads:

$$
\begin{aligned}
\overline{\mathbb{Q}}^{\text{qp}} = \Bigg\{ & 2\cos(\gamma)\left(\sum_{j=1}^{2L-2}(\sigma_j^-\sigma_{j+1}^+\sigma_{j+2}^z - \sigma_j^+\sigma_{j+1}^-\sigma_{j+2}^z + \sigma_j^z\sigma_{j+1}^-\sigma_{j+2}^+ - \sigma_j^z\sigma_{j+1}^+\sigma_{j+2}^-)\right) \\
& + \frac{\cos(\gamma)}{\sin(\gamma)}\left(\sum_{j=1}^{2L-2}(-1)^j(2(\sigma_{j+2}^-\sigma_j^+ + \sigma_{j+2}^+\sigma_j^-) + \sigma_j^z\sigma_{j+2}^z)\right) \\
& - 2\mathrm{i}\sin(\gamma)(\sigma_1^+\sigma_2^- - \sigma_1^-\sigma_2^+) + 2\mathrm{i}\sin(\gamma)(\sigma_{2L}^-\sigma_{2L-1}^+ - \sigma_{2L}^+\sigma_{2L-1}^-) \\
& - \mathrm{i}\sigma_1^z + \mathrm{i}\sigma_2^z + \mathrm{i}\sigma_{2L-1}^z - \mathrm{i}\sigma_{2L}^z \Bigg\} \frac{1}{\mathrm{i}\cos^2(\gamma)} \,.
\end{aligned}
\tag{C.3}
$$

D | ASYMPTOTIC COEFFICIENTS $\mathfrak{C}_{p,s}^{(\pm)}$

In this appendix, which is based on [34], we recall a closed form expression for the coefficients $\mathfrak{C}_{p,s}^{(\pm)}(\boldsymbol{w})$ that has been obtained in the work [133]. This is of particular interest as they enter into the quantization condition (4.108a), (4.108b). It is

$$\mathfrak{C}_{p,s}^{(\pm)}(\boldsymbol{w}) = \mathfrak{C}_{p,s}^{(0,\pm)} \, \check{\mathfrak{C}}_{p,s}^{(\pm)}(\boldsymbol{w}) \, , \tag{D.1}$$

where we have

$$\mathfrak{C}_{p,s}^{(0,\pm)} = \sqrt{\frac{2\pi}{n+2}} \quad 2^{-p \pm \frac{\mathrm{i}(n+2)s}{n}} \, (n+2)^{-\frac{2p}{n+2}} \, \frac{\Gamma(1+2p)}{\Gamma(1+\frac{2p}{n+2}) \, \Gamma(\frac{1}{2}+p\pm\mathrm{i}s)} \, . \tag{D.2}$$

This is the coefficient for $\mathtt{d} = 0$. In the more general case, they can be computed via the determinant of the $\mathtt{d} \times \mathtt{d}$ matrix:

$$\check{\mathfrak{C}}_{p,s}^{(\pm)}(\boldsymbol{w}) = \frac{(\mp 1)^{\mathtt{d}} \, \det\left(w_a^{b-1} \, U_a^{(\pm)}(b)\right)}{\prod_{a=1}^{\mathtt{d}} w_a \, \prod_{b>a}(w_b - w_a) \, \prod_{a=1}^{\mathtt{d}} \left(2p+2a-1\pm 2\mathrm{i}s\right)} \tag{D.3}$$

where

$$\begin{aligned} U_a^{(\pm)}(D) = \quad & (D-1)^2 - \left(2p+2+n\mp 2w_a + \sum_{b\neq a}^{\mathtt{d}} \frac{4w_a}{w_a - w_b}\right)(D-1) \\ + \quad & \tfrac{1}{2}\,n^2 + \left(p+\tfrac{3}{2}\right) n \mp (n+1+2p+2\mathrm{i}s)\, w_a + 2p+1 \\ + \quad & \left(\sum_{b\neq a}^{\mathtt{d}} \frac{2w_a}{w_a - w_b}\right)^2 + \left(2\left(2p+1+n\mp 2w_a\right)-n\right) \sum_{b\neq a}^{\mathtt{d}} \frac{w_a}{w_a - w_b} \, . \end{aligned} \tag{D.4}$$

E | BAE for the twisted $D_3^{(2)}$ model

This appendix is based on [33].

In this appendix, we sketch a derivation of the result (6.20) for the eigenvalue $t(u)$ of the twisted transfer matrix. The starting point is the known [146] eigenvalue of the periodic transfer matrix

$$
t(u)\Big|_{\phi_1=\phi_2=0} = (4\sinh(u-2\mathrm{i}\gamma)\sinh(u-4\mathrm{i}\gamma))^L A(u) + (4\sinh(u-4\mathrm{i}\gamma)\sinh u)^L \sum_{\ell=1}^4 B_\ell(u)
$$
$$
+ (4\sinh(u-2\mathrm{i}\gamma)\sinh u)^L C(u) ,
$$
$$(E.1)$$

where the explicit form of $A(u), B_\ell(u), C(u)$ is presented in (6.21).

Following the work [146], we apply the analytic Bethe ansatz. The monodromy matrix possesses the asymptotic behaviour

$$
\mathcal{M}(u) \underset{u\to\infty}{\sim} (\mathrm{e}^{2u-4\mathrm{i}\gamma})^L \left\{ \mathrm{diag}\left(\mathrm{e}^{-2\mathrm{i}\gamma\mathbb{h}_1}, \mathrm{e}^{-2\mathrm{i}\gamma\mathbb{h}_2}, \mathbf{1}, \mathbf{1}, \mathrm{e}^{2\mathrm{i}\gamma\mathbb{h}_2}, \mathrm{e}^{2\mathrm{i}\gamma\mathbb{h}_1} \right) + \ldots \right\} \qquad (E.2)
$$

where the ellipsis stands for unimportant off-diagonal terms. From this, we know that the twisted transfer matrix (6.8) develops the following asymptotic behaviour

$$
\mathbb{t}(u) \underset{u\to\infty}{\sim} (\mathrm{e}^{2u-4\mathrm{i}\gamma})^L \left\{ 2\,\mathbf{1} + \sum_{j=1}^2 \left(\mathrm{e}^{\mathrm{i}\phi_j}\mathrm{e}^{-2\mathrm{i}\gamma\mathbb{h}_j} + \mathrm{e}^{-\mathrm{i}\phi_j}\mathrm{e}^{2\mathrm{i}\gamma\mathbb{h}_j} \right) + \ldots \right\} . \qquad (E.3)
$$

Let us now make the following ansatz for the eigenvalue $t(u)$:

$$
t(u) = (4\sinh(u-2\mathrm{i}\gamma)\sinh(u-4\mathrm{i}\gamma))^L \, a\, A(u) + (4\sinh(u-4\mathrm{i}\gamma)\sinh u)^L \sum_{\ell=1}^4 b_\ell \, B_\ell(u)
$$
$$
+ (4\sinh(u-2\mathrm{i}\gamma)\sinh u)^L \, c\, C(u) \qquad (E.4)
$$

where the parameters a, b_ℓ, c are yet unknown. Denote by $|\Psi\rangle$ a normalised eigenstate of the transfer matrix, which is also an eigenstate of the $U(1)$ charges (6.10) with eigenvalues h_1 and h_2. We obviously have

$$
\langle\Psi|\mathbb{t}(u)|\Psi\rangle = t(u) . \qquad (E.5)
$$

We can determine the asymptotic behaviour for $u \to \infty$ of the LHS of (E.5) by keeping in mind (E.3):

$$\langle \Psi | \mathfrak{t}(u) | \Psi \rangle \underset{u \to \infty}{\sim} (\mathrm{e}^{2u-4\mathrm{i}\gamma})^L \Big\{ \mathrm{e}^{\mathrm{i}\phi_1} \mathrm{e}^{-2\mathrm{i}\gamma(L-m_1)} + \mathrm{e}^{\mathrm{i}\phi_2} \mathrm{e}^{-2\mathrm{i}\gamma(m_1-m_2)}$$
$$+ 2 + \mathrm{e}^{-\mathrm{i}\phi_1} \mathrm{e}^{2\mathrm{i}\gamma(L-m_1)} + \mathrm{e}^{-\mathrm{i}\phi_2} \mathrm{e}^{2\mathrm{i}\gamma(m_1-m_2)} \Big\}. \tag{E.6}$$

We can evaluate the RHS of (E.5) using (E.4)

$$t(u) \underset{u \to \infty}{\sim} (\mathrm{e}^{2u-4\mathrm{i}\gamma})^L \Big\{ a\, \mathrm{e}^{-2\mathrm{i}\gamma(L-m_1)} + b_1\, \mathrm{e}^{-2\mathrm{i}\gamma(m_1-m_2)}$$
$$+ b_2 + b_3 + b_4\, \mathrm{e}^{2\mathrm{i}\gamma(m_1-m_2)} + c\, \mathrm{e}^{2\mathrm{i}\gamma(L-m_1)} \Big\}. \tag{E.7}$$

A comparison of (E.6) and (E.7), suggests the relations

$$a = \mathrm{e}^{\mathrm{i}\phi_1}, \quad b_1 = \mathrm{e}^{\mathrm{i}\phi_2}, \quad b_2 = b_3 = 1, \quad b_4 = \mathrm{e}^{-\mathrm{i}\phi_2}, \quad c = \mathrm{e}^{-\mathrm{i}\phi_1}, \tag{E.8}$$

which is the result given in (6.20).

F | SYMMETRIES OF THE $D_3^{(2)}$ MODEL

This appendix is based on [33].

We briefly discuss here the proofs for a couple of the symmetries in the $D_3^{(2)}$ model noted in chapter 6.

F.1 CROSSING SYMMETRY (6.12)

To prove that $\mathbb{t}(u)$ given in (6.8) has the crossing symmetry (6.12), we start with the *transposed* transfer matrix

$$
\begin{aligned}
\mathbb{t}^t(u; \{\phi_j\}) &= \mathrm{tr}_0 \ (\mathbb{K}_0(\{\phi_j\}) \, \mathbb{R}_{0L}(u) \dots \mathbb{R}_{01}(u))^{t_0 t_1 \cdots t_L} \\
&= \mathrm{tr}_0 \, \mathbb{R}_{01}^{t_0 t_1}(u) \cdots \mathbb{R}_{0L}^{t_0 t_L}(u) \, \mathbb{K}_0^{t_0}(\{\phi_j\}) \\
&= \mathrm{tr}_0 \, \mathbb{K}_0(\{\phi_j\}) \, \mathbb{R}_{10}(u) \cdots \mathbb{R}_{L0}(u) \, .
\end{aligned}
\tag{F.1}
$$

Here, we have applied the PT-symmetry and the fact that the twist matrix (6.7) is symmetric, i.e. $\mathbb{K}^t = \mathbb{K}$, to reach the third line. Note that the transfer matrix itself can be rewritten as

$$
\begin{aligned}
\mathbb{t}(u; \{\phi_j\}) &= \mathrm{tr}_0 \ (\mathbb{K}_0(\{\phi_j\}) \, \mathbb{R}_{0L}(u) \dots \mathbb{R}_{01}(u))^{t_0} \\
&= \mathrm{tr}_0 \, \mathbb{R}_{01}^{t_0}(u) \cdots \mathbb{R}_{0L}^{t_0}(u) \, \mathbb{K}_0^{t_0}(\{\phi_j\}) \\
&= \mathrm{tr}_0 \, V_0^{t_0} \, \mathbb{R}_{10}(4\mathrm{i}\gamma - u) \, V_0^{t_0} \cdots V_0^{t_0} \, \mathbb{R}_{L0}(4\mathrm{i}\gamma - u) \, V_0^{t_0} \, \mathbb{K}_0(\{\phi_j\}) \\
&= \mathrm{tr}_0 \, \mathbb{K}_0(\{-\phi_j\}) \, \mathbb{R}_{10}(4\mathrm{i}\gamma - u) \cdots \mathbb{R}_{L0}(4\mathrm{i}\gamma - u) \\
&= \mathbb{t}^t(4\mathrm{i}\gamma - u; \{-\phi_j\}) \, .
\end{aligned}
\tag{F.2}
$$

To reach the third line, we again used the PT- and the crossing symmetry. The fourth equality is obtained by using the fact that

$$
V \, \mathbb{K}(\{\phi_j\}) = \mathbb{K}(\{-\phi_j\}) \, V \, .
\tag{F.3}
$$

Finally, for the last line of (F.2), we applied the result (F.1).

F.2 $W(0)$ SYMMETRY (6.15)

The conjugate action of $W(0)^{\otimes L}$ on the transfer matrix (6.8) yields

$$
\begin{aligned}
W(0)^{\otimes L}\,\mathbb{t}(u;\phi_1,\phi_2)\,W(0)^{\otimes L} &= W(0)^{\otimes L}\,\mathrm{tr}_0\,\left(\mathbb{K}_0(\phi_1,\phi_2)\,\mathbb{R}_{0L}(u)\ldots\mathbb{R}_{01}(u)\,\right)W(0)^{\otimes L} \\
&= \mathrm{tr}_0\,\mathbb{K}_0(\phi_1,\phi_2)\,W_L(0)\,\mathbb{R}_{0L}(u)\,W_L(0)\,\ldots W_1(0)\,\mathbb{R}_{01}(u)\,W_1(0) \\
&= \mathrm{tr}_0\,\mathbb{K}_0(\phi_1,\phi_2)\,W_0(u)\,\mathbb{R}_{0L}(u)\,W_0(u)\,\ldots W_0(u)\,\mathbb{R}_{01}(u)\,W_0(u) \\
&= \mathrm{tr}_0\,\mathbb{K}_0(-\phi_2,-\phi_1)\,\mathbb{R}_{0L}(u)\,\ldots\,\mathbb{R}_{01}(u) \\
&= \mathbb{t}(u;-\phi_2,-\phi_1)\,.
\end{aligned}
\tag{F.4}
$$

To reach the third line, we used (6.6), and to obtain the fourth equality, we have taken the following fact into account

$$
W(u)\,\mathbb{K}(\phi_1,\phi_2)\,W(u) = \mathbb{K}(-\phi_2,-\phi_1)\,.
\tag{F.5}
$$

F.3 CPT SYMMETRY (6.17)

A good starting point to prove the CPT symmetry (6.17) of the transfer matrix (6.8) is that the parity operator (6.18) acts on it as

$$
\begin{aligned}
\Pi\,\mathbb{t}(u;\{\phi_j\})\,\Pi &= \mathrm{tr}_0\,\Pi\,\left(\mathbb{K}_0(\{\phi_j\})\,\mathbb{R}_{0L}(u)\ldots\mathbb{R}_{01}(u)\right)\Pi \\
&= \mathrm{tr}_0\,\mathbb{K}_0(\{\phi_j\})\,\mathbb{R}_{01}(u)\ldots\mathbb{R}_{0L}(u)\,.
\end{aligned}
\tag{F.6}
$$

The additional conjugate action of $V^{\otimes L}$ yields

$$
\begin{aligned}
V^{\otimes L}\,\Pi\,\mathbb{t}(u;\{\phi_j\})\,\Pi\,V^{\otimes L} &= \mathrm{tr}_0\,\mathbb{K}_0(\{\phi_j\})\,V_1\,\mathbb{R}_{01}(u)\,V_1\ldots V_L\,\mathbb{R}_{0L}(u)\,V_L \\
&= \mathrm{tr}_0\,\mathbb{K}_0(\{\phi_j\})\,V_0\,\mathbb{R}_{10}(u)\,V_0\,\ldots V_0\,\mathbb{R}_{L0}(u)\,V_0 \\
&= \mathrm{tr}_0\,V_0\,\mathbb{K}_0(\{\phi_j\})\,V_0\,\mathbb{R}_{10}(u)\,\ldots\mathbb{R}_{L0}(u) \\
&= \mathrm{tr}_0\,\mathbb{K}_0(\{-\phi_j\})\,\mathbb{R}_{10}(u)\,\ldots\mathbb{R}_{L0}(u) \\
&= \mathbb{t}^t(u;\{-\phi_j\})\,,
\end{aligned}
\tag{F.7}
$$

where we used (F.3) to reach the fourth equality, and to obtain the last one, we applied (F.1).

F.4 CP SYMMETRY OF THE HAMILTONIAN (6.38)

Let us recall the expression of the Hamiltonian (6.33) after we have explicitly evaluated the derivative:

$$
\mathbb{H} \sim \mathbb{t}^{-1}(0)\,\mathbb{t}'(0) = \sum_{i=1}^{L-1} H_{i,i+1} + \mathbb{K}_L^{-1}\,H_{L,1}\,\mathbb{K}_L\,, \qquad H_{i,i+1} = P_{i,i+1}\,\mathbb{R}'_{i,i+1}(0)\,.
\tag{F.8}
$$

In the following, we will demonstrate that the bulk and boundary terms are separately invariant.

The bulk terms in (F.8) transform under parity as

$$\Pi \, H_{i,i+1} \Pi = H_{L+1-i,L-i} = P_{L+1-i,L-i} \, \mathbb{R}'_{L+1-i,L-i}(0) \,. \tag{F.9}$$

Then, the additional action of $V^{\otimes L}$ yields

$$\begin{aligned}
V^{\otimes L} \, \Pi \, H_{i,i+1} \Pi \, V^{\otimes L} &= P_{L+1-i,L-i} \, V_{L-i} \, V_{L+1-i} \, \mathbb{R}'_{L+1-i,L-i}(0) \, V_{L-i} \, V_{L+1-i} \\
&= P_{L+1-i,L-i} \, \mathbb{R}'_{L-i,L+1-i}(0) \\
&= H_{L-i,L+1-i} \,.
\end{aligned} \tag{F.10}$$

The summation over i yields

$$V^{\otimes L} \, \Pi \, \left(\sum_{i=1}^{L-1} H_{i,i+1} \right) \Pi \, V^{\otimes L} = \sum_{i=1}^{L-1} H_{L-i,L+1-i} = \sum_{j=1}^{L-1} H_{j,j+1} \,. \tag{F.11}$$

So, the bulk part is invariant under CP.

The transformation behaviour of the boundary term in (F.8) under parity is given by

$$\Pi \, \mathbb{K}_L^{-1} \, H_{L,1} \, \mathbb{K}_L \Pi = \mathbb{K}_1^{-1} \, H_{1,L} \, \mathbb{K}_1 \,. \tag{F.12}$$

Further,

$$\begin{aligned}
V^{\otimes L} \, \Pi \, \mathbb{K}_L^{-1} \, H_{L,1} \, \mathbb{K}_L \Pi \, V^{\otimes L} &= V_1 \, V_L \, \mathbb{K}_1^{-1} \, H_{1,L} \, \mathbb{K}_1 \, V_1 \, V_L \\
&= \mathbb{K}_1 \, V_1 \, V_L \, H_{1,L} \, V_1 \, V_L \, \mathbb{K}_1^{-1} \\
&= \mathbb{K}_1 \, H_{L,1} \, \mathbb{K}_1^{-1} \\
&= \mathbb{K}_L^{-1} \, H_{L,1} \, \mathbb{K}_L \,,
\end{aligned} \tag{F.13}$$

where we have used (F.3) in passing to the second line while the crossing symmetry was applied to reach the third line and to obtain the final equality, we have employed the fact that

$$[H_{L,1} \,, \mathbb{K}_L \, \mathbb{K}_1] = 0 \,. \tag{F.14}$$

So we conclude that the boundary term is also CP invariant, hence, the full Hamiltonian (F.8) is CP invariant.

Bibliography

[1] E. Ising, *Beitrag zur Theorie des Ferromagnetismus*, Z. Physik **31** (1925) 253, DOI: `10.1007/BF02980577`.

[2] R. Peierls, *On Ising's model of ferromagnetism*, Math. Proc. Cam. Phil. Soc. **32** (1936) 477, DOI: `10.1017/S0305004100019174`.

[3] H. A. Kramers, G. H. Wannier, *Statistics of the Two-Dimensional Ferromagnet. Part I*, Phys. Rev. **60** (1941) 252, DOI: `10.1103/PhysRev.60.252`.

[4] L. Onsager, *Crystal Statistics. I. A Two-Dimensional Model with an Order-Disorder Transition*, Phys. Rev. **65** (1944) 117, DOI: `10.1103/PhysRev.65.117`.

[5] A. N. Berker, L. P. Kadanoff, *Ground-state entropy and algebraic order at low temperatures*, J. Phys. A: Math. Gen. **13** (1980) L259, DOI: `10.1088/0305-4470/13/7/008`.

[6] H. Saleur, *The antiferromagnetic Potts model in two dimensions: Berker-Kadanoff phase, antiferromagnetic transition, and the role of Beraha numbers*, Nucl. Phys. B **360** (1991) 219, DOI: `10.1016/0550-3213(91)90402-J`.

[7] R. J. Baxter, *Exactly Solved Models in Statistical Mechanics*, Academic Press (1982), DOI: `10.1142/9789814415255_0002`.

[8] R. M. Nandkishore, M. Hermele, *Fractons*, Ann. Rev. Condensed Matter Phys. **10** (2019) 295, DOI: `10.1146/annurev-conmatphys-031218-013604`.

[9] B. J. Brown, D. J. Williamson, *Parallelized quantum error correction with fracton topological codes*, Phys. Rev. Res. **2** (2020) 013303, DOI: `10.1103/PhysRevResearch.2.013303`.

[10] E. Witten, *String theory and black holes*, Phys. Rev. D **44** (1991) 314, DOI: `10.1103/PhysRevD.44.314`.

[11] J. Maldacena, *The Large-N Limit of Superconformal Field Theories and Supergravity*, Int. J. Theo. Phys **38** (1999) 1113, DOI: `10.1023/A:1026654312961`.

[12] V. Schomerus, *Non-compact String Backgrounds and Non-rational CFT*, Phys. Rep. **431** (2006) 39, DOI: `10.1016/j.physrep.2006.05.001`.

[13] A. Prinsloo, V. Regelskis, A. Torrielli, *Integrable open spin-chains in AdS_3/CFT_2 correspondences*, Phys. Rev. D **92** (2015) 106006, DOI: `10.1103/PhysRevD.92.106006`.

[14] N. Bai et al., *Two-Loop Integrability of ABJM Open Spin Chain from Giant Graviton*, JHEP **03** (2019) 193, DOI: `10.1007/JHEP03(2019)193`.

[15] M. R. Zirnbauer, *The integer quantum Hall plateau transition is a current algebra after all*, Nucl. Phys. B **941** (2019) 458, DOI: 10.1016/j.nuclphysb.2019.02.017.

[16] F. Evers, A. D. Mirlin, *Anderson Transitions*, Rev. Mod. Phys. **80** (2008) 1355, DOI: 10.1103/revmodphys.80.1355.

[17] J. Teschner, *On the spectrum of the sinh-Gordon model in finite volume*, Nucl. Phys. B **799** (2008) 403, DOI: 10.1016/j.nuclphysb.2008.01.021.

[18] F. H. L. Essler, H. Frahm, H. Saleur, *Continuum limit of the integrable sl(2/1) 3-$\bar{3}$ superspin chain*, Nucl. Phys. B **712** (2005) 513, DOI: 10.1016/j.nuclphysb.2005.01.021.

[19] J. L. Jacobsen, H. Saleur, *The antiferromagnetic transition for the square-lattice Potts model*, Nucl. Phys. B **743** (2006) 207, DOI: 10.1016/j.nuclphysb.2006.02.041.

[20] Y. Ikhlef, J. L. Jacobsen, H. Saleur, *A staggered six-vertex model with non-compact continuum limit*, Nucl. Phys. B **789** (2008) 483, DOI: 10.1016/j.nuclphysb.2007.07.004.

[21] H. Frahm, M. J. Martins, *Finite size properties of staggered $U_q[sl(2|1)]$ superspin chains*, Nucl. Phys. B **847** (2011) 220, DOI: 10.1016/j.nuclphysb.2011.01.026.

[22] H. Frahm, M. J. Martins, *Phase Diagram of an Integrable Alternating $U_q[sl(2|1)]$ Superspin Chain*, Nucl. Phys. B **862** (2012) 504, DOI: 10.1016/j.nuclphysb.2012.04.019.

[23] É. Vernier, J. L. Jacobsen, H. Saleur, *Non compact conformal field theory and the $a_2^{(2)}$ (Izergin-Korepin) model in regime III*, J. Phys. A: Math. Theor **47** (2014) 285202, DOI: 10.1088/1751-8113/47/28/285202.

[24] Y. Ikhlef, J. L. Jacobsen, H. Saleur, *An integrable spin chain for the SL(2,R)/U(1) black hole sigma model*, Phys. Rev. Lett. **108** (2012) 081601, DOI: 10.1103/PhysRevLett.108.081601.

[25] V. V. Bazhanov et al., *Scaling limit of the $\mathcal{Z}_2$ invariant inhomogeneous six-vertex model*, Nucl. Phys. B **965** (2021) 115337, DOI: 10.1016/j.nuclphysb.2021.115337.

[26] N. F. Robertson et al., *Integrable boundary conditions in the antiferromagnetic Potts model*, JHEP **05** (2020) 144, DOI: 10.1007/JHEP05(2020)144.

[27] N. F. Robertson, J. L. Jacobsen, H. Saleur, *Lattice regularisation of a non-compact boundary conformal field theory*, JHEP **02** (2021) 180, DOI: 10.1007/JHEP02(2021)180.

[28] P. Dorey, R. Tateo, *Anharmonic oscillators, the thermodynamic Bethe ansatz and nonlinear integral equations*, J. Phys. A: Math. Gen. **32** (1999) L419, DOI: 10.1088/0305-4470/32/38/102.

[29] V. V. Bazhanov, S. L. Lukyanov, A. B. Zamolodchikov, Spectral determinants for Schrodinger equation and Q operators of conformal field theory, J. Stat. Mech. **102** (2001) 567, DOI: 10.1023/A:1004838616921.

[30] V. V. Bazhanov, S. L. Lukyanov, A. B. Zamolodchikov, *Higher level eigenvalues of Q operators and Schroedinger equation*, Adv. Theor. Math. Phys. **7** (2003) 711, DOI: 10.4310/ATMP.2003.v7.n4.a4.

[31] H. Frahm, S. Gehrmann, *Finite size spectrum of the staggered six-vertex model with $U_q(\mathfrak{sl}(2))$-invariant boundary conditions*, JHEP **01** (2022) 70, DOI: `10.1007/jhep01(2022)070`.

[32] H. Frahm, S. Gehrmann, *Integrable boundary conditions for staggered vertex models*, J. Phys. A: Math. Theor **56** (2023) 025001, DOI: `10.1088/1751-8121/acb29f`.

[33] H. Frahm et al., *The $D_3^{(2)}$ spin chain and its finite-size spectrum*, JHEP **11** (2023) 95, DOI: `10.1007/JHEP11(2023)095`.

[34] H. Frahm, S. Gehrmann, G. A. Kotousov, *Scaling limit of the staggered six-vertex model with $U_q(\mathfrak{sl}(2))$ invariant boundary conditions*, preprint (2023), DOI: `10.48550/arXiv.2312.11238`.

[35] K. G. Wilson, *The renormalization group: Critical phenomena and the Kondo problem*, Rev. Mod. Phys. **47** (1975) 773, DOI: `10.1103/RevModPhys.47.773`.

[36] R. Blumenhagen, E. Plauschinn, *Introduction to Conformal Field Theory*, Springer (2009), DOI: `10.1007/978-3-642-00450-6`.

[37] P. Di Francesco, P. Mathieu, D. Senechal, *Conformal Field Theory*, Springer (1997), DOI: `10.1007/978-1-4612-2256-9`.

[38] B. C. Hall, *Quantum Theory for Mathematicians*, Springer (2016), DOI: `10.1007/978-1-4614-7116-5`.

[39] E. T. Whittaker, G. N. Watson, *A Course of Modern Analysis*, Cambridge University Press (1996), DOI: `10.1017/CBO9780511608759`.

[40] M. E. Peskin, D. V. Schroeder, *An Introduction to Quantum Field Theory*, Addison-Wesley (1995).

[41] G. Mandal, A. M. Sengupta, S. R. Wadia, *Classical solutions of 2-dimensional string theory*, Mod. Phys. Lett. A **06** (1991) 1685, DOI: `10.1142/S0217732391001822`.

[42] S. Elitzur, A. Forge, E. Rabinovici, *Some global aspects of string compactifications*, Nucl. Phys. B **359** (1991) 581, DOI: `10.1016/0550-3213(91)90073-7`.

[43] J. Wess, B. Zumino, *Consequences of anomalous ward identities*, Phys. Lett. B **37** (1971) 95, DOI: `10.1016/0370-2693(71)90582-X`.

[44] E. Witten, *Global aspects of current algebra*, Nuclear Physics B **223** (1983) 422, DOI: `10.1016/0550-3213(83)90063-9`.

[45] S. P. Novikov, *The Hamiltonian formalism and a many-valued analogue of Morse theory*, Russ. Math. Sur. **37** (1982), DOI: `10.1070/RM1982v037n05ABEH004020`.

[46] E. Witten, *On holomorphic factorization of WZW and coset models*, Comm. Math. Phys. **144** (1992) 189, DOI: `10.1007/BF02099196`.

[47] R. Dijkgraaf, H. Verlinde, E. Verlinde, *String propagation in black hole geometry*, Nucl. Phys. B **371** (1992) 269, DOI: `10.1016/0550-3213(92)90237-6`.

[48] S. Ribault, V. Schomerus, *Branes in the 2D black hole*, JHEP **02** (2004), DOI: `10.1088/1126-6708/2004/02/019`.

[49] A. Hanany, N. Prezas, J. Troost, *The Partition Function of the Two-Dimensional Black Hole Conformal Field Theory*, JHEP **04** (2002) 014, DOI: `10.1088/1126-6708/2002/04/014`.

[50] J. Maldacena, H. Ooguri, *Strings in AdS$_3$ and the $SL(2, R)$ WZW Model. Part 1: The Spectrum*, J. Math. Phys. **42** (2001) 2929, DOI: `10.1063/1.1377273`.

[51] J. Maldacena, H. Ooguri, J. Son, *Strings in AdS$_3$ and the $SL(2, R)$ WZW Model. Part 2: Euclidean Black Hole*, J. Math. Phys. **42** (2001) 2961, DOI: `10.1063/1.1377039`.

[52] D. B. Ray, I. M. Singer, *Analytic Torsion for Complex Manifolds*, Annals of Mathematics **98** (1973) 154, DOI: `10.2307/1970909`.

[53] C. Candu, Y. Ikhlef, *Non-Linear Integral Equations for the SL(2,R)/U(1) black hole sigma model*, J. Phys. A: Math. Theor **46** (2013) 415401, DOI: `10.1088/1751-8113/46/41/415401`.

[54] H. Frahm, A. Seel, *The staggered six-vertex model: Conformal invariance and corrections to scaling*, Nucl. Phys. B **879** (2014) 382, DOI: `10.1016/j.nuclphysb.2013.12.015`.

[55] V. V. Bazhanov et al., *Some algebraic aspects of the inhomogeneous six-vertex model*, SIGMA **17** (2021) 025, DOI: `10.3842/SIGMA.2021.025`.

[56] A. M. Polyakov, *Conformal symmetry of critical fluctuations*, JETP Lett **12** (1970) 381.

[57] D. Friedan, Z. Qiu, S. Shenker, *Conformal Invariance, Unitarity, and Critical Exponents in Two Dimensions*, Phys. Rev. Lett. **52** (1984) 1575, DOI: `10.1103/PhysRevLett.52.1575`.

[58] A. A. Belavin, A. M. Polyakov, A. B. Zamolodchikov, *Infinite conformal symmetry in two-dimensional quantum field theory*, Nucl. Phys. B **241** (1984) 333, DOI: `10.1016/0550-3213(84)90052-X`.

[59] J. L. Cardy, *Effect of boundary conditions on the operator content of two-dimensional conformally invariant theories*, Nucl. Phys. B **275** (1986) 200, DOI: `10.1016/0550-3213(86)90596-1`.

[60] J. L. Cardy, *Operator content of two-dimensional conformally invariant theories*, Nucl. Phys. B **270** (1986) 186, DOI: `10.1016/0550-3213(86)90552-3`.

[61] H. W. J. Bloete, J. L. Cardy, M. P. Nightingale, *Conformal invariance, the central charge and universal finite-size amplitudes at criticality*, Phys. Rev. Lett. **56** (1986) 742, DOI: `10.1016/B978-0-444-87109-1.50033-9`.

[62] F. H. L. Essler et al., *The One-Dimensional Hubbard Model*, Cambridge University Press (2005), DOI: `10.1017/CBO9780511534843`.

[63] I. Affleck, *Universal term in the free energy at a critical point and the conformal anomaly*, Phys. Rev. Lett. **56** (1986) 746, DOI: `10.1016/B978-0-444-87109-1.50034-0`.

[64] C. N. Yang, *Some Exact Results for the Many-Body Problem in one Dimension with Repulsive Delta-Function Interaction*, Phys. Rev. Lett. **19** (1967) 1312, DOI: `10.1103/PhysRevLett.19.1312`.

[65] C. N. Yang, *S Matrix for the One-Dimensional N-Body Problem with Repulsive or Attractive δ-Function Interaction*, Phys. Rev. **168** (1968) 1920, DOI: `10.1103/PhysRev.168.1920`.

[66] R. J. Baxter, *Generalized ferroelectric model on a square lattice*, Stud. Appl. Math. **L** (1971) 51, DOI: `10.1002/sapm197150151`.

[67] J. B. McGuire, *Study of Exactly Soluble One-Dimensional N-Body Problems*, J. Math. Phys. **5** (1964) 622.

[68] V. V. Bazhanov, *Integrable quantum systems and classical Lie algebras*, Comm. Math. Phys. **113** (1987) 471, DOI: `10.1007/BF01221256`.

[69] A. A. Belavin, *Dynamical symmetry of integrable quantum systems*, Nucl. Phys. B **180** (1981) 189, DOI: `10.1016/0550-3213(81)90414-4`.

[70] L. D. Faddeev, *How algebraic Bethe ansatz works for integrable model*, Les Houches School of Physics: Astro. Sou. of Grav. Rad. (1996) 149, DOI: `10.48550/arXiv.hep-th/9605187`.

[71] I. V. Cherednik, *Factorizing particles on a half-line and root systems*, Theor. Math. Phys. **61** (1984) 977, DOI: `10.1007/BF01038545`.

[72] E. K. Sklyanin, *Boundary conditions for integrable quantum systems*, J. Phys. A: Math. Gen. **21** (1988) 2375, DOI: `10.1088/0305-4470/21/10/015`.

[73] L. Mezincescu, R. I. Nepomechie, *Integrable open spin chains with nonsymmetric R-matrices*, J. Phys. A: Math. Gen. **24** (1991) L17, DOI: `10.1088/0305-4470/24/1/005`.

[74] H. J. de Vega, A. González-Ruiz, *Boundary K-matrices for the XYZ, XXZ and XXX spin chains*, J. Phys. A: Math. Gen. **27** (1994) 6129, DOI: `10.1088/0305-4470/27/18/021`.

[75] A. Appel, B. Vlaar, *Trigonometric K-matrices for finite-dimensional representations of quantum affine algebras*, preprint (2022), DOI: `10.48550/arXiv.2203.16503`.

[76] J. C. Slater, *Theory of the Transition in KH2PO4*, J. Chem. Phys. **9** (1941) 16, DOI: `10.1063/1.1750821`.

[77] E. H. Lieb, *Residual Entropy of Square Ice*, Phys. Rev. **162** (1967) 162, DOI: `10.1103/PhysRev.162.162`.

[78] R. Steudel, *Chemie der Nichtmetalle*, De Gruyter (2014), DOI: `doi:10.1515/9783110307979`.

[79] H. J. de Vega, A. G. Ruiz, *Boundary K-matrices for the six vertex and the n(2n-1)An-1 vertex models*, J. Phys. A: Math. Gen. **26** (1993) L519, DOI: `10.1088/0305-4470/26/12/007`.

[80] P. P. Kulish, N. Y. Reshetikhin, *Diagonalisation of $GL(N)$ invariant transfer matrices and quantum N-wave system (Lee model)*, J. Phys. A: Math. Gen. **16** (1983) L591, DOI: `10.1088/0305-4470/16/16/001`.

[81] O. Babelon, H. J. de Vega, C. M. Viallet, *Exact solution of the $Z_{n+1} \times Z_{n+1}$ symmetric generalization of the XXZ model*, Nucl. Phys. B **200** (1982) 266.

[82] *Integrability of the D2n vertex models with open boundary*, Nucl. Phys. B **583**.3 (2000) 721, DOI: `10.1016/S0550-3213(00)00259-5`.

[83] E. K. Sklyanin, *The Quantum Toda Chain*, Springer: Lect. Notes in Phys. **226** (1985) 196, DOI: `10.1007/3-540-15213-X_80`.

[84] E. K. Sklyanin, *Quantum Inverse Scattering Method. Selected Topics*, World Scientific: Nankai Lect. in Math. Phys. (1992) 63, DOI: `10.48550/arXiv.hep-th/9211111`.

[85] Y. Wang et al., *Off-Diagonal Bethe Ansatz for Exactly Solvable Models*, Springer (2015), DOI: 10.1007/978-3-662-46756-5.

[86] R. J. Baxter, *Partition function of the eight-vertex lattice model*, Annals of Physics **70** (1972) 193, DOI: 10.1016/0003-4916(72)90335-1.

[87] R. J. Baxter, *Critical antiferromagnetic square-lattice Potts model*, Proc. R. Soc. Lond. A **383** (1982) 43, DOI: 10.1098/rspa.1982.0119.

[88] C. M. Yung, M. T. Batchelor, *Exact solution for the spin-s XXZ quantum chain with non-diagonal twists*, Nucl. Phys. B **446** (1995) 461, DOI: 10.1016/0550-3213(95)00168-R.

[89] M. T. Batchelor et al., *Exact solution and interfacial tension of the six-vertex model with anti-periodic boundary conditions*, J. Phys. A: Math. Gen. **28** (1995) 2759, DOI: 10.1088/0305-4470/28/10/009.

[90] N. Braylovskaya, P. E. Finch, H. Frahm, *Exact solution of the D_3 non-Abelian anyon chain*, Phys. Rev. B **94** (2016) 085138, DOI: 10.1103/PhysRevB.94.085138.

[91] V. V. Bazhanov et al., *On the scaling behaviour of the alternating spin chain*, JHEP **08** (2019) 087, DOI: 10.1007/JHEP08(2019)087.

[92] A. N. Krylov, *On the numerical solution of the equation by which the frequency of small oscillations is determined in technical problems*, Izv. Akad. Nauk SSSR, Ser. Fiz.-Mat. (1931) 491.

[93] W. E. Arnoldi, *The principle of minimized iterations in the solution of the matrix eigenvalue problem*, Q. Appl. **8** (1951) 17.

[94] C. N. Yang, C. P. Yang, *Thermodynamics of a one-dimensional system of bosons with repulsive delta-function interaction*, J. Math. Phys. **10** (1969) 1115, DOI: 10.1063/1.1664947.

[95] V. V. Bazhanov, S. L. Lukyanov, A. B. Zamolodchikov, *Integrable structure of conformal field theory, quantum KdV theory and thermodynamic Bethe ansatz*, Commun. Math. Phys. **177** (1996) 381, DOI: 10.1007/BF02101898.

[96] V. V. Bazhanov, S. L. Lukyanov, A. Zamolodchikov, *Integrable structure of conformal field theory. 2. Q operator and DDV equation*, Commun. Math. Phys. **190** (1997) 247, DOI: 10.1007/s002200050240.

[97] V. V. Bazhanov, S. L. Lukyanov, A. B. Zamolodchikov, *Integrable structure of conformal field theory. 3. The Yang-Baxter relation*, Commun. Math. Phys. **200** (1999) 297, DOI: 10.1007/s002200050531.

[98] A. Kluemper, M. T. Batchelor, P. A. Pearce, *Central charges of the 6- and 19-vertex models with twisted boundary conditions*, J. Phys. A: Math. Gen. **24** (1991) 3111, DOI: 10.1088/0305-4470/24/13/025.

[99] V. Y. Popkov, A. A. Zvyagin, *'Antichiral' exactly solvable effectively two-dimensional quantum spin model*, Phys. Lett. A **175** (1993) 295, DOI: 10.1016/0375-9601(93)90624-9.

[100] H. Frahm, C. Rödenbeck, *Integrable models of coupled Heisenberg chains*, Europhys. Lett. **33** (1996) 47, DOI: 10.1209/epl/i1996-00302-7.

[101] A. Klümper, *Free energy and correlation lengths of quantum chains related to restricted solid-on-solid lattice models*, Ann. Phys. **1** (1992) 540, DOI: `10.1002/andp.19925040707`.

[102] R. J. Baxter, *Potts model at the critical temperature*, J. Phys. C **6** (1973) L445, DOI: `10.1088/0022-3719/6/23/005`.

[103] L. D. Faddeev, N. Y. Reshetikhin, *Integrability of the principal chiral field model in 1+1 dimension*, Ann. Phys. (NY) **167** (1986) 227, DOI: `10.1016/0003-4916(86)90201-0`.

[104] C. Destri, H. J. de Vega, *Light-cone lattices and the exact solution of chiral fermion and sigma models*, J. Phys. A: Math. Gen. **22** (1989) 1329, DOI: `10.1088/0305-4470/22/9/022`.

[105] N. Y. Reshetikhin, H. Saleur, *Lattice regularization of massive and massless integrable field theories*, Nucl. Phys. B **419** (1994) 507, DOI: `10.1016/0550-3213(94)90342-5`.

[106] R. I. Nepomechie, A. L. Retore, *Factorization identities and algebraic Bethe ansatz for $D_2^{(2)}$ models*, JHEP **03** (2021) 089, DOI: `10.1007/JHEP03(2021)089`.

[107] G. Li et al., *Spectrum of the quantum integrable $D_2^{(2)}$ spin chain with generic boundary fields*, JHEP **04** (2022) 101, DOI: `10.1007/JHEP04(2022)101`.

[108] H. Frahm, K. Hobuß, *Spectral flow for an integrable staggered superspin chain*, J. Phys. A: Math. Theor **50** (2017) 294002, DOI: `10.1088/1751-8121/aa77e7`.

[109] Y. Miao, V. Gritsev, D. V. Kurlov, *The Floquet Baxterisation*, preprint (2022), DOI: `10.48550/arXiv.2206.15142`.

[110] A. Kuniba, T. Nakanishi, J. Suzuki, *T-systems and Y-systems in integrable systems*, J. Phys. A: Math. Theor **44** (2011) 103001, DOI: `10.1088/1751-8113/44/10/103001`.

[111] R. I. Nepomechie, R. A. Pimenta, *New $D_{n+1}^{(2)}$ K-matrices with quantum group symmetry*, J. Phys. A: Math. Gen. **51** (2018) 39LT02, DOI: `10.1088/1751-8121/aad957`.

[112] A. Doikou, *Quantum spin chain with 'soliton non-preserving' boundary conditions*, J. Phys. A: Math. Gen. **33** (2000) 8797, DOI: `10.1088/0305-4470/33/48/315`.

[113] R. I. Nepomechie, A. L. Retore, *Spin chains with boundary inhomogeneities*, JHEP **08** (2021) 053, DOI: `10.1007/JHEP08(2021)053`.

[114] É. Vernier, J. L. Jacobsen, H. Saleur, *The continuum limit of $a_{N-1}^{(2)}$ spin chains*, Nucl. Phys. B **911** (2016) 52, DOI: `10.1016/j.nuclphysb.2016.07.026`.

[115] H. Frahm, M. J. Martins, *The fine structure of the finite-size effects for the spectrum of the $OSp(n|2m)$ spin chain*, Nucl. Phys. B **930** (2018) 545, DOI: `10.1016/j.nuclphysb.2018.03.016`.

[116] H. Frahm, K. Hobuß, M. J. Martins, *On the critical behaviour of the integrable q-deformed $OSp(3|2)$ superspin chain*, Nucl. Phys. B **946** (2019) 114697, DOI: `10.1016/j.nuclphysb.2019.114697`, eprint: 1906.00655.

[117] M. J. Martins, X. W. Guan, *Integrability of the D_n^2 vertex models with open boundary*, Nucl. Phys. B **583** (2000) 721, DOI: `10.1016/S0550-3213(00)00259-5`.

[118] R. I. Nepomechie, R. A. Pimenta, A. L. Retore, *The integrable quantum group invariant $A_{2n-1}^{(2)}$ and $D_{n+1}^{(2)}$ open spin chains*, Nucl. Phys. B **924** (2017) 86, DOI: `10.1016/j.nuclphysb.2017.09.004`.

[119] Z. Tsuboi, *Universal Baxter TQ-relations for open boundary quantum integrable systems*, Nucl. Phys. B **963** (2021) 115286, DOI: `10.1016/j.nuclphysb.2020.115286`.

[120] R. Frassek, I. M. Szécsényi, *Q-operators for the open Heisenberg spin chain*, Nucl. Phys. B **901** (2015) 229, DOI: `10.1016/j.nuclphysb.2015.10.010`.

[121] P. Baseilhac, Z. Tsuboi, *Asymptotic representations of augmented q-Onsager algebra and boundary K-operators related to Baxter Q-operators*, Nucl. Phys. B **929** (2018) 397, DOI: `10.1016/j.nuclphysb.2018.02.017`.

[122] B. Vlaar, R. Weston, *A Q-operator for open spin chains I. Baxter's TQ relation*, J. Phys. A: Math. Gen. **53** (2020) 245205, DOI: `10.1088/1751-8121/ab8854`.

[123] V. V. Bazhanov et al., *A Shortcut to the Q-Operator*, J. Stat. Mech. **1011** (2010) P11002, DOI: `10.1088/1742-5468/2010/11/P11002`.

[124] P. P. Kulish, E. K. Sklyanin, *The general $U_q[sl(2)]$ invariant XXZ integrable quantum spin chain*, J. Phys. A: Math. Theor **24** (1991) L435, DOI: `10.1088/0305-4470/24/8/009`.

[125] H. Asakawa, M. Suzuki, *Finite-size corrections in the XXZ model and the Hubbard model with boundary fields*, J. Phys. A: Math. Gen. **29** (1996) 225, DOI: `10.1088/0305-4470/29/2/004`.

[126] H. J. de Vega, F. Woynarowich, *Method for calculating finite size corrections in Bethe ansatz systems: Heisenberg chain and six-vertex model*, Nucl. Phys. B **251** (1985) 439, DOI: `10.1016/0550-3213(85)90271-8`.

[127] N. M. Bogoliubov, A. G. Izergin, V. E. Korepin, *Critical exponents for integrable models*, Nucl. Phys. B **275** (1986) 687, DOI: `10.1016/0550-3213(86)90579-1`.

[128] J. Suzuki, *Simple excitations in the nested Bethe-ansatz model*, J. Phys. A: Math. Gen. **21** (1988) L1175, DOI: `10.1088/0305-4470/21/24/003`.

[129] H. Frahm, N. C. Yu, *Finite size effects in the integrable XXZ Heisenberg model with arbitrary spin*, J. Phys. A: Math. Gen. **23** (1990) 2115, DOI: `10.1088/0305-4470/23/11/032`.

[130] M. J. Martins, B. Nienhuis, R. Rietman, *An Intersecting Loop Model as a Solvable Super Spin Chain*, Phys. Rev. Lett. **81** (1998) 504, DOI: `10.1103/PhysRevLett.81.504`.

[131] J. L. Jacobsen, N. Read, H. Saleur, *Dense Loops, Supersymmetry, and Goldstone Phases in Two Dimensions*, Phys. Rev. Lett. **90** (2003) 090601, DOI: `10.1103/PhysRevLett.90.090601`.

[132] A. Voros, *Exact quantization condition for anharmonic oscillators (in one dimension)*, J. Phys. A: Math. Gen. **27** (1994) 4653, DOI: `10.1088/0305-4470/27/13/038`.

[133] G. A. Kotousov, S. L. Lukyanov, *Spectrum of the reflection operators in different integrable structures*, JHEP **02** (2020) 029, DOI: `10.1007/JHEP02(2020)029`.

[134] I. Bakas, E. Kiritsis, *Beyond the large N limit: non-linear W_∞ as symmetry of the $SL(2,R)/U(1)$ coset model*, International Journal of Modern Physics A **07** (1992) 55, DOI: 10.1142/S0217751X92003720.

[135] T. Jayaraman, K. Narain, M. H. Sarmadi, *$SU_k(2)$ WZW and Z_k parafermion models on the torus*, Nucl. Phys. B **343** (1990) 418, DOI: 10.1016/0550-3213(90)90477-U.

[136] A. Gerasimov, A. Marshakov, A. Morozov, *Free field representation of parafermions and related coset models*, Nucl. Phys. B **328** (1989) 664, DOI: 10.1016/0550-3213(89)90224-1.

[137] P. A. Griffin, O. F. Hernandez, *Feigin-Fuchs derivation of SU(1,1) parafermion characters*, Nucl. Phys. B **356** (1991) 287, DOI: 10.1016/0550-3213(91)90150-V.

[138] M. J. Ablowitz et al., *The Inverse Scattering Transform-Fourier Analysis for Nonlinear Problems*, Stud. in App. Math. **53** (1974) 249, DOI: 10.1002/sapm1974534249.

[139] V. A. Fateev, S. L. Lukyanov, *Boundary RG flow associated with the AKNS soliton hierarchy*, J. Phys. A: Math. Gen. **39** (2006) 12889, DOI: 10.1088/0305-4470/39/41/S10.

[140] A. Zamolodchikov, A. Zamolodchikov, *Conformal bootstrap in Liouville field theory*, Nucl. Phys. B **477** (1996) 577, DOI: 10.1016/0550-3213(96)00351-3.

[141] M. R. Gaberdiel, A. Recknagel, *Conformal boundary states for free bosons and fermions*, JHEP **2001** (2001) 016, DOI: 10.1088/1126-6708/2001/11/016.

[142] V. Pasquier, H. Saleur, *Common structures between finite systems and conformal field theories through quantum groups*, Nucl. Phys. B **330** (1990) 523, DOI: 10.1016/0550-3213(90)90122-T.

[143] G. A. Kotousov, S. L. Lukyanov, *ODE/IQFT correspondence for the generalized affine $\mathfrak{sl}(2)$ Gaudin model*, JHEP **09** (2021) 201, DOI: 10.1007/JHEP09(2021)201.

[144] G. von Gehlen, V. Rittenberg, G. Schütz, *Operator content of n-state quantum chains in the $c = 1$ region*, J. Phys. A: Math. Gen. **21** (1988) 2805, DOI: 10.1088/0305-4470/21/12/022.

[145] F. C. Alcaraz et al., *Operator content of the XXZ chain*, J. Phys. A: Math. Gen. **21** (1988) L117, DOI: 10.1088/0305-4470/21/3/001.

[146] N. Y. Reshetikhin, *The Spectrum of the Transfer Matrices Connected with Kac-Moody Algebras*, Lett. Math. Phys. **14** (1987) 235, DOI: doi.org/10.1007/BF00416853.

[147] M. Jimbo, *Quantum R matrix for the generalized Toda system*, Comm. Math. Phys. **102** (1986) 537, DOI: 10.1007/BF01221646.

[148] N. Y. Reshetikhin, *The functional equation method in the theory of exactly soluble quantum systems*, Sov. Phys. JETP **57** (1983) 691.

[149] H. J. de Vega, E. Lopes, *Exact solution of the $B_n^{(1)}$, $D_n^{(1)}$, $A_{2n}^{(2)}$, $A_{2n-1}^{(2)}$, $D_n^{(2)}$ and $E_6^{(2)}$ lattice models*, Nucl. Phys. B **362** (1991) 261, DOI: 10.1016/0550-3213(91)90564-E.

[150] M. J. Martins, *Unified algebraic Bethe ansatz for two-dimensional lattice models*, Phys. Rev. E **59** (1999) 7220, DOI: 10.1103/PhysRevE.59.7220.

[151] J. L. Cardy, *Logarithmic corrections to finite-size scaling in strips*, J. Phys. A: Math. Gen. **19** (1986) L1093, DOI: 10.1088/0305-4470/19/17/008.

Acknowledgements

Firstly, I thank Holger Frahm for supervising and guiding me through this academic journey. Not even a global health crisis was able to stop effective supervision and collaboration. During the first two years of extraordinary circumstances, the innumerable virtual meetings and countless instant text messages, including LaTeX-code, have provided a valuable substitute for in-person discussions. I never thought I would use the backslash button on my smartphone that often or that a chat history would become so important in my academic life. Besides the immense scientific training, I am also grateful for his moral support.

Secondly, I want to thank Andreas Klümper for agreeing to referee this thesis and for constructive advice in solving NLIEs.

Thirdly, I thank Michael Flohr for examining this thesis and Rolf Haug for chairing the examination committee.

I am also very grateful to Sergei Lukyanov for academic collaboration, for sharing his expertise about the ODE/IQFT correspondence, and for pushing me past my limits. Further, I value his lessons regarding different perspectives on approaching a scientific problem as well as scientific work and academic values, which I hope to meet in the future.

Further, I am grateful to many other researchers. I thank Rafael Nepomechie for academic collaboration, which I enjoyed very much and learned a lot from. I thank Jesper Lykke Jacobsen for proposing interesting ongoing projects and valuable discussions. I thank Ana Lucia Retore for academic collaborations and enjoyable evenings in Switzerland or Durham. Speaking of which, I thank Merlin Füllgraf for keeping my mind sane with necessary distractions outside the institute during the first two years. I want to thank Alexi Morin-Duchesne for an excellent, somehow almost private lecture series, general advice on life and extraordinary, amusing times at conferences, which I will miss a lot. I also want to thank Yacine Ikhlef for the valuable discussion about the Wiener-Hopf analysis with singular kernels. The latter was made possible by Frank Göhmann, to whom I am also grateful for his generally helpful advice about academia. I also thank Marcio Martins for his valuable lessons about football and algebraic geometry. While the former is unlikely to bear fruits, the latter helped me a lot and led to new current research projects.

I am thankful to Daria Shabetnik for sharing with me her unpublished notes about the perturbative expansion of the ODE and the ones for the Black Hole CFTs.

Also, I am thankful to Paul Winter, one of our computer admins, for all the help dealing with Fortran and the cluster.

I am indebted to Paul Hanemann, Philip Schwartz and Viktoria-Sophie Schmiesing for proofreading. Of course, I take responsibility for any remaining errors.

My last big thanks go to Gleb Kotousov for countless invaluable academic lessons. I thank you for encouraging me to develop my own new ideas and for prohibiting me from blindly approaching hard problems without having the necessary knowledge. Instead, you taught me the required methods. I sincerely thank you for this extraordinary well co-supervision,

which has broadened me in many ways. I learned so many things and methods which will continue their usefulness in the future. I am grateful for the advice on academic writing and for being introduced to new English standards, which I hope to meet at some point in my life.

Curriculum Vitae

Sascha Gehrmann, born 27.05.1997 in Hanover

since 2020:	**Leibniz Universität Hannover** Ph.D. Student in Physics
2019-2020:	**University of Cambridge** M.A.St. in Applied Mathematics
2015-2019:	**Leibniz Universität Hannover** Studies of Physics, B.Sc. Physics 2018
2007-2015:	**Hannah-Arendt-Gymnasium** Qualification for university entrance

List of publications

H. Frahm, S. Gehrmann, G. A. Kotousov: *Scaling limit of the staggered six-vertex model with $U_q\big(\mathfrak{sl}(2)\big)$ invariant boundary conditions*, preprint , arXiv: `2312.11238`

H. Frahm, S. Gehrmann, R. I. Nepomechie, A. L. Retore, *The $D_3^{(2)}$ spin chain and its finite-size spectrum*, JHEP **11** (2023) 095, DOI: `10.1007/JHEP11(2023)095`, arXiv: `2307.11511`

H. Frahm, S. Gehrmann, *Integrable boundary conditions for staggered vertex models*, J. Phys. A: Math. Theor. **56** (2023) 025001, DOI: `10.1088/1751-8121/acb29f`, arXiv: `2209.06182`

H. Frahm, S. Gehrmann, *Finite size spectrum of the staggered six-vertex model with $U_q(sl(2))$-invariant boundary conditions*, JHEP **01** (2022) 070, DOI: `10.1007/JHEP01(2022)070`, arXiv: `2111.00850`.